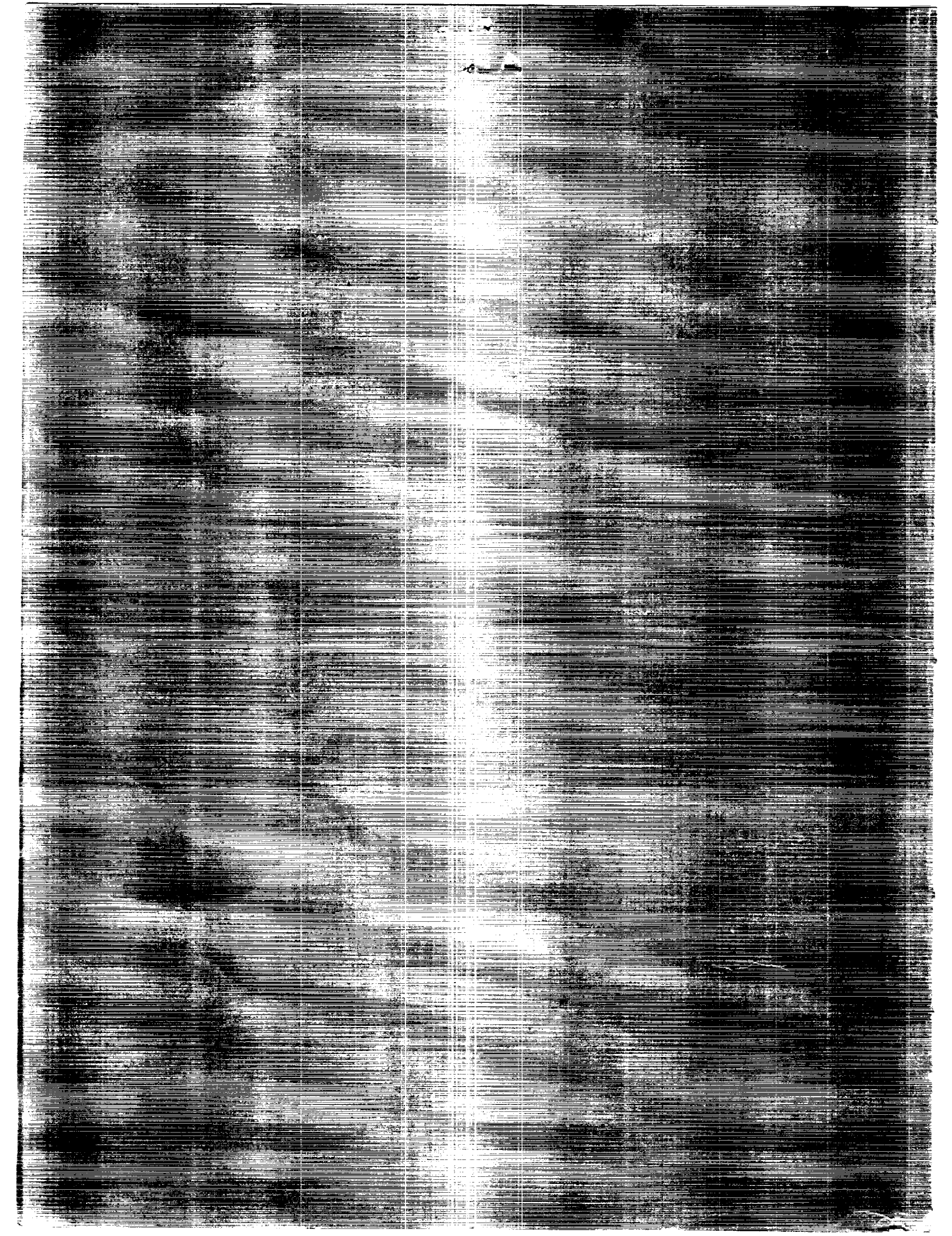

NASA Conference Publication 3046

Relativistic Gravitational Experiments in Space

Ronald W. Hellings, *Editor*
NASA Office of Space Science and Applications
Washington, D.C.

Proceedings of a workshop sponsored by
the National Aeronautics and Space Administration,
Washington, D.C., and held in
Annapolis, Maryland
June 28–30, 1988

National Aeronautics and
Space Administration
Office of Management
Scientific and Technical
Information Division

1989

TABLE OF CONTENTS

ATTENDEES

NAME	AFFILIATION
Allen Anderson	University of California-Santa Barbara
John Anderson	Jet Propulsion Laboratory
L. Anselmo	Centro Nazionale de Calcolo Elettronico
John Armstrong	Jet Propulsion Laboratory
Neil Ashby	University of Colorado
Peter Bender	University of Colorado
Charles Bennett	Goddard Space Flight Center
Bruno Bertotti	Dpt Di Fisica Nucleare e Theorica
Joe Brenkle	Jet Propulsion Laboratory
Robert Byer	Stanford University
John Chandler	Center for Astrophysics
Ignazio Ciufolini	CNR-IFSI
John Clauser	J. F. Clauser & Assoc.
Daniel DeBra	Stanford University
Rudy Decher	Marshall Space Flight Center
Francis Everitt	Stanford University
William Fairbanks	Stanford University
James Faller	Joint Institute for Laboratory Astrophysics
Richard Harms	Applied Research Corporation
Ron Hellings (Chairman)	Jet Propulsion Laboratory
Gary Horowitz	University of California
Wayne Hudson	NASA Headquarters
Timothy Krisher	Jet Propulsion Laboratory
Robert Kursinski	Jet Propulsion Laboratory
Bahram Mashhoon	University of Missouri
Richard Matzner	University of Texas
Lute Maleki	Jet Propulsion Laboratory
Peter Michelson	Stanford University
M. Moody	University of Maryland
George Newton	NASA Headquarters
Michael Nieto	Los Alamos National Laboratories
Kenneth Nordtvedt	Montana State University
Ho-Jung Paik	University of Maryland
Jody Palmer	University of Waterloo
Charles Pellerin	NASA Headquarters
Robert Reasenberg	Center for Astrophysics
Bonny Schumaker	Jet Propulsion Laboratory
Bernie Schutz	University College Cardiff
Irwin Shapiro	Center for Astrophysics
Martin Sokoloski	NASA Headquarters
David Sonnabend	Jet Propulsion Laboratory
Robert Stachnik	NASA Headquarters
Richard Stark	University of California
Robin Stebbins	University of Colorado
Richard Sydnor	California Institute of Technology
Karrick Talmadge	Purdue University
Byran Tapley	University of Texas
Joseph Taylor	Princeton University
Robert Truehaft	California Institute of Technology

Bob Vessot	Center for Astrophysics
Hugo Wahlquist	Jet Propulsion Laboratory
Joseph Weber	University of California
Edward Weiler	NASA Headquarters
Rainer Weiss	Massachusetts Institute of Technology
Clifford Will	Washington University
Eric Woolgar	University of Toronto
Paul Worden	Stanford University
Lawrence Young	Jet Propulsion Laboratory

WORKSHOP ON RELATIVISTIC GRAVITATION EXPERIMENTS IN SPACE

Meeting held at The Joint Session Meeting Room, Joint Legislative Services Building
Maryland State Capitol, Annapolis, Maryland
June 28-30, 1988

AGENDA

Tuesday (6/28/88)

9:00 AM	WELCOME	Charles Pellerin
9:20	INTRODUCTION	Ronald Hellings
9:30	I. GRAVITATIONAL WAVE DETECTION IN SPACE:	Ray Weiss, Chairman
9:30	A. Space and Laboratory Detection Experiments (R. Weiss)	
10:00	B. Advanced Doppler Tracking Experiments (J. Armstrong)	
10:25	C. Microwave Interferometer in Space (A. Anderson)	
10:50	BREAK	
11:10	D. Optical Interferometer in Space (P. Bender)	
11:35	E. Earth-Orbiting Detectors (H-J. Paik)	
12 noon	LUNCH BREAK	
2:00 PM	II. THEORETICAL BACKGROUND:	Cliff Will, Chairman
2:00	A. Gravity Waves as a Test of Relativistic Gravitation (C. Will)	
2:20	B. Gravity Wave Astronomy (B. Schutz)	
2:50	C. Detecting Gravity Waves from Binary Black Holes (H. Wahlquist)	
3:05	D. Gravity Waves from Gravitational Collapse (R. Stark)	
3:20	E. The Cosmic Gravitational Wave Background (R. Matzner)	
3:40	BREAK	
4:00	F. Metric and Non-Metric Theories (C. Will)	
4:30	G. Gravitational Consequences of Modern Field Theories (G. Horowitz)	
4:50	H. Higher-Order Tests of Relativistic Gravity (K. Nordtvedt)	
5:10	I. Tests of the Inverse-r-Square Law (M. Nieto)	
5:30	J. Applied General Relativity (N. Ashby)	

Wednesday (6/29/88)

9:00 AM	III.	ASTROPHYSICAL OBSERVATORIES AND GENERAL RELATIVITY: Ronald Hellings, Chairman
9:00		A. Pulsar Timing and VLF Gravity Waves (R. Hellings)
9:20		B. A Gravitational Redshift Test from Pulsar Timing (I. Shapiro)
9:40		C. Fast X-Ray Timing and Black Hole Detection (K. Wood)
10:00		D. Space Interferometer Measurement of Cosmic Rotation (R. Vessot)
10:30		BREAK
11:00		E. Space Telescope Searches for Galactic Black Holes (R. Harms)
11:20		F. The Cosmic Microwave Anisotropy Experiment on COBE (C. Bennett)
11:40		G. Frequency-Stable High Power Lasers in Space (R. Byers)
12 noon		LUNCH BREAK
2:00 PM	IV.	TESTS OF RELATIVITY GRAVITY IN SPACE: Irwin Shapiro, Chairman
2:00		A. GPB (F. Everitt)
2:20		B. Lageos III (I. Ciufolini)
2:40		C. Gradiometry and Gravitomagnetic Field Detection (B. Mashoon)
3:00		D. Advanced Gravitational Redshift Experiment (R. Vessot)
3:20		E. Oribiting Eotvos (P. Worden)
3:40		F. Experiments to Detect a Fifth Force (J. Faller)
4:00		BREAK
4:30		G. Icarus Lander (R. Hellings)
4:40		H. Mercury Orbiter (P. Bender)
4:50		I. Solar Probe (J. Anderson)
5:10		J. Optical Interferometers (R. Reasenberg)
5:30		K. New Tests with Old Data (J. Chandler)
6:00		Buffet dinner at the Reynolds Tavern

Thursday (6/30/88)

9:00 AM	V.	RELEVANT ADVANCED TECHNOLOGIES:	George Newton, Chairman
9:00		A. High-Stability Radio Links (R. Kursinski)	
9:20		B. Tropospheric Monitoring Technology (R. Treuhaft)	
9:40		C. Stable Clocks (R. Vessot)	
10:10		D. Improved Ranging Systems (L. Young)	
10:30		BREAK	
10:50		E. Microwave Technology in Space (R. Godfrey)	
11:10		F. Drag-Free Technology (D. DeBra)	
11:30		G. Gravity Gradiometers (M. Moody)	
11:50		H. Inertial Corrections via Dynamic Estimation (D. Sonnabend)	
12:10		I. Ultrasensitive Inertial Sensors via Neutral Atom Interferometry (I. Clauser)	
12:20		LUNCH BREAK	
2:00 PM	VI.	MEETING SUMMARY & OPEN DISCUSSION	R. Hellings, Chairman

INTRODUCTION

Gravitational physics is almost the paradigm for what the relationship between theory and observation in science should be. For over three hundred years, the process has been going on. It was the extremely precise observations of Tycho Brahe that led the young mathematician Johannes Kepler to reject the Ptolemaic and Copernican models of the solar system and discover his laws of planetary motion, laws which guided Isaac Newton in his formulation of the law of gravitation. For the next two hundred years, increasingly precise telescope observations, combined with painstaking data analysis by men like Leverrier and Newcomb, first confirmed Newton's theory in remarkable detail. But then, as the observed tiny 43 arcseconds per century of anomalous perihelion shift for Mercury stubbornly defied explanation, Newton's theory as the fundamental theory of gravitation was eventually overthrown when Albert Einstein showed that the anomaly could be explained simply as a consequence of his General Theory of Relativity. That anomalous motion of Mercury, along with a 10%-accurate observation of the bending of starlight, remained the only observational justification for Einstein's theory for fifty years. Theory had temporarily outstripped the ability of the observers. But that era is now over. Observation technology has now caught up with the demands of relativistic gravitation theory and the time has come to move ahead. What are the limits of Einstein's theory? Will it eventually fail to agree with observation? Will the next advance in precision lead the way to a new fundamental theory? These are the questions that need to be answered in order for this process that stretches back over three hundred years to continue, and these are the questions that are addressed in this workshop. It is perhaps not unreasonable to wonder if the Brahes, the Newtons, the Leverriers, and the Einsteins of the twenty-first century might not be found among the contributors in the pages of these proceedings.

There were three main goals of our workshop.

First, we sought to place experimental gravitation in its theoretical context. The predictions of theoretical astrophysics and cosmology for generation of gravitational waves were addressed. In addition, the theoretical basis for high precision tests of gravity theories was discussed, including a summary of the PPN formalism, its extension to higher order, and an exciting new idea of how classical tests of relativistic gravity might provide experimental evidence for quantum field theories of gravity. Finally, there was a discussion of some arenas where relativity has recently become a tool of the applied physicist's trade.

Second, we attempted to outline some of the current ideas and proposals for NASA projects. These included tests of relativistic gravity in space, where the goal is to continually probe the limits of validity of Einstein's theory, as discussed above. Also included were discussions of how astrophysical observatories could test relativity by looking for the effects of relativity in their measurements or by looking for black holes. Missions to detect gravitational waves were also discussed, outlining a suite of possibilities from present efforts with Doppler tracking, through a microwave interferometer, to a future laser interferometer. Gravitational wave detection experiments not only would test an aspect of gravitation but would also open a new window into the universe as gravitational wave astronomy leads to the discovery of radically new astronomical objects.

The third and last goal was to try to identify common threads of technology that would enable these missions to take place. While each mission had requirements

that were unique to it, several general fields of endeavor were identified. These included stable clock technology, improved Doppler/range microwave tracking technology, laser tracking technology, gravity gradiometry, drag-free system development, and accelerometer technology.

It is generally the hope of the participants in this workshop that an increased commitment by NASA to mission studies and to relevant technology development may lead in the next few years to a well-defined agenda for future missions in relativistic gravitation, and that by implementing such an agenda the U.S. space program may make an historically crucial contribution to the advancement of this area of science. NASA has made and will certainly continue to make important scientific discoveries and will continue to answer questions about the makeup of the universe in which we live, but there is probably no other endeavor in which NASA will work where the discoveries will be of such a fundamental nature, affecting our knowledge of the very laws the universe must obey in determining its makeup.

GRAVITATIONAL RADIATION AS A TEST OF RELATIVISTIC GRAVITY

CLIFFORD M. WILL
McDonnell Center for the Space Sciences, Department of Physics
Washington University, St. Louis, Missouri 63130

ABSTRACT

Gravitational radiation can be used to test theories of gravitation. When the waves are ultimately detected directly, their speed and polarization properties can be measured and compared with predictions of alternative theories. The multipole nature of gravitational radiation has already been tested in the binary pulsar, where observations of the decay of the orbit verify the quadrupole formula for gravitational radiation damping of general relativity and put strong constraints on dipole gravitational radiation predicted by many alternative theories.

I. INTRODUCTION

The first detection of gravitational radiation by Earth-bound detectors will usher in a new era of astronomy. The study of the waveform, spectrum, intensity, polarization, and directionality of the waves will give information about gravitational collapse, collisions between compact objects, and the gravitational-wave cosmic background (for a review of gravitational-wave astronomy, see Thorne 1987). In addition to its astrophysical and astronomical implications, gravitational radiation provides an important probe of the nature of the gravitational interaction itself, in the sense that gravitational-wave observations can be used to test the validity of general relativity versus alternative theories of gravity.

The *existence* of gravitational radiation does not provide a strong test, because any relativistic theory of gravity that incorporates Lorentz invariance, at even the most crude level, can be expected to predict gravitational waves. Instead, it is the detailed nature of the gravitational waves that can distinguish among alternative theories, in particular the speed and polarization of the waves, and the effect of the gravitational-radiation back-reaction on the source. The first two properties can be studied only via the direct detection of gravitational radiation. The third property has already been examined in detail using observations of the orbital motion of the binary pulsar.

II. SPEED AND POLARIZATION OF GRAVITATIONAL WAVES

General relativity predicts that the speed of weak gravitational waves in the geometrical optics limit should equal that of light, but other theories do not necessarily predict this equality. Table 1 shows the predicted speeds in some alternative metric theories (units are such that the speed of light is unity) (for a review, see Section 10.1 of Will 1981, and Section 7.1 of Will 1984). Differences from the speed of light in these theories typically depend on the values of parameters that relate the local geometry that describes the gravitational-wave detector to the background cosmological spacetime.

TABLE 1

PROPERTIES OF GRAVITATIONAL RADIATION IN ALTERNATIVE METRIC THEORIES OF GRAVITY (WILL 1981, 1984)

THEORY	GRAVITATIONAL WAVE SPEED	NUMBER OF POLARIZATION STATES
General relativity	1	2
Scalar-tensor theory	1	3
Vector-tensor theory	various	6
Rosen's bimetric theory	$(c_1/c_0)^{1/2}$	6
Rastall's theory	$1 + 1/2\ K^2 + O(K^3)$	5
BSLL theory	$1 + 1/2\ (\omega_0+\omega_1) + O(\omega^2)$	6
Stratified theories	*	6

*speed is complicated function of parameters.

The speed of gravitational waves can be measured by determining the time of arrival of a pulse of waves from a supernova collapse, and comparing that time with the time of arrival of the pulse of light or neutrinos (assuming that the pulses are emitted almost simultaneously at the source) (Eardley *et al.* 1973). Such a comparison has already constrained the difference of the speeds of neutrinos and photons from SN 1987A (Longo 1987, 1988; Krauss and Tremaine 1988). If v_g is the gravitational-wave speed, and T_i denotes the arrival time of the appropriate signal, then the upper limit on $|v_g - 1|$ that could be achieved by observations of a supernova at a distance d is given by

$$|v_g - 1| < \begin{cases} 10^{-9} \left(\frac{1\ \mathrm{kpc}}{d}\right) \left(\frac{T_g - T_{\gamma\nu}}{\mathrm{min}}\right) \\ 10^{-9} \left(\frac{1\ \mathrm{Mpc}}{d}\right) \left(\frac{T_g - T_{\gamma\nu}}{\mathrm{week}}\right) \end{cases} .$$

It seems likely that the first solid detection of a gravitational wave burst from a supernova will result in an interesting limit.

General relativity predicts two polarization states (corresponding to two helicity states of a spin-2 graviton) for the most general weak gravitational wave, but virtually every other metric theory of gravity predicts more states, up to six. The action of these six independent states on a ring of test particles placed in the path of a gravitational wave is shown in Figure 1. In general relativity, only the $\mathrm{Re}\Psi_4$ and $\mathrm{Im}\Psi_4$ modes are present: in the Brans-Dicke and other scaler-tensor theories, these two plus the Φ_{22} mode are present. Table 1 also notes the number of modes predicted by the theories listed (for review, see Section 10.2 of Will 1981, and Section 7.2 of Will 1984). Using an appropriate array of gravitational-wave detectors, it is possible to determine or to restrict the number of polarizations and thereby to test gravitational theories (for discussion of detection strategies see Will 1981, Section 10.2; and Eardley, Lee and Lightman 1973).

III. GRAVITATIONAL RADIATION REACTION

The discovery of the binary pulsar in 1974 provided a tool to study gravitational radiation prior to its actual detection by laboratory instruments. The unexpected stability of the pulsar "clock" and the cleanliness of the orbit allowed radio astronomers to determine the orbital and other parameters of the system to extraordinary accuracy. Furthermore, the observation of the relativistic periastron advance, and of the effects on pulse arrival times of the gravitational redshift and second-order Doppler shift, and of the Shapiro time-delay, have further constrained the nature of the system. Finally, the measurement of the rate of change of orbital period gave the first evidence for the effects of gravitational radiation damping. In general relativity, these four effects depend in a known way on measured orbital parameters and on the unknown masses m_p and m_c of the pulsar and companion (assuming that the companion is sufficiently compact that tidal and rotational distortion effects can be ignored). In the gravitational radiation case, the relevant formula is the "quadrupole formula," whose foundation is the basic fact that, in general relativity, the lowest multipole moment involved in the emission of gravitational waves (in situations where a multipole decomposition is relevant) is quadrupole. The constraints provided on the masses by these four observations are shown in Figure 2. The system is highly overdetermined (four constraints on two parameters), yet all four constraints share a common overlap region, yielding $m_p = 1.42 \pm 0.03$ and $m_c = 1.40 \pm 0.03$ solar masses: a completely consistent solution in general relativity. With these values for the masses, the predicted rate of change of orbital period agrees with the observed change to better than 5 percent (for reviews see Will 1984, Taylor 1987).

Some have argued that this provides a "strong-field" test of general relativity, in constrast to the solar-system "weak-field" tests, in the following sense. It seems likely that the companion, like the pulsar, is a neutron star, therefore both bodies contain strongly relativistic internal gravitational fields. Nevertheless, their motion and generation of gravitational waves are characteristic of their weak interbody gravitational fields and low orbital velocities, and are independent of their internal relativistic structure. This irrelevance of the internal structure is part of the so-called Strong Equivalence Principle (Sections 3.3 and 11.3 of Will 1981), a principle that appears to be unique to general relativity. It is also sometimes called the Effacing Principle (Damour 1987). The Brans-Dicke theory, for example violates SEP.

On the other hand, in most alternative theories of gravity, the motion of compact objects *is* affected by their internal structure (violation of SEP); in addition, most theories predict "dipole" gravitational radiation, whose source is the internal

gravitational binding energy of the two stars. In the binary pulsar, dipole radiation can lead to significantly larger damping than quadrupole radiation, because it depends on fewer powers of the small parameter v_{orbit}/c. Because of these two phenomena, violations of SEP, and dipole gravitational radiation, the likelihood of a consistent solution for m_p and m_c in a given alternative theory of gravity, is extremely small. For example, the Rosen bimetric theory, which otherwise agreed with solar system observations, was a casualty of this test (Section 10.3 of Will 1981).

For some theories of gravity that are in some sense "close" to general relativity, such as the Brans-Dicke theory, the binary pulsar may not be a strong testing ground for dipole gravitational radiation because of the likelihood that the two objects are neutron stars of almost the same mass. In this event, dipole radiation, even if permitted, would vanish or be negligible by virtue of the symmetry. Another possibility for testing dipole gravitational radiation is a class of close binary systems containing a neutron star and a low-mass secondary, such as the "11 minute binary," 4U 1820-30, detected in 1986. Although systems such as this are often complicated by such astrophysically "messy" phenomena as mass transfer, it may still be possible to obtain interesting and even crucial limits on alternative theories. A limit was recently set on the nonsymmetric gravitational theory of Moffat, using the reported limits on the rate of change of orbital period of 4U 1820-30, together with a reasonable model for the mass transfer (Krisher 1987). Apart from its astrophysical importance, the continued search for short-period binaries containing compact objects may provide important new arenas for testing relativistic gravity.

ACKNOWLEDGEMENTS

This work was supported in part by the National Science Foundation under Grant PHY 85-13953.

REFERENCES

Damour, T. 1987, in *300 Years of Gravitation*, eds. S. W. Hawking and W. Israel, P. 128, Cambridge University Press, Cambridge.

Eardley, D. M., Lee, D. L., and Lightman, A. P. (1973). *Phys. Rev.* , *D* **10**, 3308.

Eardley, D. M., Lee, D. L., Lightman, A. P., Wagoner, R. V., and Will, C. M. 1973, *Phys. Rev. Lett.*, **30**, 884.

Krisher, T. P. 1987, *Astrophys., J. Lett.*, **320**, L47.

Krauss, L. M. and Tremaine, S. 1988, *Phys. Rev. Lett.*, **60**, 176.

Longo, M. J. 1987, *Phys. Rev., D* **36**, 3276.

Longo, M. J. 1988, *Phys. Rev. Lett.*, **60**, 173.

Taylor, J. H. 1987, in *General Relativity and Gravitation*, ed. M. A. H. MacCallum, p. 209, Cambridge University Press, Cambridge.

Thorne, K. S. 1987, in *300 Years of Gravitation*, eds. S. W. Hawking and W. Israel, p. 330, Cambridge University Press, Cambridge.

Will, C. M. 1981, *Theory and Experiment in Gravitational Physics*, Cambridge University Press, Cambridge.

Will, C. M. 1984, *Phys. Reports*, **113**, 345.

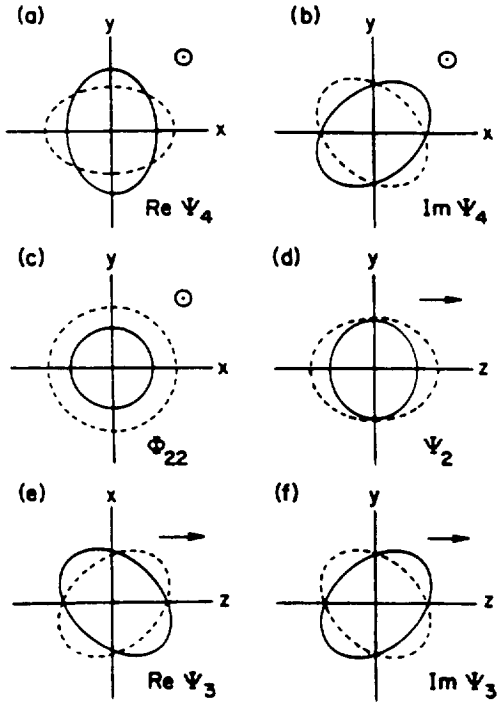

FIG. 1. — The six polarization modes of a weak plane gravitational wave permitted in any metric theory of gravity. Shown is the displacement that each mode induces on a sphere of test particles. The wave propagates in the +z direction and has time dependence cos ωt. The solid line is a snapshot at $\omega t = 0$; the broken line one at $\omega t = \pi$. There is no displacement perpendicular to the plane of the figure. In (a), (b), and (c), the wave propagates out of the plane; in (d), (e), and (f), the wave propagates in the plane.

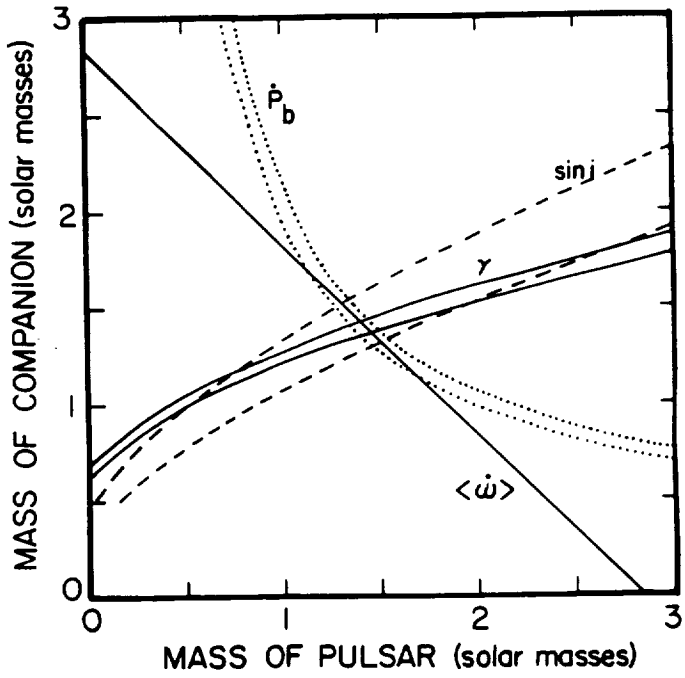

FIG. 2. — Curves showing constraints on the mass of the pulsar and its companion provided by measured values and estimated errors of the periastron shift ($\dot{\omega}$), gravitational redshift second order Doppler shift (γ), orbital period change ($\dot{P}_b$), and Shapiro time delay (sin i). All four constraints overlap in the region near 1.4 solar masses for each body.

DISCUSSION

NORDTVEDT: It seems that if strange gravitons traveled at a speed different than light, then these gravitons would Cerenkov radiate into photons or vice-versa. Can this be used to rule out strange gravitons?

WILL: That is possible, although the details depend on the particular theory in question. For example, Caves (Ann. Phys. N.Y. **125**, 35 (1977)) used such arguments to place a limit on Rosen's bimetric theory.

TREUHAFT: To what extent does a simple measurement of the difference in arrival time of gravitons and photons separate propagation characteristics from source physics (i.e. at what level can the emission times be assumed to be identical)?

WILL: The limits given above hold provided that the emission time difference is small compared to minutes (galactic source) or compared to a week (extragalactic source). Since one expects the time-scale for the processes leading to photon, neutrino and gravity-wave bursts to be on the order of milliseconds, the assumption should be valid, unless there are unforeseen delays between processes.

HELLINGS: Do you have any comment on possible scalar radiation? In particular, what theoretical limits can be set on it from experimental observations?

WILL: Measurements or limits on the possible polarizations of a detected gravitational wave could limit the existence of scalar gravitational waves, and Paik (Phys. Rev. D. 15, 409 (1977)) studied a disk gravitational-wave antenna design that would be particularly sensitive to scalar waves, represented by the mode F_{22} shown in Figure 1. The binary pulsar could in principle limit the effects of scalar gravitational radiation damping, through its contribution to dipole and quadrupole radiation. The details, however, depend on the theory in question, so for the case of Brans-Dicke type theories, the limits are disappointing compared to standard solar-system tests of those theories, because of the apparent symmetry of the system. As to scalar low-mass fields that may play a role in short-range gravity, the answer may depend on the details of the field theory that predicts the scalar field.

HELLINGS: A measurement using Peter Bender's interferometer of the phase of gravity waves from a known binary star could be used to measure the speed of gravity waves as a phase offset from the expected phase from knowledge of the optical data.

SOURCES OF GRAVITATIONAL WAVES

BERNARD F. SCHUTZ
Department of Applied Mathematics and Astronomy
University College Cardiff, Cardiff, Wales, U.K.

ABSTRACT

Sources of low-frequency gravitational radiation are reviewed from an astrophysical point of view. Cosmological sources include the formation of massive black holes in galactic nuclei, the capture by such holes of neutron stars, the coalescence of orbiting pairs of giant black holes, and various means of producing a stochastic background of gravitational waves in the early universe. Sources local to our Galaxy include various kinds of close binaries and coalescing binaries. Gravitational wave astronomy can provide information that no other form of observing can supply; in particular, the positive identification of a cosmological background originating in the early universe would be an event as significant as was the detection of the cosmic microwave background.

I. INTRODUCTION

Almost every speaker at this Workshop who has discussed methods of detecting gravitational waves from space has included a discussion of possible sources of gravitational waves at low frequencies. My aim here is not to repeat these discussions, but to put them in their astrophysical context: why is gravitational wave astronomy interesting? A good source for further reading is Thorne (1987).

In general terms, gravitational waves open up a qualitatively new window on the universe. The information they carry reflects the large-scale mass distribution of the source on distance scales of the same order as the gravitational wavelength. By contrast, observable electromagnetic radiation is of much higher frequency, and comes from small regions: atomic size for visible wavelengths, for example. As a consequence, astrophysical modelling of large-scale structures requires assumptions that enable one to go from the small-scale to the large: assumptions of local thermodynamic equilibrium, of homogeneity, of symmetry, and so on. Gravitational waves will enable more direct modelling of the source and will be complementary to electromagnetic waves when both are available.

a) A Brief Look at Sources of High-Frequency Radiation

It will help us to look briefly first at sources of high-frequency gravitational waves, even though they are of more relevance to ground-based detectors than to space-based ones. Some of them are closely related to low-frequency sources, and if they are detected from the ground they will provide further incentive for looking from space. For a review of ground-based detection, see Schutz (1988).

1) GRAVITATIONAL COLLAPSE

Collapse to form neutron stars or black holes in the mass range 1 to 10 $M_\odot$ will radiate waves in the frequency range 1 to 10 kHz with an amplitude that depends on how much asymmetry there is in the collapse. These collapses, at least sometimes, result in Type II supernova explosions. The rate at which Type II

supernovae occur is relatively well known, but the fraction of collapse events that produce strong enough gravitational waves is not. Since the characteristic period of the waves is proportional to the light-travel time around the collapsed object, the dominant frequency scales as $1/M$. For sufficiently large M, this source will produce low-frequency waves detectable from space. (See the article on gravitational collapse by Stark in this volume.)

2) COALESCING BINARIES

This is one of the most promising sources of waves detectable from the ground, once broadband laser detectors reach their expected sensitivity. The famous 'Binary Pulsar' PSR 1913+16 is a precursor of such a system: in some 10^8 years it will have evolved through gravitational radiation reaction into an almost perfectly circular orbit with a period of 20 msec and a separation between the stars of about 150 km. At this point it will be a strong source of gravitational waves at 100 Hz, within the expected observing window of laser-interferometric detectors. During the next 2 seconds the stars will spiral together and coalesce; before they coalesce, they will have emitted some 500 or so cycles of radiation at ever-increasing frequency. Because the signature of this radiation, or 'chirp,' is unique and predictable, it is possible to filter weak signals out of the noise of an interferometer. Consequently, coalescing binaries can be seen some 25 times further away than moderately strong gravitational collapses (supernovae). The expected event rate is very uncertain. Again, the frequency of the waves is inversely proportional to the mass of the system, so binaries consisting of massive black holes could be detected from space. So, too, might the precursor systems when the stars are still well separated, as in the present Binary Pulsar. I will return to this source in Section II.b.1 below.

3) PULSARS

Pulsars emit gravitational waves if they are non-axisymmetric. The frequency of the waves will be twice the rotation frequency of the star. We have little idea of what strength to expect from known pulsars, but it is unlikely that any slowly rotating, former pulsar would be a strong source of gravitational waves at low frequencies.

4) ACCRETING NEUTRON STARS

Neutron stars in X-ray binaries can be spun up by accretion, possibly until they reach a rotation rate at which they encounter a non-axisymmetric rotational instability. As Wagoner (1984) has pointed out, further accretion will drive the instability until it has sufficient amplitude so that the gravitational waves that are radiated carry away as much angular momentum as that which is being accreted. The system then becomes a steady source of gravitational waves. Several galactic X-ray sources are candidate sources. We do not know enough about the behavior of matter at neutron star densities to predict what the frequency of this radiation should be. If X-ray observations — such as those proposed for the XLA satellite (see the talk by Wood at this meeting in Michelson and Wood, this volume) — detect low-amplitude variability in X-ray sources, ground-based detectors could search for the associated waves. Successful observations would be enormously important for neutron star (and hence for nuclear) physics. It is most unlikely that any of this radiation will be at frequencies below 10 Hz.

5) STOCHASTIC BACKGROUND

There are many postulated sources of a measureable stochastic background at kiloHertz frequencies, all of them cosmological. Perhaps the most interesting are cosmic strings, which might have acted as seeds for galaxy formation. If they did, there is a firm prediction that the gravitational wave background they would have produced should have an energy density of 10^{-7} of the closure density (Vachaspati and Vilenkin 1985). There is no preferred frequency for this background, so the waves' spectrum should be scale–invariant. Detection of this background would provide strong evidence, not only for the string model of galaxy formation, but also for the particle–physics theories that lead to strings. See the talk by Matzner at this meeting for more details on backgrounds.

b) Coalescing Binaries in More Detail

The interest in coalescing binaries of neutron stars or black holes is easier to understand if we write down the formulas for the amplitude h of the gravitational waves and the timescale τ for the coalescence of the system, in terms of the total mass M_T of the system, its reduced mass μ, the frequency f of the radiation, and the distance r to the system:

maximum h (when the system is viewed down the axis)

$$h_{max} = 3.6 \times 10^{-23} \left(\frac{M_T}{2.8M_\odot}\right)^{2/3} \left(\frac{\mu}{0.7M_\odot}\right) \left(\frac{f}{100\text{Hz}}\right)^{2/3} \left(\frac{100\text{Mpc}}{r}\right) ,$$

and

coalescence timescale

$$\tau := \frac{f}{\dot{f}} = 5.6 \left(\frac{M_T}{2.8M_\odot}\right)^{-2/3} \left(\frac{\mu}{0.7M_\odot}\right)^{-1} \left(\frac{f}{100\text{Hz}}\right)^{-8/3} \text{sec.}$$

When viewed in other directions, the binary produces a wave amplitude that is h_{max} times angular factors. A network of four broadband detectors can determine these angular factors and thereby measure h_{max}.

Notice that the product $h_{max}\tau$ depends only on r: *coalescing binaries are standard candles!* It is extremely difficult in astronomy to find observable systems that can provide reliable distance measures. Coalescing binaries are of great interest for this reason. See the talk by Wahlquist at this meeting for further discussion of these binaries in the context of space-based observations.

For low-frequency observing, there are two frequencies which are useful to remember. If one expects to observe a system consisting of two 1.4 $M_\odot$ neutron stars for an observation period of 10^7 sec, then the first important number is that a binary with an initial frequency of 0.5 Hz will just reach coalescence at the end of the observing period. This is, in some sense, the optimum frequency at which to search for coalescing systems, since they are easiest to observe when they change the most in the observation period. If they are picked up at a lower frequency, they change less dramatically in 10^7 sec. Unfortunately, frequencies of 0.1 to

1 Hz are the worst from the point of view of detector noise! The second number to keep in mind is that if a system with the assumed masses has f $<7 \times 10^{-3}$ Hz, then it will not change its frequency by a measureable amount during a 10^7 sec observation. This frequency is roughly the dividing line between standard binaries and coalescing binaries from an observational point of view.

II. SOURCES OF LOW-FREQUENCY GRAVITATIONAL WAVES

There is a natural division of likely sources into two categories: cosmological sources, which are strong and distant; and galactic sources, which are local but weak.

a) Cosmological Sources

1) FORMATION OF A GIANT BLACK HOLE

Many astrophysicists believe that the most plausible explanation for quasars and active galactic nuclei is that they contain massive (10^6–$10^9\,M_\odot$) black holes that accrete gas and stars to fuel their activity. There is growing evidence that even so-called 'normal' galaxies like our own and Andromeda (M31) contain black holes of modest size (10^4–$10^6 M_\odot$) in their nuclei (Blandford 1987). It is not clear how such holes form, but if they form by the rapid collapse of a cluster of stars or of a single supermassive star, then, with a modest degree of non-symmetry in the collapse, they could produce amplitudes $h \sim 10^{-16}$ to 10^{-18} in the low frequency range observable from space. If a detector had a spectral noise density of $10^{-20} \mathrm{Hz}^{-1/2}$ (see the talk by Bender at this meeting; this might be a conservative figure), then such events could have signal-to-noise ratios (S/N) of as much as 1,000. This strong a signal would permit a detailed study of the event. If every galaxy has one such black hole formed in this way, then there could be one event per year in a detector. If no such events are seen, then either giant black holes do not exist or they form much more gradually or with good spherical symmetry.

2) STAR FALLING INTO A GIANT BLACK HOLE

If black holes power active galactic nuclei, they do so by swallowing stars and gas. Occasionally, neutron stars should fall into them. Neutron stars are compact enough not to be disrupted by tidal forces before reaching the horizon, so they will give a coherent gravitational wave burst with a frequency similar to that which the black hole gave off when if formed. Fairly reliable numerical calculations of this radiation exist (see Thorne 1987 for references), and they suggest that an event in the Virgo Cluster of galaxies would give an amplitude $h \sim 10^{-21}$ and $S/N \sim 10$. The event rate, however, is very uncertain: although the Virgo Cluster contains over 1,000 galaxies, their central black holes are quiescent and may by now have already consumed all the stars that are in orbits that take them near to the hole.

3) COALESCENCE OF GIANT BLACK HOLES

If two black holes of mass $10^6\,M_\odot$ or more, collide and coalesce, they will emit radiation which is at least as strong as we have suggested above for the formation of such holes. The waveform would have a characteristic signature from which one could identify the event with some confidence. Such collisions could result from the merger of two galaxies that both contain black holes. Merged galaxies are not uncommon, especially in the centers of clusters; after the merger, dynamical

friction could bring both holes to the center, where they would coalesce. Alternatively, it might be that giant black holes in the centers of galaxies themselves form, not by a single collapse, but by a sort of hierarachical merger of smaller black holes. Again, the event rate is very uncertain, but the events would be strong, S/N~1,000.

4) STOCHASTIC BACKGROUND OF COSMOLOGICAL ORIGIN

Gravitational waves having frequencies below 10^{-2} Hz today may be redshifted relics of waves emitted in much earlier phases of the Big Bang. See Matzner's talk at this meeting for a full discussion of the different mechanisms which might produce such waves. Among the most interesting, observationally, are inhomogeneities associated with inflation, which might produce a scale-invariant spectrum with a spectral density $\sim 10^{-21}$ $Hz^{-1/2}$ at 10^{-4} Hz; and early anisotropies, which might produce a 'line' of radiation at about 10^{-5} Hz, with spectral density 10^{-20} $Hz^{-1/2}$. If these backgrounds could be detected and identified by their spectrum, they would provide the most direct evidence that the early universe was dominated by the sort of particle physics effects that are fashionable but speculative in modern cosmological theory: inflation, spontaneous symmetry breaking, cosmic strings, and so on. The implications for cosmology and physics as a whole would be fully as significant as the discovery of the cosmic microwave background was 25 years ago. Clearly, this is one of the most important gravitational wave experiments possible from space. But it may not be easy, since as we will see below there are other backgrounds due to binary stars that could obscure any cosmological background.

b) Galactic Sources

1) COALESCING BINARY PRECURSORS

If observing from space is confined to frequencies below 0.1 Hz, then our earlier discussion of coalescing binaries in Section I.b makes it clear that no solar-mass systems will be discovered that can be followed all the way to coalescence. However, it should be possible to see some precursors as ordinary binaries (*i.e.*, below 7×10^{-3} Hz). The Binary Pulsar system itself will be just detectable at about 10^{-4} Hz if the spectral noise density of the detector is 10^{-20} $Hz^{-1/2}$. Because pulsar radiation is beamed, it is likely that there are similar systems even closer to us that we do not observe because their beams are pointed in the wrong direction. If the nearest is 2 kpc away, then it might give S/N~10 if it is favorably oriented with respect to the detector. A precursor with a frequency of 10^{-2} Hz could be seen as far away as the Andromeda galaxy (M31) with S/N~10. Since the number of precursor systems is very uncertain (see Schutz 1988), there is a good possibility that such a system, with a lifetime of only 10^4 years, would be seen.

2) CLOSE WHITE-DWARF BINARIES

Systems like this are associated with cataclysmic variables, Type I supernovae, and especially with models of the formation of isolated millisecond pulsars by the coalescence and subsequent collapse of the two white dwarfs. They are more numerous than neutron-star binaries, so the nearest may be considerably closer, with a S/N~100 or more in a 10^{-20} $Hz^{-1/2}$ detector.

3) INDIVIDUAL BINARIES

A number of nearby binary systems are known which produce radiation that is strong enough to be observed by space-based detectors. See Thorne (1987) and references therein for a list. This is one of the few certain sources of gravitational waves at these frequencies.

4) BACKGROUND NOISE FROM BINARIES

Another certain source is the vast number of ordinary binary systems, whose radiation reaches us from random directions and at random frequency. A single space-based detector will have little directional resolution, so below about 10^3 Hz it will be receiving waves from so many systems that they will be more closely spaced in frequency than the frequency resolution one can obtain in a 10^7sec observing run. (See Thorne 1987 or the talk by Bender at this meeting for details of the expected spectrum.) This background is of interest in its own right, since detecting it would give a measure of the distribution of periods in the binary population of the Galaxy. But it can also be a nuisance, obscuring other interesting sources. There are at least two possible ways to beat this noise. One is to obtain directional information about the gravitational waves, for example by flying two detectors. In any given solid angle, the confusion caused by the background will be reduced by the ratio of the solid angle to 4π. The second method is to make use of the fact that the 'noise' produced by these binaries is not true white noise: at any single frequency the amplitude is constant and the phase remains coherent over the observing period, since it is just the signal of a single binary system. This property may make it easier to filter for signals that do not have constant frequency, such as black hole bursts or waves from relatively massive coalescing binaries, since the 'noise' is not really stochastic.

III. CONCLUSION

There are a great variety of possible sources of gravitational waves at milliHertz frequencies. Some are rather speculative and some are essentially certain, considerably more certain in fact than any of the postulated sources detectable by ground-based detectors. Observations of, or even good upper limits on, some of these sources would contribute valuable information to astrophysical modelling of different types of binary star systems, neutron stars, quasars, active galaxies, and the early universe. In particular, the discovery of a gravitational wave background of cosmological origin would be of the greatest significance to astronomy and physics. Despite the great difficulties involved in building sensitive space-based detectors, the possible scientific returns make a strong case for going ahead with them.

ACKNOWLEDGEMENTS

It is a pleasure to acknowledge useful conversations with John Armstrong, Peter Bender, Ron Hellings, and Kip Thorne.

REFERENCES

Blandford, R. 1987, *300 Years of Gravitation* ed. S. W. Hawking and W. Israel (Cambridge University Press, Cambridge, U.K.), p. 277.

Shultz, B.F. 1988, *Gravitational Wave Data Analysis* (Reidel, Dordrecht).

Thorne, K. S. 1987, *300 Years of Gravitation* ed. S. W. Hawking and W. Israel (Cambridge University Press, Cambridge, U.K.), p. 330.

Vachaspati, T., and Vilenkin, A. *Phys. Rev. D*, **31**, 3052.

Wagoner, R. V. 1984, *Astrophys. J.*, **278**, 345.

DISCUSSION

HELLINGS: Peter Bender told us to expect one galactic collapse event every 1000 years. You told us we might expect one per year. Did you assume some preferred epoch of collapse to form galaxies?

SCHUTZ: No. The difference is that Peter Bender said that if all active galaxies had giant black holes, we would get 1 even per 1000 years, while I said that if all galaxies have such black holes, then it will be 1 event per year. Peter's estimate is conservative, while mine is optimistic.

HELLINGS: When you told us the spectrum to be expected from cosmic strings was scale invariant, does that mean a flat amplitude spectrum, a flat energy spectrum, or just a broad-band spectrum that you could move anywhere you chose?

SCHUTZ: It is flat in energy per decade of frequency, so that fh(f) is constant over the whole of the frequency region we are talking about, with a possible low-frequency cutoff. This will be discussed in more detail by Richard Matzner in his talk later today.

DETECTING GRAVITY WAVES FROM BINARY BLACK HOLES

HUGO D. WAHLQUIST
Jet Propulsion Laboratory
California Institute of Technology
Pasadena, California 91109

One of the most attractive possible sources of strong gravitational waves would be a binary system comprising massive black holes (BH). The gravitational radiation from a binary is an elliptically polarized, periodic wave which could be observed continuously - or at intervals whenever a detector was available. This continuity of the signal is certainly appealing compared to waiting for individual pulses from infrequent random events. It also has the advantage over pulses that continued observation can increase the signal-to-noise ratio almost indefinitely. Futhermore, this system is dynamically simple; the theory of the generation of the radiation is unambiguous; all characteristics of the signal can be precisley related to the dynamical parameters of the source.

The difficulty is that there is no clear observational evidence for their existence. The best evidence for the existence of <u>any</u> black holes comes from 3 or 4 binary systems which contain a normal star and a compact object whose mass apparently exceeds the limiting masses of white dwarfs and neutron stars. It is, of course, possible that some binaries do exist in which both stellar components have evolved into compact objects or black holes.

The lowest shaded band in Figure 1, labeled CLOSE - NORMAL, includes these possible BH binaries of normal stellar mass.

Astrophysical theory appears to require supermassive black holes to power active galactic nuclei (AGN) and quasars. The most detailed models invoke a single supermassive (10^8 - 10^9 $M_\odot$), spinning BH to explain the dynamics and configuration of the active nuclei. Evidence is accumulating that even normal galaxies may have a black hole in their nuclei; cusps in the central light emission, and rotational velocity profiles and velocity dispersions which rise within the central ~100 pc. could be explained by black holes of 10^6 - 10^7 $M_\odot$. There is some evidence that our own galaxy may contain a supermassive object, but conflicting interpretations lead to estimated masses from as low as 100 $M_\odot$ to as high as 3 x 10^6 $M_\odot$.

It has also been proposed that massive binary BH may occur quite frequently in galactic nuclei as a consequence of merging of galaxies. It has been estimated that roughly 1 in 300 galaxies could contain massive binaries and might show periodic electromagnetic emission. So far, however, periodicity has not been found observationally.

The top shaded band in Figure 1, labeled AGN, is intended to cover these possible supermassive binaries in galactic nuclei.

Another speculation on the existance of massive BH is related to the missing mass problem in galaxies. Dynamical observations of stars imply that there must be as much dark matter present in galactic disks and haloes as can be seen. It has been proposed that primordial, or pre-galatic, BH may have formed at the same time as the

globular clusters and with approximately the same range of masses (~10^6 $M_\odot$) and spatial distribution. If enough of them formed to explain the mass deficit,they could be expected to have effects on stellar dynamics similar to those observed. It is not unreasonable to assume that some of them would have formed binary systems.

The center shaded band in Figure 1, labeled HALO, includes possible BH binaries of about globular cluster mass.

In summary, the current situation is that while there is no observational evidence as yet for the existence of massive binary BH, their formation is theoretically plausible, and within certain coupled constraints of mass and location, their existence cannot be observationally excluded. Detecting gravitational waves from these objects might be the first observational proof of their existence.

Figure 1 shows the range of possible binary BH with masses between $2M_\odot$ and 2 x 10^9 $M_\odot$ and with seperations from 1 lt.-sec. to 10^8 lt.-sec. (~1pc.). The shaded bands indicate those mass ranges which have been suggested as theoretically plausible, but are not meant to imply that other mass values are impossible. The diagram can be used to distinguish the regions of likely detection.

The two dashed lines (L=30 yrs and L=10^{10} yrs) give the remaining lifetime of binaries located along those lines, based on energy loss to gravitational radiation only. Detecting a binary to the left of the L=30 yrs line, i.e., during the last 30 yrs of its lifetime, would be extraordinarily fortunate. Only the portion of the diagram to the right of this line presents reasonable probabilities of detection.

The three dotted lines (P=1000 sec, P=12 days, P=30 yrs) give the period of the binaries located along these lines, assuming a circular orbit. Periods longer than 30 yrs would require very long observation times, more than 300 yrs to detect just 10 periods of the signal. From practical considerations alone, it is not unreasonable to exclude the portions of the diagram to the right of this line.

A different problem arises in the bottom shaded band of stellar mass binaries. Any signal from a BH binary in this region is likely to be overwhelmed in the confusion of comparable signals from the multitude of ordinary, and other compact, binary systems.

These considerations serve to delimit a quadrilateral of detectability in the middle of the figure which includes the central parts of the AGN and HALO bands.

The set of eight solid lines in Figure 1 gives the amplitude of the gravitational waves from equal mass binaries located along these lines at two particularly relevant distances: first, 10^4 pc (typical distance in our galaxy), and second, 10 Mpc (distance to the Virgo cluster). It is worth noting that a gravitational wave sensitivity of H = 10^{-17} is sufficient to explore most of the detectable HALO band within our galaxy, and all of the detectable AGN band out to the Virgo cluster. However, this exploration requires detectors capable of responding to very long period waves - from hours to years.

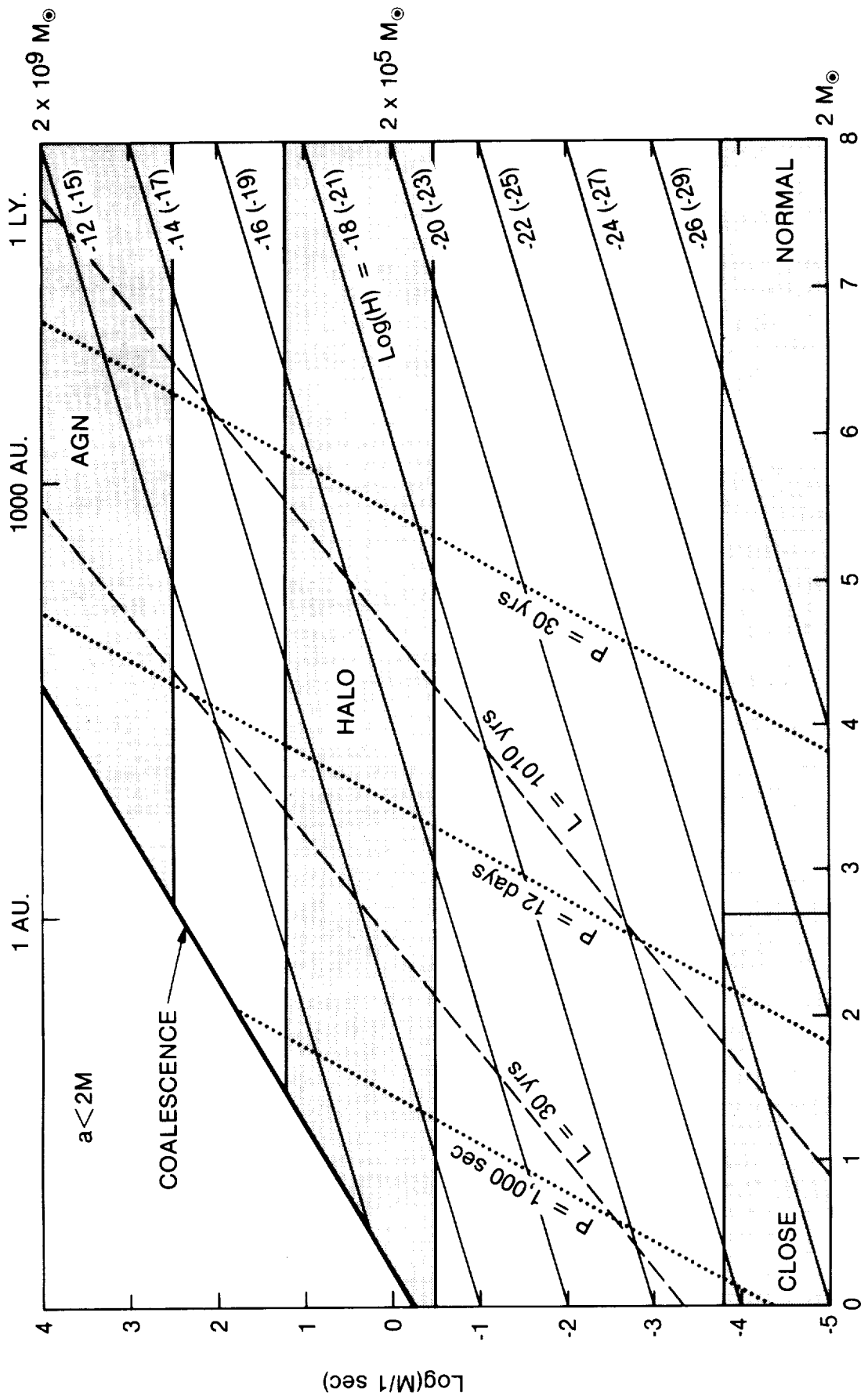

Figure 1. Possible black hole binary systems ranging in mass (M) and separation (a).

DISCUSSION

SONNABEND: It seems to me that binary B.H. of $\sim 10^5 M_\odot$ each would be rare compared to binaries with $\sim 10^5 M_\odot$ to $\sim 1\ M_\odot$, thus populating the region below the galactic halo band in your slide.

WAHLQUIST: I don't want to discourage looking for such objects, but there are plausible scenarios in which binaries of globular cluster mass form.

TAYLOR: Don't be too quick to rule out as inaccessible the region of your overlaid diagram around P $\sim 10^8$ sec. For the larger black hole masses, at least, this region is probed by millisecond pulsar timing observations.

WAHLQUIST: I concur - and will expand the detectable region in the published paper.

HELLINGS: For halo objects ($\sim 10^5\ M_\odot$), it is reasonable to look for sources in our galaxy, but for nuclear objects ($\sim 10^7$ - $10^9\ M_\odot$), since we only have one galaxy, it is probably statistically preferable to look for sources outside our galaxy.

WAHLQUIST: Yes. These supermassive binaries can be detected even out to Virgo with moderate sensitivity.

GRAVITATIONAL RADIATION FROM ROTATING GRAVITATIONAL COLLAPSE

RICHARD F. STARK
Institute for Theoretical Physics
University of California, Santa Barbara, CA 93106, U.S.A.

ABSTRACT

We find the efficiency of gravitational wave emission from axisymmetric rotating collapse to a black hole to be very low: $\Delta E / Mc^2 < 7 \times 10^{-4}$. The main waveform shape is well defined and nearly independent of the details of the collapse. Such a signature will allow pattern recognition techniques to be used when searching experimental data. These results (which can be scaled in mass) have been obtained using a fully general relativistic computer code that evolves rotating axisymmetric configurations and directly computes their gravitational radiation emission.

The results summarized here have come from a tested, fully general relativistic computer code able to evolve axisymmetric rotating matter configurations. This code numerically solves the complete coupled Einstein and hydrodynamic equations for axisymmetric systems. A more detailed description of the results, the code (and its testing), and the formalism used can be found in Stark and Piran (1985, 1986, and 1987). (A possible extension to non-axisymmetric collapse is given in Stark 1988.)

The axisymmetric rotating gravitational collapse we have studied is that of an initially pressure-deficient, 'rigidly rotating' polytrope with an adiabatic equation of state (Stark and Piran (1985, 1986, and 1987). We first set up a TOV spherically symmetric non-rotating polytrope. For the cases studied here, we have used an initial stellar radius of a $6GM/c^2$ and a fixed adiabatic index $\Gamma = 2$. We then reduce the pressure and thermal energy to a fraction f_p of their equilibrium values (with $f_p =$ 0.01 or 0.4) and simultaneously add a 'rigid body' azimuthal rotation to the star. The rotation is measured by the dimensionless angular momentum parameter $a = J / \frac{GM^2}{c}$ where J is the total angular momentum of the star. The collapse and resulting gravitational wave emission are studied for a range of angular momenta $0 \leq a < 1.5$. With our chosen equation of state, all quantities scale in an elementary fashion with M the mass of the star. Our initial conditions correspond to an initial radius of $8.8 \times 10^5 M/\mathrm{M}_\odot \mathrm{cm}$ and a central density of $1.9 \times 10^{15}(M/\mathrm{M}_\odot)^{-2}\, g cm^{-3}$ (corresponding to a somewhat unrealistic, compact, relativistic stellar core for stellar masses). (For space-based experiments one can simply scale to higher M, thus approximating supermassive or population III collapse.)

(For illustrations see the figures in Stark and Piran 1986). For $a = 0.40$ (and $f_p = 0.4$), the collapse takes place almost spherically symmetrically with the meridional velocity vector remaining closely radial, little flattening of the star, and without any shocks forming. The central density increases by a factor of ~15 and after a time of $\sim 35M$ the star 'freezes' as the lapse (which relates proper and coordinate times) drops exponentially due to black hole formation. For the collapse of a more rapidly rotating star with $a = 0.75$ (and $f_p = 0.4$), the rotational effects

become noticeable with the star soon becoming highly flattened into the equatorial plane. After a time of ~$30M$, the star bounces vertically away from the equator, but still continues to collapse radially inwards until freezing as a black hole forms, and the lapse collapses. For $a > a_{crit}$ (with $a_{crit} = 0.85 \pm 0.05$ for $f_p = 0.4$), the effects of rotation become dominant, no black hole forms, and the star ends up oscillating about a flattened rotating equilibrium configuration (see Stark and Piran 1986). (The general behavior for $f_p = 0.01$ is similar to that described, except that the star becomes rather more flattened and (for $a < a_{crit}$) collapses slightly faster).

Fig. 1 shows results obtained for the even and odd transverse traceless waveforms $h_+, h_\times$ (as defined in Stark and Piran 1987) from the collapse to black holes of stars with various $a < a_{crit}$ (and for $f_p = 0.01$). The waveforms shown have been monitored at the outer edge of the grid ($r \sim 50M$). The even and odd modes have the expected $\sin^2\theta$ and $\cos\theta\sin^2\theta$ angular dependences respectively, and these as well as the r^{-1} radial fall-off have been factored out. The waveform is well established by fairly small radii ($r \sim 25M$). The waveform consists of a broad peak at a retarded time ~0 due to the initial flattening of the star from its initial spherical configuration. (This part contributes negligibly to the total energy of the gravitational wave emission.) The main emission appears at a retarded time of ~$25M$, corresponding to when the collapsing star is only ~$3M$ in size. The main emission lasts for ~$10M$ and is followed by a decaying oscillatory tail. The most noticeable feature of these waveforms is the insensitivity of the waveform shape to the value of a. Over the range $0 < a < a_{crit}$ for black hole collapse, the shape remains closely unchanged, the waveform differing for each collapse only in its amplitude. (This is the case for $f_p = 0.4$ also.)

The maximum h_+ amplitude, $|h_+|_{max}$, from the collapse to a black hole, both for $f_p = 0.01$ and 0.4, scales very closely as a^2 and finally levels off to a maximum value as $a \to a_{crit}$. Our results are closely approximated by:

$$(r/M)|h_+|_{max} = \min\{0.1a^2, A_{max}\} \qquad (0 < a < a_{crit})$$

with $A_{max} = 0.06$, $a_{crit} = 1.2 \pm 0.2$ for $f_p = 0.01$; and $A_{max} = 0.025$, $a_{crit} = 0.8 \pm 0.05$ for $f_p = 0.4$. (As would be expected for axisymmetric collapse $|h_\times| < 0.2|h_+|$.)

The dependence of the total gravitational wave energy emitted, ΔE, on the angular momentum of the collapse (to a black hole) is shown in Fig. 2 for both $f_p = 0.01$ and 0.4. The most noticeable feature is the very low efficiency $\frac{\Delta E}{Mc^2}$. In all cases the efficiency is $< 7 \times 10^{-4}$. The emitted energy ΔE scales as a^4 (as shown by the solid line fit in Fig. 2) with a coefficient of 1.4×10^{-3} independent of f_p, and ΔE levels off to a maximum value ϵ_{max} (which depends on f_p, as shown by the dotted lines) as $a \to a_{crit}$. Our results closely follow the form:

$$\Delta E/Mc^2 = \min\{1.4 \times 10^{-3}a^4, \epsilon_{max}\} \qquad (0 < a < a_{crit})$$

with $\epsilon_{max} = 6 \times 10^{-4}$ for $f_p = 0.01$; and $\epsilon_{max} = 1 \times 10^{-4}$ for $f_p = 0.4$. In all cases $(\Delta E/Mc^2)_+ > 10(\Delta E/Mc^2)_\times$.

Corresponding to the insensitivity of the waveform shape, the shape of the energy spectra, from these collapses to a black hole is similarly insensitive. The spectra have the form of a simple peaked curve, although for values of a near a_{crit}, a low frequency component due to the initial flattening of the star appears (see Stark and Piran 1986 for detailed figures). The energy spectra peak at frequencies of $0.035 < \nu < 0.08 \left(\frac{GM}{c^3}\right)^{-1}$ Hz (*i.e.*, $7 < \nu < 16\ (M/M_\odot)^{-1}$ kHz) corresponds to wavelengths of between 12 and 28 $\left(\frac{GM}{c^2}\right)$. The peak spectral energy $F(\nu_{max})$ scales as a^4, and levels off to a maximum value as $a \to a_{crit}$. Our numerical results closely follow the relations:

$$F(\nu_{max})\ \text{erg cm}^{-2}\ \text{Hz}^{-1} = \min\{60a^4, F_{max}\}(M/M_\odot)^2\ (r/10\text{kpc})^{-2}$$

with $F_{max} = 22$ for $f_p = 0.01$; and $F_{max} = 4$ for $f_p = 0.4$.

Our waveforms are very similar in shape to those of several previous perturbation studies (see Stark and Piran 1986 for details). This broad agreement in waveform shapes suggests the importance of black hole quasi-normal mode excitation in the gravitational wave emission process. The collapsing star produces most gravitational wave emission when it is ~$3M$ in size, by which time the exterior metric is already quite similar to that of a black hole. The star thus acts as a source to excite the black hole quasi-normal modes. (The star being smaller than the peak of the black hole potential determining the normal modes.) The waveform shape reflects the properties of the black hole formed, whereas the amplitude to which the modes are excited depend on the details of the collapse. The observed insensitivity of the shape of the waveform to the rotation parameter a, corresponds to the weak dependence on a of the $m = 0$ axisymmetric modes of the Kerr black hole (Detweiler 1980). This picture is confirmed by the very good fit we obtain to the waveform from a linear combination of the two lowest modes (see Stark and Piran 1986).

We may summarize our results as follows. The most optimistic case (*i.e.*, the one producing the largest gravitational radiation) is for $a \sim a_{crit}$ and a small initial pressure ($f_p = 0.01$). For this case, we expect the maximum observable strain $|\Delta l/l|_{max}$ to be:

$$|\Delta l/l|_{max} = \begin{cases} |h_+|_{max} = 4.0 \times 10^{-19}\ (M/1.4M_\odot)\ (r/10\text{kpc})^{-1} \\ \sqrt{G/c^3\ F(\nu_{max})} = 3.6 \times 10^{-19}\ (M/1.4M_\odot)\ (r/10\text{kpc})^{-1} \end{cases}$$

where the two measures of the strain correspond to nonresonant (interferometer) and resonant (bar) experiments respectively. The maximum spectral energy, peak frequency, and full-width, half-maximum frequency are:

$$F(\nu_{max}) = 45\ (M/1.4M_\odot)^2 (r/10\text{kpc})^{-2} \text{erg cm}^{-2}\ \text{Hz}^{-1}$$

$$\nu_{max} = 10(M/1.4M_\odot)^{-1}\ \text{kHz};\ \Delta\nu_{1/2} = 4\ (M/1.4M_\odot)^{-1}\ \text{kHz}$$

For low a collapses ($a < 0.8$), the expected maximum strain and maximum spectral energy are:

$$| \Delta l/l |_{max} = 6.7 \times 10^{-19}\, a^2 (M/1.4M_\odot)(r/10\mathrm{kpc})^{-1} \qquad \text{(both cases)}$$

$$F(\nu_{max}) = 120\, a^4 (M/1.4M_\odot)^2 (r/10\mathrm{kpc})^{-2} erg\ cm^{-2}\mathrm{Hz}^{-1}$$

with ν_{max} and $\Delta\nu_{1/2}$ as above.

An important feature of the main black hole emission is that the general waveform *shape* is well defined and nearly independent of the details of the collapse. This provides a signature for the black hole collapse and will allow pattern recognition techniques to be applied to broadband experimental gravitational wave data, thus allowing greater sensitivities to be reached for these events. Further experimental implications for ground-based bar detectors of stellar collapse can be found in Stark and Piran 1986.

ACKNOWLEDGEMENTS

The work reported here was done in collaboration with Tsvi Piran.

REFERENCES

Detweiler, S. 1980, *Astrophys. J*, **239**, 292.

Stark, R.F., and Piran, T. 1985, *Phys. Rev. Lett.*, **55**, 891.

Stark, R.F., and Piran, T. 1986, In Proceedings of the fourth Marcel Grossmann Meeting on General Relativity, Ed. R. Ruffini, North Holland, Amsterdam.

Stark, R.F., and Piran, T. 1987, *Computer Physics Reports*, **5**, 221.

Stark, R.F. 1988, in Frontiers in Numerical relativity, Eds. C. R. Evans, L. S. Finn and D.W. Hobill, CUP.

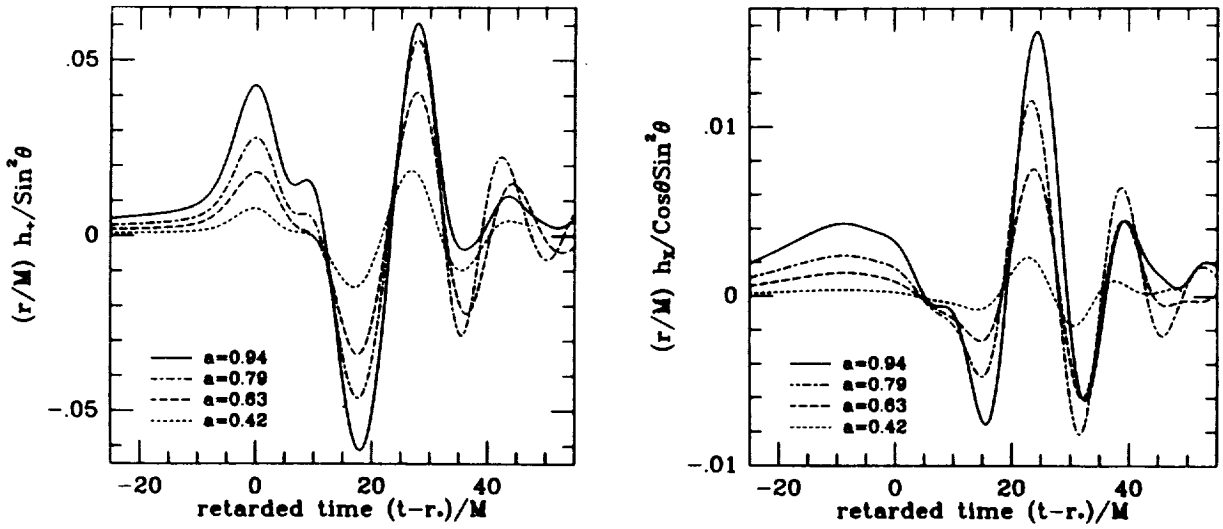

FIG. 1 — $h+$ (left) and $h\times$ (right) waveforms vs. retarded time for various a (f_p = 0.01) black hole collapses.

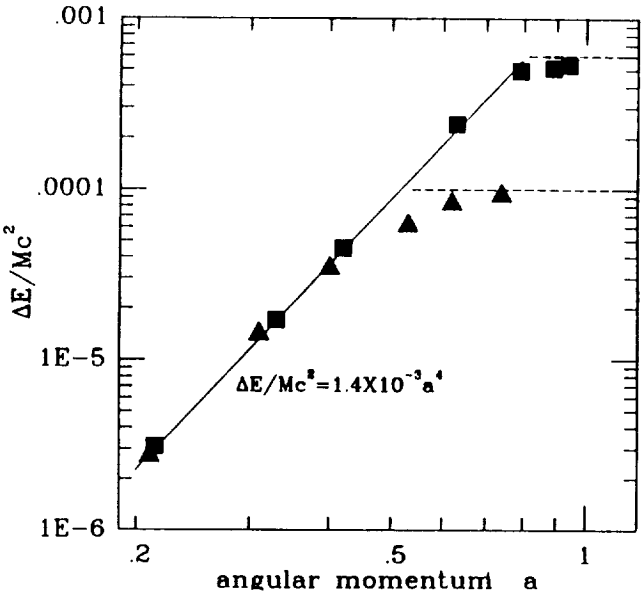

FIG. 2 — Total Gravitational wave energy (ADM) emitted vs. a for f_p = 0.01 (squares) and f_p = 0.4 (triangles) black hole collapses. Solid line fits the a^4 scaling; dashed lines mark ϵ_{max}.

DISCUSSION

ARMSTRONG: How would you expect the shape of gravitational temporal waveforms to change for non-axisymmetric collapse? Gravity wave efficiencies?

STARK: The waveforms from rotating non-axisymmetric black hole collapse can be expected to consist of a quasi-periodic phase (due to the rotation of the bar) followed by emission from the actual black hole formation and a decaying tail. Th.e main black hole emission can be expected to show similar normal mode characteristics as we have seen in the axisymmetric collapse. Thus we may expect this part of the emission to have a shape similar to that for the axisymmetric collapse, except possible at high rotations where the non-axisymmetric normal mode frequencies become appreciably split. As far as the efficiency is concerned, perturbation studies indicate that it may be at least an order of magnitude larger than for axisymmetric collapse (for an appreciable level of non-axisymmetry). We will not know for sure until numerical simulations are made. (See e.g., Stark, 1988 for work in progress).

HELLINGS: Is it true that changing "a" changes the amplitude without changing the period while changing "m" changes both in a proportional way?

STARK: The waveform amplitude from collapse to a black hole scales as a^4 for low a (where $a = J/GM^2/c$; J the total angular momentum; M the mass of the star) and then levels off before a reaches a_{crit} (the rotation above which black hole formation no longer occurs). The amplitude also scales proportionally with M. The waveform period (or more precisely, the scale of retarded time for the waveform) of the main emission from black hole formation is insensitive to a (due to the insensitivity of the axisymmetric Kerr black hole normal modes frequencies to a). The period scales proportionally with M.

SHAPIRO: Given the complexity of the system you're modelling, and the (necessarily) complicated code needed to solve the coupled equations used to represent the system's evolution, what checks have been made to try to insure that the results are correct?

STARK: It is clearly very important that a code of this kind be tested as fully as possible. We have performed an extensive series of tests which can be broadly classified into general stability tests, conservation tests, hydrodynamic tests and comparison tests against known approximate perturbation solutions. (The derivation of the equations we solve has also been checked using symbolic computer algebra). A detailed description of these tests can be found in Stark & Piran, 1987. The tests performed include: (i) Evolution of the vacuum Schwarzschild exterior ($r > 2M$) for many gravitational times; (ii) Propagation of gravitational waves (for both polarizations) along inward and outward characteristics with negligible reflection at the outer boundary; evolution to flat spacetime for low amplitude waves, and black hole formation for high initial wave amplitudes; (iii) Stable evolution of initial data consisting of flat spacetime + a small amplitude 'random data' superimposed; (iv) Evolution of stable extreme relativistic polytropes for many free fall timescales; including checking the excitation of the lowest radial mode oscillations for adiabatic indices $G > G_{crit}$, as well as the instability to collapse for $G < G_{crit}$ (with $G_{crit} = 4/3$ + general relativistic corrections); (v) Conservation of the ADM mass and the total angular momentum; (vi) Conservation of the specific angular momentum spectrum; (vii) Propagation of generalized linearized Teukolsky waves for both polarization modes; (viii) Comparison of the gravitational wave emission from the infall of a

spheroidal dust shell onto a Schwarzschild black hole with known perturbation results; and (ix) Comparison of the gravitational wave emission and hydrodynamics for uniformly rotating homogeneous spheroidal collapse with known Newtonian + quadrupole formalism results. It is also worth remarking that the waveform obtained from the full scale calculation of the axisymmetric collapse to a black hole shows a remarkable agreement with the waveform from an approximate perturbation study (Nakamura, Oohara & Kojima, Prog. Theor. Phys. Suppl., No. 90, 1987) of a rotating dust ring falling in from infinity onto a Schwarzschild black hole with a specific angular momentum comparable to that of the collapsing star. The collapsing dust ring mimics the flattening in the equatorial plane of the collapsing star. One finds very near agreement in the waveform shapes, and, on scaling up the perturbation result (beyond its actual range of validity) the amplitudes as well. (Both efficiencies then also agree at a few x 10^{-4}).

BENDER: How likely does it seem that some instability such as a bar instability would occur during collapse? What mechanisms might determine the initial axial asymmetry?

STARK: A bar mode instability is very likely for sufficiently high rotation. The amount of non-axisymmetry depends on the exact details of the microphysics and initial data. At present these are not known sufficiently well. Work in progress on non-axisymmetric collapse to a black hole (Stark, 1988) will investigate how the gravitational emission varies for a range of non-axisymmetry, but will not attempt to answer which level of non-axisymmetry is astrophysically appropriate.

SCHUTZ: I will just comment on the question of the generation of non-axisymmetry in collapse. Because it relies on an instability that grows exponentially, only a very small initial perturbation is needed. The instability is the 'bar mode' instability that has been discussed as well in the context of formation of bars and spirals in galaxies. Basically, if angular momentum is conserved in the collapse, it becomes energetically favorable for the system to deform into a tumbling bar. The hard question for numerical calculations to answer, and for which careful attention to the microphysics may be necessary, is how much angular momentum transport there may be as the object collapses.

THE PREGALACTIC COSMIC GRAVITATIONAL WAVE BACKGROUND

RICHARD A. MATZNER
Department of Physics and Center for Relativity
University of Texas at Austin

ABSTRACT

An outline is given estimating the expected gravitational wave background, based on plausible pregalactic sources. Some cosmologically significant limits can be put on incoherent gravitational wave background arising from pregalactic cosmic evolution. The spectral region of cosmically generated and cosmically limited radiation is, at long periods, $P>1$ year, in contrast to more recent cosmological sources, which have $P\sim10^{0}-10^{-3}$.

I. INTRODUCTION

This is a review paper on sources of the pregalactic cosmic gravitational radiation background and on some of the techniques that are available to study this background as well as recently developed improvements. The paper is structured first (§II) to analyze incoherent, very early (primordial) sources, which have frequencies now $\sim10^{10}$Hz, down to $\sim10^{-9}$Hz. Limits on radiation density, in various wavelengths due to knowledge of early cosmic evolution are given in §III. The results of §II–III appear in Fig. 1. Figure 2 repeats Fig. 1 but also shows the expected upper limit on the background from events occurring at low redshift due to discrete sources. In all cases we will express backgrounds in terms of the logarithmic spectral flux: νF_ν where F_ν (ergs/cm^2/sec/Hz) is spectral flux. By an accident of numerics, normal cgs units of this flux correspond to interesting cosmological energy densities. For instance:

$$\nu F_\nu \sim 6\times10^{2}\text{ergs/cm}^2\text{/sec} \tag{I.1}$$

corresponds to an energy density $\sim2\times10^{-29}$gm/cm^3, which is approximately ρ_{closure}, the critical mass density needed to recollapse the universe, assuming a Hubble constant $H_0 \sim$ 100km/sec/Mpc. Most primordial sources and all current detectors have sensitivities comparable (within a few orders of magnitude) to this value (see Figs. 1 and 2). An idea of the difficulty of detection of gravitational radiation is to compare this flux to some everyday electromagnetic radiation fluxes. Noon sunlight $\simeq 10^{6}$ergs/cm^2/sec; full moonlight $\simeq$ 1 erg/cm^2/sec $\simeq 10^{-2}\rho_{\text{closure}}$. Electromagnetic radiation at this level can, of course, be detected with no instrumentation at all.

II. SOURCES

a) Stochastic Background Sources

1) PRIMORDIAL BACKGROUND RADIATION

The most primordial source one can imagine for gravitational radiation is the Big Bang, the formation of the universe itself. By analogy to the cosmic microwave electromagnetic wave scattering (called the decoupling epoch; this probably

occurred at redshift $z \sim 1{,}000$), there should also be a low temperature gravitational radiation microwave background. The gravitational interaction becomes as strong as the electromagnetic only at energies near the Planck energy $\sim 10^{19}$GeV $\sim 10^{31}$K, which, according to classical Big Bang models, occurs at about 10^{-43} sec after the Big Bang. The gravitons would have been in thermal equilibrium then and would have shared their energy with other forms (modes) of energy present then. While the physics of that instant is very uncertain; many models predict only a few (10 to 100) total modes then. In that case, microwave gravitons of ~1K are expected (Matzner, 1969). The energy density associated with 1K microwave gravitational radiation is $\sim 8 \times 10^{-36}$gm/cm^3 $\sim 8 \times 10^{-15}$ergs/cm^3, centered at the associated wavelength of a few centimeters. Both these features put it in a very unfavorable regime for detection by any current technique. This radiation is ~2 orders of magnitude lower in density than the microwave radiation background and thus represents Ω_{gw} (thermal gravitons) $= \rho$ (thermal gravitons)/$\rho_{closure} \approx 10^{-6}$. Ω_γ is similarly defined for the electromagnetic microwave background, $\Omega_\gamma \sim 10^{-4.5}$.

2) GRAVITATIONAL RADIATION ENHANCEMENT IN VERY HIGH ENERGY (GRAND UNIFIED THEORY) PHASE TRANSITION

Here the energy is not as high as that associated with the production of gravitons but is a "mere" $T_{GUT} \sim 10^{14}$ to 10^{17}GeV. The behavior of the universe as it evolves through these temperature ranges (~10^{-42} to 10^{-40} seconds after the Big Bang) acts parametrically to pump up the gravitational wave amplitude of very long wavelengths. This is essentially an "overshoot" phenomenon, as the equation of state changes in a phase transition. If the universe, as predicted in many field theories, undergoes a period of inflation with reheating temperatures in the 10^{17}GeV range, then the enhanced radiation may turn out to be detectable. The wavelengths in question are 0.1 to 1 present horizon sizes, periods of billions of years. Radiation of this wavelength acts like large-scale distortions of the universe and is detectable in distortions of the electro-magnetic microwave background radiation. The present limits (~5×10^{-5}) in quadrupole $(\Delta T/T)_q$ (Wilkinson, 1987) put limits on the parameters of the model, and tighter limits would force the model away from $T_{GUT} \sim 10^{19}$GeV to one with typical transition energy at *smaller* values of T_{GUT} $(\Omega_{gw}/\Omega_\gamma \sim (\Delta T/T)_q^2 \sim \frac{(T_{GUT})^4}{(T_{Pl})^4}$, (Veryaskin, Rubakov, and Sazhin, 1983). In general, for small amplitude, one finds $\rho_{gw} \sim \rho_\gamma (\Delta T/T)^2$ for horizon scale waves (Misner, 1968).

3) GRAVITATIONAL RADIATION ENHANCEMENT IN HIGH ENERGY (QUARK-HADRON) PHASE TRANSITIONS

Korotun (1980), studies the effect on primordial wave spectrum of the parametric amplification that occurs during the possible phase transitions occurring in the early universe due to string interactions. The process is the same as that described in §II.2 just above; during the phase transition the universe deviates from a simple (fractional) power of t expansion function, and this leads to enhancement of gravitational wave creation. However, the net effect on gravitational waves decreases with decreasing energy scale, with

$$\frac{\Omega_{gw}}{\Omega_\gamma} \sim \left(\frac{T^*}{T_{Pl}}\right)^4 \qquad \text{(II.1)}$$

where T^* is the characteristic temperature associated with these processes. The range of these processes is $T \sim 10^{14}$GeV (maximum) for baryon synthesis (which gives $\Omega_{gw}/\Omega_\gamma \sim 10^{-20}$) and lower in temperature for other processes, which give uninterestingly small values of Ω_{gw} (Korotun, 1980).

4) GRAVITATIONAL RADIATION FROM ACOUSTIC NOISE IN STRONGLY FIRST ORDER PHASE TRANSITION

Hogan (1986) estimates the gravitational radiation produced by the random noise from random nucleation in cosmological phase transitions. He finds: $\Omega_{gw}/\Omega_\gamma \sim \delta^2(R_nH)^3v_s^6$ where v_s^2 (~1/3 for most situations) is the square of the sound speed, R_n is the typical nucleation separation, and δ is the fractional supercooling $\delta = \delta T/T$ transition, which we take here to be $\delta \sim 1$. While this spectrum is formally flat, we expect strong damping at high frequency, $\Omega_{gw}/\Omega_\gamma \sim \nu^{-1}$ (or faster) for $\nu \gg R_n^{-1}$. A second effect of phase transitions arises because of the pressure disturbances caused by different equations of state in different locations. For $\nu \sim H$ (then), $\Omega_{gw}/\Omega_\gamma$ is comparable to that found above, but for smaller ν ($\nu < H^{-1}$), the spectrum of the fall-off is $\propto \nu^3$. The nucleation length R_n can be perhaps generously estimated (Kajantie and Kurki-Suonio, 1986; Kurki-Suonio, 1988) as $R_nH \lesssim 10^{-2}$ (then). Thus $\Omega_{gw}/\Omega_{rad} \lesssim 10^{-7.5}$ or $\Omega_{gw} \sim 10^{-12}$ peak.

Hogan makes the important point that astronomically accessible gravitational wave frequencies (~10^2 Hz to ~10^{-9} Hz) correspond to possible phenomena of this type at strong interaction (or higher energies): 10^9 GeV $\leftrightarrow$ 10^2 Hz; 100 GeV (the possible temperature of the electroweak phase transition) $\leftrightarrow$ $10^{-4.5}$ Hz; 100 MeV (the quark-hadron transition) $\leftrightarrow$ 10^{-8} Hz.

5) COSMIC STRINGS

Cosmic strings are possible "topological singularities" that arose in the very high temperature early epochs of the universe. For parameters appropriate to the formation of clusters of galaxies, the associated energy is ~10^{14} GeV; the linear mass density of a string is ~10^{22} gm/cm. These objects, if formed into loops ~1 kpc on a side, have masses that can act to seed structure formation. Vachaspati and Vilenkin (1985; also Hogan and Rees, 1984) have investigated the expected gravitational radiation background in a universe in which strings contributed the seeds for the observed structure. Their analysis takes into account that cosmic string loops can be said to form when the age of the universe, t_u, reaches L/c, where L is the loop size, and we call t_i the formation time of the strings. Before that time, the loops cannot be subject to causal forces and cannot oscillate. After this time, they act as massive oscillating gravitational radiators. Following Hogan and Rees (1984), one estimates that the gravitational energy wave produced by the strings equals the horizon crossing energy fluctuations $(\frac{\delta\rho}{\rho})_{hc}$ produced by the string distribution and is essentially produced at their decay time t_{dec}. The birth time $t_i = L/c$, and the strings radiate at a constant rate $G\mu^2\gamma$, so the time of their decay is $t_{dec} = t_i/(G\mu^2\gamma)$. Because the gravitational and electromagnetic background radiation redshift the same way, one finds

$$\nu \frac{d\rho_{gw}}{d\nu} \simeq \Omega_\gamma \left(\frac{\delta\rho}{\rho}\right)_{hc} \left(\frac{1 + z_i}{1 + z_{dec}}\right) . \qquad \text{(II.2)}$$

The latter factor gives the relative enhancement due to the fact that the radiation background decays away as the strings evolve. This formula holds for strings that decay prior to the present epoch; otherwise the quantity z_{dec} must be replaced by the present: z (now) = 0. Now $(\delta\rho/\rho)_{hc} \simeq 2\pi G\mu$. If z_{dec} lies within the radiation-dominated epoch, then $(1 + z_i)/(1 + z_{dec}) = (t_{dec}/t_i)^{1/2} = (G\mu^2\gamma)^{-1/2}$, and the resulting spectrum is flat:

$$\nu \frac{d\rho_{gw}}{d\nu} \simeq \Omega_\gamma \gamma^{-1/2} (G\mu)^{1/2} \simeq (10^{-8} \text{ to } 10^{-7})\, \Omega_\gamma . \qquad \text{(II.3)}$$

This holds for loops small enough that the decay occurs before the transition to matter-dominated expansion. For larger loops, which produce lower frequencies, two effects enter. The time dependence of the redshift factor changes, $(1 + z) \propto t^{2/3}$, which gives an enhancement for lower frequencies until the decay time reaches the present. Strings whose decay time exceeds the present have not had time to decay completely, and so the spectrum falls off for very long period waves. With the parameters $G\mu \sim 10^{-6}$, $\gamma \sim 10^2$ found in a numerical survey by Vachaspati and Velinkin, the spectrum rises for periods longer than about 10 years, peaking about a factor of 100 higher than its high frequency value (*i.e.*, at $\Omega_{gw} \sim 10^{-6}$ to 10^{-5}) for period $\sim 10^3$ years and then decreasing as P^{-1} for longer periods (see Fig. 1). The short period (high frequency) cut-off of the spectrum is $\sim 10^{-11}$ seconds, *i.e.*, comparable to the thermal gravitons in frequency, although not in energy density. In Fig. 1, I also plot the gravitational wave spectrum from cosmic strings evaluated at $t = 1$ second. This is relevant to comparison to the nucleosynthesis limit (§III.a below).

6) GRAVITATIONAL WAVE PERTURBATION IN EQUIPARTITION WITH DENSITY FLUCTUATIONS

Assuming that the gravitational wave perturbation density is comparable to the fluctuations leading to galaxy formation in standard (noncosmic-string) models, Zel'dovich and Novikov,1970, obtain a long-period, gravitational wave density that is

$$\Omega_{gw} = \varepsilon^2 \Omega_\gamma \qquad \text{(II.4)}$$

where ε is the density contrast that leads to eventual galaxy formation: $\varepsilon^2 \lesssim 10^{-4}$.

7) QUASARS: "LATE" COSMOLOGICAL SOURCES

An estimate may be made for the gravitational wave density from the cosmic population of quasi-stellar objects. We present an estimate here based on one plausible model for quasars: quasars as $10^{10} M_\odot$ black holes, driven by accretion.

$M = 10^{10} M_\odot$ means the natural gravitational period associated with these black holes is $\sim 10^5$ seconds. The lifetime T of typical quasars has been variously estimated at 10^6 years.

An upper limit on the mass accretion rate is

$$\dot{M} \sim M/T$$
$$\sim 10^4 \, M_\odot/\text{year}. \qquad \text{(II.5)}$$

Assume an (unrealistically generous) efficiency of conversion to gravitational radiation:

$$\varepsilon \sim 0.1 \, . \qquad \text{(II.6)}$$

Then

$$L \simeq 10^{50} \text{ ergs/sec} \, . \qquad \text{(II.7)}$$

All quasars are at cosmological distances, $R \sim 10^{28}$ cm. A (perhaps low) estimate of the number of quasars is ~1,000.

Thus the flux from quasars in the octave centered at $\nu \sim 10^{-5}$ Hz is

$$\nu F_\nu \sim 1000 \times 10^{50} / 4\pi (10^{28})^2$$
$$\sim 8 \times 10^{-5} \text{erg/cm}^2\text{/sec}. \qquad \text{(II.8)}$$

This is marked as Q10 in Fig. 2. Other candidate models for quasars are also marked in Fig. 2: Q1, quasars as supermassive pulsars; Q2, quasars as sites of rapid stellar collapse; and Q4, quasars as relativistic star clusters (Q1, Q2, and Q4 from Rosi and Zimmerman, 1976).

b) "Recent" Cosmological Sources, SN1987a

The classical catastrophic source for gravitational radiation is supernova collapse. The gravitational flux from SN1987A can be estimated in the following way. The supernova may have converted $0.01 M_\odot$ to gravitational radiation (a generous efficiency of ~0.05%). The timescale is fixed by the total mass: $20 M_\odot$ means a typical timescale $\sim 10^{-3}$ to 10^{-2} second.

Then one has

$$\nu F_\nu(1987a) \sim (10^5 \text{ergs})/(10^{-2}\text{sec})/4\pi/(63\text{kpc})^2$$
$$\simeq 10^6 \text{ergs/cm}^2\text{/sec} \, . \qquad \text{(II.9)}$$

This is shown as 87a on Fig. 2. More conservative estimates of backgrounds from supernovae (Rosi and Zimmerman, 1976) are labeled SN in that figure.

III. LIMITS ON THE GRAVITATIONAL RADIATION BACKGROUND DENSITY

In using cosmological limits, one must be aware of the obvious fact that early universe limits only limit waves produced before the epoch at which the limit is imposed. A number of the following points have been made by Carr (1980).

a) Cosmic Nucleosynthesis

The observed light element abundances are remarkably accurately modeled by the "standard model:" a homogeneous, isotropic universe with three neutrino flavors and a present baryon density $\rho_b \sim 2 \times 10^{-31}$ gm/cm^3. Deviations in the parameters of only ~10% from standard values lead to discrepancies with observations, and despite some effort (*e.g.*, Matzner and Rothman, 1984) no deviation has been found that does not have an unmistakable signature different from the standard model results. In particular, the expansion rate at nucleosynthesis cannot be substantially perturbed as it would be if the gravitational radiation energy density then exceeded ~10% of the photon density (the dominant energy density) then. This gives different limits, depending on the wavelength of the gravitational radiation, in particular whether the wavelength was less than or greater than $\sim 3 \times 10^5$ km (*i.e.*, 1 second) at the beginning of nucleosynthesis, $T \sim 10^{10}$ K. This size corresponds to waves of 3×10^{15} km (periods ~100 years) now. Waves of shorter wavelength redshift exactly as the photon radiation, so we have the *nucleosynthesis limit*,

$$\Omega_{gw}(\nu) \lesssim 10^{-1}\Omega_\gamma \simeq 10^{-6} \text{ for } \nu \gtrsim (100 \text{ years})^{-1} . \tag{III.1}$$

Wavelengths that exceeded the horizon size but did not dominate the energy density redshift like $(1 + z)^5$ (rather than the $(1 + z)^4$ redshifting of the photons) (Misner, 1968). Thus one has

$$\Omega_{gw}(\nu) \lesssim \Omega_\gamma \left(\frac{z_h(\nu)}{10^{10}}\right)$$

where z_h is the redshift of the epoch when the wavelength finally fell within the horizon

$$z_h \sim 10^{18}\text{sec}/P_{now} \simeq ((\text{size of the universe})/\text{wavelength}) .$$

Hence

$$\Omega_{gw}(\nu) \lesssim (10^8 \text{ sec} \cdot \nu_{now})\Omega_\gamma \quad \begin{cases} \nu_{now} \lesssim 10^{-10} \text{ Hz} \\ P_{now} \gtrsim 100 \text{ years} \end{cases} . \tag{III.2}$$

These limits are reflected in Fig. 2. Both Eqs. (III.1) and (III.2) refer to waves that are present at the time of nucleosynthesis. Hence, in Fig. 2 the *dotted* cosmic string curve, giving waves produced by cosmic strings prior to $t_u = 1$ second, is the relevant one, so there is no conflict between cosmic string prediction and nucleosynthesis time.

b) Effects On Galaxy Foundation

Since galaxies must form in the expanding universe, they must be somehow gravitationally effective at $z \sim 10^3$ in order for the observed structure to have formed by now. Carr (1980) shows that this requires $\Omega_{gw} < \Omega_m^2 \sim 10^{-4}$ where Ω_m is the ratio of baryon matter to closure density; this is a limit somewhat weaker than the

nucleosynthesis limit but which may apply if the nucleosynthesis argument is somehow evaded.

c) Limits from Solar System Observations

Other upper limits on gravitational wave energy density can be obtained from the long-term effects of gravitational waves on the orbits of the moon or of the planets. For the moon, Carr (1980) finds $\Omega_{gw} \lesssim 4$ for periods $P_0 \sim 10^6$ seconds; for the planets, similar effects hold. Mashhoon (1978) finds that the effect on the phase of the moon's orbit could be more sensitive than is its semimajor axis to incident gravitational radiation.

Some very weak limits on the gravitational background can also be found by considering terrestrial and solar oscillation. Boughn and Kuhn (1984) report $\Omega_{gw}(4 \times 10^{-4}\ \text{Hz}) \lesssim 10^2$ from solar oscillations, and similarly $\Omega_{gw}(2 \times 10^{-3} - 2 \times 10^{-2}\ \text{Hz}) \lesssim 10^2$ from earth oscillations. They suggest that both earth and solar mode observations may improve by orders of magnitude and may in the future provide real limits on the density of gravitational radiation in these frequency bands.

d) Limits on the Gravitational Background from Distortions and Polarization of the Electromagnetic Microwave Background

Gravitational waves introduce anisotropy in the cosmic microwave background because the associated metric variation affects the overall redshift between source and observer. For wavelengths shorter than the horizon, the amplitude h scales as R^{-1} so the dominant effect on the microwave radiation comes from the earliest post-collisional part of the microwave photon evolution. The earliest point that the microwave background samples is thus the "decoupling epoch," which occurs at $z \sim 1{,}000$ in most models of the microwave temperature (although there have been suggestions that "late" reheating of the intergalactic in standard gas could mean that the last scattering was much more recent. Only if the decoupling redshift $\sim$ 1,000 do we obtain any usable limits from the microwave backgrounds). Gravitational radiation imprints a signature $\Delta T/T \sim h$, where h is the amplitude of the wave perturbation. For waves comparable to the size of the horizon now, the effect of waves is like that of uniform anisotropy: quadrupole $\Delta T/T$. Current upper limits on the quadrupole temperature anisotropy are $\sim 5 \times 10^{-5}$ (Lubin, Epstein, and Smoot, 1983; Fixsen, Cheng, and Wilkinson, 1983), which gives an energy content in these waves

$$\Omega_{gw} \lesssim 2.5 \times 10^{-9} \Omega_\gamma . \qquad \text{(III.3)}$$

Waves produced at decoupling might be expected to have wavelengths comparable to the horizon size at decoupling. This corresponds to angular scales minutes to degree. The limits on $\Delta T/T$ on the angular scale 10 arcminutes to 1° is $\sim 8 \times 10^{-5}$ (Wilkinson, 1987) with a somewhat tighter limit at 4.5 arcseconds $\sim 2 \times 10^{-5}$ (Uson and Wilkinson, 1984). These give

$$\Omega_{gw} \lesssim 4 \times 10^{-10} \Omega_\gamma \text{ for } P \sim 3 \times 10^8 \text{ years} . \qquad \text{(III.4)}$$

When photon scattering occurs in an anisotropic medium, polarization of the scattered photon occurs. A photon scattered at right angles must be polarized

orthogonally to the plane of its trajectory. If we consider viewing a distant thermal source, then horizontally polarized photons are all those that scattered from a horizontal orbit toward us. A gravitational wave induces an anisotropic shear $\sigma = \dot{h} = (h/P)$ in the transverse dimensions of a system. This shear leads to a differential redshift, $\Delta T/T \sim \sigma t_c$, where t_c is the mean time between collisions (assumed less than P; if $t_c \gtrsim P$ then the effect saturates). This means that vertically travelling photons pick up a different redshift between their last two collisions than do horizontally traveling photons. There is thus a net polarization induced in the radiation that reaches us. (h is a tensor that has principal axes. For "horizontal" and "vertical" above, one should strictly say "the projection on the sky of one of the principal axes;" "the projection on the sky of the other vertical axis.") Unlike the temperature fluctuations, which are diminished or destroyed by scattering, the production of polarization demands it. Since decoupling in most models is a gradual process, occurring over a factor ~2 in redshift, we expect polarization $p \sim (h/P)P \sim h \sim \Delta T/T$ (actual model calculations typically give $p \sim 0.3\Delta T/T$) induced in the microwave background from gravitational radiation. If the period P is small compared to the age of the universe at decoupling, t_{ud}, then we see the superposition of many oppositely polarized regions; so the minimum scale on which this effect can be relevant is roughly the horizon size at decoupling, and larger. Polarization limits are, in fact, comparable to temperature anisotropy limits ($p \lesssim 6 \times 10^{-5}$; Lubin and Smoot, 1981, so these results provide an upper bound on the present-day wave density consistent with the temperature anisotropic limits given above. (For essentially homogeneous waves, one calculates (with $t_c \sim t_{ud}$ at scattering) first that ($\Delta T/T$) quadrupole now $\sim(\dot{\beta} t_{ud})$. Again taking $t_c \sim t_{ud}$, we find $p \sim \Delta T/T$ consistent with the gravitational wave discussion above.)

Sunyaev, 1974 has studied the distortions in the microwave background due to the dissipation of density fluctuations in the early universe. (These would be equal to gravitational wave background under the equipartition hypothesis of Zel'dovich and Novikov, 1970). He finds the limit $\Omega_{gw} \lesssim 10^{-6.5}$ for waves of period 10^{12} sec $< P_0 < 10^{15}$ sec.

IV. CONCLUSION

As can be seen from Figs. 1 and 2, certain possible early cosmology sources can be excluded by cosmologically based limits. In particular, it seems that parametric amplification at temperatures greater than $\sim 5 \times 10^{16}$ GeV conflicts with the quadrupole anisotropy upper limit. The small scale microwave anisotropy also puts limits on the acoustic noise-induced gravitational waves arising from the QCD (quark-hadron) phase transition. (In both these cases we assume that the microwave decoupling temperature is $T \sim 3{,}000$ K ($z_{decoupling} \sim 1{,}000$).) The cosmological sources and cosmological limits) apply at longer periods than do the typical "more recent" sources and observational limits (Fig. 2). However, it is notable that as pulsar timing increases in accuracy and in length of time observed, very interesting limits on cosmological features ($P \gtrsim 10$ years) will emerge. The timing data on PSR 1937+2 1 (Rawley, Taylor, Davis, and Allen, 1987) is, for instance, very close to limiting the cosmic string-produced gravitational radiation.

Present day detectors are being supplemented by systems in process or proposed that can substantially improve sensitivity.

Allen Anderson (1987, and this volume) has described an earth orbital interferometer design. This design could reach $\Omega_{gw} \sim 10^{-5}$ at $\sim 10^{-2}$ Hz. Michaelson, 1987, has investigated the sensitivity of coincidence between cryogenic "Weber bar" detectors, which could limit $\Omega_{gw} \lesssim 10^{-7}$ for ~200 Hz; and between interferometric detectors with ~1,000 km separation, which could give sensitivities $\Omega_{gw} \sim 10^{-12}$ at 50 Hz. Even better sensitivities at ~1 to ~50 Hz could be obtained by orbiting interferometers.

ACKNOWLEDGEMENTS

I thank Dr. P. Laguna for helpful conversations on the radiation background due to cosmic strings.

REFERENCES

Anderson, A., IUGG-Vancouver (August 1987).
Anderson, J. D., and Mashhoon, B. 1985, *Astrophys. J.*, **290**, 445.
Bond, J. R., and Carr, B. J. 1984, *Mon. Not. R. A. S.*, **201**, 585.
Boughn, S. P., and Kuhn, J. R. 1984, *Astrophys. J.*, **286**, 387.
Carr, B. J. 1980, *Astron. Astrophys.*, **89**, 6.
Fixsen, D. S., Cheng, E. S., and Wilkinson, D. T. 1983, *Phys. Rev. Lett.*, **50**, 620.
Hellings, R. W., Callahan, P. S., Anderson, J. D., and Moffet, A. T. 1981, *Phys. Rev. D*, **23**, 844.
Hogan, C. J. 1986, *Mon. Not. R. A. S.*, **218**, 629.
Hogan, C. J., and Rees, M. J. 1984, *Nature*, **311**, 109.
Kajantie, K., and Kurki-Suonio, H. 1986, *Phys. Rev. D*, **34**, 1719.
Korotun, A. V. 1980, *Sov. Astron.*, **24**, 273.
Kurki-Suonio, H. 1988, *Phys. Rev. D*, **37**, 2104.
Lubin, P., Epstein, G. L., and Smoot, G. F. 1983, *Phys. Rev. Lett.*, **50**, 616.
Lubin, P., and Smoot, G. F. 1981, *Astrophys. J.*, **245**, 1.
Mashhoon, B. 1978, *Astrophys. J.*, **223**, 285.
Matzner, R. A. 1969, *Astrophys. J.*, **154**, 1085.
Matzner, R. A., and Rothman, T. 1984, *Phys. Rev. D*, **30**, 1649.
Michaelson, P. F. 1987, *Mon. Not. Roy. Astron. Soc.*, **227**, 933.
Misner, C. W. 1968, *Astrophys. J.*, **151**, 431.
Rawley, L. A., Taylor, J. H., Davis, M. M., and Allan, D. W. 1987, *Science*, **238**, 761.
Romani, R. W., and Taylor, J. H. 1983, *Ap. J.*, **265**, L35.
Rosi, L. A., and Zimmerman, R. L. 1976, *Astrophys. Space Sci.*, **45**, 447.
Sunyaev, R. A. 1974, in *IAU Symposium*, **63**, *Confrontation of Cosmological Theories with Observational Data*, p. 299, ed. M. S. Longair.
Uson, G. and Wilkinson, D. T. 1984, *Astrophys. J.*, **283**, 471.
Vachaspati, T., and Vilenkin, A. 1985, *Phys. Rev. D*, **31**, 3052.
Veryaskin, A. V., Rubakov, V. A., and Sazhin, M. V. 1983, *Sov. Astron.*, **27**, 16.
Wilkinson, D. T. 1987, in *Relativistic Astrophysics*, ed. W. P. Allen (Singapore: World Scientific).
Zel'dovich, Y. B., and Novikov, I. D. 1970, *Sov. Astron. A. J.*, **13**, 754.

SOURCES

1° K thermal gravitons: (Last equilibrium at ~10^{31} K) gravitational equivalent of the 2.7 K background radiation (Matzner 1969).

PA19: Parametric amplification of long wavelength radiation from overshoot due to phase transition at Planck epoch ~ 10^{31} K ~ 10^{19} GeV (Veryaskin, Rubakov, and Sazhin 1983).

PA17: Parametric amplification in Grand Unified Theory (GUT) phase transitions at ~10^{17} GeV (Korotun 1980).

EW: Gravitational waves generated by acoustic noise arising in the electroweak phase transition (~100 GeV) (Hogan 1986).

QCD: Gravitational waves generated by acoustic noise arising in the quark-hadron phase transition (~100 MeV) (Hogan 1986).

GALEQ: Gravitational waves produced by primordial fluctuations in an adiabatic collapse scenario for galaxy formation, assuming equipartition between density fluctuations and gravitational radiation (Zel'dovich and Novikov 1970).

Cosmic Strings: Spectrum produced by cosmic strings with dimensionless mass parameter per unit length $G\mu/c^2 \sim 10^6$ (appropriate to galaxy function). The break at period ~ P ~ 1 year is due to those that decay just at transition to matter domination in universe evolution. The peak near P = 300 years arises from the longest strings to have completely decayed by now. The P^{-1} fall-off at long periods arises because large cosmic strings have not yet completely radiated away. It must be understood that limits apply only to radiation produced prior to when the limiting mechanism is effective. See §III.A for a discussion of the apparent contradiction between the cosmic string and galaxy equilibrium production schemes and the nucleosynthesis limit. The dotted line shows the wave spectrum due to cosmic strings at the time $t \sim 1$ sec when nucleosynthesis begins.

BOUNDS

$Q\mu$: The quadrupole microwave background limits very long wavelength radiation present prior to the redshift z of last scattering (decoupling) of the radiation. The strong limit here assumes that redshift was $z \sim 1{,}000$ (Carr, 1980, and references therein).

SSm: Small scale microwave limits waves with a scale comparable to the horizon size at last scattering, here assumed to be $z_d \sim 1{,}000$. Notice that this appears to put limits on QCD noise-generated, gravitational radiation. However, both $Q\mu$ and $SS\mu$ become much weaker if $z_d < 1{,}000$, as can be the case in some reionization scenarios (Carr, 1980, and references therein).

GALFORM: Galaxies must be gravitationally effective at $z \sim 1{,}000$ in order to condense. If the gravitational wave background is too large at that time, it prevents their formation (Carr, 1980).

NUC: A limit from cosmic nucleosynthesis. For periods P shorter than ~100 years, these are waves that were shorter than the horizon scale during nucleosynthesis and that scale with the background radiation.

S74: Limit on maximum density fluctuations and associated equipartition gravitational waves, based on limits on distortion of 2.7 K microwave background from dissipation of these fluctuations (Sunyaev, 1974).

RECENT COSMOLOGICAL SOURCES

Q1: Quasars as Supermassive Pulsars (Rosi and Zimmerman, (1976)

BIN: Late evolution in spiraling binaries (binaries consisting of stellar remnants, *i.e.*, black holes, neutron stars, white dwarfs) (Rosi and Zimmerman, 1976).

BINF: Main sequence binaries (Rosi and Zimmerman, 1976).

Q10: Quasars as supermassive black holes; see §II.a-7.

SMBH: Supermassive black hole binaries ($10^2 - 10^5$ $M_\odot$)(Bond and Carr, 1984).

BHIII: Early black hole collapse from supermassive Population III stars (Rosi and Zimmerman, 1976).

BH: Black hole collapse from galactic stellar populations (Rosi and Zimmerman, 1976).

Q2: Quasars as sites of rapid stellar collapse (Rosi and Zimmerman, 1976).

Q4: Quasars as relativistic star clusters (Rose and Zimmerman, 1976).

87a: Peak flux from very optimistic estimate of supernova SN1987A (pulse length $\sim 10^{-2}$ seconds); see §II.b).

SN: Background due to galactic and extragalactic supernovae (Rosi and Zimmerman, 1976).

OBSERVATIONS (BOUNDS)

RTDA: Timing of Millisecond Pulsar PSR 1937+21 (Rawley, Taylor, Davis, and Allen, 1987).

RT: Timing of Pulsar PSR 1237+25 (Romani and Taylor, 1983).

P10: Pioneer 10 tracking data (Anderson and Mashhoon, 1985).

VI: Voyager I tracking data (Hellings, Callahan, Anderson, and Moffet, 1981).

S: Solar oscillation excitation limit (Boughn and Kuhn, 1984).

E: Earth oscillation excitation limit (Boughn and Kuhn, 1984).

L: Limit from lunar orbit constancy (Carr, 1980).

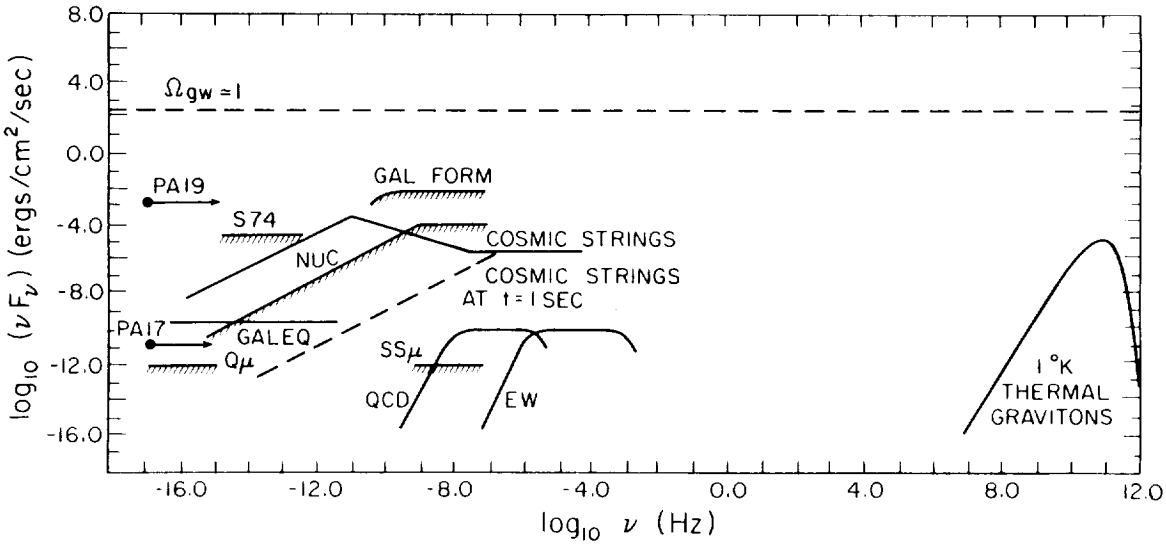

FIG. 1.— Logarithmic spectral flux for pregalactic sources of radiation and some inferred limits on their densities. Closure density $\rho_{closure} \sim 2 \times 10^{-29}$ gm/cm^3 (corresponding to $H_0 \sim 100$ km/sec/Mpc is at $\sim 6 \times 10^2$ ergs/cm^2/sec, shown here as a dotted line, so ordinary units have a significance on such a scale. For comparison, noon sunlight $\sim 10^6$ ergs/cm^2/sec, full moonlight ~ 1 erg/cm^2/sec, the 2.7 K microwave radiation $\sim 10^{-3}$ ergs/cm^2/sec. The waves appearing here are theoretical estimates for high energy, early cosmology processes; several indirect limits from cosmological observations are also indicated.

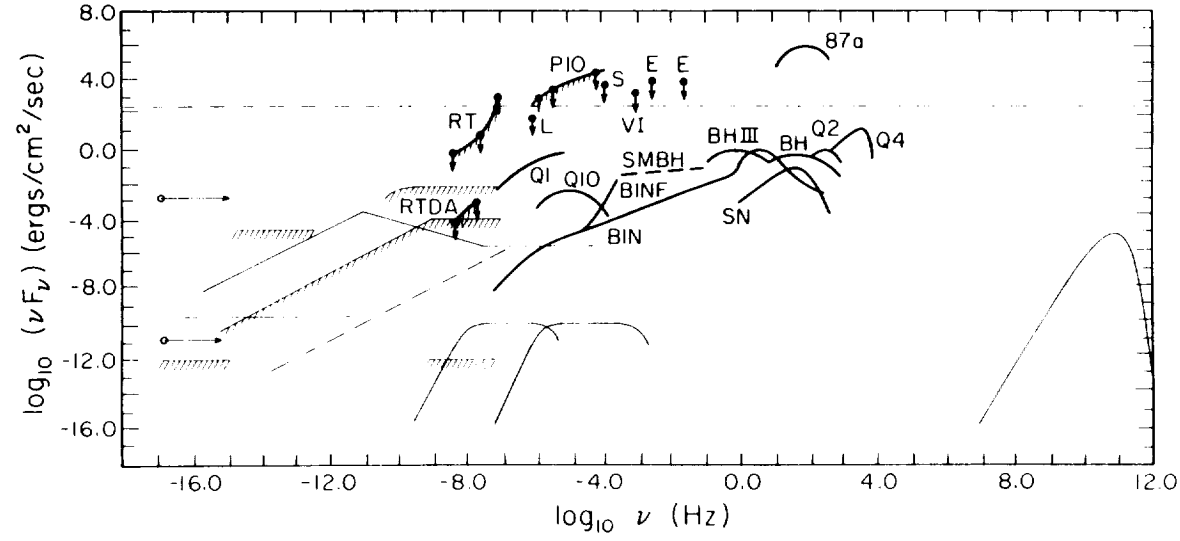

FIG 2.— Repeats Fig. 1, but includes a number of possible sources and indicates limits obtained from nonlaboratory-scale experiments (*i.e.*, including "Weber" bar and LASER detectors). It is expected that the new generation of cryogenic cooled bars and ground-based and space-based interferometers will provide sensitivity first in the dominant peak of the expected spectrum at $\sim$ 100 Hz of Ω_{gw} 10^{-2} to 10^{-3}. Later such devices have the potential to be 5 to 7 orders more sensitive than the expected background limit in the 0.1-100 Hz range.

EXPERIMENTAL CONSTRAINTS ON METRIC AND NON-METRIC THEORIES OF GRAVITY

CLIFFORD M. WILL
McDonnell Center for the Space Sciences, Department of Physics
Washington University, St. Louis, Missouri 63130

ABSTRACT

Experimental constraints on metric and non-metric theories of gravitation are reviewed. Tests of the Einstein Equivalence Principle indicate that only metric theories of gravity are likely to be viable. Solar-system experiments constrain the parameters of the weak-field, post-Newtonian limit to be close to the values predicted by general relativity. Future space experiments will provide further constraints on post-Newtonian gravity.

I. INTRODUCTION

Gravitation plays a fundamental role in our universe. On a local scale, up to 10^9 km, it determines our Earthbound environment, the nature of the Sun, the dynamics of the solar system. On scales ranging up to the largest observable distances, 10^{10} light years, it determines the structure and evolution of black holes, galaxies, clusters and superclusters of galaxies, and the universe itself. On scales ranging down to the smallest, the Planck scale, or 10^{-33} cm, gravitation forms the template against which must be meshed attempts to unify the interactions in a full quantum synthesis. It is remarkable that there exits one candidate theory of gravity, general relativity, that has the ability to treat gravitation over such a range — 60 orders of magnitude — of scales.

On the other hand, the viability of general relativity is determined by experiments that, with a few exceptions, are confined to the scale of the solar system. During the past 25 years, experiments have been spectacularly successful in verifying general relativity over this scale, and in ruling out many alternative theories of gravity. Space experiments, involving spacecraft tracking, orbiting atomic clocks, laser ranging to retroreflectors, and the like, have played a vital role in this endeavor.

But the need to extrapolate gravitational theory from solar system scales to such large and such small scales requires the most accurate verification possible at the experimentally accessible scales. Thus, despite its successes, experimental gravitation continues to be an active and challenging field, with space experiments maintaining their central role. In this paper we review the current status of experimental constraints on gravitational theory and describe the significance of future measurements.

II. CONSTRAINTS ON THEORIES OF GRAVITY: THE PRESENT PICTURE

One of the fundamental postulates of gravitational theory is the Einstein Equivalence Principle (EEP), which states: (i) test bodies fall with the same acceleration (weak equivalence principle — WEP); (ii) in a local freely falling frame, non-gravitational physics is independent of the frame's velocity (local Lorentz invariance); and (iii) in a local freely falling frame, non-gravitational physics is

independent of the frame's location (local position invariance). If EEP is valid, then gravity must be described by a "metric theory," whose postulates are that there exists a symmetric metric $g_{\mu\nu}$, whose geodesics are the trajectories of structureless test bodies and, which reduces to the Minkowski metric in freely falling frames, where the laws of physics take their special relativistic forms. The EEP divides theories of gravity into two classes: metric theories, such as general relativity, the Brans-Dicke theory, and numerous others; and non-metric theories, such as Moffat's non-symmetric gravitation theory (NGT), and others.

The observational evidence in support of EEP is very strong. For example, Eötvös-type experiments have verified WEP to better than a part in 10^{11} and improved space-borne experiments are planned. Local Lorentz invariance has been verified to high precision by several extraordinarily precise "mass-anisotropy" null experiments. Finally, gravitational redshift experiments test local position invariance: the 1976 rocket experiment (NASA's GP-A) verified this effect to two parts in 10^4. It should be noted that redshift experiments that are sensitive to effects at second order in the gravitational potential probe beyond local position invariance and *do* test alternative metric theories of gravity. (For a review of the theoretical and observational implications of EEP, see Will (1981), chapter 2; or Will (1984), sec. 2; see also Haugan and Will (1987).)

The experimental evidence in support of EEP suggests very strongly that metric theories provide the best description of gravitation. When we restrict attention to such theories and consider the weak-field, slow-motion limit appropriate to the solar system, the so-called post-Newtonian limit, then it turns out that most such theories can be described by the parametrized post-Newtonian (PPN) formalism (for a detailed review, see Will (1981), chapter 4; or Will (1984), sec. 3.3). This formalism characterizes the metric of the post-Newtonian limit in terms of a set of ten dimensionless parameters, $\gamma,\beta,\xi,\alpha_1,\alpha_2,\alpha_3,\zeta_1,\zeta_2,\zeta_3,\zeta_4$, whose values vary from theory to theory. Table 1 shows the approximate significance of these parameters, and gives their values in general relativity and in theories of gravity that possess conservation laws for momentum (semi-conservative theories and all Lagrangian-based theories) and that possess conservation laws for momentum as well as angular momentum and center-of-mass motion. Several compendia of alternative theories and their PPN parameter values have been published (see for example Will (1981), chapter 5; or Will (1984), sec. 3.4). In addition to its use as a tool for studying and classifying theories of gravity, the PPN formalism facilitates discussion of experiments because the predicted sizes of various post-Newtonian effects depend on the values of the PPN parameters; therefore the measurement of an effect is tantamount to a measurement of the corresponding PPN parameter or parameter combination.

Two important experimental tests of general relativity are the deflection of light and the Shapiro time delay of light, both measuring the same thing, the coefficient $\frac{1}{2}(1 + \gamma)$. A light ray which passes the Sun at a distance d (measured in solar radii) is deflected by an angle

$$\Delta\theta = \frac{1}{2}(1 + \gamma)\ 1''.75/d \ , \qquad \text{(II.1)}$$

Table 1. The PPN Parameters and Their Significance*

Parameter	What it measures relative to general relativity	Value in general relativity	Value in semi-conservative theories	Value in fully-conservative theories
γ	How much space-curvature is produced by unit rest mass?	1	γ	γ
β	How much "nonlinearity" is there in the superposition law for gravity?	1	β	β
ξ	Are there preferred location effects?	0	ξ	ξ
α_1	Are there preferred-frame effects?	0	α_1	0
α_2		0	α_2	0
α_3		0	0	0
ζ_1	Is there violation of conservation of total momentum?	0	0	0
ζ_2		0	0	0
ζ_3		0	0	0
ζ_4		0	0	0

*For a compendium of PPN parameter values in alternative theories together with derivations, see TEGP, Chapter 5.

and a light ray which passes the Sun on a round trip, say, from Earth to Mars at superior conjunction, suffers a delay given, for $d \gtrsim 1$, by

$$\Delta t = \frac{1}{2}(1 + \gamma)250(1 - 0.161nd)\ \mu s\ . \qquad \text{(II.2)}$$

Measurements of the deflection of light have improved steadily during the past 70 years, from the early observations of stellar positions surrounding total solar eclipses (10 to 30%), to measurements of the deflection of radio waves from quasars during the period 1969 through 1975 (1.5 %), to VLBI observations of radio source positions over the entire celestial sphere in the 1980s (approaching 1%) (Will (1984), sec. 4.1; Robertson and Carter (1984).) Orbiting optical interferometers may yield further improvements, and have the potential to probe second-order, post-post-Newtonian contributions to the deflection.

Observations of the Shapiro time delay began in the middle 1960's using radar echos from Mercury and Venus, and later made use of interplanetary spacecraft

equipped with radar transponders, such as Mariners 6, 7, and 9, and the Viking landers and orbiters. Data from Viking produced the best measurement of $\frac{1}{2}(1 + \gamma)$ to date, namely 1.000 ± 0.001, in complete agreement with general relativity (Will (1984), sec. 4.2). The time delay in a one-way signal has been recently measured using timing data from the millisecond pulsar PSR 1937+21, with results in agreement with general relativity at the three percent level (Taylor, 1987).

The perihelion shift of Mercury is another key test of general relativity. Including the possible effect of a solar quadrupole moment J_2, the predicted rate of advance is given, in arcseconds per century, by

$$d\omega/dt = 42''.98\lambda \ , \tag{II.3}$$

$$\lambda \equiv \frac{1}{3}(2 + 2\gamma - \beta) + 0.0003(J_2/10^{-7}) \ . \tag{II.4}$$

The first term in the coefficient λ is the "classical" relativistic perihelion shift contribution, which depends on the PPN parameters γ and β. In general relativity, this term is unity (see Table 1). The second term depends on the Sun's oblateness; for a Sun that rotates uniformly with its observed surface angular velocity, so that the oblateness is produced by centrifugal flattening, J_2 is estimated to be 10^{-7}, so that in such a case, its contribution to λ would be very small.

Now, the measured shift is known accurately: after the perturbing effects of the other planets have been accounted for, the excess perihelion shift is known to be about 0.5% from radar observations of Mercury since 1966, with the result that $\lambda = 1.003 \pm 0.005$. If J_2 were indeed as small as 10^{-7}, this would be in complete agreement with general relativity. However, over the past 25 years, a range of values has been reported for J_2, from 2.5×10^{-5}, inferred from 1966 visual solar-oblateness measurements, to a few parts in 10^6 from 1983 to 1985 visual observations, to an upper limit of 3×10^{-6} inferred from combined Mercury/Viking Mars ranging data, to $(1.7 \pm 0.4) \times 10^{-7}$ inferred from solar oscillation data (for a review, see Will (1984), sec. 4.3 and 4.4; and Will (1987), sec. 5.4.1). Thus, there remains some uncertainty in the interpretation of perihelion shift measurements as tests of general relativity, although conventional wisdom points toward the smaller values of J_2. An unambiguous measurement of J_2 through direct study of the Sun's gravitational field over a large range of distances could be provided by a space mission that has been under study by NASA since 1978. Known as Starprobe, it is a spacecraft that would approach the Sun to within four solar radii. Feasibility studies indicate that J_2 could be measured to an accuracy of ten percent of its conventional value of 10^{-7}. Unfortunately, it is not clear whether gravitational physics is part of NASA's current plan for this mission.

Another class of experiments tests what is called the Strong Equivalence Principle (SEP). This is a stronger principle than EEP, stating that *all* bodies, including those with self-gravitational binding energy (stars, planets), should fall with the same acceleration, and that in suitable "local" freely falling frames, the laws of *gravitation* should be independent of the velocity and location of the frame. General relativity satisfies SEP, but most other metric theories of gravity do not. Lunar laser ranging measurements since 1969 have shown that the Earth and the

Moon fall toward the sun with the same acceleration to 7 parts in 10^{12}, yielding the limit (Bender, 1988)

$$|4\beta - \gamma - 3 - \frac{10}{3}\xi - \alpha_1 + \frac{2}{3}\alpha_2 - \frac{2}{3}\zeta_1 - \frac{1}{3}\zeta_2| < 0.007 \ . \qquad \text{(II.5)}$$

If the laws of gravitation in a local system (for example, the locally measured Newtonian gravitational constant) depend on the motion of the system relative to the universe, then, according to the PPN formalism, there should occur such effects as anomalous Earth tides and variations in the Earth's rotation rate, anomalous contributions to the perihelion shifts for Mercury and Earth, self-accelerations of pulsars, and anomalous torques on the Sun that would cause its spin axis to be randomly oriented relative to the ecliptic, all among other anomalies known generically as "preferred frame" effects. Negative searches for these effects have produced strong constraints on the PPN parameters α_1, α_2, α_3, and ξ. A possible cosmological variation in Newton's gravitational constant has been constrained by analysis of Viking ranging data to be less than 10^{-11} yr^{-1} (for a review of tests of SEP, see Will (1984), sec. 5; and Nordtvedt (1987).) Apart from indirect limits, such as that shown in equation (5), the only strong limit on the conservation-law parameters ζ_i is

$$|\zeta_3| < 10^{-8} \ . \qquad \text{(II.6)}$$

from a test of Newton's third law using the Moon (Bartlett and van Buren, 1986).

The current best limits on PPN parameters are summarized in Table 2. General relativity is consistent with all of them.

III. CONSTRAINTS PROVIDED BY PLANNED OR PROPOSED PROJECTS

There are numerous ideas for probing the structure of gravity in the solar system to higher precision. Some of them provide improved values of PPN parameters, some measure PPN parameters in novel ways, some measure PPN parameters that have not been strongly constrained to date, and some begin to enter the post-post Newtonian regime. What follows is a list of some of them. Detailed discussion of many of these projects can be found in these proceedings.

a) Search for Gravitomagnetism

According to general relativity, moving or rotating matter should produce a contribution to the gravitational field that is the analogue of the magnetic field of a moving charge or a magnetic dipole. The Relativity Gyroscope Experiment at Stanford University (GP-B) is in the advanced stage of developing a space mission to detect this phenomenon. A set of four superconducting, niobium-coated, spherical quartz gyroscopes will be flown in a low polar Earth orbit, and the precession of the gyroscopes relative to the distant stars will be measured. The predicted effect of gravitomagnetism is about 42 milliarcseconds per year, and the accuracy goal of the experiment is about 0.5 milliarcseconds per year. Another proposal to look for the effect of gravitomagnetism is to measure the relative precession of the line of nodes of a pair of LAGEOS satellites with supplementary inclination angles; the inclinations must be supplementary in order to cancel the dominant nodal precession caused by the Earth's Newtonian gravitational multipole moments. A third proposal envisages orbiting a superconducting, three-axis, gravity gradiometer around the Earth to measure directly the contribution of the gravitomagnetic field to the tidal

Table 2. Current Limits on PPN Parameters

PPN Parameter	Experiment	Value or limit	Remarks
γ	time delay	1.000 ± 0.002	Viking ranging
β	perihelion shift	0.99 ± 0.02	$J_2 \approx 10^{-7}$
$\lvert\xi\rvert$	Earth tides	$<10^{-3}$	gravimeter data
$\lvert\alpha_1\rvert$	orbital preferred-frame effects	$<4 \times 10^{-4}$	combined solar system data
$\lvert\alpha_2\rvert$	Earth tides	$<4 \times 10^{-4}$	gravimeter data
	solar spin precession	$<4 \times 10^{-7}$	assumes alignment of solar equator and ecliptic are not coincidental
$\lvert\alpha_3\rvert$	perihelion shift	$<2 \times 10^{-7}$	
	acceleration of pulsars	$<2 \times 10^{-10}$	statistics of dP/dt for pulsars
$\lvert 4\beta - \gamma - 3 - \frac{10}{3}\xi - \alpha_1 + \frac{2}{3}\alpha_2 - \frac{2}{3}\zeta_1 - \frac{1}{3}\zeta_2 \rvert$	Nordtvedt effect	<0.007	lunar laser ranging
$\lvert\zeta_3\rvert$	Newton's third law for the Moon	$<10^{-8}$	lunar acceleration

gravitational force. In these and other examples of gravitomagnetic effects, the PPN parameter combination measured is $\frac{1}{2}(1 + \gamma + \frac{1}{4}\alpha_1)$.

b) Geodetic Precession

The precession of a gyroscope, or of the axis of an orbit in the curved spacetime surrounding a distant body, depends on the PPN parameter combination $\frac{1}{3}(2\gamma + 1)$. The gyroscope experiment may measure this to better than 10^{-4}. The effect of this precession on the lunar orbit (conventionally called the de Sitter effect) has been seen at the 10 per cent level (Bertotti *et al.*, 1987).

c) Improved PPN Parameter Values

A number of advanced missions have been proposed in which spacecraft anchoring and improved tracking capabilities would lead to significant improvements in values of the PPN parameters, of J_2 of the Sun, and of $\dot{G}/G$. For example, a Mercury orbiter, in a 2-year experiment, with 3cm-range capability, could yield improvements in the perihelion shift to a part in 10^4, in γ to 4×10^{-5}, in $\dot{G}/G$ to 10^{-13} yr^{-1}, and in J_2 to a few parts in 10^8. An Icarus lander could yield similar accuracies for the perihelion shift, γ and J_2. A Phobos lander, with 1.5 years of data at 15 m-range uncertainty, could improve $\dot{G}/G$ to 3×10^{-12} yr^{-1}, and could lead to refined asteroid masses.

d) Probing Post-post-Newtonian Physics

It may be possible to begin to explore the next level of corrections to general relativity beyond the post-Newtonian limit, into the post-post-Newtonian regime. One proposal is POINTS, a precision optical interferometer in space with μarcsecond accuracy. Such a device would improve the value of γ to the 10^{-6} level, and could detect the second-order term, which is of order 10 μarcseconds at the limb. Such a measurement would be sensitive to a new "PPPN" parameter, which has not been measured heretofore. Here, the experimental effort to enter the PPPN arena will have to be accompanied by theoretical work to devise a simple, yet meaningful, PPPN extension of the PPN framework (see for example, Benacquista and Nordtvedt, 1988).

e) Tests of the Einstein Equivalence Principle

The possibility of performing an Eötvös experiment in space has been studied, raising the possibility of testing WEP to 10^{-18}. The gravitational redshift could be improved to a few parts in 10^6 in an advanced redshift experiment using a hydrogen maser clock in an Earth-orbiting satellite in an orbit of 0.5 eccentricity. A hydrogen maser on Starprobe would further improve the first-order redshift, and would be sensitive to second-order corrections (these corrections are still part of the post-Newtonian limit, and depend on γ and β). Other relativistic benefits of Starprobe would be an improvement in J_2 to 2×10^{-8}, in α_1 to 0.007; J_4, and time variations in J_2, might also be detectable.

f) Testing Unconstrained PPN Parameters

Improved limits on the parameter of the Nordtvedt effect (eq. 5), together with improved limits on such parameters as ξ, α_1, and α_2 from other tests, could begin to constrain the conservation-law parameters ζ_1 and ζ_2, which are only poorly constrained to date. Further constraints could be made possible by looking for small perturbative effects in Earth-satellite and Lunar orbits (Shahid-Saless and Ashby, 1988; Will, 1971).

IV. IS THE PPN FORMALISM THE LAST WORD?

The basis for this discussion has been the PPN formalism. It is important to keep in mind that this formalism is based on a particular set of assumptions, namely the validity of symmetric metric theories of gravity, and subjective criteria of simplicity of the forms assumed for the metric. Other assumptions could be made. The extension to post-post-Newtonian gravity by Benacquista and Nordtvedt (1988) does not assume a metric, rather it assumes a many-body Lagrangian for matter, and equations of motion for light, together with some criteria of symmetry. Other formalisms based on affine theories have been developed (Coley, 1983).

Occasionally alternative theories of gravity arise that do not fit the PPN framework and that achieve some measure of fame (or notoriety!) for one reason or another. A leading example of this is the Moffat non-symmetric gravitation theory (NGT). For the most recent summary, see Moffat and Woolgar, (1988). In this theory, the metric is not symmetric, therefore according to the standard terminology, it is not a metric theory. The theory contains a parameter l^2 which may have a microscopic interpretation as depending on some combination of baryon number, lepton number, fermion number or some other quantum number of the source of gravity. The theory is purported to agree with all experiments to date, although one constraint has been placed on it using the effect of dipole gravitational radiation in the "11 minute binary" 4U 1820-30 (Krisher, 1987).

The moral is that the PPN framework, albeit a very useful tool for analyzing experiment and theory, should not be used to shackle experimentalists to a given mode of investigation of the possibilities for experiments. Instead, theorists and experimentalists should work together to devise and understand meaningful new tests of the gravitational interaction.

ACKNOWLEDGEMENTS

This research was supported in part by the National Science Foundation under grant PHY 85-13953.

REFERENCES

Bartlett, D. F., and van Buren, D. 1986, *Phys. Rev. Lett.*, **57**, 21.
Benacquista, M., and Nordtvedt, K. Jr. 1988, *Astrophys. J.*, **328**, 599.
Bender, P. 1988, private communication.
Bertotti, B., Ciufolini, I., and Bender P. L. 1987, *Phys. Rev. Lett.*, **58**, 1062.
Coley, A. A. 1983, *Phys. Rev. D*, **27**, 728; **28**, 1829; **28**, 1844.
Haugan, M. P., and Will, C. M. 1987, *Phys. Today*, **40** (5), 69.
Krisher, T. P. 1987, *Astrophys. J. Lett.*, **320**, L47.
Moffat, J. W., and Woolgar, E. 1988, *Phys. Rev. D*, **37**, 918.
Nordtvedt, K., Jr., 1987, *Astrophys. J.*, **320**, 871.
Robertson, D. S., and Carter, W. E. 1984, *Nature*, **310**.
Shahid-Saless, B., and Ashby, N. 1988, *Phys. Rev. D*, in press.
Taylor, J. H. 1987, In *General Relativity and Gravitation*, ed. M. A. H. MacCallum, Cambridge University Press, Cambridge, p. 209.
Will, C. M. 1971, *Astrophys. J.*, **165**, 409.
Will, C. M. 1981, *Theory and Experiment in Gravitational Physics*, Cambridge University Press, Cambridge.
Will, C. M. 1984, *Phys. Reports*, **113**, 345.
Will, C. M. 1987, In *300 Years of Gravitation*, ed. S. W. Hawking and W. Israel, Cambridge University Press, Cambridge, p. 80.

DISCUSSION

HELLINGS: Is it true that redshift, Eotvos, and local Lorentz invariance rule out all nonmetric theories of gravity? Could, say, some general affine theory not satisfy these limits?

WILL: The experiments in question place finite upper limits on the sizes of effects, that can be translated into constraints on the characteristics of certain classes of nonmetric theories (theories that fall within the Lightman-Lee THem framework, for example). Some theories within this class are ruled out, while others may fit within the constraints. Theories of another class, say, affine theories, may or may not fit the constraints. In other words, the experiments do not rigorously exclude all theories of a given type. On the other hand, the better the accuracy, the harder it is going to be for a given candidate non-metric theory to accommodate the constraints.

MATZNER: In the latest papers by Moffat (Moffat and Woolgar 1988), he forms a dimensionless ratio by dividing L^2 by m. Perihelion precession then depends on the difference of this ratio for the Sun and Mercury, for instance. This makes this ratio a very hard thing to observe in solar system tests. Could you comment on this?

WILL: This latest result appears to be (at last) a proper treatment of the equation of motion of bodies in Moffat's NGT. Unfortunately, many of the effects then depend on the difference of L^2/m between various bodies, so if L^2 is proportional to m, as would be true approximately if it were proportional to baryon number, then the effects will vanish. Although the limit obtained by Krisher (1987) from dipole gravitational radiation also depends on this difference, the limit may be interesting because the relativistic nature of the neutron star in 4U 1820-30 alters the value of L^2/m. I have recently noticed that the electromagnetic field equations in NGT violate EEP, so that it may be possible to place a very interesting limit on L^2/m for the Earth alone using the recent Galileo free-fall experiment with uranium and copper. Stay tuned for further details.

SHAPIRO: Has there been any independent corroborations of the solar-oscillation mode identifications made by Hill and his collaborators in their estimate of J_2 from their solar data? Would you agree that future solar oscillation experiments will solve the problem of J_2?

WILL: Unfortunately I am far from an expert in the subject of solar oscillations, so my discussion of the published results tends to be non-critical. Since we now have almost 10 years of data, and several published values for J_2, I would urge one of the experts in the field to perform a critical review of the published results. This may go some way toward answering whether this technique can confidently pin down (or has already pinned down) J_2, say to the level of 10^{-7}, or whether it could even reach the level of 10^{-8}, and thereby compete with proposals for a Mercury orbiter or Starprobe. Until then, it is difficult for neophytes like me to judge, say, Hill's mode identification or eigenfunction inversion technique against any one else's.

GRAVITATIONAL CONSEQUENCES OF MODERN FIELD THEORIES

GARY T. HOROWITZ
Department of Physics
University of California
Santa Barbara, CA 93106

I would like to discuss some gravitational consequences of certain extensions of Einstein's general theory of relativity. These theories are not "alternative theories of gravity" in the usual sense. I will assume that general relativity is the appropriate description of all gravitational phenomena which have been observed to date.

Nevertheless, there at least two reasons for considering extensions of general relativity. The first and most important is the fact that general relativity does not incorporate the observed quantum mechanical nature of matter and non-gravitational forces. The second is the common belief that at a fundamental level, gravity should be unified with the other forces of nature. In particular, this will require that gravity itself be described quantum mechanically. It is usually thought that since macroscopic amounts of matter are required for gravity to be detected and classical physics is a good approximation for macroscopic objects, these extensions of general relativity will not be observable. As I will try to explain, this is not necessarily the case.

The effects of combining gravity with quantum matter fields have been extensively studied. The most important consequence of this investigation is the following: *black holes are not really black.* This is Hawking's remarkable prediction that black holes emit thermal radiation at a temperature $T = 10^7 (M_\odot/M)^\circ K$ where $M_\odot$ is the mass of the sun and M is the mass of the black hole. For solar mass black holes this is much less than the 3° cosmic background radiation. But if much smaller black holes were formed at the time of the Big Bang, they would radiate away their mass and eventually evaporate. In particular, a 10^{15} gm black hole would be in the final stages of evaporation today, having radiated most of its mass in gamma rays. This prediction indicates a deep theoretical connection between general relativity, quantum mechanics, and thermodynamics. The observation of evaporating black holes would surely represent a major advance in physics.

Another consequence of combining general relativity with more realistic theories of matter is *cosmic strings.* These are very thin (diameter approximately 10^{-26} cm) tubes of energy that were possibly formed in a phase transition in the early universe. If they exist, they would have a number of important gravitational effects. First they could act as seeds for galaxy formation. This would avoid the difficulty of reconciling the observed isotropy of the cosmic background radiation with the amplitude of perturbations needed at the time of decoupling to evolve to form galaxies. Second, cosmic strings could act as gravitational lenses. Light from a single quasar or distant galaxy, which passes above and below a cosmic string, could be focused so that an earth-based observer sees multiple images. In fact the most likely way of detecting cosmic strings is believed to be through the observation of a series of multiple images. Finally, cosmic strings will contribute to the gravitational radiation background, since this is their main source of energy loss. This aspect of cosmic strings has been discussed by Schutz and Matzner at this meeting.

Now let us turn to the idea of unification. This work began in the 1920's with Kaluza and Klein. They showed that the two forces known at that time — gravity and electromagnetism — could be unified by postulating that spacetime had five dimensions. They argued that we only observe four because one dimension is a circle of very small radius. With the discovery of the strong and weak nuclear forces, this idea has been extended and is now incorporated in the currently popular theory known as *superstrings*. (Despite the similarity in name, these strings are quite different from ones discussed above.) This new theory not only unifies gravity with the other known forces but also with the matter. The different elementary particles and forces all arise from different excitations of a single string. At the same time, this theory is probably the first in which gravity is consistently treated quantum mechanically.

The theory of superstrings predicts that the dimension of spacetime is 10. The six dimensions we do not see are curled up into a very small ball. The size of this ball, as well as the size of the fundamental strings, is determined from Newton's constant G, Planck's constant h, and the speed of light c. This scale is known as the Planck length and is $L_P = (Gh/c^3)^{1/2} = 10^{-33}$ cm. Clearly direct observation of these extra dimensions or the strings themselves will be difficult! However, there are some intriguing new effects which may be observable at much larger distances. These effects have not yet been thoroughly investigated. Preliminary studies have yielded qualitative rather than quantitative results due to the difficulty of extrapolating over so many orders of magnitude.

Possible gravitational consequences of superstring theory:

...Short Distance Violations of the Weak Equivalence Principle (WEP). Recall that the WEP states that objects of different composition will accelerate at the same rate in a gravitational field. In the theory of superstrings, at large distances one recovers general relativity, but also an extra scalar field called the dilaton. The mass of the dilaton is known to be much less than the Planck mass ($M_P = (hc/G)^{1/2} = 10^{19}$ GeV), but has not yet been calculated reliably. If it is zero, then the dilaton couples gravitationally just like a Brans-Dicke scalar, but couples to matter in a way which violates the WEP. Since the relevant coupling constants are expected to be of order one, this is in serious conflict with the Etövös-type experiments. Furthermore, the theory predicts a unique value for the Brans-Dicke coupling constant of minus one which is also clearly ruled out by observation. For both of these reasons the dilaton must have a non-zero mass and hence a finite range. Current laboratory Etövös experiments can set lower limits on the mass of about 10^{-6} eV. However, at distances comparable to the Compton wavelength of the dilaton, one would expect violations of the equivalence principle.

More generally, one can show that theories with extra spacetime dimensions generically have scalar fields that violate the weak equivalence principle. Thus, this principle is **NOT** a fundamental building block of unified gravitational theories, but only an approximate result which is valid at large distances.

...Time Variation of the Coupling Constants. The low-energy coupling constants (gravitational, electromagnetic, *etc.*) depend on the dilaton and the size of the internal six dimensional space. In a general cosmological context, one expects these quantities to change with time. Thus, one expects the coupling constants to evolve. Once again the actual rate of change is difficult to calculate reliably.

Turning the argument around, current observational limits on their rate of change can also set limits on the masses of the appropriate particles.

DISCUSSION

PAIK: You said that the dilaton mass (Mp) is bigger than 10^{-5} eV, which corresponds to a range less than 1 cm. How do you set such a limit from the Eotvos experiment? Did you get the limit from the laboratory inverse square law? It depends on the strength of dilation coupling a. Is a of the order of unity?

HOROWITZ: Yes for both questions. The coupling for dilaton is expected to be of the order of unity. In principle, this can be calculated from the theory, but we need to better understand several non-perturbative effects (such as supersymmetry breaking) before such calculations can be made.

TALMADGE: It is my understanding that laboratory $1/r^2$ tests set limits on a only for the range from 0.1 cm to a few meters. Why then do you exclude the distance scales larger than a few meters? Does the theory predict a specific value for the relative strength of the new coupling to Newtonian gravity? Could it in principle?

HOROWITZ: There are, of course, other tests of the inverse square law for distances larger than a few meters. These experiments have set upper limits on the strength of new forces of about 1% that of gravity. Since the dilaton is expected to couple with the same strength as gravity, its range must be shorter.

TOWARD HIGHER ORDER TESTS OF THE GRAVITATIONAL INTERACTION

KEN NORDTVEDT
Montana State University
Bozeman, MT 59717

Analyses and interpretations of experiments which test post-Newtonian gravity are usually done within the assumption that gravity is a metric field phenomenon – a manifestation of space-time geometry. This, however, is unnecessary and one can start at a more primitive level – that there simply exists a phenomenological, gravitational, many-body equation of motion which must be determined by a package of observations. In fact, over the last couple decades, a diverse collection of solar system interbody tracking observations, supplemented by data from the binary pulsar system PSR 1913 + 16, has completely mapped out the first post-Newtonian order (order $\frac{1}{c^2}$ gravitational equations of motion for photons ($\vec{r}_p$) and particles ($\vec{r}_j$)), yielding (in a particular coordinate system):

$$\frac{d^2\vec{r}_p}{dt^2} = G\sum_j \frac{m_j}{r_{pj}^3}\left(2\vec{r}_{jp} - 4\vec{r}_{jp}\cdot\hat{c}\,\hat{c}\right)$$

$$\frac{d^2\vec{r}_i}{dt^2} = G\sum_j \frac{m_j \vec{r}_{ji}}{r_{ij}^3}\left[1+\frac{1}{c^2}\left(v_i^2 + 2v_j^2 - 4\vec{v}_i\vec{v}_j - \frac{3}{2}(v_j\cdot\hat{r}_{ij})^2\right)\right]$$

$$+\frac{G}{c^2}\sum_j \frac{m_j}{r_{ij}^3}\left[4\vec{r}_{ij}\cdot\vec{v}_i\vec{v}_i + 3\vec{r}_{ij}\cdot\vec{v}_j\vec{v}_j - 4\vec{r}_{ij}\cdot\vec{v}_i\vec{v}_j - 3\vec{r}_{ij}\vec{v}_j\vec{v}_i\right]$$

$$+\frac{G^2}{c^2}\sum_{jk} m_j m_k\left[\frac{\vec{r}_{ik}}{r_{ik}^3}\left(\frac{4}{r_{ij}}+\frac{1}{r_{jk}}\right) - \frac{(7/2)\vec{r}_{jk} + (1/2)\vec{r}_{jk}\cdot\hat{r}_{ij}\,\hat{r}_{ij}}{r_{jk}^3 r_{ij}}\right]$$

Actually, the photon equation of motion is of Newtonian order: the high speed of photons ($v\sim c$) produces effects which are post-Newtonian — proportional to inverse powers of c. Each of the many observations constrains some linear combination of the numerical coefficients which appear in the equations of motion (including some coefficients which are zero and don't appear above); the coefficients in the end becoming empirically fixed to accuracies which range from a percent to a part in 10^7.

After the fact, using these empirically determined equations of motion, along with some observed properties of nongravitational clocks and rulers and conservation laws for energy, momentum and angular momentum, a post-Newtonian Lagrangian can be constructed, a geometrical space-time metric field conceptual interpretation can be developed, Lorentz invariance of the equations of motion can be shown (the same equations can be used in all cosmic inertial frames), and the equations of motion are found to agree with the predictions of Einstein's gravitational theory, General Relativity, within experimental accuracy.

These fully mapped-out equations of motion include the so-called "gravitomagnetic" terms — those three terms above that are proportional to both $\vec{v_i}$ (velocity of body being accelerated) and $\vec{v_j}$ (velocity of other source bodies). Since the gravitomagnetic terms have such a historically interesting and conceptually unique interpretation (that moving matter "drags" our very inertial reference frames), a variety of experiments have been proposed to directly see these components (without participation of other components) of the above gravitational equations of motion (Ciufolini, Everitt, Mashoon, in these proceedings).

Future work in first post-Newtonian order gravity appears to primarily be two-fold: to improve the accuracy of the map of these first post-Newtonian order equations of motion; and to perform new redundant tests of the equations. A failure to confirm these equations in new contexts would require a radical revision of our basic physical assumptions.

At higher levels of precision, second post-Newtonian order $\left(\text{order}\,\frac{1}{c^4}\right)$ corrections must be made to the gravitational interaction and testing gravitational theory.

An indication that we are beginning to need $2PN$ order gravity, in order to properly interpret solar system phenomena, is the remarkable alignment of the Sun's spin axis (about 5 arc-degrees) with the solar system angular momentum vector after 4.5 billions years of existence. This implies that the Newtonian gravitational interaction is spatially isotropic (directionally independent) to a part in 10^{13} accuracy (Nordtvedt 1987) even in the presence of asymmetries in the solar system's environment — a nearby galaxy with gravitational potential $\left(\frac{GM}{c^2R}\right)_{galaxy} \sim 10^{-6}$ and a speed of the solar system (w) relative to the cosmic rest frame $\left(\frac{w}{c}\right)^2_{solar\ system} \sim 4 \cdot 10^{-6}$. The fact that both the above dimensionless environmental numbers, when squared, exceed 10^{-13} means that the spin axis history of the Sun requires the $2PN$ order gravitational interaction for its proper analysis, and in fact imposes constraints on the structure of $2PN$ order gravity.

Second-order light deflection experiments are being studied (Reasenberg in these proceedings) which will probe $2PN$ order gravity.

Since the binary pulsar system PSR 1913+16 is believed to be a pair of neutron stars in close orbit, and since the internal gravity of neutron stars is very strong, $\left(\frac{GM}{c^2r}\right)_{neutron\ star} \sim 0.1$, it is plausible that second (and higher!) post-Newtonian order gravity would be relevant to understanding the pulse-arrival-time data from such systems. We developed a formalism to examine that question (Nordtvedt 1985) in which internal gravity of celestial bodies was treated nonperturbatively while interbody orbital dynamics was treated at first post-Newtonian order. We found that under simple assumptions, *e.g.*, Lorentz invariance of the gravitational interaction, *etc.*, and accepting the first post-Newtonian order experimental constraint on the parameterized post-Newtonian (PPN) coefficients, $(4\beta - 3 - \gamma)_{exp} \approx 0$, then the equations of motion of the binary pulsar system become identical to the above exhibited $1PN$ order equations of motion for test bodies: *i.e.*, the orbital dynamics of

compact celestial bodies with strong internal gravity are not efficient probes of $2PN$ order gravity.

Consequently we have begun development of a theoretical framework for analysis and design of $2PN$ order gravitational experiments and observations. At this initial state, we assume properties of gravity which have strongest empirical support (that there exist conservation laws for energy, momentum, and angular momentum, and that the gravitational interaction is Lorentz invariant), but otherwise we start with the most general possible phenomenological $2PN$ order $\left(\text{order}\,\frac{1}{c^4}\right)$ gravitational many-body Lagrangian as a supplement to the $1PN$ order equations of motion exhibited above. A main goal of this framework is to discover what new degrees of freedom can exist in the $2PN$ order gravitational interaction under these assumptions, and what types of experiments could measure these new aspects of gravity. This framework assumes no particular theory of gravity; it is a framework for testing gravitational theory generally.

At $2PN$ order the gravitational Lagrangian consists of four, dimensionally speaking, generic classes of terms:

$$L^{2PN} = \frac{1}{16}\sum_i \frac{m_i v_i^{\,6}}{c^4} + L_2\left(\frac{Gm^2v^4}{c^4 r}\right) + L_3\left(\frac{G^2m^3v^2}{c^4 r^2}\right) + L_4\left(\frac{G^3m^4}{c^4 r^3}\right)$$

with m, v and r representing body masses, body velocities, and interbody distances. $L_{2,3,4}$ can be thought of as being two-body, three-body, and four-body interactions, respectively, although all these terms contribute to systems consisting of only two bodies.

We have found that $L_2\left(\frac{Gm^2v^4}{c^4 r}\right)$ is uniquely determined by $1PN$ order gravity plus the assumption of Lorentz invariance — no new degrees of freedom appear in this part of the $2PN$ order Lagrangian (Benacquista and Nordtvedt 1988). Under the same assumptions, $L_3\left(\frac{G^2m^3v^2}{c^4r^2}\right)$ has been found to contain only one new degree of freedom. This new parameter could be measured by a second order light deflection experiment. While $L_4\left(\frac{G^3m^4}{c^4 r^3}\right)$ cannot be constrained by Lorentz invariance, consistency with the isotropy observations of the Newtonian gravitational interaction suggests that L_4 will have two new degrees of freedom. The challenge facing the experimental and observational future in gravity is to find ways to measure these new aspects of gravity which will contribute to $2PN$ order body dynamics.

REFERENCES

Benacquista, M., and Nordtvedt, K. 1988, *Astrophys. J.*, **328**, 599.
Nordtvedt, K. 1985, *Astrophys. J.*, **297**, 390.
Nordtvedt, K. 1987, *Astrophys. J.*, **320**, 871.

DISCUSSION

SHAPIRO: Can you explain in more detail the sense in which you infer post Newtonian isotropy from the (small) inclination of the sun's spin angular momentum vector to the solar system's angular momentum vector?

NORDTVEDT: If the gravitational interaction between the matter in the oblate, rotating Sun is not spatially isotropic to a part in 10^{13}, self-torque would have precessed the Sun's axis by more than its present alignment during the past 4.5×10^{9} years. Since 10^{-13} is a smaller number than the square of the galactic potential or the fourth power of the Sun's speed through the cosmos, second post-Newtonian order gravity is constrained by this observation.

THE INVERSE-SQUARE LAW AND QUANTUM GRAVITY

MICHAEL MARTIN NIETO, T. GOLDMAN,
AND RICHARD J. HUGHES
Theoretical Division, Los Alamos National Laboratory,
University of California, Los Alamos, New Mexico 87545

I'm going to describe a program which Terry Goldman, Richard Hughes, and I are involved in at Los Alamos. As a matter of fact, it started 7 years ago when Terry and I proposed measuring the gravitational acceleration of antiprotons. We came to this idea from a particle physics point of view. I'm going to explain what I consider to be that point of view, starting with some history of physics over the last 200 years.

At the beginning of the 1800's, there were understood to be three forces: electricity, magnetism, and gravity. Through the work of Faraday, Orsted, and Maxwell, we realized that electricity and magnetism are two aspects of the same force. So, there were two forces: electromagnetism and gravity. Around 1900, manifestations began to appear of what ultimately became known as the strong and the weak forces.

In the same period, Einstein put relativity into gravity in the form we discuss it today, general relativity. If you apply general relativity to Mercury in a power series expansion you get a $1/r^3$ force. But you do not say that this is a new, nongravitational force. You say that this is a new aspect of gravity which becomes manifest when you put in relativity.

Similarly, when quantum mechanics was applied to electromagnetism, we found that there were new aspects which appeared. This was not because we changed Maxwell's equations but because we put quantum mechanics into them. To me, the prime example is the Lamb Shift. In the 1930's, this was parametrized by something that was called the Uehling potential. Nobody said that the Uehling potential manifested a new force. It was a new aspect of electromagnetism which appeared when you brought quantum mechanics into it.

In this spirit, it is the prime goal of modern particle theory to try to unify all the forces of nature in a relativistic, quantum field theory. The work of Weinberg, Salam, and Glashow, in the 1960's and 1970's, resulted in the unification of the weak and the electomagnetic forces into what we now call the electroweak force. This theory was verified in the discovery of the W and Z particles at CERN. In this unification the Z particle and the photon are two aspects of the same object: one has a mass and one doesn't.

Independently, a model of the strong force was invented. It is called QCD, for Quantum Chromo Dynamics. It is still by itself. The hope was that we could unify QCD and the electroweak theory using the group SO(5). But one of the predictions of the theory was that the proton would decay with a lifetime $<10^{32}$ years. To test this idea, people, instead of taking one proton and waiting for 10^{32} years, decided to take 10^{32} protons and wait for 1 year. Unfortunately, they waited for more than 1 year and the protons still didn't decay. So, as it stands now, even though we wish we had a successful unified theory of the strong and the electroweak forces, we don't.

However, we particle physicists are undaunted. Even though we have not unified the strong and electroweak interactions, we already are trying to unify them

with gravity. Such theories are called theories of quantum gravity. One of the manifestations of these theories is that, as with electromagnetism, new gravitational effects arise simply because quantum mechanics is brought into gravity.

But how could things be different with these new quantum gravity theories? Before I answer that I must emphasize that none of these theories produce anything like the particle spectrum which you see. In fact, every time a new accelerator goes on, people first search for the expected new particles and then say, "Wait till the next accelerator." So, all of these concepts remain theories of theories. I'm pushing them, but I have to be honest. However, they all have tantalizing phenomenological features.

In general, in these theories, the spin-2 graviton has spin-0 and spin-1 partners. The partners may couple to fermions (and therefore violate the weak equivalence principle), and they may have a finite rest mass (and so violate the inverse-square law). There are many people who have put in a lot of work: Joel Scherk, Cosmos Zachos, and I could go on and on. But let me tell you what it all boils down to. One can parametrize the static potential as

$$V = -Gm_1m_2[\ 1 + (-/+)\ a\ e^{-v/r} + b\ e^{-s/r}\ ]\ /r\ . \qquad (1)$$

The first term is normal gravity. The second term is from the spin-1 graviphoton. It has the (−) sign for matter-matter interactions (overall repulsion) and the (+) sign (overall attraction) for antimatter-matter interactions. The graviscalar term is always attractive. For matter-matter interactions these two new forces could approximately cancel and yield a small effect. For matter-antimatter interactions the two new terms add, and so could produce a relatively large effect.

But, people often wonder, does a different gravitational acceleration for antimatter violate CPT? You might think so, that if you drop antimatter it has to fall the same as if you drop matter. But actually, CPT only tells you that if you drop an apple to the earth it will fall exactly as if you drop an antiapple to an antiearth. CPT doesn't tell you what happens if you drop an antiapple to the earth.

There are two schools of thought on all of the above arguments. The loyal opposition believes that there actually may be a new force of nature. They can argue that this is just like in the days when Einstein was trying to unify electricity and gravity. He couldn't do it because he didn't know about the weak and the strong forces, so he missed the boat. So too, this school would argue, the reason why we're having trouble unifying things is because there is a "fifth force" out there and we just haven't realized it before.

Of course, the school to which I belong says that if there are new forces of approximately gravitational strength, then they are new manifestations of gravity which arise because we're bringing quantum mechanics into it: if it's approximately of gravitational strength it's gravity. That's where I'm coming from. But you know, God didn't talk to me when he built this place. So, it could indeed turn out that there is a "fifth force" of nature. This is something which experiment and theory will have to settle.

So, what are the experimental indications? As to possible Principle of Equivalence violations, Jim Faller will be talking about this tomorrow. Let us just note that the recent tests of the Principle of Equivalence have all found, with one

notable exception, a null or very small signal. Contrariwise, there have been three recent tests of the inverse-square law, on scales of the order of hundreds of meters to perhaps as much as hundreds of kilometers. All of them have found an anomaly. This includes the Australian mine results, the Air Force tower experiment, and geophysical well-logging results. So, could it possibly be that there is a lack of violation of the Principle of Equivalence and not a violation of the inverse-square law? This entire question is very exciting right now.

I want to mention two ongoing Los Alamos experiments. One is the proposal to measure the gravitational acceleration of antiprotons at LEAR, the low energy antiproton ring at CERN. This is a "Galileo" experiment which measures the antiproton's time of flight (at 4° K) up a drift tube. The experiment is approved, is underfunded and undermanned, but is going along. Equipment is being built and hopefully we're on the floor in 1991. (A complementary experiment to measure gravity on positrons is being pushed by Bill Fairbank.) An experiment to test the inverse-square law was performed last summer in the Greenland Ice Sheet. A thin bore-hole gravity meter was lowered down the DYE-3 bore-hole, which is 2 kilometers deep. This experiment is now being analyzed and the results should come out August 1.

There are many related experiments which can be done in space. Most obvious are tests of Newton's Law. For scales on the order of 10's to 100's of kilometers one could do a precise orbit analysis of a lunar positional satellite, or even analyze LAGEOS or Starlette data to higher precision. Smaller-scale tests could be done in earth orbit.

But in any event, these are exciting times for gravity. Certainly I and my collaborators are excited.

REFERENCES

For references by the many people who have contributed to this field, see our articles:
Ander, M. E., Goldman, T., Hughes, R. J., and Nieto, M. M. 1988, *Phys. Rev. Lett.*, **60**, 1225.
Goldman,T., Hughes, R. J., and Nieto, M. M. 1986, *Phys. Lett. B*, **171**, 217.

DISCUSSION

SCHUTZ: In theories where antiparticles couple to gravity differently from particles, what happens to photons, which are their own antiparticles?

NIETO: The genesis of your question was raised by the old "anti-gravity" ideas studied in the 1950's. This one asked if one could have normal tensor gravity for matter, but exactly opposite gravity for "anti-matter", then you would have "likes attract" not "opposites attract".

Such a system would violate conservation of energy. In Morrison's gedanken experiment, you could create an antiproton-proton pair in the earth's field, raise it at no cost in energy, annihilate to photons, which gain energy following, and then create a new pair with added kinetic energy. In fact, this is a variation of Wigner's perpetual motion machine if change is not conserved.

For the quantum-gravity ideas, the tensor forces are normal, and you have no change in photon dynamics. The new vector piece has 'like repel' and no coupling to photons, so this is no problem. The scalar piece could or could not couple to photons and/or not violate the principle of equivalence, depending on the particular model. Therefore, although the models are mathematically consistent on this point, different models will have restrictions imposed upon them on the size of the effects allowed by experiment.

SHAPIRO: Can you particularize the limit on the ability to "maneuver" within grand unified theories as far as the lowest "acceptable" proton decay rate is concerned?

NEITO: The simplest, most obvious, and specifically predictive "Grand Unified Theory" was SU(5), which was to break down into SU(3)-color (the strong interactions) cross the SU(2) x SU(1), the electroweak theory. This is now ruled out by the lack of proton decay. The decay rate goes as X^{-4}, where X is the massive vector boson that converts quarks into leptons. The existence of a unified coupling constant then determines rather precisely what X must be since it is the scale where all the various interaction coupling constants become the unified coupling constant. The end result is that, even with optimistic theoretical "fudges", the proton lifetime must be less than 10^{32} years. The experimental limits are now significantly greater than this number. See, e.g., T. Goldman, Ad. Nucl. Phys. 18, 315 (1987), Sec. 7.

APPLIED GENERAL RELATIVITY

NEIL ASHBY
Department of Physics
University of Colorado
Boulder, Colorado 80309-0390

I. INTRODUCTION

In this paper we discuss important relativistic effects and issues which must be considered in the interpretation of current measurements such as ranging measurements to LAGEOS and to the moon, in the implementation of the Global Positioning System, in the synchronization of clocks near the earth's surface, and in the adoption of appropriate scales of time and length for the communication of scientific results.

II. FEATURES OF GENERAL RELATIVITY

We restrict our discussion to Einstein's General Theory of Relativity (GR). GR describes events in a four-dimensional, space-time manifold (with coordinates X^μ), in which the invariant interval ds between events separated by dX^μ is given in terms of the metric tensor $G_{\mu\nu}$ by:

$$-ds^2 = G_{\mu\nu} dX^\mu dX^\nu \quad \text{(summed on repeated indices).} \tag{1}$$

The interval ds has the following interpretations. First, a test particle in free fall, such as an earth-orbiting satellite, follows a geodesic path, along which ds is an extremum. Thus, equations of motion of bodies in free fall can be derived from a knowledge of the metric tensor. Second, the proper time elapsed on a standard clock (such as an atomic clock) in free fall through the interval dX^μ will be given by $|ds|$. Third, a pulse of electromagnetic radiation will travel along a null geodesic, $ds = 0$; this is another way of stating the constancy of the speed of light.

Also, ds is a scalar quantity, invariant with respect to arbitrary transformations of coordinates. Much of the calculation entailed in working out the implications of GR involves finding coordinates in which observations can be readily interpreted. Thus, along with the knowledge of a metric tensor, in a particular coordinate system, goes a procedure for interpretation of the theory.

III. BARYCENTRIC COORDINATES

Except for small structure effects to be mentioned later, solar system bodies can be described by an approximate point mass metric derived from Einstein's field equations by Eddington and Clark (1938). The metric tensor can be written in the following interesting form, with G_{00} accurate to order (V^4) :

$$G_{00} = -1 + 2\sum_A \frac{M_A}{|\vec{X} - \vec{X}_A| \left\{ 1 - \hat{N}\cdot\vec{V}_A \right\}} \Bigg|_{ret} - 2\left(\sum_A \frac{M_A}{|\vec{X} - \vec{X}_A|} \right)^2$$

(2)

$$-2\sum_A \frac{M_A}{|\vec{X} - \vec{X}_A|} \sum_B{}' \frac{M_B}{|\vec{X} - \vec{X}_B|} + 3\sum_A \frac{M_A V_A^2}{|\vec{X} - \vec{X}_A|}$$

where the retarded time is $T' = T - |\vec{X} - \vec{X}_A(T')|/c$. Thus, in the radiation gauge used for the solution of the field equations by Eddington and Clark, a retarded Lienard-Wiechert potential (Jackson 1975) appears. The other components are:

$$G_{0i} = -4\sum_A \frac{M_A V_A^i}{|\vec{X} - \vec{X}_A|}; \quad G_{ij} = \delta_{ij}\left(1 + \sum_A \frac{M_A}{|\vec{X} - \vec{X}_A|} \right) , \tag{3}$$

where $\vec{X}_A$, $\vec{V}_A$, and $\vec{A}_A$ are the position, velocity, and acceleration of the A^{th} mass, and a prime on a summation symbol means that terms which are indefinitely large are to be omitted. M_A is the Schwarzschild mass parameter of the A^{th} mass; velocities are measured in units of c. We make use of the abbreviation $R = |\vec{X}_A - \vec{X}_B|$ which is a function of X^0 because both $\vec{X}_A$ and $\vec{X}_B$ depend on X^0. We introduce the "normalized" or external part of the metric by defining the negative of the potential in the neighborhood of the earth's mass M_E due to external sources (the subscript E denotes quantities describing the earth):

$$U^{(e)} = \sum_A{}' \frac{M_A}{|\vec{X} - \vec{X}_A|} \equiv \sum{}' M_A/R_A; \quad U_e \equiv U^{(e)}\left(\vec{X} = \vec{X}_E\right) . \tag{4}$$

Using retarded time, expanding the retarded potential gives three retardation corrections in addition to the static potential:

$$\sum_A \frac{M_A}{|\vec{X} - \vec{X}_A| \left\{ 1 - \hat{N} \cdot \vec{V}_A \right\}} \Bigg|_{ret} =$$

(5)

$$\sum_A \frac{M_A}{|\vec{X} - \vec{X}_A|} \left\{ 1 + \frac{1}{2}\left[V_A^2 - (\vec{X} - \vec{X}_A)\cdot\vec{A}_A - (\vec{V}_A \cdot \hat{N}_A)^2 \right] \right\}$$

where the unit vector $\hat{N}_A$ is given by: $\hat{N}_A = (\vec{X} - \vec{X}_A) / |\vec{X} - \vec{X}_A|$.

One can see the origin of terms of interest arising from retardation of gravitational signals in this coordinate system. Observation of such terms would be of great interest as it would provide indirect evidence for the existence of gravitational waves.

The equations of motion have been derived in detail by Moyer (1981 a,b) and others and may be written:

$$A_A^k = -\sum_B{}' \frac{M_A X_{BA}^k}{R_{AB}^3}\left(1-4U_A+V_A^2-\sum_C{}'\frac{M_C}{R_{CB}}+2V_B^2-4\vec{V}_B\cdot\vec{V}_A\right.$$

$$\left.-\frac{3}{2}\frac{\left(\vec{X}_{AB}\cdot\vec{V}_B\right)^2}{R_{AB}^2}-\frac{1}{2}\vec{X}_{AB}\cdot\vec{A}_B\right)+4\sum_B{}'\frac{M_B\left(\vec{X}_{AB}\cdot\vec{V}_A\right)\left(V_A^k-V_B^k\right)}{R_{AB}^3} \qquad (6)$$

$$-3\sum_B{}'\frac{M_B\left(\vec{X}_{AB}\cdot\vec{V}_B\right)\left(V_A^k-V_B^k\right)}{R_{AB}^3}+\frac{7}{2}\sum_B{}'\frac{M_B A_B^k}{R_{AB}},$$

where:

$$\vec{X}_{AB}=\vec{X}_A-\vec{X}_B;\quad U_A=U^{(e)}\left(\vec{X}=\vec{X}_A\right);\quad \hat{N}_{AB}=\vec{X}_{AB}/R_{AB}. \qquad (7)$$

For the case of an earth-orbiting satellite such as LAGEOS, significant perturbations arise from the term with the coefficient of $-3/2$ (which arises from retardation in this picture). This particular term could give rise to accelerations as large as 4.1×10^{-8} meters/sec^2. The Newtonian solar tidal accelerations of LAGEOS are only 10^5 larger.

IV. LOCAL INERTIAL FRAME

It is natural to do numerical computations of planetary ephemerides in solar system barycentric coordinates, using the above equations of motion that include effects due to all solar system bodies and to post-Newtonian relativistic effects. However, most observations are made from the earth — a locally inertial, freely falling platform — and do not reveal the existence of such effects. The proper interpretation of barycentric coordinates in terms of measurable quantities is key.

Our approach is to construct a transformation of coordinates from barycentric to local inertial coordinates — normal Fermi coordinates (Manasse and Misner 1963; Ashby and Bertotti 1984, 1986). In these coordinates, apart from the gravitational effects due to the Earth's mass itself, one can demand that time be measured by a standard clock near the position where the observations are made. In contrast, the coordinate time variable in the Eddington-Clark metric is measured by a standard clock at rest at infinity. Also, one can demand that the spatial coordinates be measured by standard rods or, in other words, that lengths and times be related in such a way the electromagnetic signals propagate with the defined value of the speed of light, c = 299, 792, 458 meters/sec.

Referring to Figure 1, $X^{\mu}(s)$ specifies a world line G, a timelike solution of the geodesic equations of the mass M_E in the metric given by Eqs. (2 and 3), with infinite self-interaction terms omitted. Four mutually orthonormal vectors $\Lambda^{\mu}_{(\alpha)}$, $\alpha = 0,1,2,3$ are introduced which are carried parallel to themselves along G. The zeroth member of the orthonormal tetrad is the tangent vector to the geodesic. Given a field point $P(X^{\mu})$ near G, a spacelike geodesic S is constructed which passes through P and intersects G orthogonally at proper time $x^0 = s$ as measured on a standard clock falling along G. The tetrad forms the basis for coordinates in the (almost) locally inertial frame. The first stage of the construction is finding these basic vectors.

The second stage is calculation of the transformation equations themselves by means of:

$$X^{\mu}(P) = X^{\mu}(P_0) + \Lambda^{\mu}_{(i)}\, x^i - \frac{1}{2}\,\Gamma^{\mu}_{\alpha\beta}(P_0)\,\Lambda^{\alpha}_{(i)}\Lambda^{\beta}_{(j)}\,x^i x^j$$

$$- \frac{1}{6}\,\Gamma^{\mu}_{\alpha\beta,\gamma}(P_0)\,\Lambda^{\alpha}_{(i)}\,\Lambda^{\beta}_{(j)}\Lambda^{\gamma}_{(k)}\,x^i x^j x^k + O(x^4)\ . \tag{8}$$

Lower case letters x^i are used to denote coordinates in the local frame. The coefficients of x^i in Eq. (8) are evaluated at P_0 and are functions of s (or x^0) only. The coefficients of the third and higher order terms in Eq. (8) are obtained from the equation of the space-like geodesic S. Cubic and quartic terms are necessary in order to verify that the field equations are satisfied in the local frame.

The leading terms in the resulting coordinate transformations have simple physical interpretations and can be written as follows:

$$X^0 = \int K\ dx^0 + \vec{V}_E \cdot \vec{r} = X^0(P_0) + \vec{V}_E \cdot \vec{r} + \ldots \tag{9}$$

$$X^k = X^k_E\left(X^0(P_0)\right) + x^k\left(1 - U_e - \vec{A}_E \cdot \vec{r} - \frac{1}{6}\,U_{e,mn}\,x^m x^n\right)$$

$$+ \frac{1}{2}\,V^k_E\,(\vec{V}_E \cdot \vec{r}) + \Omega^{kj}\delta_{jm}x^m + \frac{1}{2}\,r^2\,A^k_E + \ldots \tag{10}$$

In the first term in Eq. (9), the factor K is given by:

$$K^{-1} = ds/dX^0\,\Big|_G = \sqrt{\left(-G_{\mu\nu}dX^{\mu}dX^{\nu}\right)} \simeq 1 - U_e - V_E^2/2 \tag{11}$$

and gives the rate at which proper time elapses on a standard clock falling along with the origin of coordinates, with respect to barycentric coordinate time. Both special and general relativity effects are incorporated in K. U_e, the negative of the potential at the position of the falling clock due to all sources except the earth, gives rise to a gravitational frequency shift, and the term in V_E represents the second-order Doppler shift of the moving clock.

The second term in Eq. (9) arises from the well-known breakdown of simultaneity. This term plays an extremely important role in the coordinate transformation. The factor $(1-U_e)$ in Eq. (10) represents an overall length scale change, due to the external gravitational potential. The term quadratic in the Earth's velocity in Eq. (10) represents Lorentz contraction, and the term involving the antisymmetric quantity Ω^{ij} represents a slow rotation (geodetic precession) of the inertial frame axes with respect to distant stars (of about 19 milliarcsecs per year).

To describe gravitational effects in the local frame, one must perform a tensor transformation of the components of the metric, where the necessary partial derivatives, $\delta X^{\alpha}/\delta x^{\mu}$, are obtained from the coordinate transformations. One must also substitute the transformations into the expressions upon which $G_{\mu\nu}$ depends. For example, in the quantity $\left| \vec{X} - \vec{X}_E(X^0) \right|$, which occurs in the earth's potential, it is assumed the field point $\vec{X}$ and the source point $\vec{X}_E(X^0)$ are evaluated simultaneously in barycentric coordinates. The substitution must be done with exceptional care because of the relativity of simultaneity. In performing this substitution, one finds that Lorentz contractions and the relativity of simultaneity give rise to similar corrections, but that due to simultaneity is twice as large at that due to Lorentz contraction and is of the opposite sign. One finds:

$$\frac{2M_E}{\left| \vec{X} - \vec{X}_E(X^0) \right|} = \frac{2M_E}{r}\left\{ 1+U_e+\vec{r}\cdot\vec{A}_E/2+\left(\vec{r}\cdot\vec{V}_E/r\right)^2/2 \right\} . \qquad (12)$$

The term in U_e arises from rescaling of lengths, the term in V_E from a combination of simultaneity breakdown and Lorentz contraction, and the term in A_E from spatial curvature (quadratic terms in the transformation of coordinates).

There are a number of additional contributions to g_{00} which are proportional to $2M_E/r$. These are as follows:

(1) An overall multiplicative factor K^2 contributes an additional $(K^2 - 1) \times 2M_E/r \simeq (2U + V^2)\, 2M_E/r$;

(2) Nonlinear velocity correction terms to the masses which remain in G_{00} in addition to the velocity terms in the retarded potential of $3M_E V_E^2/r$;

(3) A cross-term between the external potential and the earth's potential in the squared potential term in G_{00} of $-4M_E U_e/r$;

(4) Nonlinear interaction terms in G_{00} of $-2M_E U_e/r$;

(5) Contributions from "magnetic" terms, G_{0i} of $-8M_E V_E^2/r$; and

(6) Contributions from G_{ij} of $+2M_E V_E^2/r$.

Collecting all the terms, we obtain:

$$\frac{2M_E}{r}\left\{1-\frac{1}{2}\left[V_E^2-\vec{r}\cdot\vec{A}_E-\left(\vec{r}\cdot\vec{V}_E/r\right)^2\right]\right\}\ . \qquad (13)$$

This result must now be combined with the expansion of the retarded potential, Eq. (5). It is easily seen that all corrections cancel, leaving just the static potential term $2M_E/r$ in the local frame. Thus, what appears to be a retarded potential from a moving source in barycentric coordinates appears as a static potential in a local inertial frame falling along with the mass.

Obtaining the metric tensor in the local frame by transformation is complicated; it has been illustrated above for a term of one type. This has only been carried out for a restricted class of models because of the complexity of the calculations. In the general case, one can calculate the terms linear in x^k in the local frame and find that there are about 3 dozen terms, of 16 different types, all of which cancel out. This is as one would expect on the basis of the principle of equivalence, according to which gravitational forces due to distant bodies can be transformed away locally (*i.e.*, at the origin of local coordinates), by transforming to a freely falling inertial frame.

For a model in which one considers the earth to be falling around the sun (of mass $M_\odot$) in a circular orbit, the terms quadratic in local spatial coordinates can be calculated. The contributions to g_{00} consist of: a Minkowski term, the Newtonian potential term, a contribution from the nonlinear Schwarzschild field of the earth, Newtonian solar tidal terms, nonlinear earth-sun interaction terms, nonlinear solar tides due to interaction between the sun and the earth, and higher order solar tides. The spatial part of the metric in the local frame has the usual spatial curvature term due to the earth, plus solar tidal corrections. The g_{0i} terms contribute magnetic effects.

Calculations have also been performed using the PPN metric with parameters β, γ, $\zeta 1$, and $\zeta 2$ (Shahid-Saless and Ashby, in preparation). These give rise to some interesting effects involving shifts of the center of mass of the earth-sun system. The elliptical orbit case of the earth has also been treated, assuming, however, that the earth can be treated as a test particle so certain types of nonlinear interactions can be neglected. To verify the cancellations in more realistic cases requires considerable calculation. Computer algebra programs help some, but there is a tendency for such programs to fill up memory and fail in working on this problem.

V. EQUATIONS OF MOTION

Equations of motion can be derived from the local metric in a straightforward way. Here, we shall give only estimates of the orders of magnitude of the resulting accelerations of an earth-orbiting satellite caused by post-Newtonian effects. In evaluating the orders of magnitude, it is assumed that the satellite orbit satisfies $v^2 \simeq c^2 M_E/r$. For LAGEOS $r/10^9\,\mathrm{cm} \simeq 1.2$.

TABLE 1

ESTIMATES OF ACCELERATIONS OF AN EARTH SATELLITE DUE TO RELATIVITY THE MAGNITUDES OF THE ACCELERATIONS DUE TO NEWTONIAN FORCES OF ATTRACTION TO EARTH, AND THE SOLAR TIDES, ARE GIVEN FOR COMPARISON (N. ASHBY AND B. BERTOTTI 1984).

SOURCE	MAGNITUDE	
Newtonian potential	c^2M_E/r^2	$\simeq 4\times10^2[(10^9\,\text{cm})/r]^2\ \text{cm/sec}^2$
Solar tides	$c^2M_{\odot}r/R^3$	$\simeq 4\times10^{-5}[r/(10^9\,\text{cm})]\ \text{cm/sec}^2$
Nonlinear earth field	$c^2M_E^2/r^3$	$\simeq 2\times10^{-7}[(10^9\,\text{cm})/r]^3\ \text{cm/sec}^2$
Nonlinear solar tides	$c^2M_{\odot}^2r/R^4$	$\simeq 4\times10^{-13}[r/(10^9\,\text{cm})]\ \text{cm/sec}^2$
Solar "magnetic terms"	$c^2\sqrt{[M_{\odot}^3M_Er/R^7]}$	$\simeq 8\times10^{-13}\sqrt{[r/(10^9\,\text{cm})]}\ \text{cm/sec}^2$
Earth-sun interaction	$c^2M_{\odot}M_E/R^3$	$\simeq 2\times10^{-14}\ \text{cm/sec}^2$

Note the relativistic perturbations are many orders of magnitude smaller than first calculated in the barycentric frame. This is because of the cancellations which occur upon transforming to a freely falling coordinate system. Rubincam (1977) has studied the effect of the nonlinear earth field.

The above relativistic orbital perturbations are so small that they cannot be expected to significantly affect LAGEOS's orbit. However, the nonlinear solar tidal term grows with distance from the earth and is much larger at the orbit of the moon. Combining the effects of this perturbing term on semimajor axis of the moon, eccentricity of the moon, and on the moon's mean motion, gives rise to a net perturbation on the distance between earth and moon of :

$$\delta r \simeq 4.4\ \text{cm} \times \cos(2f_M + 2\omega - 2f_E) \tag{14}$$

where f_M and f_E are the true anomalies of the moon and of the earth, respectively. This effect is unfortunately obscured by its high correlation with effects due to the solar tides themselves.

A more interesting set of effects, which have not yet been fully explored analytically, arise from multipole contributions to the earth's field. The leading quadrupole contribution is about 10^{-3} of the main monopole term and relativistic corrections arising when this quadrupole is viewed as moving in the barycentric frame can be expected to be 10^{-8} smaller, thus such relativistic accelerations can be estimated to be about $4 \times 10^{-9}\ \text{cm/sec}^2$ for LAGEOS, which is significant. Inclusion of such effects results in significant improvement in fitting the ranging data for LAGEOS (Ries, private communication).

VI. CHOICE OF TIME COORDINATE—TDT

Further transformations must be made since time standards laboratories having clocks used to define the SI second are on earth's surface, subject to additional motions due to earth rotation, and to the full gravitational potential of the earth including higher order multipole contributions to the potential.

Since the geoid is a surface of gravitational equipotential in the earth-fixed rotating frame, atomic clocks at rest on the geoid on the rotating earth all beat at the same rate. If one compares a clock near the pole with one on the equator, one finds that the one nearer the pole is close to the earth's center and is therefore beating more slowly due to a gravitational redshift effect. However it is also closer to earth's rotation axis and moving more slowly due to earth's rotation, and is subject to less time dilation (second-order Doppler shift). These effects cancel on the geoid.

The rate of a standard reference clock falling along the geodesic G, with rate correction given by the factor K in Eq. (11), does not incorporate the effects due to earth's mass and rotation. An additional correction is needed to obtain a new coordinate time x^0_{SI}, corresponding to the definition of the SI second. This is given by:

$$\frac{dx^0_{SI}}{dx^0} = 1 - \frac{1}{2}\frac{M_E}{a_1}(1 + J_2/2) - \frac{1}{2}(\omega a_1/c)^2 \qquad (15)$$

where a_1 is the equatorial radius of the earth. Then, apart from periodic terms,

$$\frac{dx^0_{SI}}{dX^0} = 1 - \frac{M_E}{2a_1c^2}(1 + J_2/2) - (\omega a_1/c)^2/2 - U_e - V_E^2/2 \equiv 1 - L \qquad (16)$$

where $L \simeq 1.55 \times 10^{-8}$; Hellings (1986) has given a more complete discussion of this. Barycentric Dynamical Time (TDB) runs at the same average rate as the SI second, so $X^O_{TDB} = (1 - L)X^O$. Thus TDB clocks beat at the same average rate as earth-borne clocks, from the point of view of an observer in the barycentric system. The TDB clocks beat more slowly, by the factor 1–L, than coordinate clocks in the Eddington-Clark metric. Therefore, to maintain a universally defined numerical value for the speed of light c, the length unit in TDB coordinates must be physically longer than the length unit in EC coordinates. Then since $(GM/c^2)_{TDB}$ represents a physical length as measured using a TDB meter stick, the numerical value of $(GM/c^2)_{TDB}$ will be less than it is in EC coordinates. But the speed of light, c, is the same in the two unit systems, so $(GM)_{TDB}$ $(1 - L)\ (GM)_{SI}$.

An outstanding issue is the definition of TDT — "terrestrial dynamical time." The problem is to define a terrestrial time scale which is as closely related to TAI in rate as is possible. Problems include how to specify the position of the master reference clock for the TDT (the geocenter is preferred), how to specify the rate of TDT in relation to TAI, and how to initialize the TDT clock since its position is not that of any clock contributing to TAI. Some synchronization convention must be adopted to resolve ambiguities.

VII. RELATIVISTIC EFFECTS IN THE GLOBAL POSITIONING SYSTEM

This area of application has been discussed elsewhere (Hellings 1986) so only a summary of the relativistic effects is given here. For clocks in GPS satellites or on the earth's surface, it is useful to synchronize to agree with hypothetical clocks synchronized in the local inertial frame. There are three residual relativistic

effects: second-order Doppler frequency shifts of moving clocks, gravitational frequency shifts, and the Sagnac effect.

To the readings of each atomic clock, systematic corrections can be applied based on the known positions and motions of the clocks, such that, at each instant, the coordinate time thus produced agrees with the reading of a fictitious standard clock with which it instantaneously coincides and which is at rest in the local inertial frame. GPS coordinate time is thus generated by systematically modifying the proper time elapsed on standard clocks.

Standard clocks on the earth's surface provide the reference rate. Due to gravitational potential and motional effects, clocks in the satellites require a fractional rate offset correction having the value:

$$\frac{3GM_E}{2ac^2} - \frac{GM_E}{a_1c^2}(1 + J_2/2) - (\omega a_1/c)^2/2 \simeq -4.465 \times 10^{-10} . \qquad (17)$$

In order for the SV clock to appear to an observer on the ground to beat at the chosen frequency of 10.23MHz, the SV clocks must be offset so that, to an observer in the SV rest frame, the frequency in $10.23 \times (1-4.465 \times 10^{-10})$MHz = 10.22999999543MHz.

An additional variable correction term, arising from a combination of gravitational frequency and second-order Doppler shifts in case the SV orbit is not circular, must be applied to the SV cock to yield GPS coordinate time:

$$\Delta t_{SV} = +4.4428 \times 10^{-10} \frac{\text{sec}}{\sqrt{\text{meter}}} e\sqrt{a} \sin E(t) \qquad (18)$$

where e is the orbit eccentricity and E is the eccentric anomaly.

For a standard clock transported near the earth's surface, the following correction must be applied:

$$\Delta t' = \int_{path} (ds/c) \left[1-(\phi-\phi_0)/c^2 + (v'/c)^2/2 \right] + 2\omega A'_E/c^2 \qquad (19)$$

where primed quantities are measured in the earth-fixed rotating frame. This gives the prescription for correcting the atomic clock reading $\int ds/c$ to account respectively for gravitational frequency shifts, second-order Doppler shifts, and the Sagnac effect. For clocks near the Earth's surface, $\phi-\phi_0 \simeq gh$, where g is the acceleration of gravity and h is the height above the geoid. The term $(v'/c)^2/2$ corrects for time dilation of clocks moving relative to the ground, and the last term expressing the Sagnac effect is equal to $2\omega A'_E/c^2$, where A'_E is the equatorial projection of the area swept out by the position vector $\vec{r}'$ of the clock in the rotating frame.

For synchronization by means of an electromagnetic signal, ds vanishes along the path. The elapsed coordinate time during propagation of the signal is:

$$\Delta t' = \int_{path} d\sigma' \left[1-(\phi-\phi_0)/c^2 \right] + 2\omega A'_E/c^2 , \qquad (20)$$

$$\Delta t' = \int_{path} d\sigma' \left[1 - (\phi - \phi_0)/c^2\right] + 2\omega A'_E/c^2 , \qquad (20)$$

where $d\sigma'$ is the increment of proper distance along the path of the signal and A'_E is the equatorial projection of the area swept out by the position vector of the electromagnetic pulse in the rotating frame. In the above expressions,

$$\phi - \phi_0 = -\frac{M_E G}{r}\left[1 - J_2 (a_1/r)^2 p_2(\cos\theta)\right] - (\omega r' \sin\theta)^2/2 + \frac{GM_E}{a_1}(1 + J_2/2) + (\omega a_1)^2/2 . \qquad (21)$$

In GR, the same Sagnac correction terms arise whether synchronizing clocks by slow transport of portable clocks or by transmission of electromagnetic signals in the rotating frame.

REFERENCES

Ashby, N. and Allan, D. W. 1979, *Radio Science*, **14**, 649.

Ashby, N. and Bertotti, B. 1984, *Phys. Rev. Letters*, **52** (7), 485.

1986, *Phys. Rev.* D34, 2246.

Eddington, A. and Clark, G. R. 1938, *Proc. Roy. Soc. London Ser.*, **A166**, 465.

Hellings, R. W. 1986, A. J., 91, 650.

Jackson, J. D. 1975, *Classical Electrodynamics*, 2nd Ed., (Wiley & Sons, New York), 654 ff.

Manasse, F. K. and Misner, C. W. 1963, *J. Math. Phys.*, **4**, 735.

Moyer, T. D. 1981a, *Cel. Mech.*, **23**, 33.

1981b, *Cel. Mech.*, **23**, 57.

Rubincam, D. 1977, *Cel. Mech.*, **15**, 21.

Shahid-Saless, B. and Ashby, N. *Phys. Rev.* (to be published).

DISCUSSION

NIETO: In the case that you have a monopole plus J_2 representing the earth, what is the motion of the geocenter about the geodesic?

ASHBY: The geocenter wobbles about a timelike geodesic with an amplitude of about a meter.

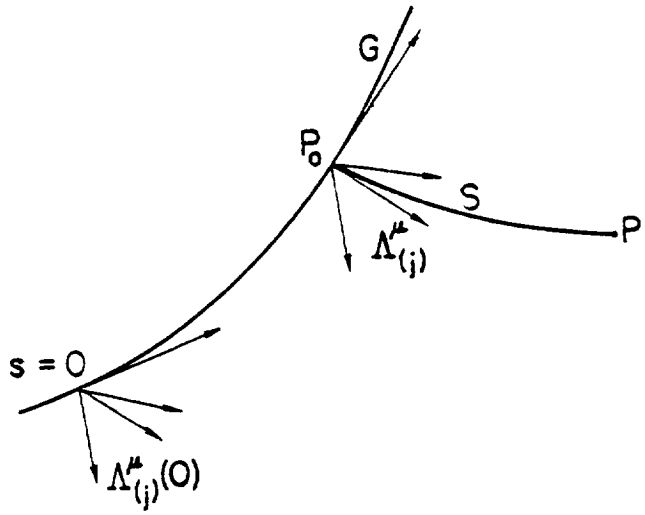

FIG. 1.—Diagram showing the local inertial frame falling freely along the geodesic G. The space-like geodesic S is constructed by dropping a geodesic from the field point P to P_0, that intersects G orthogonally.

ADVANCED DOPPLER TRACKING EXPERIMENTS

J. W. ARMSTRONG
Jet Propulsion Laboratory, Pasadena, CA 91109

ABSTRACT

The Doppler tracking method is currently the only technique available for broadband gravitational wave searches in the $\sim 10^{-4}$ to 10^{-1} Hz "low-frequency" (LF) band. In this paper I give a brief review of the Doppler method, a discussion of the main noise sources, and a review of experience with current spacecraft and the prospects for sensitivity improvements in an advanced Doppler tracking experiment.

I. RESPONSE OF DOPPLER LINK TO GRAVITATIONAL WAVES

The Doppler link between the earth and a distant spacecraft (thought of here as two free test masses separated by distance L) measures their relative dimensionless velocity $\Delta v/c = \Delta f/f_o \equiv y$ as a function of time, where Δf is the perturbation in the Doppler frequency and f_o is the nominal radio frequency of the link. An incident gravitational wave of strain amplitude h causes small perturbations in the tracking record. These perturbations are of order h in $\Delta f/f_o$ and are replicated three times in the Doppler data (Estabrook and Wahlquist 1975). The sum of the Doppler perturbations of the three pulses is zero; pulses with duration longer than ~L/c produce overlapping responses in the tracking record and the net response cancels to first order. The system has a passband to gravitational excitation: the low-frequency band edge is set by pulse cancellation to ~c/L, while thermal noises limit the high-frequency response to ~1/30 sec.

II. NOISE SOURCES

The main noise sources in spacecraft gravitational wave experiments are briefly summarized in this section. Schematic spectra of these sources are plotted in Figure 1. Spectra of actual data are given, *e.g.*, in Armstrong, Woo, and Estabrook (1979), Hellings *et al.* (1981), Anderson *et al.* (1984), Anderson and Mashhoon (1985), and Armstrong, Estabrook, and Wahlquist (1987). Transfer functions of the noises to the observable have been summarized by Armstrong (1988), along with signal processing techniques to exploit the differences between signal and noise signatures.

At frequencies higher than ~1/30 sec, thermal noise, mainly from finite signal-to-noise ratio on the downlink, dominates. This noise has a power spectrum of fractional frequency $\Delta f/f_o$ going as (Fourier frequency)^2. At lower frequencies, propagation noise and instrumental instability are important. Propagation noise results from radiowave phase scintillations imposed by irregularities in the media between earth and spacecraft (troposphere, ionosphere, solar wind). Charged particle scintillations (ionosphere and solar wind) dominate current generation (S-band radio link — $f_o \approx 2.3$ GHz) experiments (Wahlquist *et al.* 1977; Woo and Armstrong 1979). Plasma scintillation reaches a broad minimum in the antisolar direction to $\Delta f/f_o \sim (3 \times 10^{-15})$ (8.4 GHz/link radio frequency)^2. Plasma scintillation data have a "red" spectrum: $S_y \sim$ (frequency)$^{-0.7}$.

Water vapor fluctuations dominate tropospheric scintillation at microwave frequencies (Hogg *et al.* 1981; Resch *et al.* 1984; Treuhaft (this volume)), although fluctuations in the "dry component" (Shannon *et al.* 1979) may be important in future experiments. The index of refraction of tropospheric irregularities is independent of radio frequency (at microwave wavelengths), so that their level in $\Delta f/f_o$ is also independent of radio frequency. At the high elevation angles relevant to a gravity wave track, the effect, although highly variable, is typically $S_y \sim 10^{-25}$ (f/0.001 Hz)$^{-0.4}$ Hz^{-1} (Armstrong and Sramek 1982).

A fundamental low-frequency noise is instrumental instability (including clock noise), signal distribution instability, transmitter and receiver instability, mechanical stability of the antenna, spacecraft transponder stability, *etc.* Because the Doppler method is a "one-armed interferometer," frequency stability in the Doppler link is fundamental to achieving good sensitivity. The ground system aspects are discussed by Kursinski (this volume), and should enter at $\sim 5 \times 10^{-15}$ for Galileo-era experiments.

Nongravitational forces (examples are spacecraft buffeting, leaking thrusters, irregularities in the spacecraft spin rate for Doppler measurements using circularly polarized signals) are noise sources. In the Galileo-era the most important of these can be calibrated and removed with engineering telemetry to a level less than the propagation and instrumental noise levels.

III. CURRENT SENSITIVITY AND FUTURE PROSPECTS

Current generation long-duration experiments are limited by plasma scintillation noises to 1σ sensitivities $\sim 5 \times 10^{-14}$ for bursts, $\sim 1.5 \times 10^{-14}$ for broadband searches for sinusoids, and $S_y \sim 10^{-23}$ Hz^{-1} for the spectral density of a background. Using selected short-duration data sets with very low plasma noise (but still apparently plasma-limited, as evidenced by dual-frequency downlink data) sensitivities can be much better; see, *e.g.*, Figures 1 and 2 of Hellings *et al.* (1981). These levels of sensitivity can be compared with wave amplitudes at the earth from plausible sources (Thorne 1987; Wahlquist 1987; and Wahlquist (this volume)).

In the Galileo-era, X-band uplink will reduce plasma noise to parts in 10^{15} for bursts. For X-band uplink experiments, plasma noise, uncalibrated tropospheric scintillation noise, and station stability enter at comparable levels. Galileo will have lower noise levels and smaller resolution bandwidths than S-band experiments, allowing (1σ) sensitivity to sinusoids of $\sim 3 \times 10^{-16}$.

Increasing the radio frequency to, say, K-band (~32 GHz) uplink or using multifrequency links to isolate the plasma noise, gravitational wave observations can provide very high immunity to plasma noise and very sensitive gravitational wave experiments. If flight-qualified precision timekeeping becomes practical, then the possibility of onboard extraction of one- and two-way Doppler, separately, offers improved ways to discriminate gravity wave and noise signatures — see, *e.g.*, Vessot (this volume). To fully exploit the plasma noise immunity of a K-band link would require improved timekeeping on the ground and precision tropospheric monitoring; at these levels there may also be important impacts on the quality of the spacecraft transponder. Calibration of both the wet *and dry* troposphere to yield residuals smaller than than ~5% of the total would also be required to reduce residual

tropospheric noise to a level comparable with the plasma noise. Instrumental stability at $\sim 10^{-16}$ would also be required. Such a system ($f_o \approx 32$ GHz, precision tropospheric monitor, high instrumental stability, high SNR radio links) could, for long tracking arcs, have (1σ) sensitivity at $\sim 3 \times 10^{-17}$ for sinusoids.

IV. CONCLUSION

Spacecraft Doppler experiments in the Galileo-era will have substantial sensitivity improvements over the current-generation (S-band uplink) prototypes. With improvements such as higher radio frequency links, high instrumental stability on the ground and in the spacecraft, very high signal-to-noise ratio radio links, and precision tropospheric monitoring, sensitivities $\sim 3 \times 10^{-17}$ for sinusoidal waves appear possible. Improvements to sensitivities significantly better than this are, I think, impractical for observations with one station on the earth and using only the two-way Doppler observable. The difficult problems of (1) tropospheric monitoring (wet and dry components) at these levels, (2) frequency standard stability, and (3) low-level systematic errors in reliably removing the "known" motion of the station at these levels, will play roles. Sensitivity improvement in the LF band, significantly better than the levels discussed here, will likely require moving all the test masses into space and using interferometric techniques.

ACKNOWLEDGMENTS

I thank F. B. Estabrook and H. D. Wahlquist for valuable discussions on all aspects of the Doppler gravitational wave method. This work was performed at the Jet Propulsion Laboratory, under contract with NASA.

REFERENCES

Anderson, J. D., *et al.* 1984, *Nature*, **308**, 158.

Anderson, J. D., and Mashhoon, B. 1985, *Astrophys. J.*, **290**, 445.

Armstrong, J. W. 1988, "Spacecraft Gravitational Wave Experiments" in *Proceedings of NATO Advanced Research Workshop on Gravitational Wave Data Analysis* (Reidel: North Holland) (in press).

Armstrong, J. W., Woo, R., and Estabrook, F. B. 1979, *Astrophys. J.*, **230**, 570.

Armstrong, J. W., and Sramek, R. 1982, *Radio Science*, **17**, 1579.

Armstrong, J. W., Estabrook, F. B., and Wahlquist, H. D. 1987, *Astrophys. J.*, **318** ,536.

Estabrook, F. B., and Wahlquist, H. D. 1975, *GRG*, **6**, 439.

Estabrook, F. B., *et al.* 1979, "Gravitational Radiation Detection with Spacecraft Doppler Tracking: Limiting Sensitivities and Prospective Missions" in *Sources of Gravitational Radiation*, L. Smarr ed. (Cambridge University Press: Cambridge), p 37.

Hellings, R. W., Callahan, P. S., Anderson, J. D., and Moffet, A. T. 1981, *Phys. Rev.*, **D23**, 844.

Hogg, D. C., Guiraud, F. O., and Sweezy, W. B. 1981, *Science*, **213**, 1112.

Kursinski, E. R. "High-Stability Radio Links" (this volume).

Resch, G. M., Hogg, D. E., and Napier, P. J. 1984, *Radio Science*, **19**, 411.

Shannon, R. R., Smith, W. S., Metheny, W., Ceccon, C., and Philbrick, R. 1979, *Science*, **206**, 1267.

Treuhaft, R. "Tropospheric Monitoring Technology" (this volume).

Thorne, K. S. 1987, "Gravitational Radiation," in *300 Years of Gravitation*, ed. S. W. Hawking and W. Israel (Cambridge University Press: Cambridge), p. 330.

Wahlquist, H. D., *et al.* 1977, *Atti dei Convengni Lincei*, **34**, 335.

Wahlquist, H. D. 1987, *GRG*, **19**, 1101.

Wahlquist, H. D. "Detecting Gravity Waves from Binary Black Holes" (this volume).

Woo, R., and Armstrong, J. W. 1979, *JGR*, **84**, 7288.

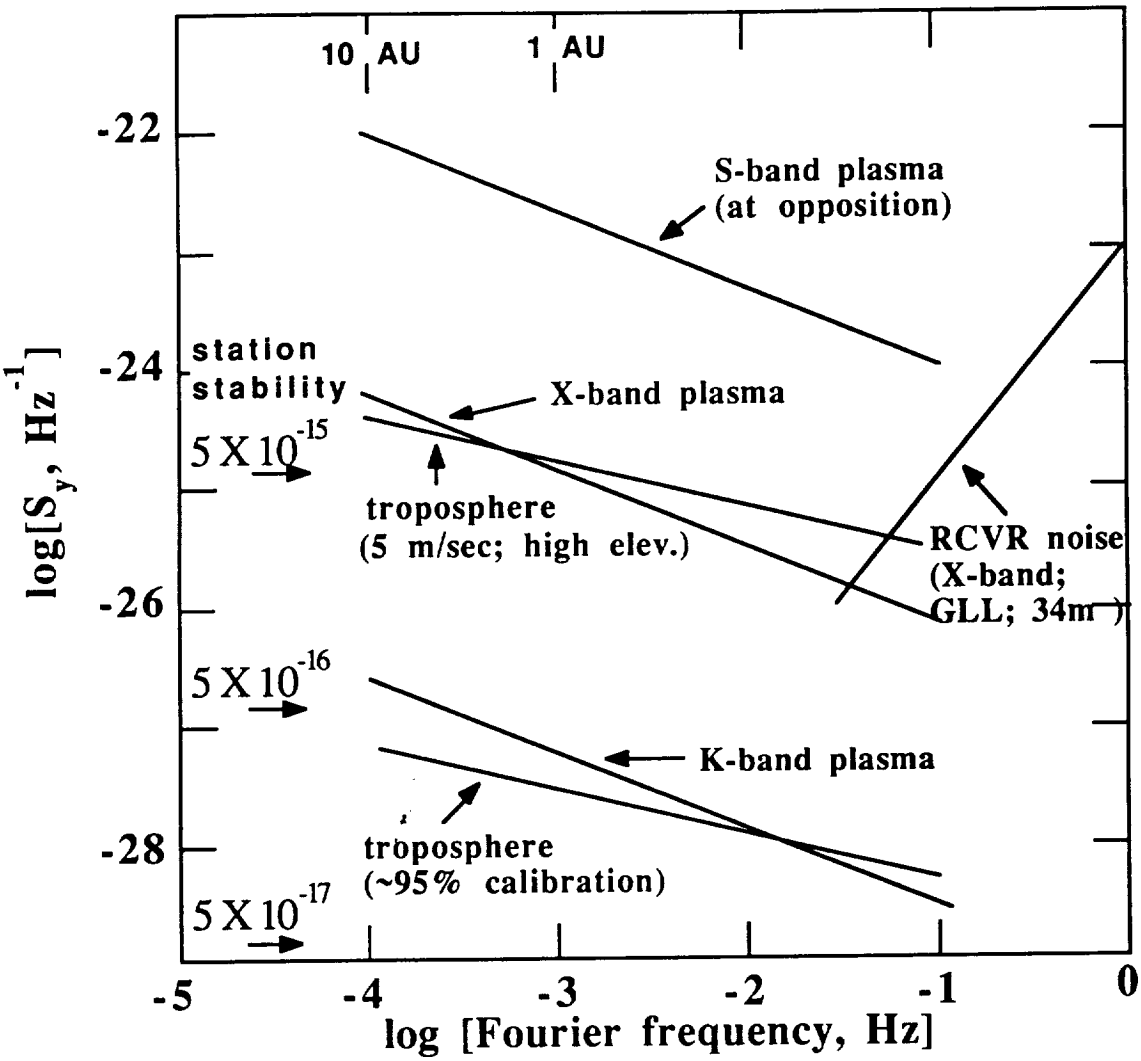

FIG. 1.—Spectra of fractional frequency fluctuations, $S_y(f)$, versus Fourier frequency, for the main noise sources in the LF band. Current generation experiments have S-band radio links and are plasma noise limited. Galileo-class experiments (X-band up- and downlinks) will have substantially reduced plasma noise; these will be limited by some combination of the X-band plasma noise, unmonitored troposphere, and station stability. Advanced experiments involving, say, K-band (32 GHz) radio links, $\sim 10^{-16}$ station stability, very high signal-to-noise ratio radio links, and precision tropospheric monitoring, could reach sensitivities $\sim 3 \times 10^{-17}$ for sinusoidal waves.

DISCUSSION

SHAPIRO: Has the problem of isolation of the transmitter from the receiver (for the X-band uplink and downlink) been solved or is it intended to use two antennas at each site, one for the transmitter and the other for the receiver?

ARMSTRONG: Galileo-era X-band gravitational wave experiments will be supported by the DSN's new 34-meter high-efficiency antennas, with both transmission and reception at the same antenna. An X-band uplink/downlink capability similar to that of the 34-meter antennas is also being planned for the 70-meter network, which could then be used with the 34-meter antennas for simultaneous two-spacecraft coincidence experiments in the 1990's.

SCHUMAKER: How well correlated are the plasma induced phase fluctuations at S- and X-band frequencies--i.e., how immune to plasma noise is a dual frequency microwave system? Can this be translated into an equivalent single higher-frequency (e.g., an optical frequency) for which the $1/f^2$ plasma noise would be as small?

ARMSTRONG: The leading contributor of plasma noise at opposition is the solar wind, which is to a good approximation collisionless and only very weakly magnetized. From cold plasma theory, refractive index squared is given by $n^2 = [1-(f_p/f)^2]$, where f_p is the plasma frequency (~30kHz for the near-earth solar wind). Since the plasma frequency is so small compared with the radio frequency, the $1/f^2$ leading term is essentially "exact". Subtle complications (e.g., geometric optics paths at the two frequencies not quite the same, imperfect plasma correlation because of different Fresnel zone sizes, collisional and magnetized plasma effects) are potential problems, but should enter at sensitivity levels well below those discussed in this paper.

THE SPACE MICROWAVE INTERFEROMETER AND THE SEARCH FOR COSMIC BACKGROUND GRAVITATIONAL WAVE RADIATION

ALLEN JOEL ANDERSON*
Planetary Geodesy and Geophysics
The University of Uppsala
S- 75590 Uppsala, Sweden

ABSTRACT

Present and planned investigations which use interplanetary spacecraft for gravitational wave searches are severely limited in their detection capability. This limitation has to do both with the Earth-based tracking procedures used and with the configuration of the experiments themselves. It is suggested that a much improved experiment can now be made using a multiarm interferometer designed with current operating elements. An important source of gravitational wave radiation, the cosmic background, may well be within reach of detection with these procedures.

It is proposed to make a number of experimental steps that can now be carried out using TDRSS spacecraft and would conclude in the establishment of an operating multiarm microwave interferometer. This interferometer is projected to have a sensitivity to cosmic background gravitational wave radiation with an energy of less than 10^{-4} cosmic closure density and to periodic waves generating spatial strain approaching 10^{-19} in the range 0.1 to 0.001 Hz.

I. INTRODUCTION

Gravitational wave research lies at the very heart of modern physics. The search for gravitational waves of astrophysical origin is one of the single most outstanding challenges for experimental physics today. This effort is currently being pursued by eminent experimental teams in several parts of the world. After two decades of experimental efforts that have been carried out both on the ground and simultaneously in space, we have reached the point where it is evident that a new generation of detectors is required if detection of gravitational waves is to be successful.

Several proposals have recently been made that aim at the construction of multiarm interferometers in space. These proposals range from direct approaches, which build upon current technologies, to more ambitious projects, which look some distance into the next century.

The situation in gravitational wave physics today is not unlike that in the particle physics community some 60 years ago. At that time, small university basement cyclotrons were just as important to the whole of physics as Fermilab, SLAC, CERN, or SSC are today. Progress and understanding in experimental physics is a methodical game. Each step along the way is supported by different groups, using different techniques, testing different methods, on different equipment.

---

*presently at Santa Barbara

II. SMILE

The Space Microwave Interferometer for Low Energy gravitational wave detection, or SMILE, combines our best current experimental knowledge and experience of present day capabilities in space gravitational wave detection. Its goal is the operation of a space multiarm microwave interferometer by the end of this century. By utilizing the most appropriate existing equipment and facilities of the various national space agencies, which are being deployed in space by other programs at considerable expense, we have designed a detection scheme which we believe is the best that can be currently achieved. This interferometer would have 10^4 to 10^5 greater sensitivity to gravitational wave energy than the best interplanetary spacecraft searches (Galileo). It would be the first in a new class of space detectors.

We have identified several experimental steps that can be carried out in the next few years. These early stages would require some new ground equipment of minimal expense but would not, however, require any special additional launch opportunities. The final stage of the proposal would require the deployment of two small probes of scout launch class to implement the full power of the interferometer. If not overburdening, these small probes might, in addition, carry equipment for the test of an even more ambitious interferometer of the next century.

At this time, it seems highly probable that the techniques developed for and utilized in the SMILE interferometer could become a primary method used for the initial set up, adjustment, and monitoring of a future interferometer of greater capability. It can be envisioned that the lessons gained from the techniques developed for SMILE could provide a reliable and necessary first step along the way to an even more highly advanced stage of space interferometry.

III. SPACE MICROWAVE INTERFEROMETER FOR LOW ENERGY GRAVITATIONAL WAVE DETECTION (SMILE)

Current major limitations with spacecraft measurements $\Delta 1/1$:

1) Troposphere* (model at best 10^{-16} at 1000 s);
2) Ionosphere* (10^{-13} to 10^{-16} at 100 s S/X band);
3) Clock* (present Vessot operational 10^{-16} at 3000 s);
4) Earth Rotation variation, Polar Motion, Atmosphere, Ocean and Tidal Loading parameters* (model to 10^{-16} at 1000 s); and
5) Plasma (10^{-13} to 10^{-16} at 1000 s S/X band).

SMILE will:

1) Eliminate Troposphere,
2) Eliminate Ionosphere,
3) Eliminate clock,
4) Eliminate Earth Rotation variation, PM, A, O and TL parameter errors,
5) Reduce plasma by 2 orders in $\Delta 1/1$,

*RTLT correlated creating problem for G-wave detection

6) Provide 4 to 5 orders improvement in G-wave energy sensitivity detection over Galileo,

7) Measure a G-wave background energy to less than 10^{-4} cosmic closure density in the range 0.1 to 0.001 Hz, and

8) Measure periodic G-waves generating spatial strain approaching 10^{-19} in the range 0.1 to 0.001 Hz.

The following is a series of experimental steps that have been identified and can now be conducted with the present TDRSS spacecraft for evaluation prior to design commitment of the space interferometer.

Step 1. *Design and carry out a TDRSS open loop tracking experiment.*

Configuration: TDRSS, one antenna, tracking earth orbiting Doppler beacon spacecraft in wideband. Transmit wideband signal to White Sands, record and do open loop recovery and Fourier analysis. Compare with TDRSS discrete Doppler readout. Develop open loop recording and analysis procedures. Develop algorithms and model spacecraft dynamics from data.

Step 2. *Design and carry out a TDRSS open loop tracking experiment.*

Configuration: TDRSS, two antennas, both tracking simultaneously same earth orbiting spacecraft in wideband. Transmit both wideband signals to White Sands, record and do open loop recovery of both signals, Fourier analysis and comparison. Model complex spacecraft dynamics.

Step 3. *Design and carry out a TDRSS White Sands frequency standard H-maser experiment using transmit through and receive on TDRSS with wideband reception.*

Configuration: TDRSS, one antenna, tracking earth orbiting transponder spacecraft. Use TDRSS precise Doppler transmit mode. Transmit wideband to White Sands, record and do open loop recovery, Fourier analysis.

Step 4. *Design and carry out a TDRSS White Sands frequency standard H-maser experiment using transmit through and receive on TDRSS with wideband reception on two antennas.*

Configuration: TDRSS, two antennas, both tracking simultaneously same earth-orbiting transponder spacecraft. Use TDRSS precise Doppler transmit mode. Transmit both wideband signals to White Sands, record and do open loop recovery of both signals, Fourier analysis and comparison. Evaluate system in detail.

SCHUMAKER: In a previous vu-graph you said that plasma noise entered in at levels 10^{-13} - 10^{-16}. You gain by a factor of 10 going from X to KA-band, and another factor of ten between 100-S and 1000-S arms. Is this factor of 100 what allows you to expect a sensitivity of 10^{-18}? And, if so, isn't this optimistic, and only appropriate for directions away from the sun?

ANDERSON: Yes, it is a realistic value. The full range of 10^{-13} to 10^{-16} to $\Delta L/L$ equivalent effect for X-band was primarily to indicate the vast range of plasma effects over the whole solar angle and solar cycle period. The experiment would be so configured as to minimize the plasma effects and periods of operation at $\Delta L/L$ of 10-18 is realistic (see comment by Hellings).

HELLINGS: The increase in sensitivity in the interferometer comes from a factor of 10 due to the change from X to K band and another factor of about 5 from the fact that the round-trip light-times will be only 100 seconds compared to the 10^4 seconds in the interplanetary spacecraft. The plasma noise is stronger at low fourier frequencies, and the shorter light time avoids these low fourier components.

SHAPIRO: The uncertainty of theoretical predictions in this field notwithstanding, what is the theoretical basis for your assumption that the gravitational stochastic background will match the power in the microwave background?

ANDERSON: I believe it is correct to say that there is no other measurement which comes within 2 or 3 orders of setting a limit of 10^{-4} closure density for G-wave energy in this waveband. There are a lot of potential sources in this waveband making the accumulated incoherent gravitational wave energy flux a major source. Estimates of the incoherent flux from close binaries in our own galaxy, for example, indicate a total summed flux causing spatial strain around 10^{-18} $\Delta L/L$ in a broad band throughout this waveband. Therefore I believe the chance of detecting this incoherent background with these methods is very good.

TREUHAFT: Your estimate of tropospheric fluctuations of 10^{-16} at 1000 sec seems between one and two orders of magnitude too low. From the recent TDRSS experiment, the earth-based baseline (Japan-Australia) was much more stable then baselines to TDRSS. How do you plan to get around satellite motion, or whatever is determined to be the ultimate cause of the low coherence on TDRSS baseline (for times >500 sec)?

ANDERSON: (1) In my first overhead I have purposely indicated the most optimistic values, that is, those that are the best possible. Those for the troposphere are for high desert sites, and are based partly upon measurements inferred from the VLA for spatial coherency as reported by Armstrong, 1981, in Radio Science. Armstrong concluded that about 10% of the time data taken was equivalent to plasma + troposphere disturbance at 5 parts in 10^{15} or better. The experiment itself was unable to set an absolute smaller limit beyond this number. I have therefore noted for brevity on the overhead that spacecraft tracking experiments done from earth tracking stations are limited by unmodellable tropospheric disturbances at 10^{16} and very unlikely to ever be better than this number using our current methods of measurement and present understanding. Your objection that you cannot do well by modelling is probably correct using current methods. (2) Concerning the TDRSS experiment itself, we would not do the classical VLBI experiment, which measures baseline length, but rather we would measure Doppler and we believe this can be done at about 3 orders more accurate. Appropriate tests using TDRSS can be carried out to confirm this estimate.

BERTOTTI: What is the level at which you need to measure or to control the non-gravitational accelerations in your final experiment?

ANDERSON: In this experiment there are two approaches. The first one is to beat down the noise in the detector by building up a large number of observations, spectrally separating the general broadband noises caused by individual members of the interferometer from the specific gravitational wave autocorrelation signature. To reach a level of 10^{-18} $\Delta L/L$ for this detection we would need about 20 days of data. The second approach is to limit the broadband noises. Here the payoff would only be commensurate with the other characteristics of the system being improved at the same time. In this experiment unmodelled drag forces of 10^{-9} to 10^{-10} g in the waveband of the detection are tolerable.

OPTICAL INTERFEROMETER IN SPACE

P. L. Bender,* J. E. Faller,* J. L. Hall,* D. Hils, R. T. Stebbins and M. A. Vincent**
Joint Institute for Laboratory Astrophysics
University of Colorado and National Institute of Standards and Technology
Boulder, Colorado 80309

ABSTRACT

The present design concepts for a Laser Gravitational-Wave Observatory in Space are described. Laser heterodyne distance measurements are made between test masses located in three spacecraft separated by roughly 10^6 km. The major technology issues are: the reduction of spurious acceleration noise for the test masses to below 2 x 10^{-15} cm/sec^2/Hz$^{0.5}$ from 10^{-5} to 10^{-3} Hz; and the measurement of changes in the difference of the antenna arm lengths to 5 x 10^{-11} cm/Hz$^{0.5}$ from 10^{-3} to 1 Hz with high reliability. The science objectives are: to measure discrete sinusoidal gravitational wave signals from individual sources with periods of 1 second to 1 day; to measure the stochastic background due to unresolved binaries; and to search for gravitational wave pulses with periods longer than 1 second from possible exotic sources such as gravitational collapse of very massive objects.

1) INTRODUCTION

It seems likely that several of the proposals in different countries for large ground-based laser gravitational wave detectors will be funded in the next 2 or 3 years. If so, the prospects appear good for the direct detection of gravitational wave signals within a decade. However, the sensitivity which can be achieved in ground-based detectors at frequencies below about 10 Hz is strongly limited by environmental noise sources. Even if complete isolation of the test masses from ground motions is possible, the gravity gradient noise due to naturally occurring density variations in the ground and atmosphere would cause the instrumental strain sensitivity to get worse as roughly the inverse fourth power of the frequency (Saulson 1984).

Since a number of types of gravitational wave sources which may provide unique kinds of astrophysical information exist only at frequencies below 1 Hz, we have carried out studies of the sensitivity which could be achieved at frequencies of 10^{-5} to 1 Hz with a three-satellite interferometric antenna for a Laser Gravitational-Wave Observatory in Space (LAGOS). A lot more work is needed, particularly on methods for minimizing the time-varying spurious acceleration of the test mass in each spacecraft at periods from 10^{-5} to 10^{-3} Hz. However, the general characteristics of the LAGOS antenna design (Stebbins et al. 1988) and the types of gravitational wave sources which could be observed with it (Hils et al. 1986) have become fairly well established. The antenna design characteristics are described briefly in this article, with particular emphasis on the problem of reducing spurious accelerations of the test masses at frequencies of 10^{-5} to 10^{-3} Hz.

---

* Staff member, Quantum Physics Division, National Institute of Standards and Technology

** Now at: Jet Propulsion Laboratory, Pasadena, CA 91109

2) Basic Antenna Design

Our present baseline case for the LAGOS antenna location and geometry are shown in Fig. 1. The three spacecraft are located about 30° behind the Earth in orbit around the sun. The center one is in a circular orbit with one year period. By choosing the orbits for the other two correctly, one can achieve a right-angle geometry, with the two end spacecraft keeping nearly constant and equal distances of roughly 10^6 km from the center one (Faller and Bender 1984). They will appear to go around the center spacecraft with one year period in a plane which is tipped 60° with respect to the ecliptic.

In the absence of planetary perturbations, the variations in the arm lengths would have amplitudes of 0.16% for 10^6 km arm lengths. The largest planetary perturbations are the resonance ones due to the Earth. Computer calculations of these have been carried out by Vincent, and maximum variation of ±0.6% over a ten year period were found. This corresponds to a maximum relative velocity of about 1 m/sec.

The test mass in each spacecraft floats freely within a cavity which is designed to produce very little spurious acceleration of the test mass. In the simplest form of the antenna, a beam-splitter would be mounted in the center test mass and a mirror in each end test mass to form an interferometer. However, with 50 cm diameter telescopes used for transmitting and receiving the light, only about 10^{-7} of the transmitted light is received at the far end. Thus this light is sent to a photo-detector after it is received and beat against a small amount of light from a laser in the end spacecraft. The resulting signal is used to phase-lock the laser, and the main part of the laser light is transmitted back to the center spacecraft. This coherent transponder approach, which is common in optical communications systems, is necessary in order to obtain a sufficiently high signal level. The lasers are assumed to be laser diode pumped Nd YAG lasers, with high efficiency, long lifetimes, and about 1 watt of transmitted power at the 530 nm second harmonic wavelength. The lasers are locked tightly to stable Fabry-Perot cavities in order to obtain good short term phase stability.

Back at the center spacecraft, the received beams from the two ends are beat against the local laser to give output signals at the two Doppler frequencies, which correspond to the rate of change of the two arm lengths. These signals can be down-shifted for convenience, filtered with narrow-band tracking filters, and then sent to continuously counting phase meters which record the phase perhaps every 0.1 sec. Digital filtering methods also need to be considered. The desired phase measurement stability is roughly 2×10^{-6} cycle/$Hz^{0.5}$ from 1 to 10^3 sec intervals. Thus care in the design of the phase measurement system and thermal stability in the optical system are necessary. The required data transmission rate back to the Earth is probably not more than 2 kilobits/sec, depending on the amount of auxiliary data needed.

The data analysis method is based on the fact that there are essentially no unknown perturbations of the arm lengths with periods of 10^5 sec or shorter due to the planets, their satellites, or other solar system bodies. Since the spurious accelerations of the test masses will be kept very small, the apparent unmodeled changes in the sum of the length of the two arms can be taken as a measure of the fluctuations in the laser wavelength (Faller et al. 1985). The changes in the difference of the two arm lengths for the interferometer, corrected for the laser

wavelength fluctuations, provide the gravitational wave signal. For a small fractional difference in the interferometer arm lengths, the only negative effect of this laser wavelength correction method will be a comparable fractional error in the amplitude and phase of the detected gravitational wave signals.

It has been recognized from the beginning that minimizing spurious accelerations of the test masses would be the main technological challenge in designing the LAGOS antenna. However, there was not time to do more during the Workshop talk than to show a list of the spurious acceleration sources considered and describe a few of them very briefly. Since most of the discussion after the talk was on this topic, and in view of the helpful questions raised by D. B. DeBra, most of the remainder of this brief summary will be devoted to some of the spurious acceleration issues.

3) Time-Varying Spacecraft Mass Attraction

The gravitational potential due to all of the spacecraft except the test mass can be expressed as a spherical harmonic expansion about a point near the center of the test mass cavity. Because of practical construction tolerances and unknown variations in material densities, the coefficients of the different potential terms will have various uncertainties. We can reduce the low degree coefficients to the level allowed by the uncertainties, in order to minimize the gravitational acceleration of the test mass, but at least the second and third degree potential terms will have to be measured in flight and then cancelled out by displacing small compensating masses. The measurements can be made for all of the important terms by displacing the spacecraft with respect to the test mass by programmed offset vectors and observing the resulting changes in the interferometer arm length difference. This is part of the antenna set-up procedure, and may have to be repeated as frequently as each week.

Terms which cannot be determined by the above procedure are the first degree terms. These give test mass accelerations which are independent of the spacecraft position. They would be balanced to the level of 10^{-11} g, which was the design goal at zero frequency for the TRIAD mission, by careful weighing of spacecraft parts and by adjustments. Other potential terms give forces which vary with spacecraft displacement. The effects of such terms would be minimized by servo control of the spacecraft position so that it doesn't move with respect to the test mass by more than 1 micron. This is feasible because the amplitude of solar wind and solar radiation pressure force variations on the spacecraft at the periods of interest will be quite small with respect to the average radiation pressure force.

Two important questions raised by D. B. DeBra concern the spacecraft potential changes caused by fuel motion and by thermal distortion. We have assumed so far that cold gas thrusters using perhaps N_2 would provide the acceleration of roughly 10^{-8} g needed in order to counteract the solar radiation pressure. Preliminary estimates indicate that, for the end spacecraft, the N_2 for a ten year mission could be located in two spherical tanks opposite each other and at 90° to the interferometer arm. However, they would need to be far enough away so that either about half the Shuttle bay would be needed to hold the three LAGOS spacecraft or the tanks would be deployable after launch. The changes in the second degree potential terms due to fuel usage would need to be cancelled out by pre-programmed motions of small compensating masses, but the accuracy requirements on the motion are not severe. For the center spacecraft, the fuel tanks would be along the axis of the spacecraft.

One other possibility would be to use ion thrusters if they have been developed and qualified for other purposes before Phase B studies for a possible laser gravitational wave mission are started, but this cannot be assumed at present.

The second question concerning thermal distortion of the spacecraft is probably best handled by a combination of good thermal design and correction to the received data. The main driver for such distortions will be solar intensity variations with periods of 10^3 to 10^5 sec, coupled with asymmetric thermal properties of the spacecraft. We have previously discussed the use of a two-stage thermal shield for the main optical system of the spacecraft, plus an extra stage for the test mass cavity and the beam-splitter/detector package (Stebbins et al. 1988). Two insulating blankets with roughly fifty layers each would be used in the two-stage thermal shield, with an outer thermal load structure between them and the main instrument package serving as the thermal load for the inner blanket. The main thermal distortion effects are likely to be from the outer blanket and the outer thermal load, rather than from the inner parts of the spacecraft. Fortunately, it appears that the solar intensity fluctuations can be measured well enough so that the transfer function to the difference in antenna arm lengths can be determined and removed from the data.

4) Non-Gravitational Test Mass Perturbations

At very low frequencies, it appears impossible to avoid serious problems from the solar intensity fluctuations. An important effect, pointed out to us initially by R. W. P. Drever, is anisotropic thermal radiation pressure fluctuations acting on the test mass due to a fluctuating temperature difference across the cavity. With three stages of thermal shielding, we estimated that this effect will give noise which increases in amplitude as $f^{-16/3}$ at frequencies below about 10^{-5} Hz.

Another potentially limiting effect is random collisions of residual gas molecules with the test mass. This well-known effect would give roughly 10^{-15} cm/s^2/Hz$^{0.5}$ acceleration noise for a fairly dense 10 kg test mass and 10^{-11} torr pressure. Care is needed in avoiding virtual leaks in the test mass cavity, and some initial warming of the cavity to speed up outgassing may be desirable. Based mainly on the random gas molecule collisions and time-varying spacecraft mass attraction, we are currently using 2×10^{-15} cm/s^2/Hz$^{0.5}$ as the desired error budget level for spurious accelerations over the frequency range from roughly 10^{-5} to 10^{-3} Hz.

For electrical forces, the main problem is charging up of the test mass due to cosmic ray impacts. The charge on the test mass has to be sensed by applying a sinusoidal drive field, and then kept low by injecting the opposite charge. The fluctuations in the test mass potential should be kept below 3×10^{-6} volts/Hz$^{0.5}$ if the stray electric field level in the cavity is 1 volt/meter.

The magnetic susceptibility requirement for the test mass will depend on how low the magnetic field gradient from the spacecraft can be kept. The main fluctuating magnetic force on the test mass is likely to be from the interaction of the fluctuating interplanetary field with the dipole moment induced by the gradient of the spacecraft magnetic field. For a spacecraft magnetic field of 10^{-3} Gauss due to current loops 1 meter from the test mass, and for 3×10^{-3} Gauss/Hz$^{0.5}$ fluctuations in the interplanetary field, the susceptibility requirement for the test mass is roughly 10^{-7}.

The effects of momentum transfer due to cosmic ray impacts also have been considered. Protons with energies below roughly 100 MeV will not reach the test mass, and the energy deposited by higher energy particles will be of this order. For galactic cosmic rays, the directions of arrival are nearly isotropic and the arrival times are random. The resulting fluctuating test mass acceleration level is more than an order of magnitude below our current error budget level. For solar cosmic rays, the flux of particles with energies above 100 MeV is believed to be very low, except at the times of major solar flares. At such times, the momentum transfer to the test masses would be large, and would ruin the usefulness of the data for gravitational wave observations for a day or two. This is the only time we know of when the antenna would not get useful data, except for the possibly weekly spacecraft gravitational potential checks.

5) Expected LAGOS Antenna Performance

Based on the error models discussed above, plus the shot noise limit for 1 Watt of transmitted laser power, the expected antenna sensitivity is given as a function of frequency in Fig. 2. It appears that other sources of noise in measuring the test mass separation can be kept below the shot noise limit at frequencies above 1 x 10^{-3} Hz. The overall antenna sensitivity curve shown should be regarded as the current goal for the antenna, since a great deal of work is needed in order to determine whether this goal can be achieved within realistic mission constraints. We believe that the most important challenge for such a mission will be achieving a high degree of reliability, despite the need for three separate spacecraft and the requirement of very low spurious acceleration levels for the test masses at frequencies of 10^{-5} to 10^{-3} Hz. However, this must be accomplished within mass constraints of something like 300, 300, and 400 kg for the three spacecraft, in order to keep the mission costs from escalating.

The antenna sensitivity curve shown in Fig. 2 is roughly an order of magnitude below the level of the expected power spectrum of gravitational wave signals from 10^{-5} to 10^{-3} Hz (Hils et al. 1986). These signals are due to a number of types of galactic binaries, including ordinary main-sequence binaries, contact binaries, cataclysmic variables, close white dwarf binaries, and neutron star binaries. Since many such binaries exist in even as narrow a band as 0.1 cycle/year, they generally will not be resolvable except for frequencies near 10^{-3} Hz or higher, where many individual binaries can be observed. Instrumental noise levels can be checked by observing changes in the signal level as the center of the galaxy goes through the nulls in the antenna pattern, and the direction to individual resolved binaries can be determined in the same way. The antenna sensitivity also is sufficient for detecting possible pulses due to the collapse of very massive objects to form black holes near the time of galaxy formation. More information about the observable types of signals will be published soon.

ACKNOWLEDGMENTS

This work has been supported by the NASA Innovative Research Program under Award Number NAGW-822, and by the National Institute of Standards and Technology.

REFERENCES

Faller, J. E. and Bender, P. L., "A possible laser gravitational wave experiment in space" in *Precision Measurement and Fundamental Constants II, ed.* B. N. Taylor and W. D. Phillips (NBS Spec. Publ. 617, 1984), 689-690.

Faller, J. E., Bender, P. L., Hall, J. L., Hils, D. and Vincent, M. A., "Space antenna for gravitational wave astronomy" in Proc., Colloquium *Kilometric Optical Arrays in Space* (ESA SP-126, Noordwijk, The Netherlands, 1985), 157-163.

Hils D., Bender, P. L., Faller, J. E. and Webbink, R. F., "The gravitational wave sky at micro-Hz to Hz frequencies' in *Eleventh Int. Conf. on General Relativity and Gravitation: Abstracts of Contributed Papers, Vol. II* (Univ. of Stockholm 1986), 509.

Saulson, P. R., "Terrestrial gravitational noise on a gravitational wave antenna," Phys. Rev. *D30*, 732-736, 1984.

Stebbins, R. T., Bender, P. L., Faller, J. E., Hall, J. L., Hils, D. and Vincent, M. A., "A laser interferometer for gravitational wave astronomy in space" in *Proc. Fifth Marcel Grossman Conf.* (Univ. of Western Australia, Perth, 8-13 Aug. 1988), in press.

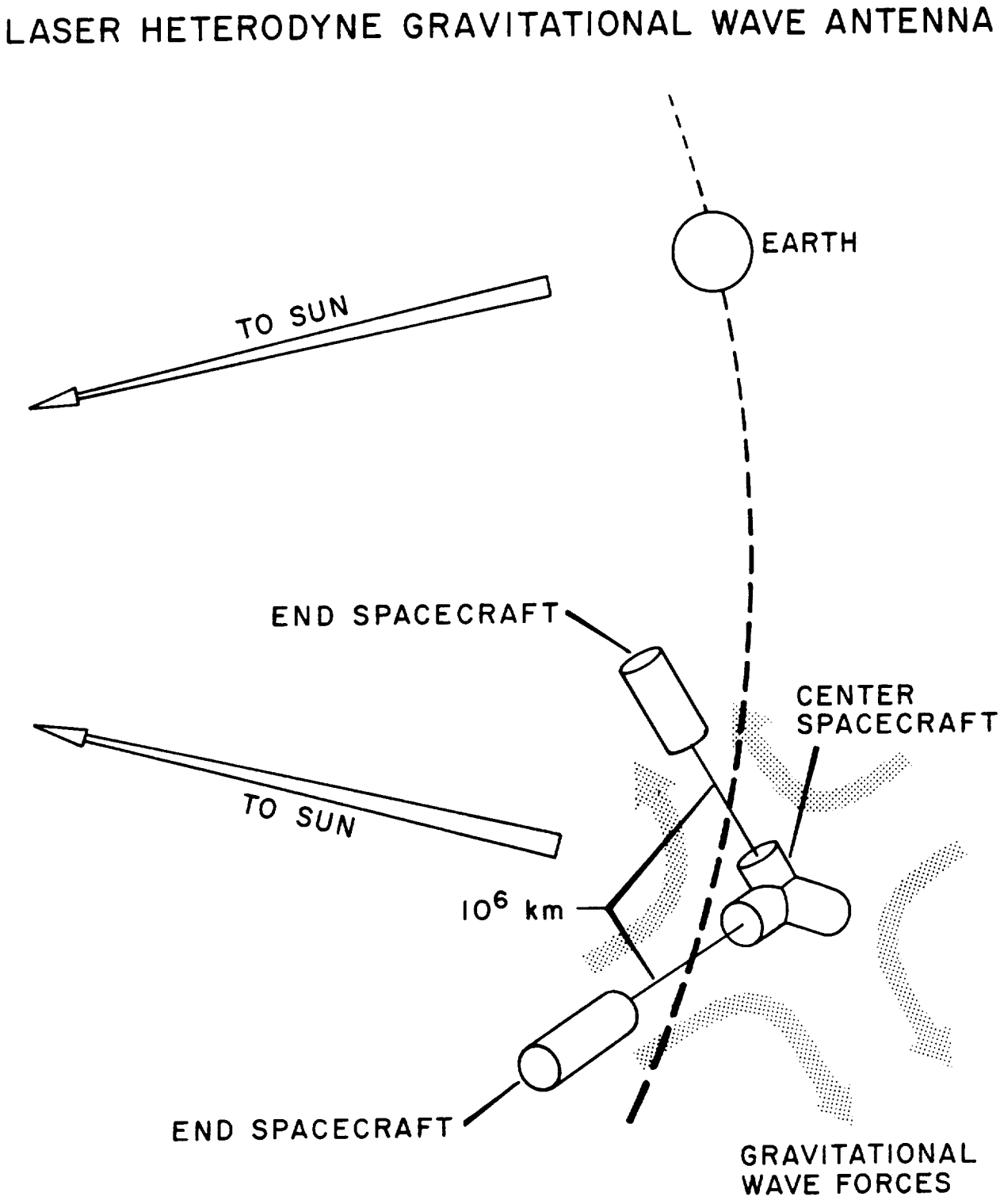

FIG. 1 — Laser Heterodyne Gravitational Wave Antenna

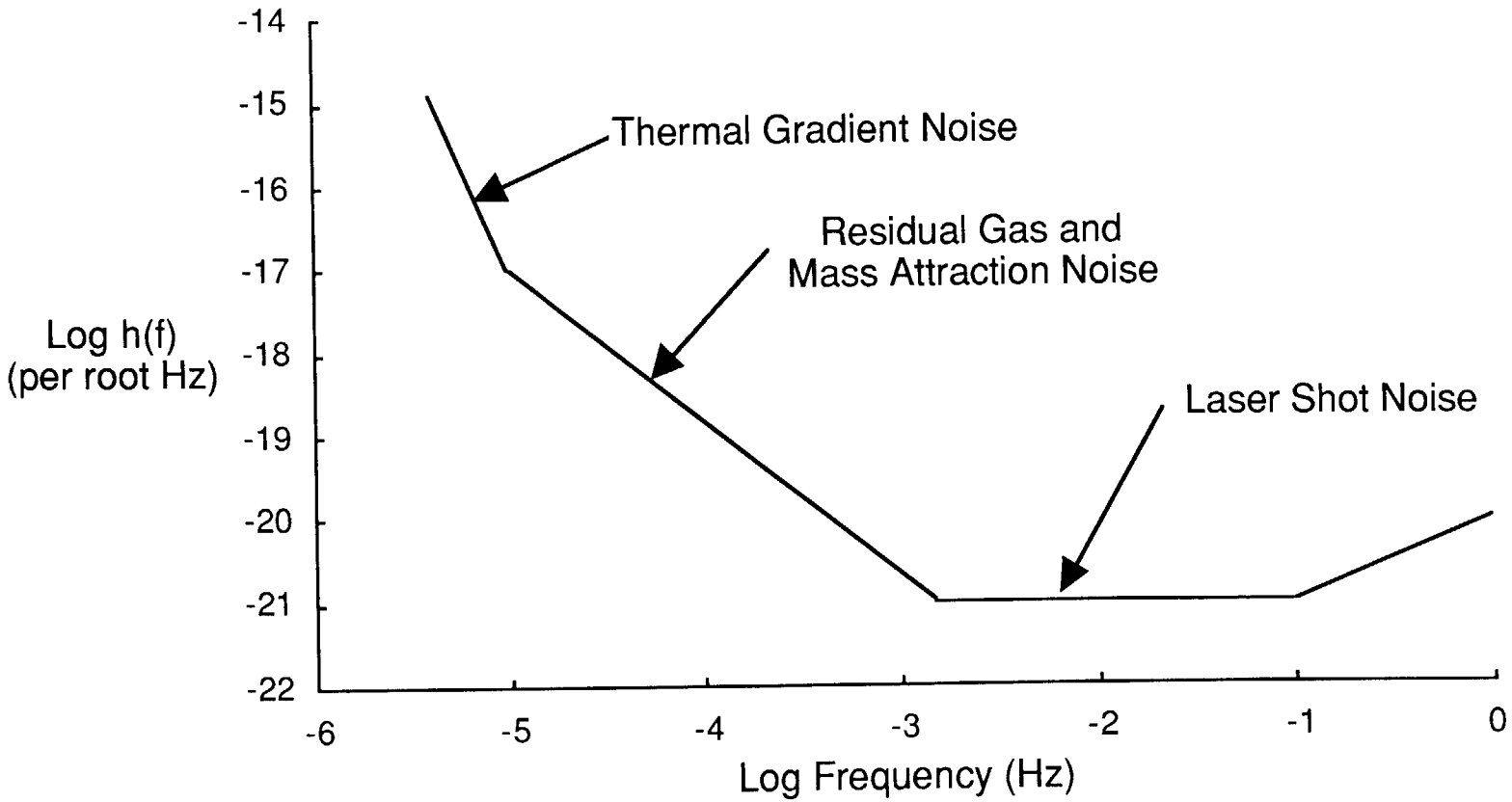

FIG. 2 — Antenna Sensitivity

DISCUSSION

ARMSTRONG: I think it is remarkable that you are talking about confusion-limited vs. flux-limited gravitational wave astronomy, at least at low frequencies!

MATZNER: How active are these satellites? (For instance, to maintain orientation and drag-free behavior.) What is the expected gas consumption rate, and what is the expected lifetime?

BENDER: The expected fuel consumption rate for cold gas thrusters is about 10 grams per day. The mission lifetime would be 10 years.

SHAPIRO: How do you envision obtaining the "geometry" of the system, and its change with time, with sufficient accuracy to acquire fringes with the laser interferometers?

BENDER: We expect to take about a week to determine and refine the spacecraft orbits with the DSN antennas before releasing the test masses and starting the measurements.

CLAUSER: How do you release the proof mass to guarantee no rotation? With 1w of laser power, won't the proof mass charge up quickly? Will the charge be truely uniform on the mass? How do you discharge it?

BENDER: We haven't worked on the release mechanism problem yet. Clearly this is a very sensitive part of the procedure if we use a non-rotating test mass. We plan on having only a small part of the laser power hit the test mass. The main charging mechanism is expected to be cosmic ray impacts. Even using carefully applied gold or other coatings, there will be varying work functions on the surface and some non-uniformity in the charge distribution. The proof mass charge probably would be neutralized by spraying charge onto it.

HELLINGS: What would the sensitivity of your interferometer be if you did not have a drag-free system?

BENDER: The largest spurious accelerations of the spacecraft are expected to be roughly 10^{-11} g. For differing effects on the different spacecraft which are 1% this large and last for a few thousand seconds, the apparent signal would be about 10^{-15}.

SONNABEND: Have you considered reducing the gas pressure variations on the proof mass by a cryogenic housing?

BENDER: Yes. But the cryogen supply would limit the mission length, and the spacecraft is already complicated enough.

SCHUMAKER: (Re. his comment on problem of rapid fringe-rate.) Couldn't you overcome that problem just by using two local oscillators, tuned to compensate for the expected Doppler shifts?

BENDER: Yes, using frequency-offset local oscillators might well be desirable.

EARTH-ORBITING RESONANT-MASS GRAVITATIONAL WAVE DETECTORS

HO JUNG PAIK
Department of Physics and Astronomy
University of Maryland, College Park, MD 20742

ABSTRACT

Earth-based gravitational wave detectors suffer from the need to support the large antenna masses against the earth's gravity without transmitting a significant amount of seismic noise. Passive vibration isolation is difficult to achieve below 1 Hz on the earth. Vibration-free space environment thus gives an opportunity to extend the frequency window of gravitational wave detection to ultralow frequencies. The weightless condition of a space laboratory also enables construction of a highly symmetric multimode antenna which is capable of resolving the direction of the source and the polarization of the incoming wave without resorting to multiantenna coincidence. In this paper, we consider two types of earth-orbiting resonant-mass gravitational wave detectors. One is a skyhook gravitational wave detector, proposed by Braginsky and Thorne (1985). The other is a spherical detector, proposed by Forward (1971) and analyzed by Wagoner and Paik (1976).

I. SKYHOOK GRAVITATIONAL WAVE DETECTOR

The skyhook detector is an extension of the shuttle-borne skyhook, proposed by Colombo *et al.* (1974), now known as Tethered Satellite System. As a gravitational wave detector, two end masses (mass m_o each) are connected by a long, thin cable (length L) to form a dumbbell antenna with a spring at its center (fundamental longitudinal resonance frequency $\omega_o/2\pi$ and quality factor Q). As it orbits the earth, the cable would be stretched radially by the earth's tidal gravitational field. Gravitational waves would pull the masses apart and together in a oscillatory fashion. Their motion would be transmitted to the spring by the cable and a sensor would monitor the spring's resulting motion. Due to the relatively large motion produced in the spring, the sensor noise is deemed negligible, thus making the skyhook a broadband detector.

Four serious noise sources have been identified for the skyhook: Nyquist noise produced by the fluctuating part of the skyhook's internal dissipation, fluctuations in the cable length produced by fluctuations in solar and earth heating, fluctuating forces due to the gravity gradients of the high harmonics of the earth, and fluctuating electric and magnetic forces. In order to have a detection bandwidth of 10 mHz to 100 mHz, one could choose m_o = 20 kg, L = 25 km, $\omega_o/2\pi$ = 35 mHz and Q = 10^5. The Nyquist noise expressed in gravitational-wave units is

$$h_N = \left(\frac{32}{\pi}\frac{kT\omega_o}{mL^2\omega^3 Q}\right)^{1/2} = 3\times 10^{-17}\left(\frac{f}{30\ mHz}\right)^{-3/2}.$$

In order to keep the noise due to fluctuations in heating below this level, the fractional oscillation in irradiating heat flux must either be below 3×10^{-6} or be monitored to this sensitivity by an instrument on board the skyhook. The gravity gradient noise could be made negligible by choosing an altitude greater than 1,000

km. A nonconducting cable is proposed to minimize the effect of electric and magnetic fields. During some micropulsations, the disturbance is expected to greatly exceed the level given by the Nyquist noise. Thus, it will be necessary to carry on board the skyhook one or more electric field probes to monitor the vertical gradient of the vertical electric field fluctuations. The skyhook altitude must also be chosen to be below 6,000 km to maximize the time spent in quiet E-field regions.

The skyhook could be a relatively inexpensive broadband earth-orbiting detector, with sensitivity $h \cong 3 \times 10^{-17}$ in the frequency band 10 to 100 mHz, intermediate between present detectors (spacecraft Doppler tracking and earth modes) and the envisioned interferometric systems.

II. FISH-EYE GRAVITATIONAL WAVE TELESCOPE

Present Weber-bar antennas, laser interferometers, and Doppler tracking systems are all single-degree-of-freedom detectors of gravitational waves. As a result, many detectors in various orientations have to be used in coincidence to discriminate against nongravitational disturbances and to construct the direction of the source and the polarization of the waves. This problem could be overcome by using a resonant-mass detector whose modes exhibit the highest degree of degeneracy; *i.e.*, a spherically symmetric mass. A sphere has five degenerate quadrupole modes. By measuring the amplitudes of these five modes simultaneously, one could determine the four unknowns: the source direction (θ, ϕ) and the amplitudes of two independent polarizations of the wave $(\psi_+, \psi_\times)$. The remaining fifth degree of freedom could be used to reject nongravitational disturbances. The monopole mode of the sphere could also be monitored to have further anticoincidence rejection and to test theories, such as the Brans-Dicke theory, that predict existence of a scalar wave. The sphere is equally sensitive to waves coming from any direction, due to its symmetry, thus making the antenna a unique "fish-eye gravitational wave telescope."

Operation of such a spherical detector in a terrestrial laboratory is hampered on account of the difficulty of supporting the system against gravity without violating the spherical symmetry. In space, the antenna can float inside a spacecraft, providing excellent vibration isolation without disturbing the mode characteristics of the sphere. It is, however, difficult to improve the sensitivity of a lumped resonant-mass detector much beyond those of earth-based detectors due to a practical limit in putting a large mass into an earth orbit.

We consider, as an example, an aluminum sphere with radius (R) of 1.2 m, which will have a mass (M) of 2×10^4 kg and the quadrupole mode frequency $(\omega_2/2\pi)$ of 1 kHz. The quantum-limited sensitivity of this detector is

$$h_{QL} = \left(\frac{2h}{M\omega_2 R^2}\right)^{1/2} \cong 10^{-21}$$

By cooling the antenna to 1 K and efficiently matching its output to a quantum-limited SQUID, one could achieve this sensitivity. If the sensitivity of $h \cong 10^{-21}$ is found to be sufficient to detect bursts of gravitational waves, an orbiting gravitational wave observatory carrying a fish-eye telescope could be constructed.

REFERENCES

Braginsky, V. B., and Thorne, K. S. 1985, *Nature*, **316**, 610.

Colombo, G., Gaposchkin, E. M., Grossi, M. D., and Weiffenbach, G. L. September 1984, "Shuttle-borne Skyhook: A New Tool for Low-Altitude Research," Smithsonian Astrophysical Observatory Reports in Geoastronomy, No.1.

Forward, R. L. 1981, *Gen. Rel. and Grav.*, **2**, 149.

Wagoner R. V., and Paik, H. J. 1977, in *Experimental Gravitation* (Academia) (Nazionale dei Lincei, Rome).

DISCUSSION

SHAPIRO: What analysis has been carried out (re: the proposed skyhook gravitational wave detector) to show that the (broad band) plasma processes in the vicinity of the skyhook will not cause serious problems?

PAIK: The disturbance by the ambient electromagnetic field has been considered. I am not sure whether the plasma processes have been fully analyzed.

SCHUTZ: Why do you only need to go down to $1^{o}K$? Isn't the noise at that temperature still larger than the quantum limit?

PAIK: It depends on the quality factor of the antenna and the bandwidth. For a detector with Q of 10^8 and a fractional bandwidth $\Delta f/f$ of 0.1, cooling to $1^{o}K$ is enough to reach the quantum limit. If one cools down the antenna further, requirement on the transducer Q and coupling will be reduced.

ANDERSON: With regard to the skyhook, when we looked at this, we came to the conclusion that it was necessary to know the gravity gradient field of the Earth to 4 or 5 orders better than it is presently modelled. We therefore came to the conclusion that it might possibly work as a gravity gradiometer for earth gravity modelling--but not as a good gravitational wave detector. Is that so?

PAIK: In fact, Braginsky and Thorne point out that the skyhook is a very good gravity gradiometer for earth gravity. But, by putting the skyhook at high enough altitude, above 1,000 km according to their calculation, they bring down the effect of the earth's gravity gradient to the level of $h=10^{-17}$.

BERTOTTI: I wonder if the noise produced by the low order harmonics of the gravity field of the earth has been studied in the skyhook gravitational wave detector. Since the orientation of the wire will change, there is an additional change in tension due to unknown harmonics.

PAIK: Yes. This gravity gradient effect is attenuated exponentially as a function of altitude. There is a pendulum mode of the skyhook, which makes the end masses rock sideways. However, the additional time-varying tension due to this motion will be narrow-banded.

WEISS: Could you explain the relative merits in sensitivity and costs of putting a spherical antenna in space vs. putting cylindrical bar antennas on the ground. What cannot be done on the ground that must be done in space?

PAIK: In principle, five or six bar detectors oriented in proper directions may accomplish the same purpose as a spherical antenna. However, it may not be easy to support them against the Earth's gravity in various required orientations in three dimensions on Earth.

PULSAR TIMING AND GRAVITATIONAL WAVES

Ronald W. Hellings
Jet Propulsion Laboratory
Pasadena CA 91109

In the last few years, several researcher Detweiler, 1979, Hellings et al. 1983, Romani, et al, 1983 and Davis, et al., 1985) have used timing data from pulsars to search for ultra-low frequency (ULF) gravitational waves (waves at periods from a few days to a few years), especially for the waves making up the stochastic cosmic background such waves. It is the purpose of this talk to discuss how these limits are obtained and to point out several precautions that must be taken in the analysis of these data.

In pulsar timing, the times of arrival of pulses are measured and compared with a model. The UTC times of arrival τ are transformed to TDB times of arrival τ via well-known algorithms (Hellings, 1986 and Backer, et al., 1986). The t's are related to the TDB times of emission T by

$$ct = cT + \mathbf{k}\cdot(\mathbf{R}-\mathbf{r}) - (1+\gamma)\sum_p \frac{GM_p}{c^2}\ln\left[\frac{\mathbf{k}\cdot\mathbf{r}_p + r_p}{\mathbf{k}\cdot\mathbf{R}_p + R_p}\right]$$

where $\mathbf{R} = \mathbf{R_0} + \mathbf{V}T$ is the location of the pulsar at time T, $\mathbf{r}$ is the position of the radio observatory on the earth, $\mathbf{k}$ is a unit vector toward the pulsar, and $\mathbf{r_p}$ and $\mathbf{R_p}$ are the position of intervening body p relative to the earth and the pulsar, respectively, at the time when the signal passes closest to the body. The $(1+\gamma)$ term is of course the Shapiro time delay, with PPN parameter γ parametrizing the curvature of space. The position of the observatory may be written as $\mathbf{r} = \mathbf{q} + \xi$, where $\mathbf{q}$ is the position of the center of the earth, determined from numerically-integrated planetary ephemerides, and ξ is the geocentric position vector of the observatory, determined from observatory coordinates and from a model of the physical ephemeris of the earth.

The actual times of arrival may be compared with the predicted times of arrival to give timing residuals, δt. Among the noise sources contributing to these residuals might be the variation of the spacetime metric created by the passage of a gravitational wave. The rate of change of the timing residuals will be proportional to the dimensionless amplitude of the wave

$$\frac{d}{dt}(\delta t) = \frac{\Delta\nu}{\nu} = h(t).$$

If there is only a single pulsar being observed, then the spectral density of cosmic gravitational waves is simply less than or equal to the spectral density of the residuals. However, if there are several pulsars being observed over the same period of time, it is possible to dig into much larger noise to detect the gravitational wave noise source since it will be a common signal in the time series for each pulsar. Thus we may write the frequency residuals from the i^{th} pulsar as (Hellings et al., 1983)

$$\frac{\Delta\nu_i}{\nu} = \alpha_i h(t) + n_i(t),$$

where α_i contains geometrical factors, resulting from the relation of the polarization and propagation vectors of the gravitational wave to the line-of-sight from the earth

to the pulsar, and $n_i(t)$ is the independent noise in the data from each pulsar. Cross-correlating the data from pulsars i and j, one finds

$$\nu^{-2} \langle \Delta\nu_i \Delta\nu_j \rangle = \alpha_i \alpha_j \langle h^2 \rangle + \alpha_i \langle h n_j \rangle + \alpha_j \langle h n_i \rangle + \langle n_i n_j \rangle,$$

where the brackets indicate cross-correlation. Since n_i and n_j are independent of each other and of h, all of these terms will tend to zero as the square-root of the number of data points except for $\langle h^2 \rangle$, which is the autocorrelation function of the gravitational wave amplitude.

Using data from the single millisecond pulsar, PSR1937+21, limits have been set[4] for gravitational waves of periods less than one year. Using data from several quiet normal pulsars, limits were set[2] using the cross-correlation technique at periods from a few months to five years. These limits are compared with other direct limits and with possible critical energy densities in Figure 1 (Zimmerman et al., 1980).

There is one caution which must be observed in analysis of pulsar data. This is that in order to reduce the timing residuals to the levels that appear in the literature, several deterministic signals have had to be subtracted away. These signals correspond to unknown (and therefore erroneous) values for the period, period derivatives, position, proper motion, and possible parallax of the pulsar and, as data accumulates for the most precise pulsars, the parameters of the earth's orbit and perturbing solar system parameters. The point of this for gravitational wave analysis is that there might have been enormous gravitational wave signatures in the data originally, but, if there had been, they would have been subtracted away by adjusting one of the adjustable parameters of the model.

The method which must be used to take this process into account is to treat the parameter adjustment process as a data filter and to compute the transfer function of the filter. A transfer function is the function which multiplies the input spectrum, frequency be frequency, to produce the output spectrum. The spectrum of the post-fit residuals must therefore be divided by this transfer function to give the realistic limits that may be inferred on the original gravitational wave noise in the timing data records.

Blandford, et al. (1984) computed the transfer function for a filter that adjusted the pulsar parameters only. We have recently worked out the transfer function for a combined adjustment of the pulsar parameters and adjustment of solar system parameters, consistent with the level at which these parameters are known from other solar system astrometric data. Since the solar system model is based on numerical integration, it was not possible to produce an analytical expression for this transfer function. Rather a Monte Carlo analysis was performed in which twenty years of pulsar timing data were simulated, one point per week, and these data added to the combined set of solar system data while all parameters, pulsar and solar system, were adjusted. Twenty such simulated data sets were analysed and the pre- and post-fit power spectra were compared to get the transfer function for each set. A mean transfer function was found as a average of the twenty transfer functions. The results of this analysis are shown in Figure 2. It should be noted that there has been a noticeable subtraction of power at Mars's orbital period and that other longer period planetary perturbations combine to subtract almost all power at periods longer than about five years. The strong absorbtion line at one year combines

period planetary perturbations combine to subtract almost all power at periods longer than about five years. The strong absorbtion line at one year combines uncertainty in Earth orbital parameters and uncertainty in pulsar position and proper motion (the latter $t \sin t$ parameters acting to keep the line relatively broad).

REFERENCES

Backer, D. C. and Hellings, R. W. 1986, *Ann. Rev. Astron. Astrophys.* **24**, 537.
Blandford, R., Narayan, R., andRomani, R. 1984, *J. Astrophys. Astron.* **5**, 369.
Davis, M. M., Taylor, J. H., Weisberg, J. M., and Backer, D. C. 1985, *Nature* **315**, 547.
Detweiler, S. 1979, *Ap. J.*, **234**, 1100.
Hellings, R. W., *Astron. J.* 1986, **91**, 650.
Hellings, R. W. and Downs, G. S. 1983, *Ap. J. Lett.* **265** L39.
Romani, R. W. and Taylor, J. H. 1983, *Ap. J. Lett.* **265** L35.
Zimmerman, R. L. and Hellings, R. W. 1980, (original of this figure) *Ap. J.* **241**, 475.

Figure 1. Limits on the spectrum of cosmic gravitational radiation energy density from several direct gravitational wave experiments. The line labeled "critical densities" represents the locus of peaks of a set of broad-band spectra, each of which would provide a critical energy density. The line labeled "PULSARS" is from the analysis of Hellings and Downs (1983). The line labeled "1937+21" comes from the results of Davis et al (1985).

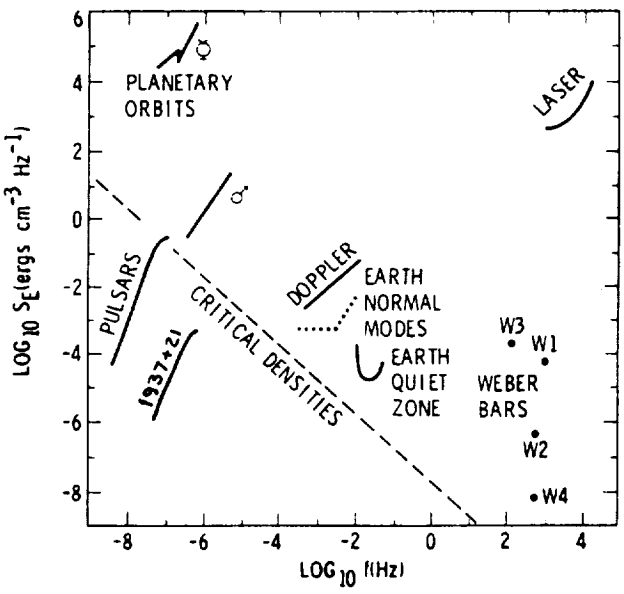

Figure 2. Mean transfer function of the solar system data analysis filter. Ordinate is relative power. Abscissa is frequency in inverse days.

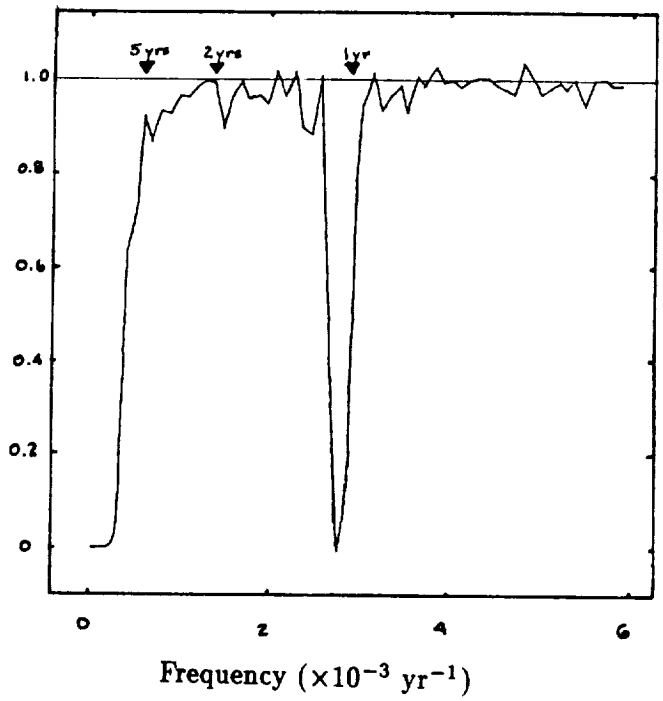

DISCUSSION

SCHUTZ: Could you clarify one point please? Although an increasing sum of data may not lower the minimum frequency at which you can set limits, presumably it does continue to improve limits on the gravitational wave background at higher frequencies?

HELLINGS: Yes.

TREUHAFT: Would VLBI positions of the millisecond pulsar help eliminate parameters from your fit of pulsar data?

HELLINGS: Yes. Roger Linfield at JPL has some data to do that in the can, but it hasn't yet been analyzed. Of course, this assumes a tie between the VLBI reference frame and the planetary ephemeris reference frame, in which the timing positions will be given.

N90-19956

X-RAY TIMING OBSERVATIONS AND GRAVITATIONAL PHYSICS

PETER F. MICHELSON
Department of Physics
Stanford University
Stanford, California 94305

KENT S. WOOD
Naval Research Laboratory
Washington, D.C.

Photon-rich X-ray observations on bright compact galactic sources will make it possible to detect many fast processes that may occur in these systems on millisecond and submillisecond timescales. Many of these processes are of direct relevance to gravitational physics because they arise in regions of strong gravity near neutron stars and black holes where the dynamical timescales for compact objects of stellar mass are milliseconds. To date, such observations have been limited by the detector area and telemetry rates available. However, instruments such as the proposed X-ray Large Array (XLA) would achieve collecting areas of about 100 m^2. This instrument has been described elsewhere (Wood and Michelson 1988) and was the subject of a recent prephase A feasibility study at Marshall Space Flight Center. Observations with an XLA class instrument will directly impact five primary areas of astrophysics research: the attempt to detect gravitational radiation, the study of black holes, the physics of mass accretion onto compact objects, the structure of neutron stars and nuclear matter, and the characterization of dark matter in the universe. In this talk we will focus on those observations that are most directly relevant to gravitational physics: the search for millisecond X-ray pulsars that are potential sources of continuous gravitational radiation; and the use of X-ray timing observations to probe the physical conditions in extreme relativistic regions of space near black holes, both stellar-sized and supermassive ($>10^6$ solar masses). These observations can be used to find answers to gravitational physics questions such as the following.

- Are rapidly-spinning neutron stars subject to relativistic instabilities that lead to the emission of gravitational radiation?
- Do marginally stable orbits exist around neutron stars?
- Do accreting neutron stars in binaries evolve primarily by orbit decay associated with gravitational radiation emission?
- Are light curves of predicted binary millisecond X-ray pulsars modified by gravitational lensing?
- What are the submillisecond temporal characteristics of galactic black holes?
- What are the angular diameters of X-ray emitting regions around compact objects in active galactic nuclei?
- What is the extent of X-ray emission associated with halos of clusters of galaxies, and does it imply the presence of dark matter?

The direct detection of gravitational radiation is perhaps the primary goal of experimental gravitational physics. While emission of such radiation has been inferred from radio observations of a neutron star binary system, efforts to directly detect gravity waves have not yet succeeded. The predicted sources of gravitational

radiation may be broadly subdivided according to whether emission is produced in a short burst, as a stochastic background, or as a continuous wave at a single frequency. Continuous wave emission is of interest in connection with bright accreting neutron stars in binaries.

Rapidly rotating neutron stars become secularly unstable when subjected to viscous dissipative forces or gravitational radiation reaction (Chandrasekhar 1970, Friedman and Schutz 1978). Modes that grow via gravitational radiation reaction are damped by viscosity and vice versa. This process, often referred to as the Chandrasekhar-Friedman-Schutz (CFS) instability, was originally considered applicable to a situation in which a neutron star is born with a spin period near 1 ms and then deaccelerated by the torque associated with gravitational radiation. In a reference frame rotating with the star, the CFS mode manifests itself as a nonaxisymmetric deformation of the star (with mode number m = 3 or 4) that counter-rotates. For the CFS mechanism to deliver CW gravitational radiation over a prolonged time, the angular momentum radiated away must be replenished. Nature provides an appropriate situation when a neutron star with a weak magnetic field accretes material from a binary companion. In an accretion environment, the neutron star need not start with a short period. Accretion provides a spin-up torque that can first drive the neutron star into the unstable regime and then keep it there, ultimately reaching an equilibrium in which angular momentum lost by gravitational radiation equals that gained from accretion. This scenario was recently described theoretically by Wagoner (1984). The model requires that the star have a weak magnetic field in order that the accretion disk extend to the stellar surface and deliver angular momentum continuously.

In equilibrium, gravitational radiation is emitted at a frequency f associated with the pattern speed of the nonaxisymmetric distortion as seen in the observer's frame. This frequency depends on details of the neutron star's structure and its viscosity. It is predicted to lie in the range 200 Hz < f < 800 Hz, below the rotation frequency of the star.

X-ray radiation is emitted as a consequence of the accretion process. Indeed, most of the gravitational energy of the accreting matter is released in X-rays, while most of the angular momentum is removed by gravitational radiation. Because of the nonaxisymmetric distortion of the star, the X-ray flux is expected to be weakly modulated at the same frequency as the gravitational radiation. This situation constitutes a new kind of binary X-ray pulsar that has never been detected, probably because the frequency is very high, the level of modulation is very low, and the pulsar is in a binary system. All of these conditions make detection with a small aperture detector very difficult. An XLA class instrument enormously improves the detection probability.

Detection in either the X-ray or the gravity wave channel facilitates the search in the other channel. One could discover the pulsar in X-rays and use knowledge of the frequency to search for the gravity wave signal. Detection of the X-ray pulsations by itself would be significant, settling some major issues in astrophysics. The period of the X-ray modulation would give information about the equation of state of matter at high densities and information about the viscosity. The theory of the X-ray pulsation mechanism in these systems could be tested. Dual-channel detection of the source in both X-rays and gravity waves would provide two measures of the neutron star distortion and would lead to a variety of new observational tests, *e.g.*, tracking the angular momentum as it is added by accretion and removed by gravitational radiation.

We now turn to consideration of how X-ray timing applies to the study of black holes. These gravitationally collapsed objects are an allowed endpoint of evolution of massive bodies in General Relativity. Specific astrophysical candidates have been identified in two very different mass ranges: stellar candidates such as Cygnus X-1 and active galactic nuclei (AGN), with masses from about 10^5 to perhaps more than 10^7 solar masses. Black holes play a fundamental role in astrophysics, in large part because accretion onto black holes is thought to be the energy release mechanism that powers the quasars and other AGNs.

X-ray and even gamma-ray observations have contributed enormously to the identification and study of black hole candidates, mainly because it is in these high-energy channels that the sources are highly luminous and well-isolated. Since the radiation emitted by accretion can vary on the relevant dynamical timescales, fast timing and time-resolved spectroscopy are crucial, just as for neutron stars. However, we must acknowledge that no high-energy observations by themselves have yet provided a rigorous observational demonstration that a black hole is present in these systems. For the stellar mass cases in particular, the experimental approach most often used is proof by mass determination: if the compact, accreting object exceeds the maximum stable mass of a neutron star, then it must be a black hole. The mass determination is usually made by optical observations of the companion that determine the mass function of the accreting binary system. X-ray observations establish the compact nature of the source. This approach is indirect in that it establishes a black hole by excluding a particular alternative, a stable non-collapsed configuration, rather than by observing some distinctive signature indicative of an event horizon in the system. Excluding alternatives is not quite the same as demonstrating a horizon.

One of the ways that X-ray observations can be used in the study of black holes is to observe strong gravitational field effects associated with the hole that can be isolated in the short timescale X-ray variability of the source. (Another tool is X-ray polarimetry measurements. See R. Stark's contribution in this volume.) For example, the mass and angular momentum of a black hole are two properties that can, in principle, be determined by external measurements. These properties of the hole determine the innermost marginally stable orbit around the hole, which, in turn, sets the inner boundary of the accretion disk. For a known mass, the period of the innermost stable orbit is a function of the magnitude and direction of the angular momentum of the hole. Thus, if we knew the mass and could measure the innermost stable orbit period, the angular momentum of the hole could be determined.

There is some evidence that emission from the inner disk can be isolated. From observations of the rapid X-ray variability from Cygnus X-1, Meekins, *et al.* (1984) found that a substantial fraction of the emission was modulated near a preferred timescale of 3 milliseconds. Order of magnitude considerations show that the timescale and magnitude of these fluctuations require an origin in the inner accretion disk. In addition, a turnover in the variability power was found on timescales shorter than 3 ms. This may signal detection of the inner edge of the disk.

It must be stressed that these results were based not on the detection of single bursts but rather from the study of long strings of data. In other words the bursts are not studied singly but in a statistical aggregate. An XLA class instrument is needed to see individual burst events and measure their temporal profiles and energy

spectra. These observations should lead to a much improved theory of the inner edge of the disk and therefore its use as a probe of the gravitational metric in this region.

In this talk we have stressed two applications of X-ray timing observations with a large area detector. There are many others. In conclusion, we point out that the historical experience in X-ray timing, from the UHURU satellite onward, has been one of continual surprise. EXOSAT (launched 1983) is particularly remembered for the discovery of quasiperiodic oscillations in neutron stars: a phenomenon that was unforseen when EXOSAT was launched. In the age of the NASA Space Station, it will be possible to construct instruments with 100 m^2 aperture and the commensurate data handling capability that will make possible X-ray timing observations on timescales as short as a few tens of microseconds. These timescales are at least a factor of 1,000 shorter than the shortest accessible with past and current generation satellites and about 10^5 shorter than typical capabilities. This is a largely unknown territory but, based on past experience, we can anticipate many important discoveries.

REFERENCES

Chandrasekhar, S. 1970, *Phys. Rev. Lett.*, **24**, 611.

Friedman, J. L., and Schutz, B. F. 1978, *Astrophys. J.*, **222**, 281.

Meekins, J. F., *et al.* 1984, *Astrophys. J.*, **278**, 288.

Wagoner, R. V. 1984, *Astrophys. J.*, **278**, 345.

Wood, K. S., and Michelson, P. F. 1988 in *Experimental Gravitational Physics*, P. F. Michelson and Hu En-ke, eds. (World Scientific Publishing Co., Singapore).

DISCUSSION

SCHUTZ: I'd like to reinforce what you said about the relation of this experiment to ground-based gravitational wave detectors. If we could detect Wagoner's accretion-driven unstable neutron stars we would learn a great deal about neutron star structure and the equation of state of neutron matter. But even broad-band laser interferometers may not have sufficient sensitivity to detect the gravitational waves without using narrow-banding techniques to enhance sensitivity at the frequency of the wave. So they will need to know this frequency ahead of time, and XLA can make a big contribution to gravitational wave astronomy.

WOOD: Yes, that's correct. In principle one could use either type of detector, gravitational wave or X-ray, for initial discovery of the continuous-wave signal and then look in the other channel at the frequency that had been discovered. It appears that prospects for initial discovery are far better in X-rays. I should stress that it is important to know not only the frequency of the CFS signal in the center-of-mass frame of the neutron star but also the orbital elements of the binary system, because orbital motion introduces a substantial frequency modulation. The large X-ray aperture overcomes the FM by providing sufficient sensitivity for detection in a small fraction of an orbital period, and once the signal is found, it can be used to work out the necessary orbital elements. The X-ray and gravitational wave observations contribute complementary information about the source.

WEISS: Can you compare XLA with XTE? (The X-ray Timing Explorer).

WOOD: XLA represents the genera and has far greater capability. XLA is 200 times larger and has a maximum telemetry data rate several hundred times greater than that of XTE, both of which are needed for working at higher signal-to-noise on very short timescales. The two experiments operate in the same energy range and can isolate essentially the same set of sources (excepting transients active for one and not the other). XLA can make all the observations that XTE's proportional counter array can make, but it also can carry out other observations that go far beyond XTE's capabilities. These latter observations are the ones that have been discussed here. Being 100 times larger does not make it 100 times as expensive. There should be very significant economies of scale in the manufacture of many proportional counters. Some of the functions of the free-flyer satellite that carries XTE are in the case of XLA provided by the Space Station, for example power and telemetry. The Space Station provides maintenance access as well.

HELLINGS: Can this detector act as a polarimeter in the sense of Richard Stark's suggestion?

WOOD: There is a possibility that polarimetry capability could be incorporated, by measuring the pulse rise time as well as the amplitude for each X-ray event. This approach was examined some years ago and found to be sufficiently sensitive only when there are very large numbers of photons, but that is exactly what the large area of XLA provides. This issue needs to be re-examined in the XLA context. In any X-ray polarimetry it is essential to be able to distinguish real polarization effects from spurious effects of instrumental origin. Laboratory work on that is needed.

SHAPIRO: What sort of angular resolutions do you expect to obtain with your array and how do you plan to achieve them?

WOOD: The basic proportional counter units have mechanical collimators that provide a field of view of 1 square degree. This is sufficient to isolate the bright sources that will be used for the timing work, i.e., the 2000 brightest sources in the sky. It would be straightforward to have a co-aligned monitor imaging detector observing the field simultaneously. (A coded aperture could monitor the field with resolution of a few arcminutes.) We regard this as an option, not absolutely essential, because in those cases where it was desirable to monitor the field of view it might be possible to arrange simultaneous observation with another instrument such as AXAF.

Very high angular resolution for mapping on fine scales is achieved by using XLA in conjunction with a distant occulting edge that moves slowly across the field of view, either a natural occulter (the moon) or an artificial one. The angular resolution achievable varies with the source and observing configuration, but it would be possible to reach milliarcseconds on sources as faint as the brighter quasars and active galactic nuclei. One must be able to see the source at sufficient signal-to-noise in the time the occulter sweeps the angular scale of interest. This is roughly a thousandfold better than the best angular resolution achievable in X-rays by other means.

FAIRBANK: What is the angular resolution if you provide a knife edge with another satellite?

WOOD: There are several reasons to provide an artificial satellite with a smooth edge that can be steered around to provide artificial occultations. The machined edge removes the necessity for knowing the lunar terrain in the region that provides the occultation, which means that the limit on angular resolution with a bright source will be set by diffraction and might become as fine as 100 micro-arcseconds. It is possible to steer the artificial occulter to any point on whole sky, so that there is access to a much larger sample of targets, and the artificial occultations can be scheduled to occur at convenient times.

To get the occulter to move slowly enough it must be at roughly the distance of the moon. The technical problems involved in realizing precision navigation of a satellite is such a high orbit are (i) minimizing the control impulse (propellant) required for navigation and (ii) the error budget, that is, determining what correction to apply to achieve occultation. A study done by NRL and Stanford showed that both problems could be solved by placing the satellite in an orbit perpendicular to the lunar orbit and suitably phased so that the gravitational pull of the moon advances the orbit plane without fuel expenditure. Control impulse is applied only to in-track maneuvering.

GENERAL RELATIVISTIC X-RAY (UV) POLARIZATION ROTATIONS AS A QUANTITATIVE TEST FOR BLACK HOLES

RICHARD F. STARK
Institute for Theoretical Physics,
University of California, Santa Barbara, CA 93106, U.S.A.

ABSTRACT

It is now 11 years since a potentially easily observable and quantitative test for black holes using general relativistic polarization rotations was proposed (Stark and Connors 1977, and Connors and Stark 1977). General relativistic rotations of the X-ray polorization plane of 10 to 100 degrees with X-ray energy (between 1 keV and 100 keV) are predicted for black hole X-ray binaries. (Classically, by symmetry, there is no rotation.) Unfortunately, X-ray polarimetry has not been taken sufficiently seriously during this period, and this test has not yet been performed. A similar (though probably less clean) effect is expected in the UV for supermassive black holes in some quasars and active galactic nuclei. Summarizing: (i) a quantitative test (proposed in 1977) for black holes exists; (ii) X-ray polarimetry of galactic X-ray binaries sensitive to at least 1/2% between 1 keV and 100 keV is needed (polarimetry in the UV of quasars and AGN will also be of interest); and (iii) proportional counters using timerise discrimination have been shown in laboratory experiments able to perform X-ray polarimetry and this and other methods need to be developed.

Measurement of the energy dependence of the direction of the plane of linear polarization of the X-ray emission from accreting black hole candidate binary systems will allow a direct and quantitative experimental test for the presence of a black hole in these systems (Stark and Connors 1977, Connors and Stark 1977, and Stark 1980). While classically there can be no continuous rotation of the plane of polarization with observed X-ray energy for such axisymmetric systems, general relativistic effects due to a black hole will result in an energy-dependent rotation of several tens of degrees in this polarization plane for energies between 1 and 100 keV which will provide a signature for the presence of a black hole. Measurement of this energy-dependent rotation, together with the corresponding general relativistic effects on the energy dependence of the net observed degree of linear polarization of the X-ray emission, will allow us to test whether a black hole is present and to quantitatively measure the spin of the black hole, as well as to probe the geometry of the accretion process.

The reason that the X-ray polarization properties are so sensitive to the strong gravitational field of the black hole, comes from the fact that the rotation of the plane of polarization of the X-rays propagating from the accreting gas near the black hole to the observer is of the same order as the amount of gravitational bending which these rays undergo. (The radiation is polarized because of electron scattering and other processes occuring during the radiative transfer within the gas surrounding the black hole.) Since, for a black hole, this bending can amount to 10 to 100 degrees, similarly large general relativistic polarization rotation effects will exist. These polarization effects are therefore intimately related to one of the most well known effects of gravitation: that of light bending — but are measured in tens of degrees rather than the usual seconds of arc!

Detailed calculations (Stark and Connors 1977, Connors and Stark 1977, and Stark 1980), for the X-ray polarization properties of the standard black hole disk model, show rotations of 10 to 100 degrees in the direction of the net observed plane of linear polarization with X-ray energy between 1 and 100 keV, (Fig.1). The magnitude of these polarization rotations becomes bigger with increasing angular momentum of the black hole and for decreasing observer polar angles. Typically we find for energies between 1 and 100 keV a polarization angle rotation of 40 degrees in the X-ray emission from accretion onto a nonrotating Schwarzschild black hole and 90 degrees for accretion onto a maximally spinning Kerr black hole. General symmetry arguments do not allow such continuous polarization rotations with energy for classical (*i.e.*, weak gravitation), axisymmetric systems, so that detection of this unique polarization feature can indicate both the existence of a black hole, and that the accretion is in the form of a disk all the way to the inner region. A similar behaviour of the plane of polarization with energy is also expected from most other disk models which have strongly radially dependent physical conditions. General relativistic effects will also modify the X-ray energy dependence of the degree of linear polarization (Fig. 2) — it being reduced typically by a factor of 2 from the classical result.

Detailed calculations (Connors and Stark 1977; Connors, Piran, and Stark 1980; Stark 1980) have also been performed for other black hole accretion models: standard disk models for the outer region and an optically thin inner disk region or a geometrically thick cloud surrounding the black hole. For these types of accretion, we expect the polarization properties to follow the standard disk results for low energies (up to 1 to 10 keV), while above these energies, the polarization properties become energy-independent with a plane of polarization differing from the lower energies by an angle different from 90 degrees (the classical result; Lightman and Shapiro 1975). Observation of a continuous rotation of the polarization angle with X-ray energy at low energies, followed by a jump different from 90 degrees, would indicate the existence of a black hole and that the accretion in the inner region is optically thin. Further information would be obtained from the energy dependence of the degree of linear polarization. Monte-carlo calculations of the effects of a large cloud of scattering material surrounding the binary system show that these general relativistic rotations would remain observable even for optical depths of scattering material up to 0.5 (Connors, Piran, and Stark 1980; and Stark, 1980).

As well as observing the energy dependence of the plane and degree of X-ray polarization, one may also expect long-term, temporal variations in these polarization properties at a fixed observer energy. Observers may detect changes in the plane and degree of X-ray polarization if the size of the accreting cloud or disk varies, giving rise to a general relativistic time-dependence of these polarization properties. Such changes could be associated with spectral and intensity changes. In particular, it would be important to see if there are any temporal changes in the polarization features of Cygnus X-1 which are correlated with the spectral intensity changes between the two states of this source.

X-ray polarization observations would be able to rule out nongeneral relativistic contributions to this rotation of the polarization plane with X-ray energy. A twisted nonaxisymmetric disk, resulting from the nonalignment of the spin axis of the black hole with that of the binary system, could lead to such a rotation. This possibility is unlikely, however, since general relativistic dragging of inertial frames effects are expected to align the X-ray emitting inner region of the disk into the equatorial plane of the black hole (Bardeen and Patterson 1975). Any remaining

effects from a twisted disk could be discovered observationally (and distinguished from general relativistic rotations) by looking for a time-dependence of the polarization properties with a period equal to that of the orbital period of the binary system. A second additional source of energy-dependent polarization rotation at low X-ray energies (on top of the general relativistic rotation) would occur from Faraday rotation if a strong homogeneous magnetic field is present. A more likely magnetic field configuration, because of the differential rotation present, would be a chaotic field which would influence the degree and not the plane of polarization. In any case, even for the maximum magnetic field possible, these magnetic effects would only be significant below 1 to 10 keV, and they would be observationally distinguished from general relativistic effects by the E^{-2} dependence of the magnetic depolarization with energy E (Gnedin and Silant'ev 1977). The measurements of Long, Chanan, and Novick (1980) of 3% linear polarization in Cygnus X-1 at 2.6 keV, if positive, suggest that such depolarization does not take place in this source.

What difference can we expect between a black hole and neutron star? The difference in surface boundary conditions and magnetic fields can be expected to lead to observationally distinct polarization properties between a black hole as opposed to a neutron star X-ray binary. (In general, we would expect neutron star binaries to be more highly polarized.) If, however, we assume a nonmagnetized neutron star and neglect the difference in boundary conditions, then we can estimate a factor of ~5 difference between the general relativistic polarization rotations for a Kerr black hole and that for a neutron star, and a factor of (1 to 2) between a Schwarzschild black hole and neutron star. Experimentally we would look for a statistical correlation between X-ray binaries with high mass compact objects (indicating black holes) and those showing the larger polarization rotations. Further evidence would be given by the energy dependence of the degree of polarization.

In laboratory experiments, Sanford, Cruise, and Culhane (1970) have demonstrated the ability to use timerise discrimination in proportional counters to perform X-ray polarimetry. The charge cloud of cascade electrons has a shape dependent on the polarization of the X-ray photon inducing the photoelectron process. As the cloud drifts toward the anode, the shape determines the timerise characteristics of the signal and hence the incoming polarization can be measured. This method seems to show great promise and it is surprising that it has not been exploited more. (Above 30 keV to 50 keV, where the photoelectric opacity drops, a compton polarimeter would probably be necessary.)

Similar general relativistic effects can be expected for supermassive black holes. The magnitude of the general relativistic polarization rotations remains the same independent of the black hole mass. The mass simply determines where in energy the rotation takes place. Thus, for disk accretion about a supermassive black hole (mass $5 \times 10^8 M_\odot$) rotations of 10 to 100 degrees can occur (when free-free opacity and Faraday effects are not dominant) in the UV, beginning around 10 to 20 eV (Stark and Connors 1988). (Polarization swings with timescales of hours to days from orbiting hot spots may also be observable; Connors, Piran, and Stark 1980; and Stark 1980.) Black hole accretion is a possible model for quasars and some active galactic nuclei, and it would be of great interest to have accurate polarimetry of these objects at these frequencies. Observations of a UV excess in the flux of some quasars have already allowed an estimate of the disk contribution and hence estimates of the black hole mass and accretion rate (*e.g.*, Malkan 1983). Knowing the mass and accretion rate, a definite prediction for the general relativistic polarization

rotation and degree of polarization as a function of frequency can be made (Stark and Connors 1988). Unfortunately, accurate polarimetry at these frequencies does not presently exist in order to make a comparison with these theoretical predictions. It should be noted, though, that model-dependent details are much more uncertain in the supermassive case as compared to the galactic X-ray binary case. X-ray polarimetry of X-ray binaries is thus preferred over UV quasar observations as providing the cleanest quantitative test for black holes.

ACKNOWLEDGEMENTS

The work reported here was done in collaboration with Paul Connors, and in part with Tsvi Piran.

REFERENCES

Bardeen, J. M., and Petterson, J. 1975, *Astrophys.. J. Lett.*, **195**, L65.

Connors, P. A., and Stark, R. F. 1977, Nature, **269**, 128.

Connors, P. A., Piran, T., and Stark, R. F. 1980, *Astrophys. J.*, **235**, 224.

Gnedin, Yu. G., and Silant'ev, N. A. 1977, *Sov. Astr. Lett.*, 3, 136.

Lightman, A. P., and Shapiro, S. L. 1975, *Astrophys. J. Lett.*, **198**, L173.

Long, K. S., Chanan, G. A., and Novick, R. 1980, *Astrophys. J.*, **238**, 710.

Malkan, M. A. 1983, *Astrophys. J.*, **268**, 582.

Sanford, P. W., Culhane, J. L., and Cruise, A. M. 1970, in *Non-solar and X-ray astronomy, IAU proceedings*, ed. L. Gratton.

Stark, R. F. 1980, *Electron Scattering, Polarization and General Relativity*, Ph.D. thesis, Oxford University, Unpublished.

Stark, R. F., and Connors, P. A. 1977, Nature, **266**, 429.

Stark, R. F., and Connors, P. A. 1988, To be published.

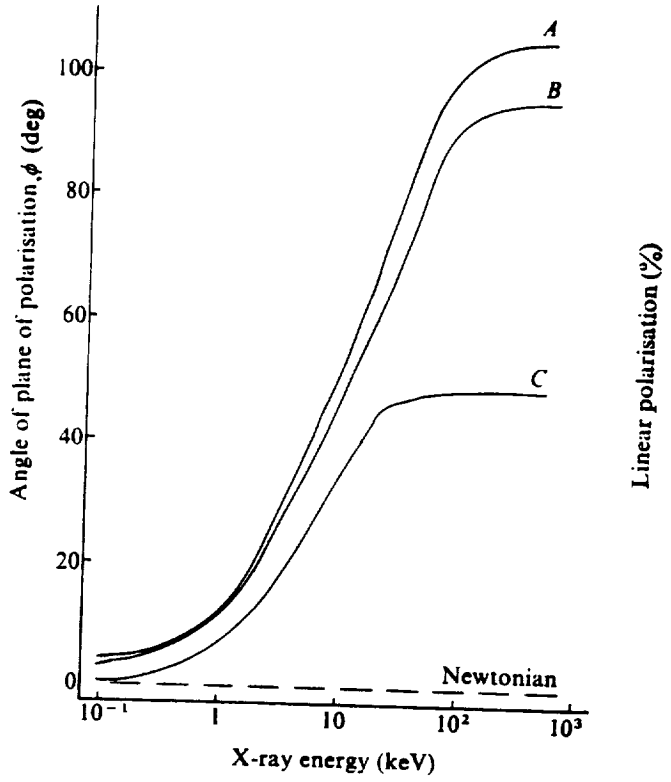

FIG. 1.—Variation of plane of polarisation with energy for $\theta_0 = 41.1$ for the one-temperature model with *A*, $a/m = 0.9981$; *B*, $a/m = 0.9$; C, $a/m = 0$, where viscosity parameter, $\alpha = 0.1$; mass of black hole, $M = 9M_\odot$; mass accretion rate $= 7 \times 10^{17}$ gs^{-1}.

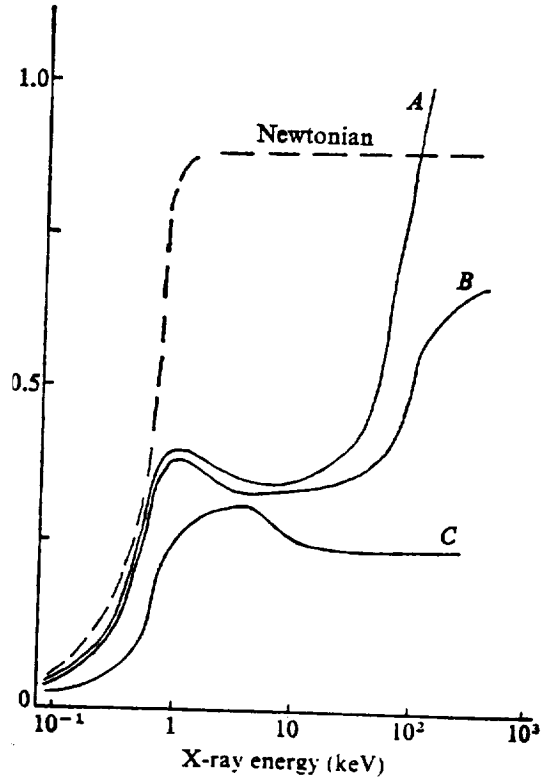

FIG. 2.—Variation of linear polarisation with energy for the one-temperature model, with *A*, $a/m = 0.9981$; *B*, $a/m = 0.9$; C, $a/m = 0$. Same parameters as Fig. 1.

DISCUSSION

SHAPIRO: It was not clear to me that the distinction between black holes and neutron stars would be so simple to make reliably. Could you comment in more detail on the means for such distinctions?

STARK: The pick-out (both radially and azimuthally) of the most blue shifted rays which are the dominant contribution to the polarization rotations (see Stark & Connors, 1977) allows us to estimate the size of the polarization rotations for neutron stars. (Neglecting, for the moment, the surface boundary differences). Comparing the general relativistic rotations (with X-ray energy) from fairly extreme neutron stars with the black hole results (for the same observer angle) we find a factor ~ 5 difference between a maximal Kerr black hole and a neutron star, and ~1-2 between a Schwarzschild black hole and a neutron star. There is a clear distinction between a rapidly spinning black hole and a neutron star; but less so for a Schwarzschild black hole. The X-ray polarization properties of neutron stars can, however, be expected to be also observationally distinct from black holes because of the radiative differences in the inner regions arising from surface boundaries and magnetic fields. (Higher degrees of polarizations can be expected from neutron stars). The energy dependence of the degree of polarization together with that of the polarization rotations may allow us also to distinguish between Schwarzschild black holes and neutron stars, if this is true. It will also be important to correlate X-ray polarization data with other observations. Thus, we will expect to see statistically higher X-ray polarization rotations with energy in those binaries which have higher mass compact objects (those beyond the neutron star mass limit, and therefore black hole candidates).

HELLINGS: Is the width of the x-ray spectrum sufficiently narrow that you can pick out the shift of frequency.

STARK: I'm not sure I exactly understand the question. The polarization rotation test has no direct relation to frequency shifts. The polarization measurements are performed on the continuum X-ray flux and have nothing to do with any particular spectral features.

SPACE TELESCOPE SEARCHES FOR BLACK HOLES IN GALACTIC NUCLEI

RICHARD J. HARMS
Applied Research Corporation

ABSTRACT

The Hubble Space Telescope (HST) will allow astronomers to obtain luminosity profiles, rotation curves, and velocity dispersions at angular scales that are an order of magnitude superior to those obtained previously. This enhanced spatial resolution will greatly improve our sensitivity for detecting centrally condensed matter in nearby galactic nuclei including, possibly, black holes.

I. INTRODUCTION

The determination of the total masses and mass distributions of various types of galaxies has been an active area of astronomical research throughout the past approximately 15 years. Reviews by Faber and Gallagher (1979) and by Trimble (1987) summarize many of the results obtained from ground-based observations and their implications for the existence of black holes in the nuclei of some galaxies. Many of these observations concentrate on determining the mass content of galaxies out to large distances from their nuclei in order to estimate their total masses and its forms. However, other observations have been directed at determining the mass and luminosity distributions of galaxies as far toward their nuclei as practicable. Because they are so nearby, M31 and M32 have been especially good candidates for seeking black holes in their nuclei. Observations by Tonry (1987), Dressler and Richstone (1988), and Kormendy (1988) strongly suggest the possible presence of black holes in both these nearby galaxies.

The Hubble Space Telescope (HST) will routinely obtain images with spatial resolution of 10s of milliarcseconds throughout the UV to near-IR region. Spectroscopy of regions through apertures as small as 0.1 arcseconds will also be possible throughout most of the same spectral region. This increase in angular resolution will enable astronomers using the HST to obtain luminosity profiles, rotation curves, and velocity dispersion profiles of the central regions of galaxies with spatial resolution at least an order of magnitude improved over what has been possible to date from the ground. Limited angular resolution is the primary limiting factor for detecting the presence of centrally condensed matter in the nuclei of galaxies, so that the availability of the HST Observatory will greatly improve our sensitivity for detecting black holes in the nuclei of galaxies.

II. APPROACH

From images of a galaxy taken through one or more broad-band filters, along with certain assumptions about the galaxy's orientation and symmetry, one directly obtains the luminosity profile L(R). From these data and additional models of the fractions of stellar types, the luminosity distribution yields an estimate of that portion of the mass distribution due to stars. Non-uniqueness of the conversion from observed luminosities and spectra to stellar sources, and uncertainty in the true orientations and symmetry of the galaxy, produce rather large uncertainties in the determination of $M_{stellar}(R)$ for any particular galaxy.

The total mass distribution of the galaxy can be estimated from the effects of gravity acting on the luminous matter. Spatially-resolved spectra of spiral galaxies produce rotation curves, V(R), of the (line-of-sight) velocity of stars versus position in the galaxy. Because elliptical galaxies generally are not supported by rotation, one sees in their spectra primarily a dispersion, $\sigma_V(R)$, in the (line-of-sight) velocities with position. Within uncertainties set by unknown inclination effects, symmetry, and dominant orbit types (radial, circular, isotropic), one can obtain estimates of M(R), the total mass within radius R, for both spirals and ellipticals. (Note that the velocity dispersion, $\sigma_V(R)$, as R-->0 will provide useful information about the matter in both spiral and elliptical galaxy nuclei.)

The signature of a black hole in the nucleus of a galaxy will be a normal luminosity and a high value of mass as R-->0. If the inferred density of invisible material within the nucleus becomes great enough, it can be argued that the matter very probably has collapsed into a black hole simply because separate masses so closely crowded will not be stable against gravitational collapse. Such an argument is unlikely to be absolutely conclusive in any given case, but the likelihood of a black hole can become extremely high if one can detect the existence of substantial mass within a small enough volume. Thus, the measurements of L(R) and M(R), the latter through either V(R) or $\sigma_V(R)$, at small R are crucial for detecting any possible black holes in galactic nuclei.

III. SENSITIVITY OF HST FOR FINDING NUCLEAR BLACK HOLES

It is the factor-of-10 increase in angular, and therefore spatial, resolution that will make the HST a powerful tool for finding black holes (if they are there) in the nuclei of galaxies, or for setting improved upper limits to their presence. Two major reasons explain why increased spatial resolution enhance so dramatically our sensitivity for detecting black holes in galaxies:

(1) The measured spectral effects become stronger as R-->0 since both V(R) and $\sigma_V(R)$ scale as $(M/R)^{1/2}$, and

(2) Observations at smaller values of R enhance the intrinsic contrast between total mass M(R) and the mass $M_{stellar}(R)$ due to stars.

The functional dependence of the spectral signature strength, proportional to $(M/R)^{1/2}$ (Item 1), suggests that the HST will be about 10 times more sensitive than a ground-based telescope for detecting a black hole in a particular galactic nucleus. However, it is the contrast enhancement (Item 2) arising from the ability to "home in" more sharply on the central region of the galaxy that really increases our sensitivity to a central black hole. Sampling R 10 times closer reduces the contribution to M(R) from stars by a factor of 1,000 if the central stars are uniformly distributed, and even more if (as is likely) their density increases toward the center of the galaxy.

Table 1 provides examples of the spatial resolution which will become possible with the HST. Images sampled on an angular scale as fine as 7 milliarcseconds will be possible, while spectra will be obtained through apertures as small as 0.1 arcseconds in diameter. Spectra taken from the HST will allow determination of V(R) and $\sigma_V(R)$ to at least 100 km/sec accuracy. Table 2 illustrates typical masses of black holes which will be detectable with the HST at various distances.

TABLE 1

SPATIAL SAMPLING IN PARSECS FOR VARIOUS BLACK HOLE DOMICILES

RESOLUTION (arcsec)	RESOLUTION (pc) ON CERTAIN TARGETS			AVAILABLE INSTRUMENTS
	M31 AND M32 D = 0.35 Mpc	M87 9 Mpc	NGC 6251 70 Mpc	
0.007	0.03	0.6	5	FOC
0.022	0.08	2	15	FOC
0.044	0.15	4	31	FOC,WF/PC
0.10	0.35	9	70	FOC,WF/PC,FOS
0.2	0.88	23	175	FOC,WF/PC,FOS,GHRS
1.0	3.5	90	700	HST and GROUND-BASED

FOC = Faint Object Camera (on HST)
WF/PC = Wide-Field/Planetary Camera (on HST)
FOS = Faint Object Spectrograph (on HST)
GHRS = Goddard High Resolution Spectrograph (on HST)

TABLE 2

HST CAPABILITY FOR DETECTING BLACK HOLES IN GALAXIES AT VARIOUS RANGES

DISTANCE (Mpc)	$RV^2/G \approx$ MIN DETECTABLE BH ($M_\odot$)
0.35	$8 * 10^5$
9	$2 * 10^7$
70	$2 * 10^8$

For M31 and M32, we will be sensitive to black holes of the size ($\approx 10^6 M_\odot$) suspected to exist at the nucleus of our own galaxy [see, for example, Serabyn and Lacy (1985)]. The HST observations will be able to prove conclusively the presence or absence of black holes in M31 and M32 of the masses ($10^{6.5-8.0} M_\odot$) suggested by the observations of Tonry (1987), Dressler and Richstone (1988), and Kormendy (1988).

IV. CONCLUSIONS

The HST will provide a powerful tool for finding black holes in the nucleus of nearby galaxies. The factor-of-10 increase in angular resolution of the HST, compared to ground-based telescopes, will increase our sensitivity to detect black holes in galactic nuclei by factors of 10 to 1,000. For the neighboring galaxies M31 and M32, we will be able to detect black holes of the same size ($\approx 10^6 M_\odot$) as may exist in our own Milky Way Galaxy, and will conclusively confirm or refute the presence of $M \approx 10^{6.5-8.0} M_\odot$ black holes hinted at by current ground-based data.

REFERENCES

Dressler, A., and Richstone, D. O. 1988, "Stellar Dynamics in the Nuclei of M31 and M32: Evidence for Massive Black Holes," *Astrophys. J.*, **324**, 701-713.

Faber, S. M., and Gallagher, J. S. 1979, "Masses and Mass-to-Light Ratios of Galaxies," *Ann. Rev. Astron. Astrophys.*, **17**, 135-187.

Kormendy, J. 1988, "Evidence for a Supermassive Black Hole in the Nucleus of M31," *Astrophys. J.*, **325**, 128-141.

Serabyn, E., and Lacy, J. H. 1985, "[NeII] Observations of the Galactic Center: Evidence for a Massive Black Hole," *Astrophys. J.*, **293**, 445-458.

Tonry, J. L. 1987, "A Central Black Hole in M32," *Astrophys. J.*, **322**, 632-642.

Trimble, V. 1987, "Existence and Nature of Dark Matter in the Universe," *Ann. Rev. Astron. Astrophys.*, **25**, 425-472.

DISCUSSION

SONNABEND: Will HST give sufficient resolution at, say, the center of M31 to see individual high-velocity stars (if they exist), and thus provide a better test for a central black hole than just the velocity curve?

HARMS: Very high velocity stars (projected) near galactic nuclei would be very good indicators of condensed central matter which might be black holes, so we will certainly be looking for them. The cameras on the HST will provide images with spatial resolutions ranging from 7 to 44 milliarcseconds per pixel. At the distance of M31, this corresponds to spatial sampling on a scale of 0.03 parsecs to 0.15 parsecs, assuming a distance to M31 of 0.7 Mpc. Spectroscopy throughout a broad wavelength region from the UV through the near-IR is possible on a spatial scale of 100 milliarcseconds, corresponding to 0.35 parsecs at M31. While HST will not truly resolve individual stars in M31, individual bright stars near the nucleus may dominate the light emission in a given spatial sample, which would allow us to measure velocities of individual stars. If these stars show high velocity dispersions, this would provide strong evidence for centrally condensed matter in the galactic nucleus. The images from HST will allow us to determine whether such central matter is luminous or not with spatial resolution generally even better than will be attainable for spectra.

THE COBE COSMIC 3 K ANISOTROPY EXPERIMENT: A GRAVITY WAVE AND COSMIC STRING PROBE

CHARLES L. BENNETT
Laboratory for Astronomy and Solar Physics
NASA Goddard Space Flight Center
and
GEORGE F. SMOOT
Lawrence Berkeley Laboratory
University of California, Berkeley

ABSTRACT

Among the experiments to be carried into orbit next year, by the COBE satellite, are differential microwave radiometers. They will make sensitive all-sky maps of the temperature of the cosmic microwave background radiation at three frequencies, giving dipole, quadrupole, and higher order multipole measurements of the background radiation. The experiment will either detect, or place significant constraints on, the existence of cosmic strings and long wavelength gravity waves.

I. INTRODUCTION

The microwave radiometer experiment on the Cosmic Background Explorer (COBE) satellite will be a sensitive probe of long wavelength gravity waves and cosmic strings. This anisotropy experiment will make full sky maps of the temperature of the cosmic microwave background radiation (CMBR) at three frequencies to a sensitivity of $\Delta T/T \sim 3 \cdot 10^{-5}$ for each of 1,000 independent pixels on the sky, where $T = 2.7$ K is the temperature of the CMBR. The sensitivity to a quadrupole term will be $\Delta T/T \sim 5 \cdot 10^{-6}$, approximately an order of magnitude more sensitive than previous experiments which give limits of $3 \cdot 10^{-5}$ (Klypin *et al.* 1988) and $7 \cdot 10^{-5}$ (Lubin *et al.* 1985, Fixen *et al.* 1983, and Cheng *et al.* 1979). This increased sensitivity will result in stringent limits on density perturbations at decoupling, anisotropic expansion, and the energy density in the Universe due to long wavelength gravity waves, and with a field of view of ~7°, CMBR anisotropies due to large cosmic string loops and horizon length cosmic strings.

The COBE satellite is to be launched by NASA in May 1989 on a Delta rocket. COBE carries three experiments:

(1) an absolute radiometer, to measure the cumulative emission from the earliest galaxies being formed;
(2) a spectrophotometer, to measure the spectrum of the CMBR and map it over the whole sky; and
(3) differential microwave radiometers, to measure the large angular scale anisotropy of the CMBR over the entire sky.

The focus here, the differential microwave radiometer experiment, is a three-frequency experiment designed to measure sensitively small temperature differences in the sky. The radiometers at 31 GHz, 53 GHz, and 90 GHz each have a pair of horns with fixed 60° separation. The radiometers are mounted on a spacecraft which spins at 0.8 rpm while in polar orbit. With these motions, the experiment rapidly measures temperature differences over large areas of the sky.

The largest expected source of systematic errors is Galactic emission, including thermal radiation from dust, free-free radiation from electrons, and synchrotron radiation from the relativistic electrons spiraling around the magnetic field lines. Observing at the three frequencies separates the Galactic and CMBR emission since each source of radiation has a fairly well-defined spectrum which is distinguishable given the three frequency operation.

II. GRAVITY WAVES

If there is a significant background of gravity waves in the universe, then at least one such wave might be passing through the earth (and the observer, COBE) at the present time. Consider a single, weak, linearly polarized plane wave with a sufficiently long wavelength to appear static to us. The wave perturbs the metric and thereby stretches the wavelenghts of the CMBR photons. Burke (1975) calculated the effect of such a gravity wave and showed that the expression for the observed frequency shift, as a function of the Θ between the source of emission and the propagation direction of a wave with polarization angle Φ, is given by $z(\Theta,\Phi) = 1/2(A_1-A_0)\ (1-\cos\Theta)\ \cos 2\Phi$, where A is the proper strain ($\delta l/l = h/2$ where $g_{ik} = g_{ik}^{(\circ)}+h_{ik}$) observed between freely falling observers, A_0 is the amplitude at emission (or last scattering), and A_1 is the amplitude at the receiver. The change in frequency appears as a Doppler shift of the spectrum, which is equivalent to a temperature shift by the same factor.

The energy density of such a gravity wave is $\varepsilon_{GW} = \omega^2 c^2 h^2/32\pi G$. Expressed in terms of the critical density, $\rho c = 3H_o^2/8\pi G$, and measured anisotropy amplitude, ΔT, one finds $\Omega_{GW} = \varepsilon_{GW}/\rho_{crit}c^2 = \pi 2c^2h^2/e\lambda^2 H_o^2$, or

$$\Omega_{GW} = 1.6 \cdot 10^{-3}\ \frac{[(\Delta T/T)/(0.1\text{mK}/2700\text{mK})]^2}{(\lambda/10\ \text{Mpc})^2\ (H_o/100\ \text{km}\cdot\text{s}^{-1}\cdot\text{Mpc}^{-1})^2}\ .$$

A chaotic sea of gravity waves will produce distortions in the CMBR intensity. Calculations by Lindner (1988) show the finite thickness of the last scattering surface can cause dilution of the anisotropy produced by gravity waves with wavelengths less than 100 Mpc. He estimated that the anisotropy power spectrum will peak at ~1°, but extend out to large angles. For the COBE anisotropy experiment, which measures the difference between 7°-wide patches on the sky 60° apart, there would be a measurable anisotropy for a significant field of gravity waves. While the COBE microwave anisotropy experiment is not ideally designed to look for a chaotic gravity wave field, it will be able to set cosmologically significant limits on the energy density of long-wavelength gravity waves.

It is possible that there are some very long wavelength gravity waves. We might expect that any primordial gravitons existing from around the Planck time ($\sim 10^{-43}$ secs) would be thermalized; however, Grishchuk (1977) showed that that might not be the case and that there is a mechanism that could produce a nonthermal spectrum.

Grishchuk and Zel'dovich (1978) showed that gravity waves with wavelengths larger than the horizon of the universe can be observed through the resulting anisotropy in the CMBR, making the assumption that the phases of the gravity waves do not conspire to make our location uniquely privileged to have a flat background

inside our horizon. The effect of a superhorizon length gravity wave on the CMBR isotropy depends both upon its amplitude and time dependence.

III. COSMIC STRINGS

Cosmic strings are line-like topological defects in the universe that are produced naturally in many particle physics gauge theories as the universe undergoes a phase transition from very high temperatures to very low temperatures (Vilenkin 1985). Strings are characterized by a mass per unit length, μ, which deforms flat space to conical space. This makes cosmic strings unusual in that they act as gravitational lenses whose bending angle, $\Delta\Theta = 8\pi G\mu/c^2$, is independent of impact parameter. This, by itself, does not produce an anisotropy in the CMBR, since the CMBR has highly uniform surface brightness. However, the string also has tension, μ, so that the string tries to straighten itself at relativistic speeds. Due to the motion of the string, photons passing on one side are boosted to higher frequencies and on the other side pulled back to lower frequencies. The maximal discontinuity occurs when the velocity of the string is perpendicular to the line of sight where one finds a step in the brightness of the CMBR across the string to be $\Delta T/T = 8\pi G\mu\beta\gamma/c^2$, where β and γ are the usual relativistic parameters.

Not all strings are long strings stretching from horizon to horizon. Some strings form closed loops which are oscillating and radiating gravity waves at an enormous rate (Vilenkin 1981). These closed loops also produce temperature anisotropies and several examples have been calculated (Stebbins 1988).

An example of a candidate string is presented by Turner *et al.* (1986). Turner *et al.* (1986) suggested the possibility of a 2.6 arcminute linear gravitational lens. Such a string would produce an anisotropy step across the string of about 2 mK. Stark *et al.* (1987) searched for this effect and they did not see it at the 1 mK level, and later Lawrence *et al.* (1986) set a 0.1 mK limit, so alternate explanations for the object have been advanced.

For questions of energy density and galaxy formation the natural mass per unit length, $G\mu/c^2$, is the 10^{-6} to 10^{-4} giving anisotropy levels resulting in anisotropies in the range of 0.03 to 3 mK. Stebbins (1988) calculates examples of distortions of the CMBR for sample closed loops. Veeraraghavan *et al.* (1988) consider the effects of horizon-length strings.

IV. CONCLUSION

The microwave anisotropy experiment on the COBE satellite should detect, or provide a stringent limit on, long wavelength gravitational radiation. It will also be a sensitive probe of the perturbation to the cosmic background photons caused by cosmic strings.

ACKNOWLEDGEMENTS

This work was supported by the NASA COBE Project.

REFERENCES

Burke, W. L. 1975, *Astrophys. J.*, **196**, 329.
Cheng, E. S., Saulson, P. R., Wilkinson, D. T., and Corey, B. E. 1979, *Astrophys. J.*, **232**, L139.
Fixen, D. J., Cheng, E. S., and Wilkinson, D. T. 1983, *Phys. Rev. Lett.*, **50**, 620.
Grishchuk, L. P. 1977, *Ann. New York Acad. Sci.*, **302**, 439.
Grishchuk, L. P. and Zel'dovich, Ya. B. 1978, *Soviet Astr.*, **22**, 125.
Klypin, *et al.* 1988, *Soviet Astr. Letters*, **13**, 104.
Lawrence, E. V. *et al.* 1986, *AJ*, **92**, 1235.
Lindner, 1988, *Astrophys. J.*, **326**, 517.
Lubin, P., Villela, T., Epstein, G., and Smoot, G. 1985, *Astrophys. J.*, **298**, L1.
Stark, A. A., Dragovan, M., Wilson, R. W., and Gott, J. R. 1987, *Nature*, **322**, 805.
Stebbins, A. 1988, *Astrophys. J.*, **327**, 584.
Turner, *et al.* 1986, *Nature*, **321**, 142.
Veeraraghavan, S., Stebbins, A. and Silk, J. 1988, in preparation.
Vilenkin, A. 1981, *Phys. Lett.*, **107B**, 47.
Vilenkin, A. 1985, *Physics Reports*, **121**, 263.

DISCUSSION

SHAPIRO: You mentioned that the Berkeley, Princeton, and USSR results on the microwave background anisotropies were discrepant. Could you elaborate on the details of these discrepancies?

BENNET: The Soviet data was contaminated by radiation from the Earth, picked up by the sidelobes of the horn. They did extensive work to attempt to eliminate this source of systematic error, but to my eye, these remain features in the map due to Earth radiation. The dipole results are:

	USSR	Berkeley	Princeton
ΔT(mk)	3.16±0.12	3.44±0.21	3.18±0.21
α(hrs)	11.3±1.6	11.2±0.1	11.2±0.1
δ(degrees)	-7.5±2.5	-6.0±1.5	-8±2

THE GRAVITY PROBE B RELATIVITY GYROSCOPE PROGRAM

C. W. F. EVERITT, B. W. PARKINSON AND J. P. TURNEAURE
W. W. Hansen Laboratories of Physics
Stanford University, Stanford, California 94305-4085

I. OVERVIEW OF PROGRAM

The idea of testing general relativity through observations on Earth-orbiting gyroscopes was suggested in 1959-1960 independently by G. E. Pugh (1959) and L. I. Schiff (1960). Both recognized that the direction of spin of a suitably oriented gyroscope should change with respect to the line of sight to a guide star for two reasons: a geodetic effect from the motion of the gyroscope through the curved space-time around the Earth, and a frame-dragging effect from the Earth's rotation. In a 600-km polar orbit, the predicted effects are respectively 6.718 arcsec/yr and 0.043 arcsec/yr.

NASA began supporting laboratory research on the experiment, now called Gravity Probe B, in 1964. Technologies for it were progressively established in the 1960's and 1970's, and an error analysis, completed in 1974 (Everitt 1974), demonstrated the potential of measuring frame-dragging to 1% to 2% and the geodetic effect to 1 part in 10^4. Later analyses, discussed below, suggest possibilities for further improving those precisions each by a further factor of 10.

In 1984, after technical and scientific reviews by the Space Science Board and other bodies, and completion by NASA Marshall Center of a Phase B Study, the NASA Administrator approved the start of a program known as STORE (Shuttle Test Of the Relativity Experiment). The purpose of STORE is to verify the final Gravity Probe B science payload, perform on the Shuttle a 7-day "experiment rehearsal" (including sophisticated gyro tests in low gravity), and then return the payload to Earth for refurbishment and integration into the Science Mission spacecraft.

The payload (Figure 1) comprises four gyroscopes, a telescope, and a "drag-free proof mass," all mounted in a "quartz block assembly" within an evacuated magnetically shielded probe, which in turn is inserted into a 10-ft long, 6-ft diameter liquid helium dewar, operating at 1.8° K and maintaining low temperature for 2 years. Stanford is responsible for developing the quartz block assembly; Lockheed, under contract to Stanford, developed the dewar and the probe. STORE is manifested on Shuttle OV-105, for launch MSSN 69 in February 1993. The Science Mission is set tentatively for June 1995.

II. THE GYROSCOPE

The gyroscope is a sphere of fused quartz 38 mm in diameter, coated with a thin (~1 μm) layer of superconducting niobium, and suspended within a spherical cavity by voltages applied to 3 mutually perpendicular saucer-shaped electrodes. The rotor-electrode gap is about 40 μm; the support voltages about 1 kV on Earth and 0.1 V in space. The rotor is spun up to 170 Hz through a differential pumped channel inside the housing, after which the pressure is reduced to about 10^{-11} torr and the rotor coasts freely. The spin-down rate, governed by gas damping, is about 0.0025% per year.

The gyroscope's most novel feature is its "London moment readout." A spinning superconducting sphere of radius r, angular velocity ω_s develops a magnetic moment $M_L = (mc/2e)r^3\omega_s$ G-cm^3 aligned with its instantaneous spin axis. This magnetic marker is read out by surrounding the sphere with a tightly coupled superconducting loop (Figure 2) connected to a SQUID (Superconducting QUantum Interference Device) magnetometer. The London moment readout has four key merits: (1) it can be applied to an ideally round and homogeneous rotor, (2) it offers 1 milliarcsec resolution in a 2-hour observation period, (3) it is insensitive to miscentering of the ball in the loop, and (4) it causes negligible readout reaction torque.

Since 1975, we have gained some 20,000 hours of gyro test data, with speeds up to 179 Hz, precise London moment readout, and drift performance corresponding to 0.6 milliarcsec/yr at 10^{-10} g.

III. PERFORMANCE LIMITS ON THE EXPERIMENT

A sound experiment needs: (1) drift-free gyroscopes, (2) precise determination of the gyro spin directions with respect to a guide star, and (3) knowledge of the star's proper motion with respect to distant quasars. Current uncertainty in the proper motion of our guide star, Rigel, sets limits on the experiment at 0.9 to 1.7 milliarcsec/yr, but since future astrometric missions (HIPPARCOS and POINTS) should remove that problem, we ignore proper motion and ask what the internal limits on the experiment are.

Earlier analyses of gyro drift performance were deliberately conservative. Take the simple but critical mass-unbalance torque due to variations $\Delta\rho/\rho$ in the density of the gyro rotor. It causes a drift-rate $\Omega_\rho < 0.25\ (\Delta\rho/\rho)\ f/\omega_s$, where ω_s is the gyro angular velocity and f is the mean transverse acceleration on the spacecraft. With $\Delta\rho/\rho \sim 3\times10^{-7}$ and $f \sim 10^{-10}$ g, the drift-rate is 0.05 milliarcsec/yr - essentially the result used, with other error terms, to compute the earlier overall estimated worst-case Newtonian drift of 0.3 milliarcsec/yr. Now, Gravity Probe B is a drag-free satellite, and it rolls (10-min period) about the line of sight to the guide star, which is also the gyro spin axis. In that configuration, the assumption of a 10^{-10} g mean transverse acceleration is extraordinarily conservative. Even 10^{-11}g is conservative. This term can safely be reduced by least a factor of 10, though it should be added that, as of now, nonuniformities in the rotor coating would make a larger (0.06 milliarcsec/yr for 10^{-11} g) contribution to gyro drift.

Other refinements to the error budget come from (1) a greatly improved understanding of gyro suspension torques, (2) a demonstrated capability of operating at pressures as low as 10^{-11} torr (as compared with the earlier 10^{-10} torr), and (3) a decision to fly Gravity Probe B in an orbit (established via an on-board Global Positioning System sensor) whose mean is within 100 m of the poles. A revised analysis, to be published elsewhere, yields a worst-case total Newtonian drift no higher than 0.06 milliarcsec/yr.

The issues in determining the gyro spin direction with respect to the guide star are somewhat different. Here the analysis combines gyro readout noise, telescope errors, calculation of the gyro scale factor (achieved by using the

aberration of starlight as a "natural yardstick"), and calibration of the spacecraft roll orientation. In earlier Kalman filter covariance analyses (Vassar *et al.* 1980), the limits dominated by SQUID noise in the gyro readout were in the range of 0.6 to 0.9 milliarcsec/yr. A recent analysis by J. V. Breakwell and X. H. Qin, taking into account already demonstrated improvements in SQUID technology plus the extension of the mission lifetime from 1 to 2 years, reduces this figure in measurement of the frame-dragging effect to 0.06 to 0.13 milliarcsec/yr for a single gyroscope.

It would be premature to offer a final revised figure for the overall performance of Gravity Probe B, but an improvement by as much as a factor of 10 over earlier estimates is not out of the question.

IV. INTEGRATION AND IN-FLIGHT CALIBRATION

The STORE program commenced in February 1985. The main tasks so far have been to develop flight quality gyroscopes and design and build a First Integrated Systems Test (FIST) (Bardas *et al.*). The FIST comprises a full-scale dewar probe/quartz block assembly (Figure 1, inner part), interfaceable with the flight dewar, for use in ground tests in a laboratory dewar of comparable length but smaller diameter. First cool down is June 1989. Design of the science payload/Shuttle test unit begins September 1988, fabrication February 1990. Between February 1989 and September 1990, competing spacecraft predesign studies will be performed by two yet-to-be-selected aerospace companies.

In-flight calibration is a critical issue for the Science Mission. Gravity Probe B is unusual among tests of general relativity in that it is a physics experiment rather than an observation of given astrophysical or solar system phenomena. The system is under experimenters' control and allows a profusion of reliability checks. Some deliberately enhance certain errors for brief periods, for example, by introducing an inertially fixed 10^{-7} g bias into the drag-free controller to magnify and calibrate mass-unbalance and suspension torques. Others, such as the use of starlight aberration to calibrate the gyro scale factor, are built into the experiment. Six distinct principles of in-flight calibration have been established (Everitt 1988) to form a comprehensive validation scheme.

ACKNOWLEDGEMENTS

Gravity Probe B was initiated jointly by L. I. Schiff, W. M. Fairbank, and R. H. Cannon. Among present colleagues we thank especially D. Bardas, J. V. Breakwell, S. Buchman, W. S. Cheung, D. E. Davidson, D. B. DeBra, D. Gill, R. Hacker, G. M. Keiser, J. A. Lipa, J. Lockhart, M. Taber, R. A. Van Patten, Y. M. Xiao, with C. Everson, M. Mintz, R. Parmley, J. Salmon and 32 others at Lockheed. Currently, there are 31 graduate and undergraduate students associated with the program.

REFERENCES

Bardas, D. *et al.* "Hardware Development for Gravity Probe B," *SPIE Proc* **619**, 29.

DeBra, D. B. in this volume.

Everitt, C. W. F. 1974, *Experimental Gravitation* ed. B. Bertotti, 331, Varenna, Italy.

Everitt, C. W. F. 1988, "The Stanford Relativity Gyroscope Experiment (A): " ed. J. D. Fairbank *et al.*, *Near Zero: New Frontiers of Physics*, W. H. Freeman, New York, in press.

Pugh, G. E. November 1959, WSEG Memorandum No. 11, The Pentagon, Washington, D.C.

Schiff, L. I. 1960, "Possible New Experimental Tests of General Relativity Theory" *Physical Review Letters*, **4**, Number 5, 215-219.

Vassar, R. A., *et al.* 1980, *J. Spacecraft* **19**, No. 1, 66, AIAA 80-1671R, New York.

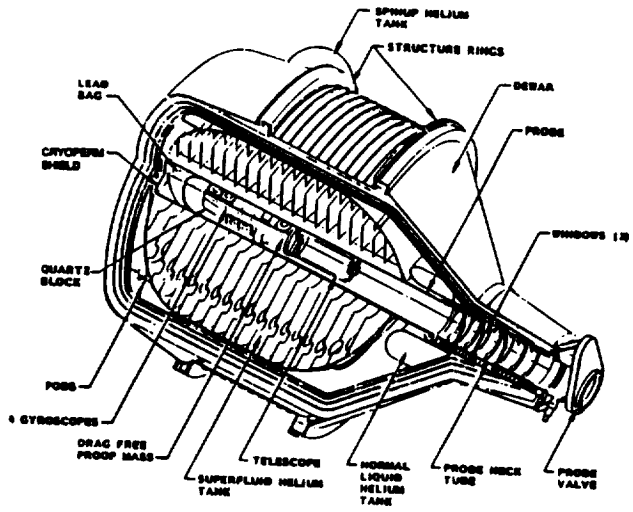

FIG. 1. — Gravity Probe B Science Payload as Tested on Shuttle in the STORE program.

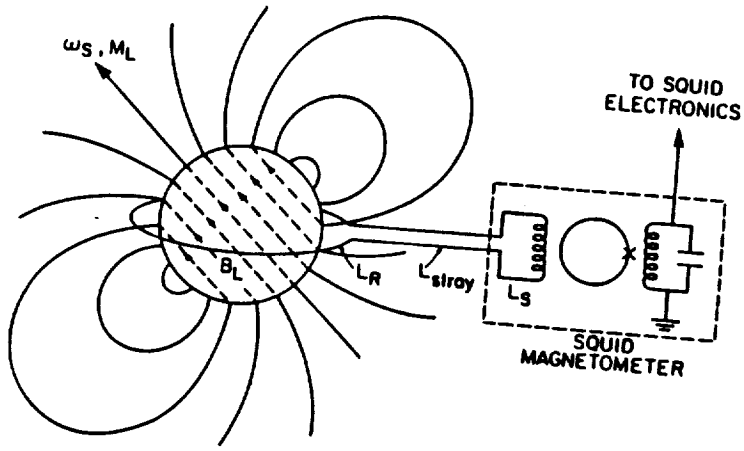

FIG. 2. — Reading Out the Gyro Spin Axis via the London Moment.

DISCUSSION

SHAPIRO: What tests will be performed on the 7-day shuttle flight of the gyroscope experiment?

EVERITT: The Shuttle flight fulfills two functions. First is an "experiment rehearsal" that will enable us to evaluate the overall performance of the dewar instrumentation package under semi-realistic space conditions. In that mode we will go through the fairly complex logistics of gyro spin-up, alignment, and low gravity operation; and also study a large number of mundane but important operational parameters such as gyro pressures and temperatures, dewar boil off, performance of the multilevel suspension system under different acceleration conditions, SQUID performance, response of system to launch environment, and so forth. Second, the Shuttle flight provides the first opportunity for extended gyro tests under low gravity conditions. These will be based on intercomparisons between the gyros. To enhance the information gained from the gyro tests we have reached agreement in principle with the Shuttle program office to have two two-hour periods per day in which the Shuttle will be rolled slowly (10 minute period) approximately about the gyro spin axes. We plan also to spin two gyros at full speed and two at reduced speed. Some consideration has been, and will continue to be given, to reducing the mean transverse acceleration on the gyros by applying the gyro suspension signals to the Shuttle control system, in order to make the Shuttle quasi drag-free. This data has interest for many other people besides ourselves, but we may suspect that in the end the bureaucracy will prevent it from happening.

SHAPIRO: What changes of the individual gyroscopes might be made (one with respect to another) to eliminate possibly important common-mode errors?

EVERITT: As the basic operation of the gyroscope we have four gyros all aligned essentially parallel with the line of sight to the guide star, two spinning clockwise and two counterclockwise; each with its own unique mass-balance, asphericity, and surface patch effect patterns. Having the gyroscopes in two opposed pairs makes them respond oppositely to certain classes of disturbance; for example, any effect of the Earth's gravity gradient on the centrifugally induced oblateness of the gyro star (but see answer to Ciufolini's first question below), and magnetic torques from the interaction of the London Moment with some common-mode transverse magnetic field (though the only known example of such a field that can begin to cause error, trapped flux in the surrounding magnetic shield, is heavily averaged by the roll of the spacecraft). Conversely, having innate differences in asphericity, mass-unbalance, etc. for the individual gyroscopes, means that they will respond differently to mass-unbalance and suspension torques generated by transverse accelerations on the spacecraft. If, therefore, in basic gyro operation, all four gyroscopes are seen to agree with each other to the performance level calculated in advance, significant constraints will have been established on any common mode errors from these known sources.

Another built-in difference among the four gyroscopes is that each is at a different distance (ranging from 10 cm to 45 cm) from the spacecraft center of mass. Hence we get a further autocratic check (of a very favorable kind) on mass-unbalance and suspension torque terms. The reasoning is as follows. Although we tune up the orbit initially so that its mean plane over the lifetime of the experiment is very exactly polar and aligned with the line of sight to the guide star, the orbit-plane is subject to lunisolar perturbations that make it oscillate back and forth, principally with respect to the line of sight, with 14 days and 6 month periods. These

motions introduce transverse accelerations, different for each gyro, because of the gyros' displacement from the orbit plane. These accelerations give rise to very small drift terms, with six month and fourteen day periodicities, in the plane of the geodetic precession. (Note that there is no such effect in the plane of the frame dragging precession). Both terms are small, (the fourteen day one exceedingly so) but by searching for them we set a definite upper limit on such torques (from a criteria different from these described above) and so strengthen confidence in the experimental result. Alternatively if the observed were much larger than anticipated, one could attempt to diagnose their cause, and apply corrections to back out the relativity data.

The question of deliberately applying changes to the system, different for each gyroscope, is part of the larger question of post-flight calibration tests discussed by Everitt (1988). There is a balance, discussed in that paper, between the physicist's desire to vary every parameter he can, and the engineer's desire not to mess with a working system. It is easy enough to raise the suspension preload voltages on each gyro independently and thereby change a certain class of suspension torques; it is also easy to apply known magnetic fields to each gyro to find any anomalous magnetic disturbances. On the other hand, we should be considerably more cautious about changing rotor speed after spin-up. See Everitt (1988) for further discussion.

CIUFOLINI: Another possible use of the GP-B experiment outcome may be to place limits on the existence of torsion (antisymmetric connection), that may propagate in vacuum in some gravity theories. A part of the eventual torsion may in fact comply with the spin of the gryoscope and give a precession, additional to the Lense-Thirring-Schiff and De Sitter precessions.

EVERITT: This comment is appreciated. I hope Dr. Ciufolini will continue his researches into these interesting theoretical questions.

CIUFOLINI: What is the order of magnitude of the spin precession of the gyroscope due to the coupling between the static part of the Earth field and the quadrupole moment of the quartz sphere due to its rotation?

EVERITT: For a gyroscope with quadrupole coefficient J_2, in circular orbit about a spherical central body, the secular component of drift for gravity gradient coupling is, by Laplace's formula, $W = 3/4$ or $3J_2\ g'/4w_SP\ \sin 2\alpha$, where R is the orbit radius, α the angle between spin axis and orbit plane, g' the gravitational acceleration at altitude R, and w_S the gyro's angular velocity. For the Gravity Probe B gyroscopes the centrifugally induced J_2 with $w_S = 1068$ rad/s (170 Hz) is 3×10^{-6}; there is also an intrinsic J_2, because of mass inhomogeneities, of order 10^{-7}. For an orbit whose mean inclination and alignment are, as indicated in the response to Shapiro's second question above, within 100 m of the Earth's polar axis and line of sight to the star, the resulting near precession rate of the gyro spin axis for the centrifugally induced J_2 is 4.6×10^{-4} marc-s/yr. There are also minute six month and fourteen day periodic terms in the orbit plane from the effects of lunisolar perturbations discussed above.

CIUFOLINI: What is the current value of the altitude at which the gyroscope should be injected?

EVERITT: Relativity makes it desirable to have a low altitude; atmosphere drag, which affects the amount of gas required for drag-free control, to have a higher altitude. Current discussion ranges from 550 km - 650 km, with the most likely value being 600 km as specified in the text of the paper.

LAGEOS III AND THE GRAVITOMAGNETIC FIELD

IGNAZIO CIUFOLINI
Center for Space Research
The University of Texas at Austin
Austin, Texas 78712

I. IMPORTANCE OF THE GRAVITOMAGNETIC FIELD

a) A Never-measured Field of Nature

In electrodynamics, in the frame at rest with an electrically charged sphere we have an electric field. If we then rotate the sphere we observe a magnetic field, which strength is proportional to the angular velocity.

Similarly, in Einstein geometrodynamics (Misner *et al.* 1973, Wheeler 1964) (general relativity), a non-rotating, massive sphere produces the standard Schwarzschild field. If we then rotate the sphere we have the occurrence of the gravitomagnetic field, whose strength, in the weak field limit, is proportional to the sphere angular velocity. In the weak field approximation of the Kerr metric, the gravitomagnetic field is (Thorne *et al.* 1986):

$$\vec{H} = \vec{\nabla} \times \vec{\beta} \equiv 2 \left[\frac{\vec{J} - 3 (\vec{J} \cdot \hat{r}) \hat{r}}{r^3} \right] \qquad (1)$$

where $\vec{\beta} \equiv (0,0, -\frac{2J}{r^3})$ is the gravitomagnetic or Lense-Thirring potential and J is the angular momentum of the central body.

We observe that gravitomagnetism and gravitational waves are the two main aspects, still to be measured, of Einstein geometrodynamics analogous to magnetic field and electromagnetic waves of electrodynamics.

b) At the Foundations of Inertia in Einstein General Relativity

In Einstein geometrodynamics (Misner *et al.* 1973, Wheeler 1964), to solve the initial value problem (York 1979, Choquet-Bruhat and York 1980) as a part of the initial conditions, we need to specify on a Cauchy hypersurface Σ the conformal mass-energy current density: $\vec{j}$ base. Through the initial conditions, with the field equations, we then solve for the geometry $g_{\alpha\beta}$ of the universe and eventually, we determine the local inertial frames (where $g_{\alpha\beta} \to \eta_{\alpha\beta}$) all over the spacetime. The axes of the local inertial frames (gyroscopes) are therefore influenced, and partially determined, by the mass-energy currents in the universe (dragging of inertial frames).

This agrees with some kind of general relativistic formulation of the Mach principle, according to the ideas of Einstein and Wheeler (Wheeler 1988, Carifolini and Wheeler 1987). "Nothing would do more to demonstrate the inertia-influencing effect of mass in motion than to detect and measure the Einstein-Thirring-Lense-predicated gravitomagnetism of the earth" (Wheeler 1988).

c) A Key Role in Theories of Quasars and Active Galactic Nuclei

In high-energy astrophysics, some theories of energy storage, power generation, jet formation and jet alignment of quasars and active galactic nuclei are based on the existence of the gravitomagnetic field of a supermassive black hole (Thorne *et al.* 1986).

In particular, this field may explain the constant direction of the jets over millions of light years and therefore over a time of several millions of years. Through the standard Navier-Stokes equations, in which one includes the gravitomagnetic field of the central object, one can show (Bardeen and Petterson 1975) that the accretion disk tends to be oriented into the equatorial plane of the central body — Bardeen-Petterson effect. The jets are then ejected normally to the accretion disk, that is, normally to the equatorial plane of the central body. The angular momentum vector of the central black hole acts, therefore, as a gyroscope and this may explain the constant direction of the jets.

II. LAGEOS III
LASER RANGED SATELLITES TO DETECT THE GRAVITOMAGNETIC FIELD AND SUPPLEMENTARY INCLINATION SATELLITES TO AVOID GRAVITY FIELD UNCERTAINTIES

Many experiments have been proposed to measure the gravitomagnetic field.

The GPB experiment (Everitt 1974, Lipa *et al.* 1974) intends to measure the Lense-Thirring-Schiff (Lense and Thirring 1918) precession of gyroscopes orbiting the earth.

Polar satellites have been proposed to measure the Lense-Thirring precession of the orbital plane — an enormous gyroscope (Schiff 1960, Yilmaz 1959) and two guided, drag-free, counter-rotating, polar satellites have been suggested to avoid orbital inclination errors (Van Patten and Everitt 1976). We recall that a polar satellite: $I \cong 90°$, has a null classical nodal precession.

Here, we briefly summarize the new idea (Ciufolini 1985, 1984, 1987, 1988) to measure the gravitomagnetic drag of the nodes of two nonpolar, supplementary inclination, laser ranged satellites. This idea can be decomposed into two parts:

(1) Position measurements of laser ranged satellites, of LAGEOS (Smith and Dunn 1980, Yoder *et al.* 1983, Cohen *et al.* 1985) type, are accurate enough to detect the tiny effect due to the gravitomagnetic field: the Lense-Thirring precession.

(2) To cancel out the uncertainties in the enormous perturbations due to the nonsphericity of the earth gravity field, we need (Ciufolini 1985, 1984, 1987) a new satellite, LAGEOS III, with semimajor axis and eccentricity, a and e, equal to those of LAGEOS, but with supplementary inclination: $I_{III} \cong 70°$.

The LAGEOS (Smith and Dunn 1980, Yoder *et al.* 1985) semimajor axis is $a = 12270$ km, the period $P = 3.758$ h, the eccentricity $e = 0.004$ and the inclination $I = 109.94°$. The period of the node $P(\Omega) = 1046$ days.

The Lense-Thirring nodal precession is for LAGEOS (Ciufolini 1984).

$$\dot{\Omega}^{\text{Lense Thirring}}_{\text{LAGEOS}} = \frac{2GJ_{\oplus}}{c^2 a^3 (1-e^2)^{3/2}} \cong 31 \text{ milliarcsec/year} \qquad (2)$$

where $J_{\oplus} \cong 5.9 \times 10^{40}$ g • cm2/sec $\cong 1.5 \times 10^2$ cm^2 is the earth angular momentum.

Unfortunately, the Lense-Thirring precession cannot be extracted from the measured value of the LAGEOS nodal precession, because of the uncertainty in the theoretical classical precession due to the quadrupole and higher mass moments of the earth:

$$\dot{\Omega}^{\text{Classical}}_{\text{LAGEOS}} \cong 126^{\circ}/\text{year}$$

However, a new satellite, of LAGEOS type: LAGEOS-III, with supplementary inclination: $I_{\text{LAGEOS III}} \cong 70°$, would have a classical precession equal in magnitude and opposite in sign to that of LAGEOS. By contrast, since independent of the inclination, the Lense-Thirring precession (2) would be the same, both in magnitude and sign for the two satellites. Therefore, from the sum of the measured nodal precessions, we should be able (Ciufolini 1985, 1984, 1987, 1988) to measure the Lense-Thirring effect.

III. ERROR SOURCES
ORBITAL INJECTION ERRORS, GRAVITATIONAL AND NONGRAVITATIONAL PERTURBATIONS AND MEASUREMENT ERRORS

(1) Errors from gravitational perturbations arise from uncertainties in modeling the LAGEOS gravitational nodal perturbations. These errors may be subdivided into:

(a) Errors from orbital injection errors (Ciufolini 1988) due to the uncertainties in the knowledge of the static part of the even zonal harmonic coefficients, J_{2n}, of the earth gravity field. These errors are, *a priori*, zero for the two supplementary inclination satellites. However, any deviation of the orbital parameters of LAGEOS III from the optimal values will introduce uncertainties which must be evaluated.

(b) Errors from other gravitational perturbations (Ciufolini 1988). Static odd zonal harmonic perturbations; static nonzonal harmonic perturbations; nonlinear harmonic perturbations; solid and ocean earth tides. De Sitter (or geodetic) precession (Bertotti *et al.* 1987); sun, moon and planetary tidal accelerations; nonlinear, n-body, general relativistic effects; other very tiny relativistic deviations from geodesic motion of LAGEOS. The main error source is, however, due (Ciufolini 1987, 1988) to the uncertainties in modeling the dynamical part of the earth gravity field, that is, to the uncertainties in modeling solid and ocean earth tides.

(2) Errors from nongravitational perturbations (Ciufolini 1987, 1988). Direct solar radiation pressure; earth albedo; satellite eclipses; anisotropic thermal

radiation; Poynting-Robertson effect; infrared radiation; atmospheric drag; solar wind; interplanetary dust; earth magnetic field. The main error sources are, however, due to uncertainties in modeling the earth albedo, anisotropic thermal radiation, and atmospheric drag (Ciufolini 1987, 1988).

(3) Errors from measurement uncertainties in the orbital parameters (Ciufolini 1988). These errors are due to the uncertainties in the measurement of the LAGEOS orbital parameters and, in particular, to the errors in the measurement of the inclination I and the nodal longitude Ω, relative to an asympotic inertial frame (Ciufolini 1988).

IV. PRELIMINARY ERROR ANALYSIS
A PRELIMINARY 10% MAXIMUM ERROR, OVER THE PERIOD OF THE NODE

A major problem in modeling the LAGEOS orbit is the average secular decrease (Cohen *et al.* 1985, Rubincam 1988) of the LAGEOS semimajor axis of about 1 mm per day. This corresponds to an along-track acceleration of about -3×10^{-10} cm/sec^2. This acceleration may be explained by three mechanisms (Rubincam 1988, Afonso *et al.* 1988):

(1) Neutral and charged particle drag (Rubincam 1982, Afonso *et al.* 1985).

(2) Thermal drag from the earth infrared radiation (Rubincam, 1987 and 1988) and the thermal lag of the LAGEOS retroreflectors, due to their thermal inertia. The re-emission causes an along-track acceleration opposite to the satellite motion.

(3) Thermal drag from the sun radiation plus satellite eclipses by the earth (Afonso *et al.* 1988). The sun radiation is absorbed and then re-emitted by the satellite. This phenomenon may be important when the satellite orbits are partially in the shadow of the earth.

The effect of these three perturbations on the node has been investigated in relation to the supplementary inclination configuration (Ciufolini 1988, Farinella 1988). The preliminary result is that their effect should not be larger than 1% $\dot{\Omega}^{\text{Lense-Thirring}}$ due to particle drag (Ciufolini 1987, 1988). This is negligible over the period of the node for two supplementary inclination satellites due to infrared radiation (Ciufolini 1988, Farinella 1988) and not larger than 2% $\dot{\Omega}^{\text{Lense-Thirring}}$ due to thermal drag plus satellite eclipses (Ciufolini 1988).

To support these preliminary figures, we observe that to give a secular nodal precession, a force must: 1) be perpendicular to the orbital plane, and 2) change sign in half a period. Even in this worst case, an acceleration with amplitude $\sim 3 \times 10^{-10}$ cm/sec^2 can, at most, cause a LAGEOS nodal precession of 5% $\dot{\Omega}^{\text{Lense-Thirring}}$, as it is easily calculated (Ciufolini 1988) from the Lagrange equation for the node. Ciufolini (1988) has carried out a comprehensive preliminary analysis. The result is that, using 2 nonpolar, laser ranged satellites with supplementary inclinations, the maximum error, over the period of the node of

~3 years, should not be larger than ~10% of the gravitomagnetic effect to be measured.

A study group, composed of University of Texas at Austin and Italian scientists, is, at present, performing a comprehensive computer simulation and covariance analysis of the experiment.

ACKNOWLEDGEMENTS

I thank C. Alley, E. Amaldi, J. Anderson, P. Bender, N. Cabibbo, M. Cerdonio, D. Christodoulidis, R. Eanes, F. Everitt, P. Farinella, P. Knocke, L. Guerriero, R. Hellings, H. Mark, R. Matzner, K. Nordtvedt, T. Regge, D. Rubincam, I. Shapiro, D. Smith, K. Thorne, M. Watkins, S. Weinberg, J. A. Wheeler, and C. Will.

REFERENCES

Afonso, G., Barlier, B., Berger, C., Mignard F., and Walch, J. J. 1985, *J. Geophys. Res.*, **90**, (B11), 9381.

Afonso, G., Barlier, F., Carpino, M., Farinella, P., Milani, A., Nobili, A. M. 1988, submitted to *Ann. Geophys.*

Bardeen, J. M., and Petterson, J. A. 1975, *Astrophys. J. Lett.*, **195**, L65.

Bertotti, B., Ciufolini, I., and Bender, P. L. 1987, *Phys. Rev. Lett.*, **58**, 1062.

Choquet-Bruhat Y., and York, J. W., Jr. 1980, in: General Relativity and Gravitation, A. Held, ed. (Plenum, New York).

Ciufolini, I. October 1984, *Bull Am. Phys. Soc.*, Cleveland, Ohio **6**, 1169, (1985).

Ciufolini, I. 1986, *Phys. Rev. Lett.*, **56**, 278 [submitted October 1984].

Ciufolini, I. 1987, *Cel. Mech.*, **40** ,19.

Ciufolini, I. March 1988, *Bull. Am. Phys. Soc.*; Austin, Texas, APS meeting.

Ciufolini, I. March 1988, A Comprehensive Introduction to the LAGEOS Gravitomagnetic Experiment, to be published.

Ciufolini I., and Wheeler, J. A. 1987, Geometrodynamics, Inertia Here is Ruled by Mass There (University of Texas Press, Austin, in preparation).

Everitt, C. W. F. 1974, in Experimental Gravitation, B. Bertotti, ed. (Academic Press, New York), p. 331.

Cohen, S. C., King, R. W., Kolenkiewicz, R., Rosen, R. D., and Schutz, B. E., eds. 1985, *J. Geophys. Res.*, **90**, 9215.

Farinella, P. 1988, to be published.

Lense, J., and Thirring, H. 1918, *Phys. Z.*, **19**, 156.

Lipa, J. A., Fairbank, W. M., and Everitt, C. W. F. 1974, in Experimental Gravitation, B. Bertotti, ed. (Arcade mic Press, New York), p. 361.

Misner, C. W., Thorne, K. S., and Wheeler, J. A. 1973, Gravitation (Freeman, San Francisco).

Rubincam, D. P. 1982, *Celest. Mech*, **26**, 361.

Rubincam, D. P. 1987, *J. Geophys. Res.*, **92**, 1287.

Rubincam, D. P. 1988, Thermal Drag on LAGEOS, *J. Geophys. Res.*

Schiff, L. I. 1960, *Phys. Rev. Lett.* **4**, 215.

Smith, D. E., and Dunn, P. J. 1980, *J. Geophys. Res. Lett.*, **7**, 437.

Thorne, K. S., Price, R. H., and MacDonald, D. A. 1986, eds., Black Holes, the Membrane Paradigm (Yale University Press, New Haven and London), p. 72.

Van Patten, R. A., and Everitt, C. W. F. 1976, *Phys. Rev. Lett.*, **36**, 629.

Wheeler, J. A. 1964, Geometrodynamics and the Issue of the Final State, in Relativity, Groups and Topology: 1963 Les Houches Lectures (Gordon and Breach, New York), p. 317.

Wheeler, J. A. 1988, in IV USSR Seminar on Quantum Geometry, M.A. Markov, ed. (World Scientific, Singapore).

Yilmaz, H. January 1959, *Bull Am. Phys. Soc.*, **4**, New York, p. 65.

Yoder, C. F., Williams, J. G., Dickey, O., Schutz, B. E., Eanes, R. J., and Tapley, B. D. 1983 *Nature*, 303, 757.

York, J. W., Jr. 1979, in: Sources of Gravitational Radiation, L. Smarr, ed. (Cambridge Univ. Press, Cambridge), p. 83.

DISCUSSION

SHAPIRO: LAGEOS-II will of course help to understand the partially unmodeled secular variation of the semimajor axis.

CIUFOLINI: Certainly; however this unmodeled variation should not be a problem for the gravitomagnetic experiment. In fact, even in the worst case that a comparable acceleration would be acting perpendicularly to the orbital plane and changing sign in half a period, that is, even in the case of a maximum contribution to the nodal rate, the total nodal drag due to this acceleration would not be more than 5% of the Lense-Thirring effect.

NORDTVEDT: Why do you quote a dJ_2/J_2 uncertainty limitation, when you might use the LAGEOS orbit, itself, as a measure of J_2?

CIUFOLINI: Unfortunately the nodel precession and the rates of change with time of the other orbital parameters are due, not only to the earth quadrupole moment, but to other harmonics too. A solution would be to orbit several high-altitude, laser-ranged satellites, of LAGEOS type, to measure each even zonal harmonic coefficient, to the proper order, plus one satellite to measure the Lense-Thirring effect. Another solution is to orbit polar satellites (Yilmaz 1959, Everitt and Van Patten 1976), since they have a null classical precession. Another solution is to use supplementary inclination satellites to cancel out the classical precession (LAGEOS III, Ciufolini 1984).

SHAPIRO: (Comment on question by K. Nordtvedt). The even zonal harmonics (J_2, J_4, ...) affect other orbital parameters, as well as W, and these effects for the orbit of LAGEOS I, as well as for other satellites, allow estimates to be made of the values of J_2, J_4, ... It was to the residual errors, or uncertainties, from these estimates that Ignazio referred.

GRADIOMETRY AND GRAVITOMAGNETIC FIELD DETECTION

BAHRAM MASHHOON
Department of Physics and Astronomy
University of Missouri
Columbia, Missouri 65211

I. GRAVITATIONAL "MAGNETIC" FIELD

Gravitomagnetism was apparently first introduced into physics about 120 years ago when major developments in electrodynamics and the strong similarity between Coulomb's law of electricity and Newton's law of gravity led to the hypothesis that mass current generates a fundamental force of gravitational origin analogous to the magnetic force caused by charge current. Holzmüller (1870) and Tisserand (1872, 1890) showed that this novel interaction led to the precession of planetary perihelia. The ratio of this velocity-dependent force to the Newtonian force of attraction contained only the speed of propagation of gravity as a new parameter. This parameter was taken to be the speed of light. The excess motion of perihelia would disappear if the speed of propagation approached infinity. There were attempts to use this fact to account for the excess perihelion precession of Mercury (Whittaker 1951). However, Einstein's relativistic field theory of gravitation provided a natural explanation for the excess perihelion motion. It is due to a small relativistic correction to the "Newtonian" gravitoelectric field of the Sun. Furthermore, Hans Thirring showed, in 1918, that the rotation of a massive body does indeed generate a gravitational "magnetic" field according to general relativity. The general investigation of the excess motion of planets and the moons due to the gravitomagnetic field is due to Lense and Thirring (1918). The resulting perihelion precession turned out to be much smaller than, and in the opposite sense of, the excess motion of Mercury (Mashhoon *et al.* 1984).

According to general relativity, the rotation of a body leads to the dragging of the local inertial frames. In the weak-field approximation, the dragging frequency can be interpreted, up to a constant proportionality factor, as a gravitational "magnetic" field. There is, as yet, no direct evidence regarding the existence of such a field. This work is concerned with the possibility of detecting the gravitomagnetic field of the Earth by gravity gradiometry.

II. GRAVITY GRADIOMETRY IN GENERAL RELATIVITY

Imagine two neighboring particles falling freely in an external gravitational field characterized by a Newtonian potential ϕ. The relative motion of the particles can be described in Newtonian theory by

$$\frac{d^2\xi^i}{dt^2} + K_{ij}(t)\xi^j = a^i \tag{1}$$

to first order in the relative displacement ξ. Here a is the relative acceleration caused by nongravitational forces and $K_{ij} = \partial^2\phi/\partial x^i \partial x^j$ is the tidal matrix. The tidal matrix is symmetric, and its trace is proportional to the local density of matter with the proportionality constant determined by the Newtonian constant of gravitation. The situation in general relativity is remarkably similar, except that equation (1) holds in the local inertial frame with t replaced by the proper time τ along the path of the

particles, and the tidal matrix is given by certain components of the Riemann curvature tensor as measured in the local frame carried along the path (Mashhoon 1977). Specifically, let $R_{\mu\nu\rho\sigma}$ be the spacetime curvature for the exterior field of a rotating mass such as the Earth. In Schwarzschild-like coordinates, the components of the Riemann tensor would contain contributions from the mass M, angular momentum J, and higher multipole moments of the Earth. Let $x^\circ = x^\circ(\tau)$, and $x^i = x^i(\tau)$ represent the orbit of a gradiometer freely falling in the Earth's field. An orthogonal parallel-propagated set of three local space-like directions ("gyroscopes"), $\lambda^\mu_{(i)}$, is necessary so that the orthonormal tetrad $\lambda^\mu_{(a)}$, with $\lambda^\mu_{(o)} = dx^\mu/d\tau$, could be used to define a local inertial frame. With respect to such a frame, equation (1) holds with Newtonian time replaced by τ and

$$K_{ij}(\tau) = R_{\mu\nu\rho\sigma}\lambda^\mu_{(o)}\lambda^\nu_{(i)}\lambda^\rho_{(o)}\lambda^\sigma_{(j)} \tag{2}$$

The equation of motion with respect to any other local frame can be obtained from equation (1) by means of a transformation,

$$\xi'^i = M_{ij}(\tau)\xi^j \ . \tag{3}$$

A gradiometer measures the relative acceleration $d^2\xi'/d\tau^2$, hence, effects of gravity gradients are mixed with terms arising from the deviation of actual gradiometer axes from the local inertial frame.

It is important to note that (K_{ij}) contains, besides the "electric" parts of the field, the Lense-Thirring orbital precession as reflected in the tangent to the worldline $\lambda^\mu_{(o)}$, the gravitomagnetic precession and nutation of gyro axes as reflected in $\lambda^\mu_{(i)}$, as well as the contribution of the gravitational "magnetic" field to the spacetime curvature. Consider, for instance, a gradiometer on a circular (equatorial or polar) orbit about the Earth (Braginsky and Polnarev 1980, Mashoon *et al* 1985). The components of the tidal matrix are simple when expressed in terms of the local polar coordinate system $(\hat{r}, \hat{\theta}, \hat{\varphi})$, which is essentially the Earth-pointing orientation. The tidal matrix consists of a diagonal Newtonian part of order $\omega_o^2 = GM/r^3 \simeq 10^{-6}$ sec^{-2} for a near-Earth orbit, a diagonal relativistic "electric" part of magnitude $3(GM/c^2r)\omega_o^2$, which is $\simeq 10^{-9}$ of the Newtonian part, and a "magnetic" part with amplitude of order $6(J\omega_o/c^2M)\omega_o^2$, which is $\simeq 10^{-10}$ of the Newtonian part. The "magnetic" part is constant and diagonal for an equatorial orbit and off-diagonal for a polar orbit. These off-diagonal elements contain harmonic and mixed terms of frequency ω_o.

To detect the gravitomagnetic field of the Earth, it is therefore necessary to use a highly sensitive gravity gradiometer such as the low-temperature device developed by Paik (1985).

III. PAIK'S SUPERCONDUCTING GRAVITY GRADIOMETER

During the past year, Ho Jung Paik, Clifford Will, and the author have studied-in the context of a wide class of gravity theories (Will 1984) the feasibility of detecting the Earth's gravitomagnetic field using Paik's superconducting gravity gradiometer (Paik *et al.* 1987). The main conclusions of our rather preliminary investigation can be stated as follows.

(1) The gravitomagnetic effect must be separated from local frame effects; this requires that the local frame be defined at the same level of precision as in the Stanford gyro experiment (GP-B). Hence the orientation of the gradiometer must be controlled such that the pointing errors remain below $\sim 10^{-3}$ arc second $Hz^{-1/2}$ at signal frequency $2\nu_o \simeq 3.4 \times 10^{-4}$ Hz appropriate for local inertial orientation determined by gyroscopes. This general conclusion is expected to hold even if the orientation of the gradiometer is defined using telescopes. Hence GP-B's superconducting gyros or cryogenic telescopes are essential for such an experiment.

(2) The error due to the internal misalignment of gradiometer axes, *i.e.*, the deviation of the axes of gradiometer from perfect orthogonality, turns out to generate second-order effects for Paik's rigid three-axis gradiometer. The misalignment error must therefore be kept below $\sim 10^{-6}$.

(3) It is possible to separate the gravitomagnetic signal from the Newtonian and post-Newtonian gravitoelectric effects of the mass of the Earth by a signal differencing scheme. Consider, for instance, a Paik gradiometer in polar orbit. In the Earth-pointing orientation, the subtraction of gradiometer outputs in the $(\hat{r} + \hat{\varphi})$ and $(\hat{r} - \hat{\varphi})$ directions, or the $(\hat{\varphi} + \hat{\theta})$ and $(\hat{\varphi} - \hat{\theta})$ directions, would essentially eliminate gravitoelectric effects.

(4) This subtraction is complete if the two sensitive axes of the gradiometer are identical. There is, therefore, a strict scale factor stability requirement of 5×10^{-9} $Hz^{-1/2}$ at the signal frequency of $2\nu_o$.

On the basis of requirements that follow from our preliminary analysis, it is projected that Paik's superconducting gravity gradiometer can resolve the expected gravitomagnetic signal in 1 year of data collection with a signal-to-noise ratio of 10^2. It thus appears, that the cryogenic, as well as drag-free technology, associated with GP-B can be combined with Paik's work to provide a novel method of detecting the gravitomagnetic field of the Earth.

ACKNOWLEDGEMENTS

It is a pleasure to acknowledge fruitful discussions with H. J. Paik and C. M. Will.

REFERENCES

Braginsky, V. B., and Polnarev, A. G. 1980, *JETP Lett.*, **31**, 415.

Holzmüller, G. 1870, *Z. Math. Phys.*, **15**, 69.

Lense, J., and Thirring, H. 1918, *Phys. Z.*, **19**, 156.

Mashhoon, B. 1977, *Ap. J.*, **216**, 591.

Mashhoon, B., Hehl, F. W., and Theiss, D. S. 1984, *Gen. Rel. Grav.*, **16**, 711.

Mashhoon, B., and Theiss, D. S. 1982, *Phys. Rev. Lett.*, **49**, 1542.

Paik, H. J. 1985, *IEEE Transactions on Geoscience and Remote Sensing*, **GE-23**, 524.

Paik, H. J., Mashhoon, B., and Will, C. M. 1987, *Proc. International Symposium on Experimental Gravitational Physics* (Guangzhou, China).

Theiss, D. S. 1985, *Phys. Lett.*, **109A**, 19.

Tisserand, F. 1872, *Compt. Rend.*, **75**, 760.

Tisserand, F. 1890, *Compt. Rend.*, **110**, 313.

Whittaker, E. T. 1951, *A History of the Theories of Aether and Electricity* (Nelson, London), **Vol. 1**, pp. 207-208.

Will, C. M. 1984, *Phys. Rep.*, **113**, 345.

DISCUSSION

HELLINGS: What do you use as a reference for the pointing requirement for your gravimetric axes?

MASHHOON: Thus far we have used the local inertial frame as defined by ideal orthogonal gyroscopes. This system is related to the Earth-pointing orientation along a circular orbit by a rotation of frequency w_o. A reference system based on telescopes requires a separate investigation since aberration effects need to be taken into account.

CLAUSER: What have you assumed for the gradiometer sensitivity of Paik's experiment?

MASHHOON: 10^{-5} E $Hz^{-1/2}$.

NORDVEDT: What do you exactly mean by 'gravitomagnetism has never directly been detected?' I know of quite a few phenomena for which the gravitomagnetic interaction is needed and to explain the observation.

MASHHOON: It is certainly true that information regarding the gravitomagnetic interaction has been obtained from observations within the framework of parameterized post-Newtonian approximation scheme. On the other hand, general relativity predicts that an isolated uniformly rotating mass would cause a dragging of the local inertial frames that is independent of the motion of the observer relative to the rotating mass. That is, the gravitomagnetic field is present even when the observer is at rest with the rotating mass. This is a fundamental proposition that deserves to be tested directly.

CIUFOLINI: It is interesting to observe that the first one to calculate one effect of the gravitomagnetic field, after general relativity was discovered, has been de Sitter in 1916. He calculated the tiny precession of the perihelion of Mercury due to the angular momentum of the Sun an effect, he found, much smaller that the Schwarzschild perihelion precession.

MASHHOON: In his (first) 1916 paper (published in Monthly Notices) on the astronomical consequences of general relativity, de Sitter considered, among other things, the perihelion precession of a planet in an equatorial orbit due to the axial rotation of the Sun. However, the general discussion of the gravitomagnetic field and its consequences for orbital motion is due to Thirring and Lense.

NIETO: A historical comment. It turns out that Maxwell also noted the similarity between Newton's Law and Coulomb's Law as contained in his theory of electromagnetism. In his great treaties on electromagnetism, Maxwell tried to develop a (vector) theory of gravity which would be similar to his electromagnetic theory. However, because he had to change the sign of the energy (like charges or masses had to attract), the system was a run-away. It did not conserve energy. This is an analogue of the non-conservation of energy in "anti-gravity" theories.

THE STANFORD EQUIVALENCE PRINCIPLE PROGRAM

PAUL W. WORDEN JR., C. W. FRANCIS EVERITT, AND M. BYE
Physics Dept., Stanford University

The Stanford Equivalence Principle Program (Worden, Jr. 1983) is intended to test the uniqueness of free fall to the ultimate possible accuracy. The program is being conducted in two phases: first, a ground-based version of the experiment, which should have a sensitivity to differences in rate of fall of one part in 10^{12}; followed by an orbital experiment with a sensitivity of one part in 10^{17} or better. The ground-based experiment, although a sensitive equivalence principle test in its own right, is being used for technology development for the orbital experiment.

A secondary goal of the experiment is a search for exotic forces. The instrument is very well suited for this search, which would be conducted mostly with the ground-based apparatus. The short range predicted for these forces means that forces originating in the Earth would not be detectable in orbit. But detection of Yukawa-type exotic forces from a nearby large satellite (such as Space Station) is feasible, and gives a very sensitive and controllable test for little more effort than the orbiting equivalence principle test itself.

The present limit on violations of the equivalence principle is a few parts in 10^{11}. The orbital version of this experiment may improve on this by a factor of a million, allowing very significant tests of several theories. Proper choice of materials for a particular test can enhance this improvement significantly; to check the gravitational response of the strong interactions one could use test masses of copper and hydrogen to gain an additional factor of 30. In 1955, Lee and Yang predicted an apparent violation of the equivalence principle (due to a new long-range force) to explain proton stability. The force has never been detected, but neither has the decay of a proton: the question of a new force therefore becomes more interesting. Moffat's Nonsymmetric Gravitation Theory (Moffat 1987) predicts a $1/R^5$ component of gravity that would be easily detectable in a slightly eccentric orbit. Both of these theories would be strongly tested by the orbital experiment.

We think of the experiment as a highly refined version of Galileo's supposed experiment at the Leaning Tower of Pisa. Two masses fall with slightly different accelerations; the separation between them is proportional to the distance of fall. In the orbital experiment (Fig. 1), the masses fall all the way around the Earth, repetitively. The sensitivity of the experiment depends less on being able to measure their separation than on being able to guarantee that they are not disturbed by uninteresting effects. The key to this is to put the test masses in a "drag-free" spacecraft, which, in its simplest form, is a shield that flies along with them and protects them from gas drag and the environment. The spacecraft body keeps up with the test masses, by means of small jets, without disturbing them. Another consideration is the effect of gravity gradients. If the masses are not at the same height, they will have different accelerations due to the Earth's gravity gradient. The difference in acceleration from gravity gradients has half the period of the orbit, while any signal from a violation of equivalence will have the same period as the orbit. It is therefore possible to separate the gravity gradient acceleration from the equivalence principle signal and use it as an error signal to force the centers of mass of the test bodies into coincidence. The effect of gravity gradients then

vanishes. If a torsion balance were used instead of independent masses, it would experience a torque from gravity gradients acting on its residual quadrupole moment, which could not be reduced sufficiently because the moment is not easily adjustable. We expect the limiting disturbance on the orbital experiment to be due to one of several gas pressure effects; if any significant amount of residual gas surrounds the test masses, they will be blown around by gas currents from thermal gradients, outgassing, and spacecraft motion.

The Earth-based experiment uses a "scaled-down" version of the apparatus envisioned for the orbital experiment, which can be used for development in addition to equivalence principle tests. The major difference in experimental concept is that the source of gravitational acceleration is the Sun rather than the Earth. The masses fall towards the Sun along with everything else on Earth; the apparent direction of fall is modulated once per day by the Earth's rotation. An Eötvös-type experiment is also possible, in which the apparatus is smoothly rotated about the local vertical, with a 1/2 hour period. This balances part of gravity against the Earth's centrifugal field, which is significantly larger than the Sun's acceleration. Although technically more difficult, the Eötvös-type experiment is about three times more sensitive and, furthermore, the rotating apparatus can be used for a very definitive search for a "fifth force," at several hundred times the sensitivity of present tests.

The apparatus used for both the ground-based and orbital experiments (Fig. 2) may be thought of as a differential accelerometer which is insensitive to everything except the difference in gravitational acceleration between its test masses. The test masses are arranged concentrically to eliminate any response to gradients, and are cylindrical to allow access to the inner mass. The masses are supported and constrained by precision superconducting magnetic bearings; these ideally allow force-free motion along the cylinder axis and rigid constraint radially. The mass positions are measured by a superconducting inductance bridge circuit connected to a SQUID magnetometer. This circuit can measure displacements to 0.001 Angstrom, and has other benefits as well. By adjusting the amount of trapped current in different parts of the bridge, the sensitivity to motion of either mass can be made equal and opposite. The position detector then responds only to differences in mass motion, and ignores the common motion which may be due to environmental noise. Better still, the position detector exerts a restoring force on each mass, which can be adjusted somewhat independently of the sensitivity. If the periods of the masses are also adjusted to be the same, the masses respond identically to external disturbances such as seismic noise. Then the differential mode of the system is not excited, as it would be if the masses responded differently. Then only the differential force is detected by the position detector circuit. The sensitivity of the system is effectively multiplied by the common mode rejection ratio; with a seismic background of 10^{-7} cm/sec^2 (at one cycle per day) and CMRR approaching 10^5, we expect to be able to see a signal of 10^{-12} cm/sec^2, which is the basis for our sensitivity limit on the ground-based experiment.

The ground-based experiment is currently in an advanced stage of development. We near the end of a long period of development of the magnetic bearings, crucial to the performance of the experiment, and have demonstrated the operation of the other subsystems of the apparatus.

REFERENCES

Lee, T.D. and Yang, C.N. 1955, *Phys. Rev.*, **98**, 1501.

Moffat, J. 1987, "Test Particle Motion in the Nonsymmetric Gravitation Theory", *Phys. Rev. D*, **35**, 3733.

Worden, P.W., Jr. 1983, Cryogenic Equivalence Principle Experiment: Discussion and Present Status: Proc Third Marcel Grossman Meeting on General Relativity (Hu Ning, Ed.) North Holland, pp. 771-779.

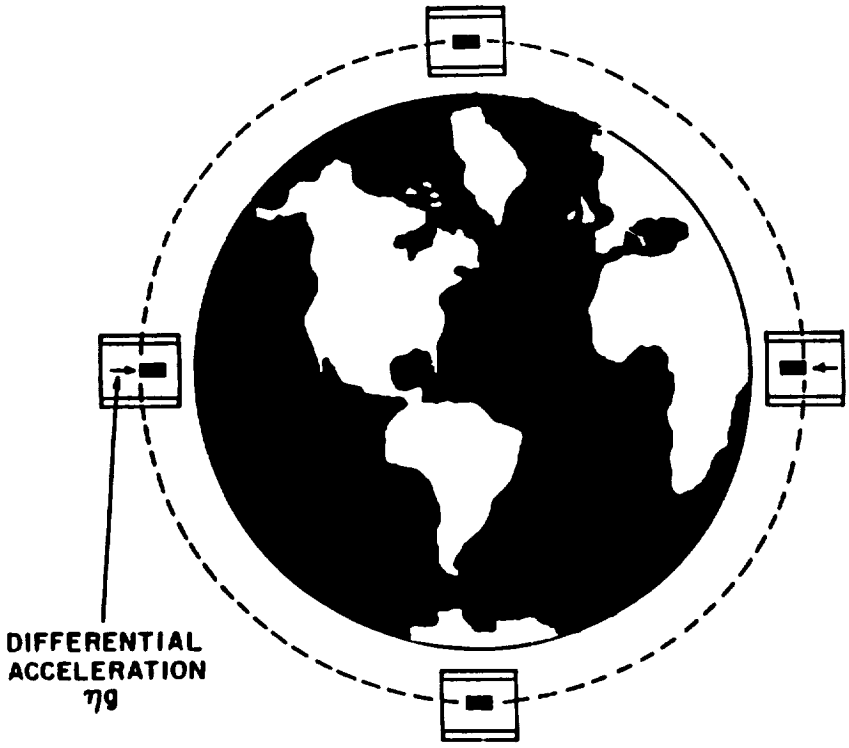

FIG. 1. — Orbital Experiment

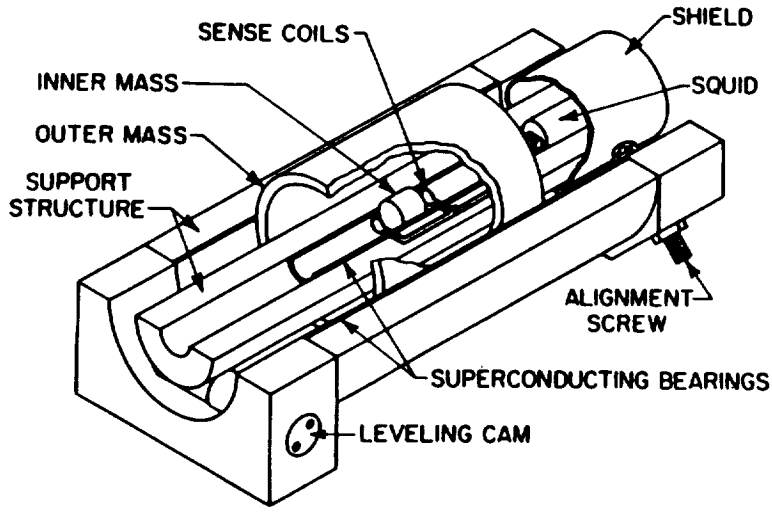

FIG. 2. — Equivalence Principle Accelerometer

NIETO: If you are going to test for new (gravitational or 'fifth') forces you are going to need a site. Do you have one in mind? On this point, I wish someone would do an experiment at Thieberger's Palisader site (the only new experiment that obtained a large positive result), or at the Grand Canyon.

WORDEN: At the present time we are considering one of the end chambers at Stanford's High Energy Physics Laboratory for preliminary tests. There are also some quarries near Stanford which would be less convenient for testing, but would provide better tests for forces with a range of 200 meters or more. A semiportable version of the apparatus is possible.

ICARUS LANDER

RONALD W. HELLINGS
Jet Propulsion Laboratory
Pasadena CA 91109

Icarus is one of the earth-crossing asteroids. It has a semi-major axis of 1.078 AU, giving it a period of 1.12 years, and an eccentricity of 0.827. The perihelion distance is thus 0.187 AU. The inclination of Icarus's orbit is 23°. Although it is a small body (radius ≈ 1km), it it still massive enough to be essentially immune to non-gravitational forces. These orbital and physical qualities make it an attractive target for testing General Relativity. The close passage to the sun means that it will be subject to a large relativistic perihelion precession; the high eccentricity makes the precession easy to measure; the high inclination allows the solar quadrupole moment (J_2) to be simultaneously determined via the nodal precession it predicts. The degeneracy between the relativistic effect and the effect of J_2 in the perihelion precession may thus be broken.

In this talk, I will present results from a preliminary study of a possible trajectory design for an Icarus lander and from a covariance study of the scientific return to be expected from such a mission.

The same properties of Icarus's orbit that make it so attractive for tests of General Relativity — its high inclination and high eccentricity — make it a difficult target to reach. Nevertheless a seven-year trajectory has been found[1] which has a $\Delta\upsilon$ requirement which is attainable. The mission events are as follows:

Depart Earth — 1/2/93 ($\Delta\upsilon$ = 0km/sec)

First Maneuver — 1/7/94 ($\Delta\upsilon$ = 1.51km/sec)

Gravity Assist/Earth — 2/28/95 ($\Delta\upsilon$ = 0.47km/sec)

Gravity Assist/Jupiter — 7/25/96 ($\Delta\upsilon$ = 0km/sec)

Second Maneuver — 10/25/99 ($\Delta\upsilon$ = 0.80km/sec)

Icarus Encounter — 10/13/00 ($\Delta\upsilon$ = 2.86km/sec)

The total $\Delta\upsilon$ is thus 5.64 km/sec. This is a difficult but a reasonable requirement.

A preliminary covariance study[2] to determine the scientific value of range data from an Icarus lander has been completed. In this study it was assumed that range data had an inherant accuracy of 10 cm. (It has been suggested that such an accuracy is attainable with the DSN. A feasability study of this would be a worthwhile task.) Two years of data were assumed with one data point per day. It was further assumed that the data from Icarus would be so accurate that they would overwhelm the information content of all other solar system data for the parameters of interest, an assumption which is almost certainly true at the assumed 10 cm accuracy, so all other solar system data were neglected. The parameters of interest were the orbital

1. The trajectory design was performed by A. Khatib.
2. The study used POSCOV, a program written by J.D. Anderson and E.L. Lau.

elements of Icarus and of the Earth, the GM of the sun, and PPN parameters β, γ, and the solar J_2. The *a priori* uncertainties for these parameters were 1% for β, 0.2% for γ, and 10^{-6} for J_2. The post-fit uncertainties are shown as functions of time in Figures 1-3.

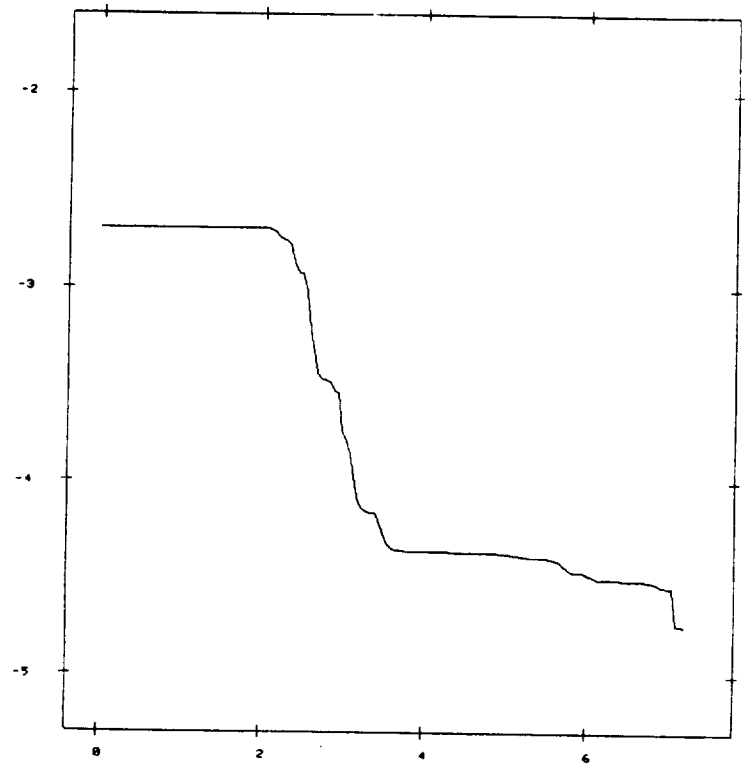

Figure 1. Log_{10} of the uncertainty in γ as a function of Icarus tracking time. There is no improvement until the first solar conjunction at t=300 days, which allows a measure of the gravitational time delay. Final formal uncertainty in γ is 1.8×10^{-5}

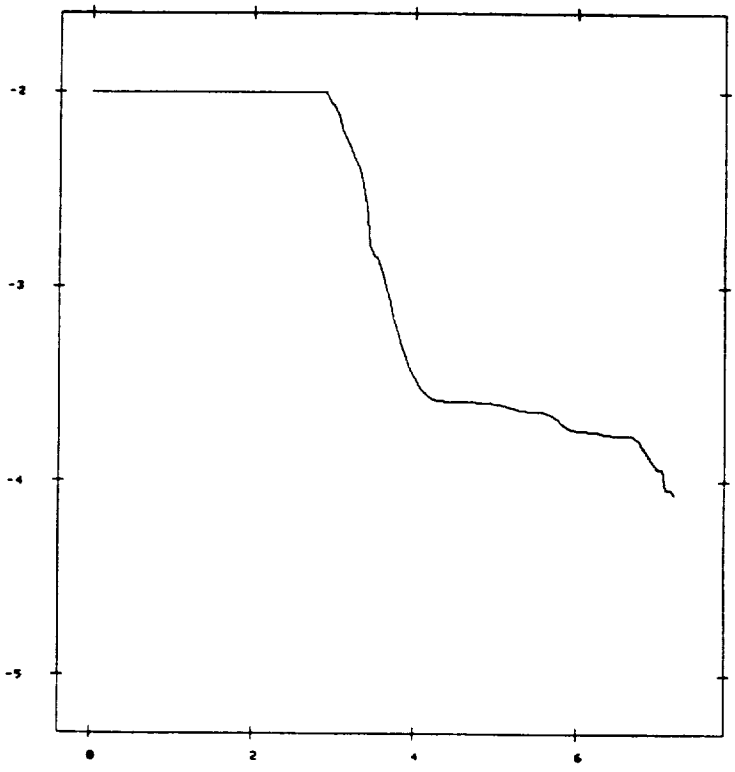

Figure 2. Log_{10} of the uncertainty in β as a function of Icarus tracking time. The strong correlation between β and γ in perihelion precession prevents improvement until the solar conjunction separates the two parameters. Final formal uncertainty in β is 9×10^{-5}.

Figure 3. Log_{10} of the uncertainty in J_{2o} as a function of Icarus tracking time. The strong correlation between J_{2o} and γ in perihelion precession prevents improvement until the solar conjunction separates the two parameters. The separation between J_{2o} and β comes as a result of the determination of node precession. Final formal uncertainty in J_{2o} is 5.3×10^{-8}.

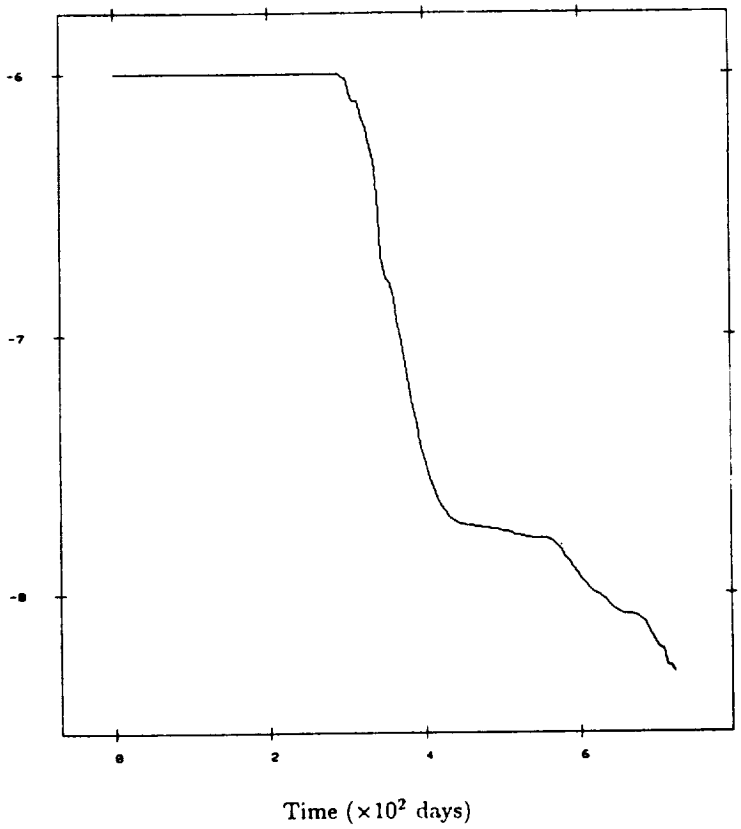

DISCUSSION

Questions and answers at the end of Bender's paper (p. 147)

SMALL MERCURY RELATIVITY ORBITER

Peter L. Bender and Mark A. Vincent *

Joint Institute for Laboratory Astrophysics
University of Colorado and National Institute of Standards and Technology
Boulder, Colorado 80309

ABSTRACT

The accuracy of solar system tests of gravitational theory could be very much improved by range and Doppler measurements to a Small Mercury Relativity Orbiter. A nearly circular orbit at roughly 2400 km altitude is assumed in order to minimize problems with orbit determination and thermal radiation from the surface. The spacecraft is spin-stabilized and has a 30 cm diameter de-spun antenna. With K-band and X-band ranging systems using a 50 MHz offset sidetone at K-band, a range accuracy of 3 cm appears to be realistically achievable. The estimated spacecraft mass is 50 kg.

We have carried out a consider-covariance analysis to determine how well the Earth-Mercury distance as a function of time could be determined with such a Relativity Orbiter. The minimum data set is assumed to be 40 independent 8-hour arcs of tracking data at selected times during a two year period. The gravity field of Mercury up through degree and order 10 is solved for, along with the initial conditions for each arc and the Earth-Mercury distance at the center of each arc. The considered parameters include the gravity field parameters of degree 11 and 12 plus the tracking station coordinates, the tropospheric delay, and two parameters in a crude radiation pressure model.

The conclusion from our study is that the Earth-Mercury distance can be determined to 6 cm accuracy or better. From a modified worst-case analysis, this would lead to roughly 2 orders of magnitude improvement in our knowledge of the precession of perihelion, the relativistic time delay, and the possible change in the gravitational constant with time. For an 8 year tracking period, the accuracy for the solar quadrupole moment J_2 would be 1×10^{-9} if general relativity is assumed to be correct, or 1×10^{-8} in the general case.

1) General Discussion

To obtain a major improvement in solar system tests of gravitational theory, accurate measurements of the Earth-Mercury distance over an extended period of time are needed. Studies of the new information achievable as a function of the systematic error level in the distance measurement data have been carried out by Ashby et al. (1989), using a modified worst case analysis. The Parameterized Post-Newtonian (PPN) formulation of gravitational theory was used. The uncertainties in the PPN parameters β, γ, α_1, α_2, α_3, and ζ_w were determined for mission durations of 1, 2, and 8 years. The uncertainties in the solar quadrupole moment J_2 and in the rate of change of GM for the sun also were determined.

---

* Now at: Jet Propulsion Laboratory, Pasadena, CA 91109

The desired Earth-Mercury distance data could be obtained by ranging from the Earth to a lander on Mercury. However, a lander on Mercury in the foreseeable future probably would be small and would not have an Earth-pointed antenna. Thus, ranging to a Mercury Orbiter appears to be very attractive, provided that the orbit can be determined accurately enough so that the measured Earth-spacecraft distance can be converted into the Earth-Mercury distance with little loss in accuracy. This may not be possible for a spacecraft with high eccentricity, low periapsis, or high area-to-mass ratio. To avoid these limitations, we have studied the orbit determination problem for a Small Mercury Relativity Orbiter in a nearly circular polar orbit with roughly 2400 km altitude (Vincent and Bender, 1989). The results showed that 6 cm Earth-Mercury distance accuracy could be achieved, based on 1×10^{-14} Doppler accuracy for 10 minute observation times and 3 cm range accuracy. Since the range accuracy limitation is likely to be mainly from systematic errors, and therefore will not average out as the square root of the number of observations, only one range measurement was assumed per 8 hour arc of tracking data.

2) Conceptual Design of Spacecraft and Transponder System

The basic configuration of the spacecraft in the conceptual design is quite similar to the Pioneer Venus Orbiter, but scaled down by roughly a factor 4 in all dimensions. The spacecraft is cylindrical and is spin-stabilized about the normal to Mercury's orbit, with a de-spun antenna pointed toward the Earth. A sketch of the spacecraft is shown in Fig. 1. The dual-frequency antenna is 30 cm in diameter. The spacecraft body is 60 cm in diameter and 25 cm high, with the absorption of the sides relatively low at solar wavelengths. The sides are thermally insulated from the inside of the spacecraft to reduce the total heat input.

The dual-frequency Doppler and ranging system uses coherent transponders, with downlink frequencies of approximately 8.4 GHz (X-band) and 34.5 GHz (K-band). For each band, the modulation code bandwidth for the ranging signals is 6 MHz. An additional signal is included, which is offset by 50 MHz from the main K-band carrier. The phase of the beat frequency between these two signals is used to determine the range, subject to 2π phase ambiguities, which correspond to 3 m ambiguities in the range. The transmitted power levels when ambiguity resolution is not occurring are roughly 200 mW total at K-band and 500 mW at X-band. The expected average total spacecraft power requirement during an 8 hour tracking session is 10 W.

With the above spacecraft Doppler and ranging system and one of the 38 m diameter Deep Space Network (DSN) antennas, the signal-to-noise ratio for the Doppler signals should be high. The expected DSN accuracy for the dual frequency Doppler tracking data during the Galileo gravitational wave observing periods (S-band and X-band downlink) is 5×10^{-15} for 100 to 1000 s averaging times. The availability of K-band capability is not currently scheduled for the DSN, but there is considerable interest in adding this capability for use in other missions. The dual-frequency sidetone ranging system would give sufficient signal-to-noise ratio for 3 cm accuracy in 10 min observing times, after correction for the interplanetary and ionospheric electron density along the path.

Since the 8 hour measurement intervals are assumed to occur only about every other day, the average power required is about 2 watts. This power would be supplied by solar cells and a battery charging system. The mass of the required long-lifetime batteries and charging system for about 100 watt hours storage capacity is estimated

to be 10 kg. This mass plus the required structural mass of the spacecraft are the main items in the mass budget. It is believed that a total spacecraft mass of 50 kg is achievable, although no studies of the spacecraft structure have been carried out. This mass plus the spacecraft dimensions given earlier yield an area-to-mass ratio of 0.005 m^2/kg, which was the value used in the orbit determination studies.

ACKNOWLEDGMENTS

This work was supported in part by the NASA Innovative Research Program under Award No. NAGW-822.

REFERENCES

Ashby, N., P. L. Bender, and J. M. Wahr, "Accuracy of gravitational physics tests and of the solar quadrupole moment from ranging to a Mercury Orbiter", *Astrophys. J.*, submitted (1989).

Vincent, M. A. and P. L. Bender, "Orbit determination and gravitational field accuracy for a Mercury transponder satellite, "J *Geophys. Res.*, submitted (1989).

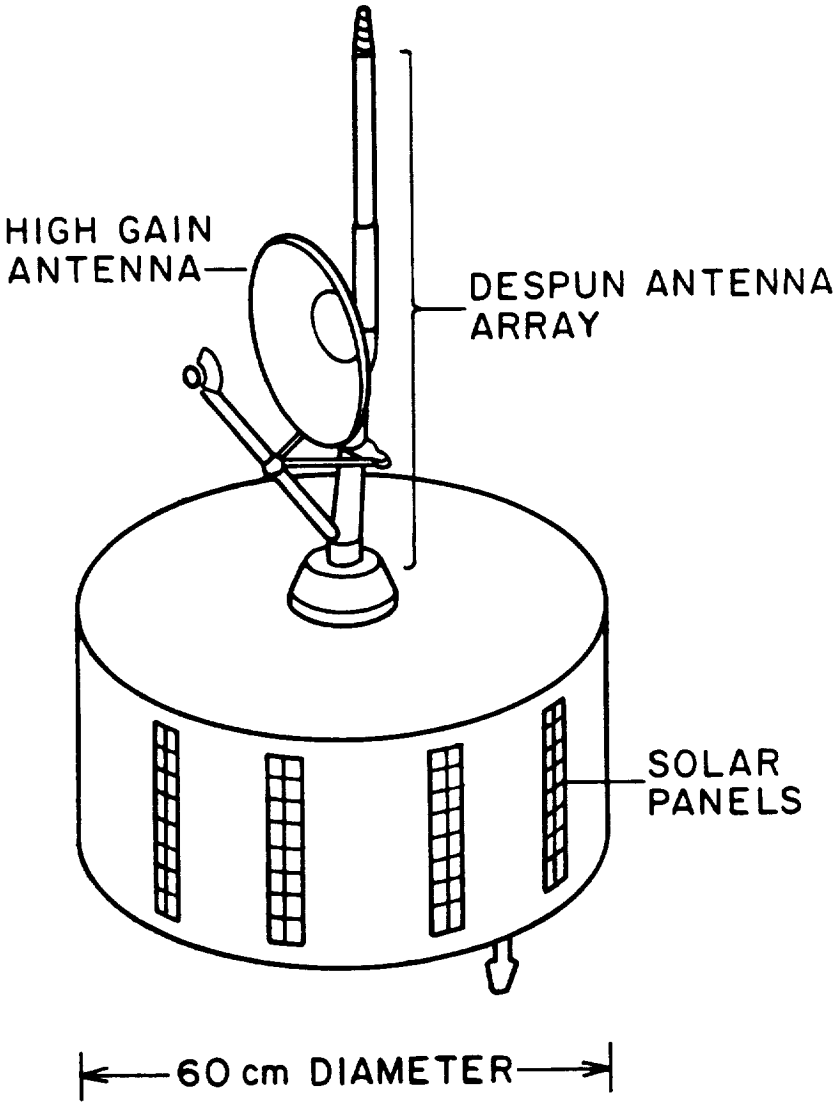

FIG. 1. -- Small Mercury Relativity Orbiter

DISCUSSION

SHAPIRO: In your respective error analyses using simulated observations, what was the smallest angular separation between the sun and the target (with the target on the far side of the sun)?

HELLINGS & BENDER: Five degrees

SONNABEND: If the initial estimate of J_{2O} were seriously worsened, would there be any significant change in the latter evolution of the covariance?

HELLINGS & BENDER: Almost no effect for either mission.

GRAVITATIONAL EXPERIMENTS ON A SOLAR PROBE MISSION: SCIENTIFIC OBJECTIVES AND TECHNOLOGY CONSIDERATIONS

JOHN D. ANDERSON
Mail Stop 301-230
Jet Propulsion Laboratory
California Institute of Technology
Pasadena, California 91109

1. INTRODUCTION

On June 5, 1975, Professor Giuseppe Colombo came to JPL as a consultant on a number of mission studies. One of these studies, occupying a duration of about one year, concerned the concept of a solar impact probe (Colombo, 1976). In the summer of 1976 Lou Friedman and I, working in close collaboration with Colombo, began a more detailed study of a solar probe (either solar plunger or sun grazer) with the hope that a joint Phase A study effort might be undertaken between ESA and NASA. Such a study never materialized, but we did publish the results of our own small study in the proceedings of a conference on experimental relativity in Pavia, September 17-20, 1976, sponsored by the Accademia Nazional dei Lincei (Anderson, et al., 1977). This led to the initiation of a NASA study at JPL in 1978 on the engineering and scientific feasibility of a Solar Probe Mission, named Starprobe during the study, in which a spacecraft is placed in a high eccentricity orbit with a perihelion near 4 solar radii.

The Starprobe study, headed by J. E. Randolph at JPL, showed that the concept was feasible and in fact preliminary mission and spacecraft designs were developed. During this period Colombo introduced the concept of a "solar parachute" that could reduce the final orbital period of a solar probe to the Sun (Randolph, 1978). Such a probe would go to Jupiter first and then use the giant planet's gravity field to change the spacecraft's trajectory so that it would go to the Sun. The parachute, actually a small solar sail relying on solar radiation pressure for thrust, would be deployed following the Jupiter swingby and would change the period of the spacecraft about the Sun from four years to one year, thus permitting multiple flybys of the Sun with a reasonable interval of time between encounters.

In the early stages of the Solar Probe studies the emphasis was placed on gravitational science, but by the time of a workshop at Caltech in May 1978 (Neugebauer and Davies, 1978) there was about an equal division of interest between heliospheric physics and gravitation. During that workshop several individuals and science groups presented preliminary descriptions of experiments in the areas of solar interior and general relativity, the solar surface, solar energetic particles, solar neutrons, solar wind, interplanetary dust, and gravitational waves. By 1980 sufficient interest had developed in the mission that NASA formed three ad hoc science study teams (see Table 1). The reports of these teams were published in a single document (Underwood and Randolph, 1982) along with the most recent thinking on the mission and system design concepts.

Those of us who had conceived of Solar Probe as a gravity mission viewed the influx of solar physicists with some trepidation, and indeed the prognosis for a mission of sufficient compexity to support gravitational science deteriorated rapidly in the 1983 fiscal year. It became increasingly clear to NASA that if a solar-probe mission were flown, it would be less costly if the science were restricted to the area of particles and fields. The main concern was the requirement for a drag compensation

system to support gravitational science, though the Randolph study had indicated that the addition of such a system to a basic fields and particles spacecraft would increase the total cost of the mission by only 10 percent.

The last of the gravitational studies for Solar Probe was conducted at JPL in 1983 (Mease et al., 1984). Since that time, the Committee on Solar and Space Physics (CSSP) of the National Academy of Sciences has recommended the pursuit of a focused mission, featuring fields and particles instrumentation and emphasizing studies of the solar wind source region. Such a Solar probe mission is currently listed as the 1994 Major New Start candidate in the Office of Space Science and Applications Strategic Plan. More recently in October 1988 a Solar Probe Science Study Team was convened by the Space Physics Division for the purpose of studying the possible science return from the recommended focused mission.

In the remainder of this review I will reiterate the unique gravitational science that can be accomplished with a solar probe mission. In addition I will address the technology issues that were identified in 1980 by the ad hoc working group for Gravity and Relativity Science.

II. SCIENTIFIC OBJECTIVES

The primary scientific objectives of a solar probe mission from the viewpoint of gravitational science is the determination of the quadrupole coefficient J_2 in the Sun's gravity field. This objective was identified as the most important single measurement during the early studies in the 1970's, and it was reaffirmed by the ad hoc group in 1980. As shown in Figure 1, an accuracy of 2×10^{-8} is feasible. No other technique could yeild a measurement to this accuracy. Even if the other second degree harmonics are assumed nonzero, and the J_2 coefficient is assumed to vary sinusoidally with a period of 160 min, the accuracy in the mean value of J_2 is degraded to only 2.5×10^{-8} (Mease et al., 1984). A drag compensation system accurate to 10^{-10} g_e is required, but a system at 10^{-9} g_e could still produce a respectable accuracy in J_2 of 3×10^{-8}.

An accurate measurement of J_2 would yeild information on the state of rotation of the solar interior, particularly the core, and at the same time it would remove the solar oblateness as a source of error in other solar system tests of General Relativity. For example, an error of 3×10^{-8} in J_2 would result in an error of only 3.8×10^{-3} arcsec per century in the precession of Mercury's perihelion. A direct and relatively accurate determination of the PPN parameter would be possible from observations of Mercury (see for example Misner, Thorne, and Wheeler, 1973, p. 1072 for a definition of PPN parameters).

OTHER POSSIBLE SCIENTIFIC OBJECTIVES

1) A Measurement of J_4 of the Sun.

Ulrich and Hawkins (1980) have suggested that differential rotation could cause a large value of J_4, on the order of $J_2/10$. Because the effect of J_4 falls off by a factor of r^{-2} faster than J_2, it would have a negligible effect on the orbit of Mercury, but at a distance of 4 solar radii it could conceivably be detected with Solar Probe. Hill (1986) has reported the detection of a large J_4 (-2.5×10^{-6}) by means of visual

oblateness observations at SCLERA in 1983. The value of J_2 from the same observations is $(5.2 \pm 1.7) \times 10^{-6}$. Such a large value of J_2 is disputed by others (Duvall et al., 1984) who derive $(1.7 \pm 0.4) \times 10^{-7}$ based on solar free oscillations. Solar Probe could resolve this dispute and at the same time provide a possible detection of J_4 if it is as big as analysis of the 1983 SCLERA data indicates.

2) A Measurement of the Time Variability of J_2.

The studies by Mease et al. (1984) showed that the amplitude of a 160 min sinusoidal variation could be determined to an accuracy of about 2×10^{-8}. Solar oscillations with a 160 min period have been reported (Scherrer and Wilcox, 1983). Christensen-Dalsgaard and Gough (1980) have suggested that these oscillations might give rise to an oscillatory quadrupole moment.

3) Total Angular Momentum of the Sun.

This would have to be determined by using the solar probe to measure the dragging of the Sun's inertial frame by the solar rotation. The studies by Mease et al. (1984) indicated that the expected effect is too small to be detected by the dynamics of the solar flyby.

4) Redshift Experiment

By including an atomic frequency standard on board Solar Probe, it might be possible to measure post-Newtonian corrections to the gravitational redshift. Bechhoeffer et al. (1988) have shown that with a four-frequency four-link Doppler tracking system, it is potentially possible to measure the fourth-order term in the gravitational redshift. This would seem to offer an excellent opportunity to measure effects in the solar system one order beyond Einstein's predictions. Unfortunately this experiment places requirements on a 1994 Solar Probe mission that would be hard to meet, given the recommended narrow focus on solar physics, but it deserves study, particularly from the point of view of the tracking system and the amount of drag compensation needed, if any.

5) Preferred-frame Parameter a_1.

The study by Mease et al. (1984) showed that the preferred-frame PPN parameter a1 could be determined with accuracy of 0.007, assuming that the motion of the solar system in the Earth mean equator and equinox system of 1950.0 is (-353.44, 28.93, 34.08) km s^{-1}.

6) Moffat Parameter in NGT Theory.

According to the NGT theory of Moffat (1983) there is a non-PPN parameter l that can be determined from orbital dynamics. According to the studies of Mease et al. (1984) this parameter for the Sun could be measured with an accuracy of 880 km. A failure to detect this parameter would place severe restrictions on NGT as a viable alternative to General Relativity.

In addition to the specific objectives mentioned above, the NASA ad hoc working group also recognized that the radio system on Solar Probe might be advantageous to a search for gravitational radiation. Similarly, the radio system, in conjunction with

a favorable Jupiter-centered flyby trajectory during the Jupiter gravity assist, might lead to new information on the gravity field of Jupiter and its ephemeris. The studies by Mease et al. (1984) suggest that no new information would become available on the PPN parameters b and g as a direct result of the solar flyby trajectory, but as pointed out by the ad hoc working group, a significant indirect determination of b in combination with other data, particularly observations of Mercury, would definitely be possible.

III. TECHNOLOGY CONSIDERATIONS

The NASA ad hoc working group identified three areas of technology which are of particular importance to gravitational physics. They recommended that all three areas should be studied in more detail before a final system design is selected for Solar Probe.

1) Tracking System

The specification and configuration of the tracking systems needs to be determined, both with respect to the required accuracy during solar encounter and with respect to Doppler and range capability.

2) Drag Compensation System

The non-gravitational accelerations on Solar Probe during the critical period of solar encounter (± 1 day) are unacceptably large for gravitational experiments. A reduction by a factor as large as 10^5 is required by means of some sort of drag compensation system. For a given proposed system it is important to evaluate its effect on the scientific objectives, particularly with regard to the environment of ionizing solar radiation and the expected noise spectrum of the drag-compensation accelerations on Solar Probe.

3) On-Board Atomic Frequency Standard

An atomic frequency standard on board Solar Probe, and operational for the period of solar encounter, would permit added flexibility in the tracking system, but more importantly, it would be required for a meaningful fourth-order redshift measurement. A study of proposed frequency standards should address the question of the reliability of the flight unit as well as its physical parameters and stability specifications.

TABLE 1. NASA Ad Hoc Science Study Teams, 1980

Gravity and Relativity Science

R. D. Reasenberg, Chairman, MIT
J. D. Anderson, JPL
D. B. DeBra, Stanford
I. I. Shapiro, MIT
R. K. Ulrich, UCLA
R. F. C. Vessot, CfA

Particles and Fields Science

F. L. Scarf, Chairman, TRW
B. E. Goldstein, JPL
A. Barnes, ARC
W. C. Feldman, Los Alamos
L. Fisk, U. of New Hampshire
G. Gloeckler, U. of Maryland
S. M. Krimigis, APL
K. N. Ogilvie, GSFC
C. T. Russell, UCLA

Imaging Sciences

A. B. C. Walker, Jr., Chairman, Stanford
A. Title, Lokheed Palo Alto
A. Kreiger, American Science and Engineering
J. Kohl, CfA
H. Zirin, Caltech
J. Underwood, JPL
E. Frazier, The Aerospace Corporation
R. Munro, High Altitude Observatory, Boulder
G. Timothy, Laboratory for Atmospheric and Space Physics, Colorado
G. Withbroe, Harvard Observatory
J. Davis, American Science and Engineering
E. Rhodes, USC

REFERENCES

Anderson, J. D., Colombo, G., Friedman, L. D., and Lau, E. L., "An Arrow to the Sun," *Gravitazione Sperimentale*, 393-422, Accademia Nazionale dei Lincei, Rome, 1977.

Bechhoeffer, J. D., Eardley, D. M., and Vessot, R. F. C., "Relativistic Measurements with a Solar Probe Mission," to appear in the proceedings of the "Symposium on Relativistic Gravitation" held at the XXVII meeting of COSPAR, July 18-29, 1988 in Espoo Finland.

Christensen-Dalsgaard, J. and Gough, D. O., "Perturbations in Gravitational Potential Associated with Solar Oscillations," *Nonradial and Nonlinear Stellar Pulsation*, eds. H. A. Hill and W. A. Dziembowski, pp. 369-380, Springer-Verlag, New York, 1980.

Colombo, G., "An Alternative Option to the Dual Probe, Out of Ecliptic Mission Via Jupiter Swingby," paper presented at the GSFC Symposium on the Sun and the Interplanetary Medium, 1975, NASA TM-X-71097, March 1976.

Duvall, T. L., Dziembowski, W. A., Goode, P. R., Gough, D. O., Harvey, J. W., and Leibacker, J. W., Nature, *310*, 22.

Hill, H. A., "Solar Oscillations, Gravitational Multipole Field of the Sun and the Solar Neutrino Paradox, *Mathematical Aspects of Gravity and Supergravity*, proceedings of the NATO Advanced Workshop held July 21-24, 1986 at Utah State University, Logan, Utah.

Mease, K. D., Anderson, J. D., Wood, L. J., and White, L. K., "Tests of General Relativity Using Starprobe Radio Metric Tracking Data," Jour. of Guidance, Control, and Dynamics, **7**, 36-44, 1984

Misner, C. W., Thorne, K. S., and Wheeler, J. A., *Gravitation*, Freeman and Company, San Francisco, 1973.

Neugebauer, M. and Davies, R. W., eds., *A Close-Up of the Sun*, NASA/JPL Doc. No. 78-70, 1978.

Randolph, J. E., "Solar Probe Mission Options," JPL Doc. No. 660-77, Appendix C, 1978.

Scherrer, P. H. and Wilcox, J. M., *Solar Physics* **82**, 42, 1983.*8*

Ulrich, R. K. and Hawkins, G. W., "The Solar Gravitational Figure - J_2 and J_4," JPL Internal Document 10M 312/80.5 - 763, Att. 4-1, 1980.

Underwood, J. H. and Randolph, J. E., eds., *S*tarprobe Scientific Rationale, A Report of the Ad Hoc Working Groups, JPL Publication 82 - 49, 1982.

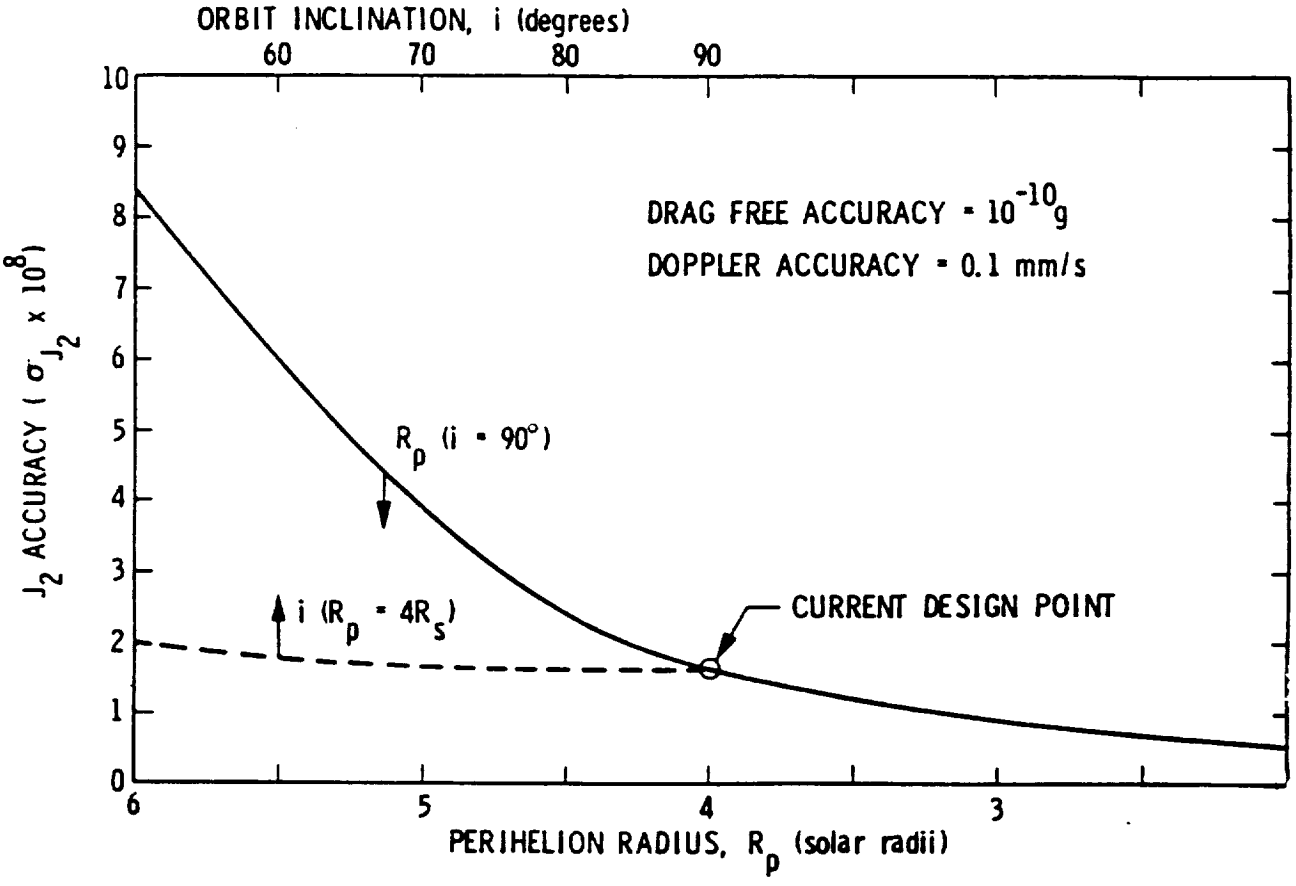

Fig. 1 - Estimated accuracy of a determination of the quadrupole moment in the Sun's gravity field from the Doppler tracking of Solar Probe. The solid curve shows the degradation in accuracy as the perihelion distance is increased from the design point of 4 solar radii. The dashed curve shows a small sensitivity to the orbital inclination to the ecliptic, but this is only realistic under the assumption that all gravity harmonics except the quadrupole moment are negligible. Under the assumption of white noise during the solar encounter, the Doppler accuracy of 0.1 mm/s represents an estimate of the one-sigma accuracy of reduced range-rate measurements at a sample interval of 60 s. Under the assumption that the error in the drag-free system is dominated by the DC component, the solid and dashed curves represent realistic estimates of the error for a drag-free accuracy of 10^{-10} g_e, but they are too optimistic if the drag-free system contains significant noise components with periods on the order of 10,000s (10^{-4} Hz).

OPTICAL INTERFEROMETERS FOR TESTS OF RELATIVISTIC GRAVITY IN SPACE

R. D. REASENBERG
Smithsonian Astrophysical Observatory

I. INTRODUCTION

We consider a space-based astrometric interferometer with a large optical bandwidth. POINTS (Precision Optical INTerferometry in Space) would measure the angular separation of two stars separated by about 90 deg on the sky with a nominal measurement error of 5 microarcseconds (μas). For a pair of mag 10 stars, the observation would require about 10 minutes. We estimate the instrument would measure daily the separation of two stars for each of about 60 pairs of stars; a random sequence of such measurements, if suitably redundant, contains the closure information necessary to detect and correct time-dependent measurement biases to well below the nominal measurement accuracy. The 90 deg target separation permits absolute parallax measurements in all directions.

A redundant observing schedule for 300 stars and 5 quasars (1,500 star-star observations and 250 star-quasar observations) would provide extra redundancy to compensate for the quasars' higher magnitude. If a nominal 30-day observation sequence were repeated 4 times per year for 10 years, we would obtain means stellar parameter uncertainties of: 0.6 μas, position; 0.4 μas/y, proper motion; and 0.4 μas, parallax (Reasenberg 1986). This set of well-observed stars and quasars would form a "rigid frame" and the stars would serve as reference objects for measurements of all additional targets, as well as being targets of direct scientific interest.

In the following sections we consider the instrument global data analysis science objectives including a relativity test and technology. A compressed version of the VuGraphs shown follows the text.

II. INSTRUMENT

The POINTS instrument comprises two starlight interferometers and a metrology system. Each interferometer has a baseline 2 m long, and 2 afocal telescopes, each with a primary mirror 25 cm in diameter. The axes of the interferometers are separated by an angle $\varphi = \varphi_o + \Delta$, where φ_o is 90° and $|\Delta|$, the absolute value of the articulation angle, is less than 3. The instrument determines θ ($\approx$90 deg), the angular separation between two stars, by measuring φ and, independently, δ_1 and δ_2, the offsets of the target stars from their respective interferometer axes. Once a target star is in the field of an interferometer, the corresponding δ is measured through the analysis of the dispersed fringe which forms a "channelled spectrum." The use of this technique simplifies the instrument by making the fringe easy to see; it eases the pointing requirements to about ± 3 arcsecond. The nominal limiting magnitude is 17, but depends on the level of disturbance that the instrument suffers. Techniques exist to extend the limiting magnitude by five, provided detector noise does not dominate. Central to the design is the real-time metrology of (1) the angle between the interferometers, and (2) the starlight optical path; each of these metrology systems uses a laser interferometer scheme based on technology that is either currently available or under development and expected to be available soon.

The control of systematic error is the key to achieving the nominal accuracy of 5 μas. We address this problem at three levels: (1) stable materials, structural design, and thermal control; (2) real-time metrology; and (3) the detection and correction of systematic error in conjunction with the global data analysis. For a 2-m baseline, the nominal 5-μas uncertainty corresponds to a displacement of 1 end of the interferometer toward the source by 50 picometers (pm). (See Table 1.) Since similar displacements of internal optical elements are also important, the instruments require real-time metrology of the entire starlight optical path accurate to a few pm. This metrology does not pose an overwhelming problem because (1) the precision is needed only for a narrow bandwidth ($\approx 10^{-3}$ Hz, since higher frequency errors will tend to average out during a single star-pair observation), and (2) a slowly changing bias in the measurement is acceptable, as discussed below.

TABLE 1

PRELIMINARY POINTS ERROR BUDGET OF 50 PM*

I.	Starlight determination of δ_1 and δ_2	43 pm	
	A. Photon statistics		40 pm
	B. Detector		10 pm
	C. Suboptimal estimator and loss of fringe tracking		10 pm
II.	Metrology determination of ø	20 pm	
	A. FAM		10 pm
	B. Laser gauges		10 pm
	C. Fiducial blocks		10 pm
	D. Lasers		10 pm
III.	Modeling errors	10 pm	
	A. Structure (including vibration)		
	B. Ephemeris error		
	C. Geometry		

*(5mas ≈ 2.5 × 10^{-11} radians) × 2 m = 50 × 10^{-12} m ≈ 50 pm.

The angle, φ, between the baselines of the two interferometers is determined by measuring the six distances among four fiducial blocks in the system. Each of the six distances is measured by a laser gauge which must meet the following requirements: (1) precision of a few pm; (2) measurement accuracy not sensitive to small changes in distance (*i.e.*, not a null device and free of bias periodic in distance); (3) ability to keep track of significant distance changes (*i.e.*, many wavelengths); and (4) ability to operate without the calibration that would be made possible by making multiwavelength changes in the distance measured. We are developing such a laser gauge (Phillips and Reasenberg 1988) and suitable solid-state sources are expected in the next few years. "Full-Aperture Metrology" (FAM) surveys the optical components that transfer the starlight from the primary mirrors to the beamsplitter in each stellar interferometer. FAM provides three significant advantages over conventional approaches.

(1) FAM removes complexity. The usual metrology systems use a large number of laser gauges to determine the locations of the elements individually. From these measurements, the optical path through the system is computed. FAM directly measures the optical path through the system.

(2) FAM measures the correct quantity. Because the metrology signal fully illuminates the surface of each optical element that determines the starlight phase at the beamsplitter, the phase of the metrology signal is representative of the average starlight path through the system.

(3) FAM provides the basis for an operational definition of the direction of the interferometer baseline. It results in a pair of "fiducial points" located in the "fiducial blocks" in front of each interferometer. These fiducial points, which lie on lines parallel to (or held at fixed small angles to) the interferometer baselines, are used to determine φ, the angle between the two interferometers' optical axes.

Each fiducial block is a collection of optical elements which joins the ends of the metrology paths.

III. GLOBAL DATA ANALYSIS

When an observation set has sufficient redundancy, it can be analyzed to yield a rigid frame; it serves to determine the angular separation of all pairs of observed stars. The redundancy is measured by M, the ratio of the number of observations to the number of stars observed. With moderate redundancy, M = 4.2, the uncertainty in the separation of any two stars (including those not simultaneously observed) is about equal (on average) to the instrument measurement uncertainty. The star grid is free of regional biases and may be further strengthened by additional data obtained when the grid stars are used as reference stars for additional science targets.

The metrology system that is described above is capable of providing the required precision, but contains finite-sized optical components, each of which will introduce a bias into the measurement of the angle. This bias will surely be time-dependent at the microarcsec level. Both the determination and correction of that bias naturally occur when the observations are combined in a least-squares estimate of the individual stellar coordinates (including proper motion and parallax), the instrument model parameters, and the expected biases. In particular, our covariance studies have shown that, even without the introduction of a special observing sequence, it is possible to estimate simultaneously the stellar coordinates and several instrument bias parameters per day without significantly degrading the stellar coordinate estimates. Thus, we have latitude in the instrument design: metrology biases and related errors can be allowed to change on a time scale of hours without significantly degrading the performance of the instrument. The covariance studies also show that the baseline lengths, systematic errors in φ, and other instrument parameters are naturally determined in the data analysis.

A discussion of some astrophysical applications of POINTS is given by Reasenberg *et al.* (1988) and in less detail by Reasenberg (1984). These applications include (1) a light-deflection test of general relativity, perhaps to second order in the solar potential, but 10^3 times more accurate than the present best test (Fomalont and Sramek 1977); (2) a search for other planetary systems, which will either find such systems or show that they are considerably less common than is now projected; (3) development of a distance scale based on direct parallax determinations for a large number of Cepheids; (4) a determination of the masses of stars in binary systems and those close enough to apply the method of perspective acceleration; (5) parallax measurements yielding both absolute stellar magnitudes and, in conjunction with mass estimates and other data, a sharpened mass-color-luminosity relation; (6) a vastly improved global reference frame and a tie to existing ones; (7) a refinement of our knowledge of the mass distribution in the Galaxy; (8) a strictly geometric (*i.e.*, coordinate and parallax) determination of the membership of star clusters; and (9) a bound on, or a measurement of, quasar proper motions. In addition, there are applications to solar-system studies and to the navigation of spacecraft, particularly in the outer solar system.

We have performed a series of covariance studies of a POINTS light-deflection test using a common set of 100 Monte Carlo stars which includes ten constrained to be within 0.2 deg of the ecliptic. Over a 2-year experiment, quarterly observations were made of all pairs simultaneously observable with Δ chosen to yield M = 5. Whenever one of the 10 "special stars" was between L_G (glare limit) and L_P (pre-emptive limit), it was observed continuously, cycling among the stars within Δ of 90 deg of it. On any day when one of the special stars was between L_P and L_D (daily survey limit), it was observed once with each other star within Δ of 90 deg from it.

For each star (except for the two held fixed to prevent degeneracy) we estimated five parameters: location (2), proper motion (2), and parallax. Along with the 492 star parameters, we simultaneously estimated 4 relativistic-solar parameters: γ (PPN coefficient), Λ (second-order coefficient), J_2 (solar quadrupole coefficient), and I (solar angular momentum). [See Epstein and Shapiro (1980) for a discussion of these four parameters and the deflection to second order.] The results are shown in Table 2.

We conclude that a POINTS mission could improve the first-order test 2 to 3 orders of magnitude beyond the present uncertainty of 0.002 for γ, but that it would yield only a marginal result for Λ with the instrument's present nominal specifications. There are, however, several factors in the specifications that could be altered to change the sensitivity in either direction. For example, the 5-μas nominal measurement uncertainty could be improved by choosing bright target stars, increasing the photon detection probability from its nominal 2%, expanding the baselines, or enlarging the primary mirrors. The instrument's metrology system would have to be improved correspondingly. On the other hand, the solar glare limit, L_G, is undoubtedly the single most critical factor in the second-order test, as expected, since the second-order deflection varies as the inverse-square of the impact parameter. Note especially the dramatic decrease in $\sigma(\Delta)$ that comes from decreasing L_G to 0.25 deg (limb grazing) and, by contrast, the lack of improvement from extending L_D to 8 deg.

TABLE 2

COVARIANCE STUDY FOR ESTIMATION OF RELATIVITY PARAMETERS

OBSERVATION PROGRAMS FOR COVARIANCE STUDY

PARAMETER	SPECIFICATIONS				
Solar glare limit (L_G deg)*	0.5	0.25	0.5	0.75	.0
Pre-empt limit (L_P deg)	1.0	0.75	1.0	1.25	1.5
Daily survey limit (L_D deg)	8	4	4	4	4
Total observations	7293	6104	5996	5901	5846

COVARIANCE STUDY RESULTS

MODEL PARAMETER	NOMINAL VALUE	UNCERTAINTY (STANDARD DEVIATION)				
γ (10^{-6})	10^6	2.2	1.2	2.4	3.7	5.1
Λ	1.0	2.2	0.5	2.4	5.8	11
J_2 (10^{-6})↑	0.1	4.4	0.4	4.5	17	43
I (10^{-6})↑	0.5	0.9	0.3	1.0	2.2	3.7

*L_D is taken as an effective limit representing the gradual degradation of the instrument performance as the sun-target angle is decreased. All three limits are in degrees from the center of the sun.

↑The "dimensionless" quantities J_2 and I are, respectively, the quadrupole moment and the angular momentum of the Sun in units of solar mass and radius and the speed of light. The nominals are based on the standard model of the central condensation of the sun and the assumption that the spin rate is uniform.

V. TECHNOLOGY

None of the technology thus far identified as being required for POINTS is far beyond the present state of the art. For the most challenging problem, the internal metrology, we have solutions in principle. However, these do require a continuation of our ongoing development at CFA. Some of the required technologies are developing rapidly for reasons unrelated to POINTS. A list of the most important technology areas is given in Table 3. Note that these technologies are not peculiar to POINTS, but will have broad application to advanced space instrumentation.

TABLE 3

POINTS TECHNOLOGY CHALLENGES

Space qualified zone-plate mirror
Fabrication of fiducial blocks
Laser gauges
Photon-counting detectors of high efficiency and long life — space qualified
Microdynamics of the optical bench
Pointing and isolation (especially if instrument is on Space Station)
Computation at spacecraft

The technology to be demonstrated in the POINTS program will have a fundamental impact on the development of future optical interferometers for placement in space. In particular, we believe that the application of laser metrology to measure critical optical path lengths and instrument geometry would simplify the design of at least three classes of future interferometric instruments:

(1) "Not-quite-imaging" devices are generally linear arrays of two or more apertures which, in some cases, are made movable. They provide an incomplete sample of the so-called u-v plane. However, such information is useful for learning about the target when it has a strong symmetry, but is hard to resolve.

(2) Fully imaging interferometric devices are discussed extensively in a report prepared by Perkin-Elmer for NASA-Marshall (Final Study Report for Astronomical Interferometric Systems Technology Requirements [AISTR], Revision A, May 1986, NASA Contract #NAS8-26105, P-E# ER991A, and available from Mr. Max Nein at NASA-Marshall), as well as in the proceedings of the Workshop on High Angular Resolution Optical Interferometry from Space (BAAS, 16(3,II), 1984), in the proceedings of the Colloquium on Kilometric Optical Arrays in Space (ESA, SP-226, 1984), and in the Final Report of the Cambridge Workshop on Imaging Interferometry (March 1987, Battelle, Columbus, Ohio, supported by NASA-Astrophysics, D. Mouvard, Ed.).

VI. DISCUSSION

It is now widely recognized that interferometric instruments will play a major role in many aspects of space-based optical astronomy. (See, for example, the three volumes cited in the preceding paragraph.) Results of major importance will come from imaging interferometers with higher resolution and more light-gathering power than the Hubble Space Telescope (HST). However, such instruments must be large to achieve their advantage over existing instruments. POINTS, which is small, could perform a significant test of general relativity, open new areas of astrophysical research, and change the nature of the questions being asked in some old areas. It could be the first of a new class of powerful instruments in space and could prove the technology for the larger members of that class to follow.

REFERENCES

Epstein, R. and Shapiro, I. I. 1980, *Phys. Rev. D*, **2**, 2, 947.

Fomalont, E. B., and Sramek, R. A. 1977, *Comments on Astrophysics*, **7** (1), 19-33.

Phillips, J. D. and Reasenberg, R.D. to be presented at the OSA Topical Meeting on Space Optics for Astrophysics and Earth and Planetary Remote Sensing, North Falmouth, 27-29 September 1988.

Reasenberg, R. D., in *Proceedings of the Workshop on High Angular Resolution Optical Interferometry from Space* (Baltimore, 13 June 1984), edited by P. B. Boyce and R. D. Reasenberg 1984, BAAS **16**, 758.

Reasenberg, R. D. 1986, in *Astrometric Techniques*, proc. of IAU Symp. 109, ed. H. K. Eichhorn and R. J. Leacock, (Reidel), pg 321.

Reasenberg, R. D., Babcock, R. W., Chandler, J. F., Gorenstein, M. V., Huchra, J. P., Pearlman, M. R., Shapiro, I. I.,Taylor, R. S., Bender, P., Buffington, A., Carney, B., Hughes, J. A., Johnston, K. J., Jones, B. F., and Matson, L. E. 1988, *Astron. J.*, in press.

DISCUSSION

FAIRBANK: How accurately could you measure the proper motion Rigel?

REASENBERG: If Rigel were included as one of the grid stars, then after a ten-year mission we would know its proper motion with an uncertainty of under 0.5 microarcseconds per year. Even a few observations made within the first two years of a mission would yield proper motion for Rigel uncertain by less than 5 microarcseconds per year. In short, we could easily exceed the needs of GP-B. As a matter of scientific priority, I would expect that a highly redundant and robust observing schedule would be selected for Rigel.

HELLINGS: It seems like several systematic errors (such as thermal effects driven by the Sun) would have signatures identical to the relativity deflection you want to measure. How would you estimate such a bias?

REASENBERG: Although a solar-driven thermal bias is unlikely to look identical to the relativity effect, it may have a sufficiently similar signature to be a problem. To first order, the effect of instrument heating caused, for example, by looking at a target near the sun should be corrected by the Full-Aperture Metrology system. However, at some level this correction will fail. Pre-launch tests should tell us the characteristics of the failure and these characteristics should be confirmed by experiment in an early phase of the mission. For example, we might point the instrument to a bright pair of stars away from the Sun, measure their separation, then briefly swing the instruments so as to expose one of the interferometers to excessive heating. Finally, by pointing back to the bright pair, we could watch the decay of the residual distortion due to solar heating. When we better understand the failure mechanisms and characteristics for the FAM system, we will be able to devise more highly targeted post-launch tests.

TREUHAFT: To what extent do star or quasar structure fluctuations contribute to reference frame instabilities at the microarcsecond level?

REESENBERG: I know of no basis for discussing quasar structural fluctuations at the microarcsecond level. However, for stars much is known. I believe that for active stars, star spots can shift the center of light of a star by as much as a few percent of the stellar radius. However, most stars are not nearly so active, and the center of light shift should be well under one percent of the radius. One percent of a solar radius is a microacrsecond at 45 parsecs.

SCHUMAKER: How is your precision hurt by the nonpointlike nature of a target? For example, what about the probably large number of binaries that are undetected, especially those that are indistinguishable spectroscopically and comparable to each other in brightness?

REESENBERG: It is inevitable that some of our selected targets will be undetected binaries and we therefore have investigated the response of POINTS to such a target. When the two sources are close together compared to the fringe spacing (50 mas), the instrument treats the source as if it were at the center of light. For sources of different temperatures and either similar or dissimilar magnitudes, the instrument can determine the angular separation between the sources with almost the same precision as the position of the fainter source alone would have been determined, provided only that the binary nature of the source has been discovered. In this case, virtually no confusion results in the astrometric measurement. For an undetected companion, of the same temperature and at least one magnitude fainter than the target star, there is a measurement bias which is zero mean, periodic in the star-companion separation, and proportional to the ratio of the brightness of the companion to the brightness of the target. The envelope of the bias can be made to fall as the cube of the target-companion separation, dropping below 1 microarcsecond at less than an arcsecond separation for a companion one magnitude fainter than the target.

NEW TESTS WITH OLD DATA

JOHN F. CHANDLER
Harvard-Smithsonian Center for Astrophysics
Cambridge, Massachusetts

The discussion of new tests of relativity must begin with a definition of the word "new." I propose to include, under that rubric, not only tests that have never been attempted before or never produced a useful result, but also those that may be repeated with significantly improved results. Thus, this paper will discuss the classical tests insofar as they have been recently refined and will give the results obtained by my colleagues and me at the Center for Astrophysics (CFA). I will also go on to describe a new test of relativity via the detection of the de Sitter precession of the Moon's orbit. These tests, when considered in the parameterized post-Newtonian (PPN) framework, have all involved determining combinations of "β" and "γ."

A further topic of consideration is that of "old" data. In attempting to improve a test of relativity, particularly when the effect to be discerned is a secular one, such as the relativistic perihelion advance of Mercury, it is important to maintain the original set of data, so that the experiment need not start all over. Even in an era of rapid advances in technology, a data set composed just of the observations made by the latest space probe (for example) will be at a disadvantage compared to one that includes earlier measurements. Still, for old data to be useful in performing new tests, they must be preserved in an accessible form, *i.e.*, not just published in scientific journals and the like, but retained along with instrument calibrations and measurement uncertainties on machine-readable media with accompanying format specifications and field descriptions. Empirically, the best way of ensuring the continued usability of old data is to continue using them.

Let us turn first to the deflection of light by massive bodies, such as the Sun. The PPN formula for the deflection (to first order in the mass of the deflecting body) has a coefficient of (1 + "γ"), where "γ" takes on a value of 0.0 in the Newtonian case and 1.0 in general relativity, and the test is to observe the deflection and thereby determine "γ." The classical experiment, of course, was to observe stars near the Sun during a solar eclipse. The results have been consistent with a value of one, but the difficulties of observing stellar positions near the Sun, even during an eclipse, have prevented a very decisive test using optical wavelengths. Still, position measurements at radio frequencies using very-long-baseline interferometry (VLBI) can greatly improve on the optical results, and preliminary analysis of such an experiment by the VLBI group at CFA indicates that a standard error of 0.002 for "γ" should be attainable.

The perihelion advance of Mercury provides another test of gravitational theories. In fact, it was the basis for the original "new" test with old data, since Einstein was able to explain the previously unexplained excess in the perihelion rate for Mercury. However, that excess represents a small residual after removing the purely Newtonian perturbations due to the other planets. The PPN coefficient of the anomalous perihelion advance is (2 + 2 "γ" – "β"), and if we assume that "γ" is known from other tests, the perihelion rate can be treated as a test of "β." Clearly, measuring the rate of advance requires observing Mercury for a long time to track the perihelion. Indeed, in order to distinguish the relativistic effect from the possibly negligible one of the solar quadrupole moment (a purely Newtonian advance of the perihelion), it is necessary to (1) track two different planets to take advantage of the different radial dependences of the two effects, or (2) determine the quadrupole

moment from other methods. This kind of test will obviously always be "renewable" in the sense that an improved external constraint on the solar quadrupole moment will immediately reduce the uncertainty in the excess (post-Newtonian) rate of perihelion advance. The results for this test are, again, consistent with general relativity, but the uncertainty in the estimate of "β" depends strongly on whether the solar quadrupole moment is also estimated or is assumed to have a value consistent with the Sun's surface rotation rate and standard models of the solar interior. From a combination of data, including ground-based radar delay and Doppler observations of Mercury and ranging to the Viking Landers on Mars, we found the "β" standard error to be 0.05 when the quadrupole moment is also estimated, and 0.02 when the latter is held fixed at the assumed value.

A third test consists of measuring the Shapiro time-delay effect in the propagation of signals passing near a massive body. The PPN formula for the delay has a geometric part and, like the first-order light deflection, a coefficient of $(1 + \text{"}\gamma\text{"})$. The simplest method is to observe the round-trip time of signals "bounced" off objects near superior conjunction with the Sun, and the most sensitive time-delay test to date followed this pattern except that the "bounces" consisted of signal returns by active transponders on the Mariner 9 and Viking spacecraft. Our combined data set covered four separate conjunctions of Mars, though with varying levels of accuracy. The resulting estimate of "γ," again, is consistent with general relativity, and the standard error of the estimate is 0.002.

A brief examination of the second and third tests reveals yet another kind of experiment (one that we have done at CFA), namely, to test "everything" at once. In this context, "everything" refers to our comprehensive model of the solar system, including not only the PPN parameters, but also the masses and orbital elements of all the significant bodies; the parameters describing the rotation of the Earth, Moon, and planets; and others too numerous to mention. The key to the method is to observe everything available (and relevant) and combine the data in a simultaneous parameter estimation procedure, taking into account the relative errors associated with each type of observation. The result is a solar-system model with "something for everyone" in it, and a means of extracting maximum information from the data. Such a global test is perpetually "renewable," and there are other advantages, as will be seen presently.

Another test of relativistic gravitation, though not of relativity *per se*, lies in the search for time variations in the gravitational coupling constant, a concept that gained wide attention with Dirac's "large number hypothesis." Indeed, the hypothesized variation can have two interpretations: either a variation of the coupling constant G, or a variation of the dynamical time scale as measured in atomic units. Such a hypothesis can be tested quite easily (and has been) in the context of our solar-system model. We have added the hypothesis parametrically to the model in each of its two forms, and thus, our "grand" solutions can be used to test either form by means of estimating the corresponding coefficient. To date, the results have been negative, that is, no variation of G can be discerned, and our estimate of the standard error in either parameter amounts to 2×10^{-11} parts per year. This represents a large factor times the formal standard deviation of the parameter estimate, partly because of limitations in our model for want of knowledge of asteroid masses. Thus, this test is especially "renewable" to the extent that asteroid masses may be determined.

A new test of relativity (and one that makes use of old data) consists of measuring the geodesic precession of the Earth-Moon system and comparing the rate

with that predicted by de Sitter in 1916. As he pointed out, a satellite orbit in a system freely falling in the Sun's gravitational field undergoes a relativistic precession proportional to the solar potential. The PPN expression for the rate has a coefficient of (1 + 2 "γ"), and a value (when "γ" = 1) of about two seconds of arc per century for the Moon. The effect was simply too small to detect until quite recently, when the increasing sensitivity and growing time coverage of the lunar laser ranging observations, in combination with the other data types used in our solar-system analysis, brought it within reach. Since this effect is simply a consequence of general relativity, and since there is no single term or small group of terms in the theory that leads to the effect, we found it necessary to add an *ad hoc* precession to our model with an adjustable coefficient to account for a possible departure from the predicted rate. We then estimated that coefficient and found no such departure. We obtained a standard error for the estimate of 0.04 arcsec per century, or 2% of de Sitter's rate.

In sum, as these tests illustrate, the ideal test of relativity makes use of the broadest possible collection of data.

DISCUSSION

HELLINGS: It appears that your uncertainty in $\dot{G}/G$ is still about twice ours. Are you planning to publish the geodetic precession results soon?

CHANDLER: Yes, soon.

TAYLOR: Could you expand on the analysis discrepancy in the $\dot{G}$ limit?

CHANDLER: Since the underlying formal standard deviation is about the same in both analyses (and much smaller than either quoted uncertainty), the discrepancy is due to differences in the choice and interpretation of numerical experiments with the data, and to differences in the details of the respective models. We (SAO and JPL) are slowly working on the comparison between the models.

N90-19969

FREQUENCY STABLE HIGH POWER LASERS IN SPACE

ROBERT L. BYER
Department of Applied Physics
Stanford University
Stanford, CA 94305

I. INTRODUCTION

Two years ago during a visit to Boulder, Colorado, Professor Peter Bender introduced me to his dream of a laser heterodyne gravity wave antenna that would operate in solar orbit with a one million kilometer path length. I was asked what progress might be expected in laser technology that would be appropriate for operation of this space-based gravity wave detector.

The rapid progress in diode lasers (Streifer *et al.* 1988) coupled with the energy storage and potentially sub-Hertz linewidths of solid state lasers (Byer 1988, Fan and Byer 1988) and the possibility of efficient frequency conversion by nonlinear optical techniques (Kozlousky *et al.* 1988) defines a technology that is appropriate for laser interferometry in space.

This paper summarizes the present status of diode-laser-pumped, solid-state lasers and projects future progress in areas of linewidth control, high average power, operating efficiency, and operational lifetimes that are essential for space-based applications.

II. DIODE LASER PUMPED ND:YAG LASER OSCILLATOR

In 1985, Zhou *et al.* demonstrated a diode-laser-pumped standing wave monolithic Nd:YAG laser oscillator that operated at 1,064 nm. That experiment illustrated that diode pumping of Nd:YAG was feasible with only a 2 mW cw threshold and with a slope efficiency of 25%. Further, the monolithic 5-mm-long crystal oscillator was isolated from most laboratory-induced sources of acoustic noise and operated with a linewidth of less than 3 kHz. The standing wave geometry, however, was susceptible to feedback of optical radiation and did not oscillate in a single frequency at higher output power levels.

To overcome the limitations of the standing wave oscillator and yet retain the advantages of the monolithic structure, Kane and Byer (1985) invented the monolithic nonplanar ring resonator. This oscillator combined the elements of an optical diode, which forced oscillation in a single direction, with the stability of the millimeter-dimensioned monolithic construction. With diode laser pumping, over 50 mW of single frequency output power was obtained with kilohertz linewidths (Kane *et al.* 1987a). The nonplanar ring oscillator has been an essential element in progress in laser linewidth studies, in efficient nonlinear frequency conversion into the green, and in the demonstration of coherent laser radar at 1,064 nm. The nonplanar ring oscillator's immunity to optical feedback, its single frequency output at high power levels, and its high resonator, Q, make it the oscillator of choice for linewidth-reduction studies. Figure 1 shows a schematic of a diode-laser-pumped nonplanar ring oscillator. Recent work has demonstrated that these oscillators operate with linewidths less than1 kHz, that they can be offset frequency-locked, and that they can be phase-locked. Future work is expected to reduce the linewidth to less than 1 hertz and to lock the frequency-doubled output onto the 300 kHz-wide subdoppler hyperfine component of the iodine molecule at 532 nm. Beyond that, it is

possible to conceive of stabilization of the output of these monolithic devices using ions, or a single ion, stored in an optical or radio frequency trap as an optical clock.

III. 56%-EFFICIENT, SECOND-HARMONIC GENERATION

Techniques must be used to increase the power level in nonlinear crystals to efficiently frequency double the milliwatt power level, cw diode-pumped Nd:YAG oscillators to generate green output at 532 nm. Internal second-harmonic generation (SHG), where the nonlinear crystal is placed within the laser resonator, is one approach for SHG (Fan *et al.* 1986, Baer 1986). Early experiments yielded milliwatt output power levels in the green at conversion efficiencies near 10%. However, internal SHG requires that optical elements be placed within the laser resonator, thus foreclosing the option of the stable monolithic designs and adding complexity to the laser oscillator structure.

An alternative is to externally resonate the fundamental field within the nonlinear crystal. Kozlovsky *et al.* recently demonstrated 56% SHG efficiency using the external resonant approach and converted 52 mW of 1,064 nm to 30 mW of cw 532 nm which had the stability and linewidth of the infrared laser source (Kane *et al.* 1986). The experiment, which used a monolithic ring resonator in a $MgO:LiNbO_3$ nonlinear crystal is shown in Figure 2. Kozlovsky *et al.* (1988) used a diode-laser-pumped nonplanar ring oscillator as the laser source in these elegant experiments. The generation of green radiation allows frequency locking onto hyperfine components of the iodine molecule as a first step toward an absolutely stable laser oscillator. The high conversion efficiency into the green also allows the contemplation of a green source of radiation to replace the argon ion laser as the preferred laser source for gravity wave interferometry.

IV. HIGH-AVERAGE POWER, HIGH-EFFICIENCY LASER OSCILLATORS

To meet the future requirements for gravity wave interferometry in space, the diode-laser-pumped, solid-state laser power must be substantially increased. Fortunately, work is underway with the goal of improving the power level and the efficiency of diode-laser-pumped, solid- state laser oscillators.

The first approach taken to increase the available power, from narrow linewidth laser oscillators, was the demonstration of a 62 dB gain multipass slab geometry Nd:YAG laser amplifier which amplified cw input power at the milliwatt level to kilowatt peak powers for microsecond-long pulse durations (Kane *et al.* 1986). The output of this amplifier was used to demonstrate the first coherent laser radar at 1,064 nm. The Stanford coherent laser radar system used the diode-laser-pumped, nonplanar ring oscillator, the multipass slab amplifier, and single mode glass fiber to collect the returned signal and mix it with the local oscillator (Kane *et al.* 1987b).

In a second approach to obtain higher power levels, a two- dimensional diode laser array was used to pump miniature slabs of Nd:YAG and Nd:Glass. This experiment demonstrated over 0.5 Watt of average output power at 4% overall electrical-to-optical efficiency, and demonstrated that the slab geometry had advantages for diode laser pumping (Reed *et al.* 1988). Since these early results, electrical-to-optical efficiencies of greater than 10% have been demonstrated (Byer 1988).

Based on the diode array pumping of a miniature slab geometry laser oscillator, scaling to higher output power levels is now possible with high confidence. Since the present cost of a two-dimensional array of diode lasers is prohibitive, an alternative approach, shown in Figure 3, has been proposed (Fan and Byer 1988). In this approach, many individual diode lasers, coupled through fibers, are used to pump a slab geometry solid- state laser. The advantages of this approach are the lower cost of the individual diode laser sources, the separation of the diode laser cooling and electrical circuits from the laser itself, and the soft failure mode inherent in many-source pumping. An added benefit is that the laser can be upgraded easily by replacing diodes by increased power diodes, as the technology allows, without redesigning the entire laser system. This design also takes advantage of the projected decrease in cost per Watt of diode laser power by a factor of four each year.

To meet the gravity wave interferometry requirements, we propose to demonstrate a 20 W, cw, single frequency, slab geometry Nd:YAG laser oscillator pumped by 60 1-Watt diode lasers. The overall efficiency of this laser is expected to exceed 10%. That is, for 200 W of electrical input, the laser will generate 20 W of optical output at 1,064 nm. We plan to injection-lock this power oscillator with a nonplanar ring oscillator to obtain single frequency operation. We also plan to frequency double this laser oscillator using external resonant doubling in $MgO:LiNbO_3$. This source should be both a direct replacement for the argon ion laser and the first step toward a laser oscillator that can meet space-based operational requirements.

SUMMARY

Recent progress in diode-laser-pumped, solid-state lasers and in efficient nonlinear frequency conversion has opened new possibilities for coherent laser interferometry. The next generation of laser sources should meet the most demanding requirements for gravity wave interferometry. With further evolution, narrow linewidth lasers should open the possibility of deep space coherent communication or additional relativistic measurements based on astrometry.

REFERENCES

Baer, T. 1986, *J. Opt. Soc. Am B*, **3**, 1175.
Byer, R. L. 1988, "Diode Pumped Solid State Lasers," *Science* **239**, 742.
Fan, T. Y., *et al.* 1986, *Opt. Letts.* **11**, 204.
Fan, T. Y., and Byer, R. L. 1988, *IEEE Journ Quant Electr.* **QE-24**, 895.
Kane, T. J., and Byer, R. L. 1985, *Optics Letts* **10**, 65.
Kane, T. J., *et al.* 1986, *Opt. Letts.* **11**, 216.
Kane, T. J., *et al.* 1987a ,*Opt. Letts.* **11**, 175.
Kane, T. J., *et al.* 1987b, *Opt. Letts.* **12**, 239.
Kozlovsky, W. J., *et al.* 1988, *IEEE Journ Quant. Electr.* **QE-24**, 913.
Reed, M. K., *et al.* 1988, *Opt. Letts.* **13**, 204.
Streifer, W., *et al.* 1988, "Advances in Diode Laser Pumps," *IEEE Journ Quant. Electr.* **QE-24**, 883.
Zhou, B. K., *et al.* 1985, *Optics Letts* **10**, 62.

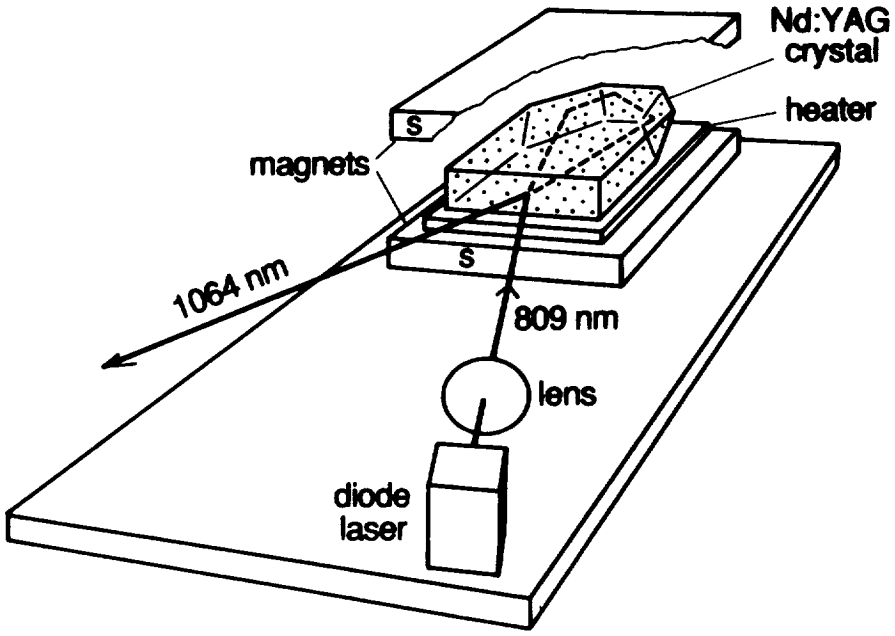

FIG. 1.—A diode-laser-pumped nonplanar ring oscillator

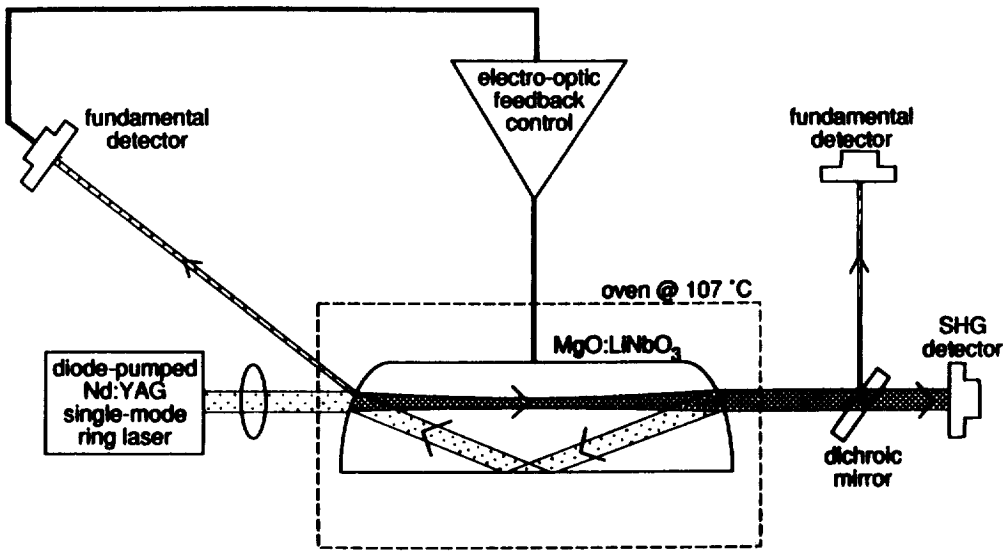

FIG. 2.—The 56%-efficient, external resonant ring doubler

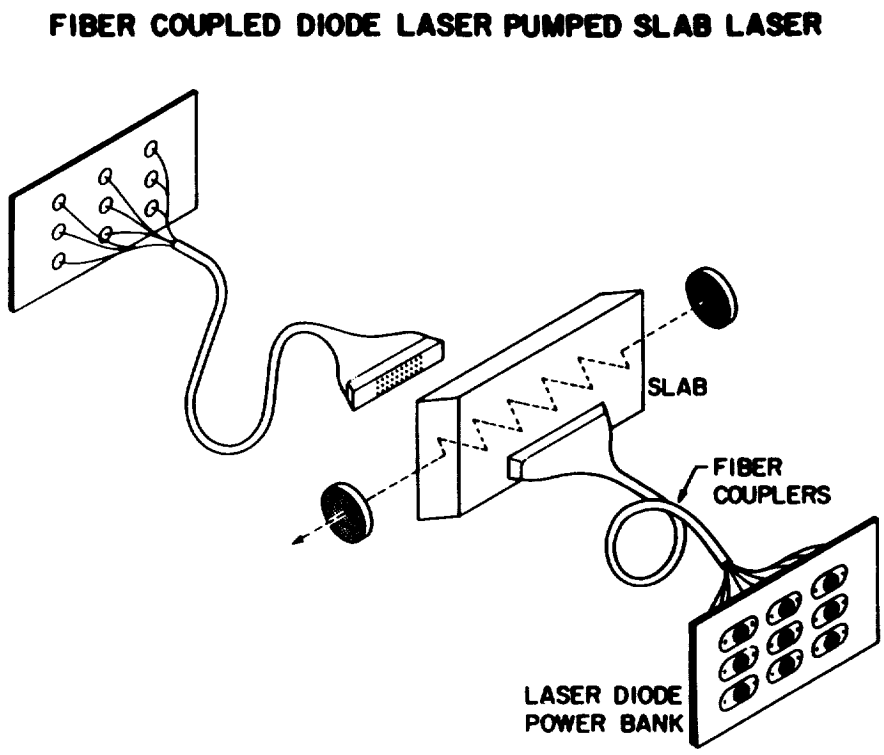

FIG. 3.—Slab laser pumped by many diode lasers coupled through optical fibers

HIGH STABILITY RADIO LINKS

E. ROBERT KURSINSKI
Jet Propulsion Laboratory
Pasadena, California 91109

I. INTRODUCTION

Radio telecommunication links are used for communication with deep space probes. These links consist of sinusoidal carrier signals at radio frequencies (RF) modulated with information sent between the spacecraft and the earth. This carrier signal is a very pure and stable sinusoid, typically derived from an atomic frequency standard whose frequency and phase are used to measure the radial velocity of the probe and from this and other data types derive its trajectory. This same observable can be used to search for space-time distortions cased by low frequency (0.1 to 100 mHz) gravitational radiation (Estabrook and Wahlquist 1975). The purpose of this paper is to discuss how such a system works, what its sensitivity limitations are, and what potential future improvements can be made.

II. OVERVIEW OF EXPERIMENT CONFIGURATION

The instrument or acquisition system discussed here consists of NASA's earth-based Deep Space Network (DSN) of tracking stations, deep space spacecraft, and the data analysis facilities of the general relativity experimenters. Much, if not all, of this same system is also used for spacecraft navigation, VLBI and other types of spacecraft radio science experiments such as the measurement of planetary mass densities and planetary and solar osculations. Examples of the experiments done with the Voyager spacecraft are given by Tyler (1987).

Figure 1 is a schematic representation of how the system works. The basic concept is that an extremely stable monochromatic signal is generated and radiated from the earth to the spacecraft, which receives and retransmits the signal back to earth. At the earth, the signal is received and its frequency is differenced with the same reference signal from which it was originally generated. Any known systematic effects are then removed from this difference leaving a detrended frequency versus time series in which to search for effects of gravitational radiation.

The version of this system currently operating in the DSN consists of an S-band uplink and coherent S-band and X-band downlink signals. A new system is presently being implemented consisting of an X-band uplink and coherent S-band and X-band downlink signals. The first such installation is planned to be completed at the new 34 meter antenna in the Deep Space tracking station complex in Australia this fall, including the test equipment needed to measure and calibrate the system performance, and will first be used with the Galileo spacecraft. For future missions, Ka-band and optical frequencies are planned in order to support higher telemetry rates and further reduce the plasma-induced scintillations on the phase of the propagating signal. The radio frequencies are listed in Table 1.

TABLE 1

DEEP SPACE LINK FREQUENCIES (IN GHz)

BAND	UPLINK	DOWNLINK
S	2.1	2.3
X	7.2	8.4
Ka (proposed)	34	32

RELATIVE PLASMA INSTABILITIES (DELTA-F/F):

S p/down = 12 × X p/down = 225 × Ka p/down

III. LIMITATIONS IN SENSITIVITY

The sensitivity of this system is characterized by its normalized frequency stability, referred to as delta-f/f, which is the uncertainty or instability of the frequency estimates from the system divided by the radio frequency of the signal being measured. This quantity is useful because it is comparable to the dimensionless amplitude of an incident gravitational wave (Estabrook and Wahlquist 1975).

The short and long period limits, which set the time scales over which this type of system is sensitive, are set respectively by the signal strength to noise ratio (SNR) and the time it takes the signal to travel to the spacecraft and back again: the so-called Round Trip Light Time (RTLT) (Estabrook and Wahlquist 1975). The SNR is limited by factors such as transmitter power, antenna gain, receiver amplifier noise, and the distance between the earth and the spacecraft. With all other things being equal, use of higher RF signal frequencies will improve the SNR because antenna gain is proportional to link frequency squared, resulting in delta-f/f improving proportionally with the inverse of the signal frequency cubed.

For the current S-band uplink system, measurements by Armstrong, *et al.* (1987) indicate the short- and long-term limits for the system are due respectively to the downlink SNR and plasma-induced phase scintillations on the S-band uplink signal to the spacecraft. Separation of the plasma noise from the clock noise for certain long integration times has been achieved by Armstrong (1988), and the measured clock noise delta-f/f is 6×10^{-14}.

In the new X-band uplink system, the earth-based equipment has been designed for improved phase stability over that of the S-band uplink system to take advantage of the lower plasma scintillations on the X-band uplink signal. Table 2 is a summary of the expected performance of the new X-band uplink system. It contains a list of error sources and expected levels, measured in square root of Allan variance of frequencies, measured with a 1 Hz filter, for a 1,000-second integration time. The numbers in this table can be viewed as the expected "raw" performance of the system, in the sense that they reflect the stability of the frequency and phase data

after the RF signal has been detected but, do not reflect any of the methods which can be used to dig further into the data such as those discussed by Armstrong (1988).

TABLE 2

EXPECTED PERFORMANCE FOR X-BAND UP/DOWN

	COMPONENT	ALLAN SIGMA * 1.0×10^{15} AT 1,000 SECONDS
Earth Transmission	Frequency Distribution	2
	Translation & Amplification	2
	Antenna at Transmission	1
Spacecraft	Amplifiers, Transponder	2
Earth Reception	Antenna at signal reception	1
	low noise amplifier	0.2
	receiver	2
	frequency distribution	2
Frequency Source	H-maser including change over round trip light time (8 hours)	2
	RSS	5
Propagation Troposphere		<0.6 to 5
	plasma (sep > 150 degrees)	1.5 to 15
	Total	5 to 17

Unfortunately, in a system such as this there is very little common mode noise cancellation. The system can be viewed as one arm of an interferometer and would need another arm to provide cancellation of many of the instrumental effects. A spaceborne microwave interferometer, which would use technologies similar to those discussed here and take advantage of such cancellation effects, is discussed in the Allen Anderson paper elsewhere in this volume.

A primary example of the lack of cancellation is the stability of the frequency standard from which the radiated signal frequency is derived. The instability of this standard, during the integration time over which the signal frequency and phase are detected as well as over the RTLT, limits the knowledge of both the radiated and received signal frequencies as well as their difference. It is for this reason that the system is designed with the downlink signal frequency being generated from the ground frequency reference making it as stable as possible. The best frequency standards available are active-type hydrogen masers, which are used by the DSN and currently cannot be flown on deep space spacecraft. The values in Table 2 represent typical active hydrogen maser stabilities for the DSN.

The major equipment improvements made with the X-band uplink capability have been primarily in the areas of frequency distribution and phase coherence, particularly for periods of 1,000 seconds or more where any mechanical movement or changes in temperature can be translated into phase shifts in this equipment. The distribution into the antennas of reference frequencies which retain the stability of the hydrogen maser source has been achieved through the use of an active phase correction loop. Improvements in the phase coherence of the transmitting and receiving equipment, that is, how well they follow the phase and frequency of the reference signal from the frequency standard, have been achieved by reducing the percentage of the uplink signal frequency and the receiver heterodyning frequencies which are derived from tunable elements. In addition, particularly temperature-sensitive components have been ovenized. The transmitter phase errors were reduced with a phase correction loop around the translation equipment (exciter) and the transmitter allowing the exciter to correct for the phase shifts in the transmitter. Measurements of many of these improvements were made in a prototype configuration by Otoshi and Franco (1987). Trowbridge (1975) measurements of the X-band traveling wave maser, and preliminary results of measurements of FET and HEMT low-noise amplifiers employed in the DSN, indicate these devices cause little instability relative to the other system components.

The spacecraft radio equipment sits in a much more thermally and mechanically benign environment than the earth-based equipment and therefore provides excellent stability to the level stated in Table 2 without any modifications specifically for this application. The large parabolic dish antennas, used on the earth, suffer from structural deformations caused by the earth's gravity as they track the spacecraft position across the sky. These distortions change the focal length and hence the signal path length. The values in Table 2 represent a conservative estimate of the residual errors after calibration and removal of these effects.

Phase scintillations due to the earth's troposphere are expected to be the ultimate limit for this type of system even with calibration. The troposphere effects are modeled as wet and dry components that are due respectively to fluctuations of water vapor and the density of the atmospheric constituents (oxygen, nitrogen, *etc.*). The wet component is presently the dominant of the two effects but R. Treuhaft indicates elsewhere in this volume that the dry may not be far behind. The value stated on Table 2 is from Armstrong and Sramek (1982) from measurements taken at the VLA.

As mentioned, plasma irregularities limit the long-term stability of the S-band uplink system. These instabilities as measured by delta-f/f, are proportional to the inverse of the transmission frequency squared, making this frequency very important and an area of continual potential improvement for this system. The relative instabilities for different radio frequencies are listed in Table 1. On the other hand, the inverse frequency dependence allows the plasma effects to be measured and removed by differencing the phase between two-phase coherent signals of different frequencies. The range of values estimated in Table 2 are from the work of Armstrong *et al.* (1979).

IV. POTENTIAL FUTURE IMPROVEMENTS

Table 3 lists some areas of potential major improvement, including what equipment might be involved, and other areas that would mutually benefit from the

improvements. All improvements listed here would be beneficial to other spacecraft radio science experiments as well as to VLBI and spacecraft navigation. The items mentioned here are discussed in the DSN Long Range Plan (1988).

As indicated in Table 2, many of the effects are of the same order, implying that improvements will have to be made in a number of different areas to increase the sensitivity by another order of magnitude. Two items in particular in Table 3, namely calibrating the troposphere and improving frequency standards, appear to be the most difficult technical problems to overcome due to the lack of available technologies which will enhance their performance. There is no method currently of calibrating the troposphere at the levels needed. One promising technology for calibrating the wet component is the water vapor radiometer (WVR) which measures water vapor in the antenna beam. However, it is far from being an operating phase calibration system. This and other possibilities are discussed in R. Treuhaft's paper in this volume.

TABLE 3

FURTHER POTENTIAL MAJOR IMPROVEMENTS

CAPABILITY	IMPROVEMENT	EQUIPMENT DEVELOPMENT REQUIRED	COMMON GOOD
Higher frequency links	Reduced plasma & thermal noise instabilities	Exciter, receiver, transmitter, low noise amplifier, spacecraft transponder	Higher TLM rates, closer probing of solar corona GR time delay
Dual frequency links	Calibration of plasma phase effects	Exciter, microwave distribution, spacecraft transponder	GR time delay
Troposphere monitoring	Calibration of tropospheric phase	Water vapor radiometer (wvr)	VLBI and navigation
Optical fiber distribution	Reduced mechanical and thermal instabilities	Optical fiber transmitters and receivers	Connected element interferometer
Beam waveguide (BWG) antenna	Reduced mechanical and thermal instabilities	BWG antenna, laser ranging monitoring of BWG optics	Ease to modify front-end equip.
Improved frequency standards	Stability over shorter and longer periods	Trapped ion superconducting cavity OSC, low temp H-maser, saphire dielectric resonator OSC	VLBI, navigation, spacecraft O SC

The current level of stability provided by the active hydrogen maser has been, and apparently will continue to be for some time, the best frequency standard in the range of minutes to hours until there is a breakthrough of some kind. The frequency standards listed in Table 3 are promising research projects at JPL and elsewhere. Improvements in both ground and spaceborne frequency standards would help both searches for gravitational radiation and other types of spacecraft radio science experiments. Robert Vessot, in particular, has pointed out that if simultaneous measuring systems similar to the system described here were implemented on both the spacecraft and the earth, they would provide information that would allow cancellation of the earth's troposphere. In order to be useful, of course, the spaceborne standard would have to have excellent stability approximately equal to that of the ground standard.

V. CONCLUSION

Much work has be done towards understanding the limitations of this system. The expected sensitivity of the X-band uplink system communicating with the Galileo spacecraft, should provide frequency data with stabilities in the range of 5×10^{-15} for integration times in the thousands of seconds. This represents an improvement over the S-band uplink system of more than an order of magnitude, which has been achieved primarily through the use of a higher uplink frequency and improved radio and timing equipment on the earth. As indicated in Table 2, there are many sources of instability of comparable levels in reaching this level of sensitivity, and therefore a number of areas exist in which technological improvements will be required to gain another order of magnitude of sensitivity. Of these, there appear to be two, namely troposphere calibration and improved frequency standards, which, due to the lack of current technologies which will lead to their further improvement, are the largest technical obstacles that are limiting further increases in sensitivity.

REFERENCES

Armstrong, J. W., Woo, R., and Estabrook, F. B. 1979, *Ap. J.*, **230**, 570.

Armstrong, J. W., and Sramek, R. 1972, *Radio Science*, **17**, 1579.

Armstrong, J. W., Estabrook, F. B., and Wahlquist, H. D. 1987, *Ap. J.*, **318**, 536.

Armstrong, J. W., 1988, Spacecraft *Gravitational Wave Experiments*, NATO Advanced Research Workshop on Gravitational Wave Data Analysis, Editor: B. Schutz, (Reidel).

Estabrook, F. B., and Wahlquist, H. D. 1975, *Gen. Rel. Grav.*, **6**, 439.

Otoshi, T. Y., and Franco, M. M. January-March 1987, *TDA Progress Report*, **42-89**, 1.

Trowbridge, D. L. 1975, *JPL DSN Progress Report*, **42-28**, 69.

Tyler, G. L. 1987, IEEE Proc., **75**, 1404.

Deep Space Network Long Range Plan, JPL D-3079, Issue B, 801-1, January 15, 1988.

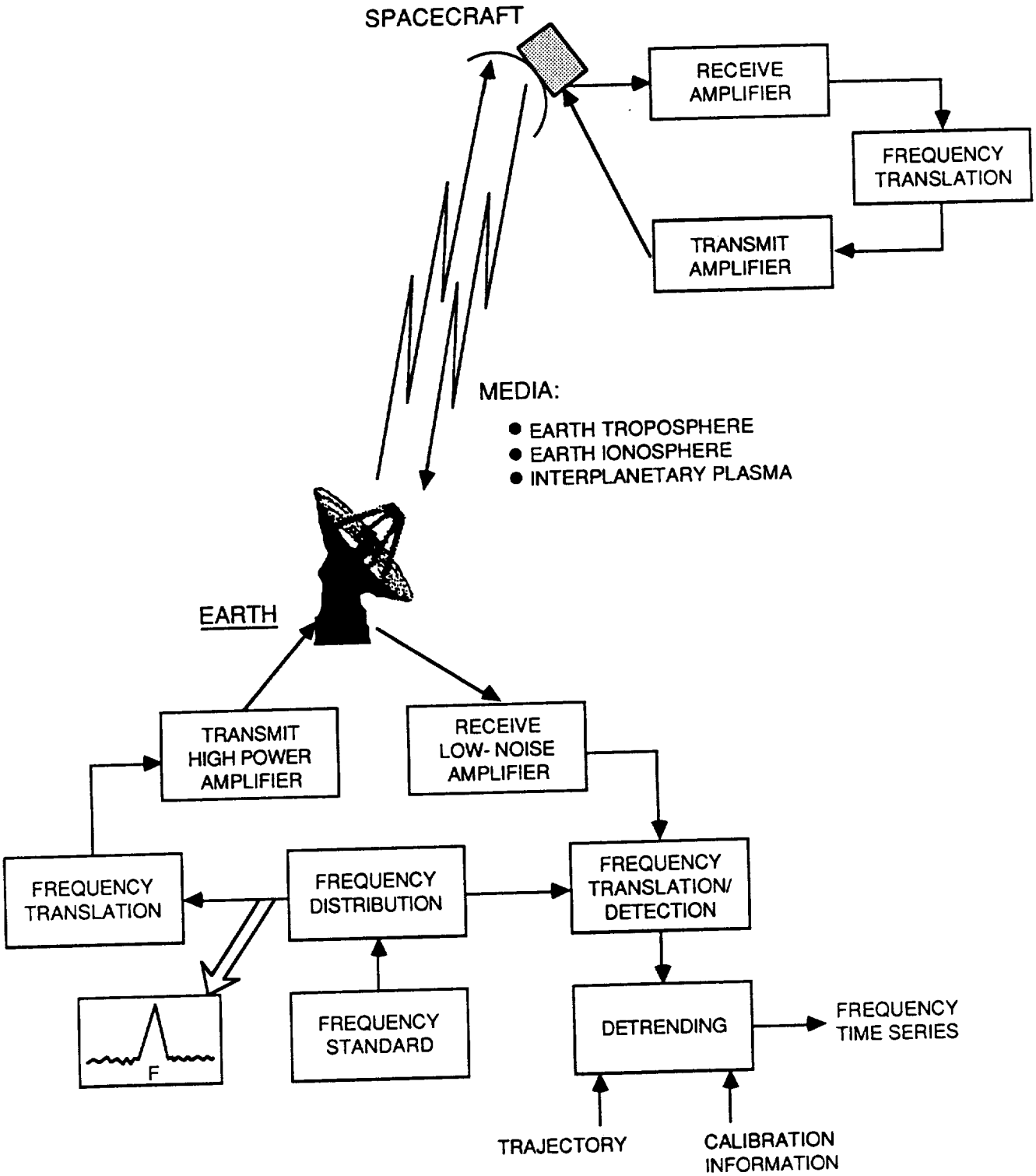

FIG. 1. — Functional Overview

DISCUSSION

REASONBERG: Why is the spacecraft up/down ratio not the same for S, X, and K-band links? Failure to make these ratios the same will make eventual dual-band "up & down" systems less effective than they should be at removing the effect of plasma on the delay and Doppler observables.

KURSINSKI: If two-phase coherent uplink the downlink signals of different frequencies are used, the differential phase between these two signals can be used to estimate and substantially reduce the plasma effects on the phase of the signals. In order to isolate the hi-power transmitted signal from the very weak received signal on the same antenna, it has been necessary to separate the uplink and downlink frequencies via multiplication ratio. Unfortunately, as is apparent in Table I of 'High Stability Radio Links,' there is a difference between the up/down ratios for S- and X-band frequencies. This was done to be compatible with the deep space frequency band allocations assigned by the International Telecommunication Union (ITU). This, unfortunately, means that the plasma effects on the signal cannot be completely isolated via a simple estimate of the differential phase between the two signals received at the earth.

SHAPIRO: Regarding the near future, why can't one use; dual-band (S- and X-band) uplink as well as downlink (the S-band uplink capability already exists and it is not clear why it needs to be dropped) and VLBI calibration techniques, already well developed, to calibrate the relevant electrical paths on the transmitter and receiver parts of the ground system?

KURSINSKI: To isolate the plasma effects, in this situation, implies that the plasma effects on the uplink would have to be estimated via a differential phase measurement between the two uplink signals at the spacecraft and then perhaps one of the uplink signals would be used as the reference to generate the two coherent downlink signals. Such a scheme has been proposed by Jay Breidenthal at JPL using existing equipment and the Galileo spacecraft. Simultaneous S-band and X-band uplink signals could be radiated from different antennas at the same complex and the Galileo transponder, because of its design, may unintentionally be able to simultaneously receive both signals. One method suggested for separating the uplink plasma effects is to offset the two uplink signals from their relative 11/3 ratio by some factor like 1 Hz, which would result in a beat frequency in the downlink signal from which the uplink plasma effects could be measured separately from the downlink effects.

Concerning calibration of the relevant electrical paths, usage of the techniques developed for VLBI is a possibility. The DSN is developing a calibration and monitoring technique for the X-band uplink capability and based on this question, I will have the modifications necessary to make this compatible with the S-band uplink examined.

TROPOSPHERIC MONITORING TECHNOLOGY FOR GRAVITY WAVE EXPERIMENTS

R. N. TREUHAFT AND G. M. RESCH
Jet Propulsion Laboratory
Pasadena, California

ABSTRACT

Tropospheric refractivity fluctuations are an important error source for gravity wave detection by Doppler tracking in that they alter the phase and phase rate of electromagnetic signals. The goals of this paper are to present estimates of the effect of tropospheric fluctuations on the Doppler signal and to suggest some examples of methods which minimize the effect. A model of the fluctuations is utilized to achieve those goals. The levels of wet and dry fluctuations for a single path through the atmosphere are estimated to be approximately 4×10^{-14} and 9×10^{-15} sec/sec for 20 degree elevations at 1,000 seconds. At the 40 degree elevations intended for the gravity wave experiment, the wet and dry fluctuation levels are approximately 2×10^{-14} sec/sec and 6×10^{-15} sec/sec at 1,000 seconds, respectively. Four possible methods for reducing the fluctuation effect are suggested: 1) observation and analysis strategies, which separate the atmospheric and gravity wave signatures; 2) water vapor radiometry for the wet component; 3) calibration using Global Positioning System (GPS) satellites; and 4) Doppler observations from multiple antennas to average fluctuation effects. The last two techniques could be used to calibrate both wet and dry fluctuations, or could be used in conjunction with water vapor radiometry to calibrate only the dry component. For example, combining water vapor radiometry and the proposed GPS technique could reduce the total 1,000 second fluctuation effect to approximately 6×10^{-15} sec/sec at 20 degree elevations, or 2×10^{-15} sec/sec at 40 degree elevations.

I. APPROACH

Fluctuations in the refractivity at microwave frequencies are an important nondispersive error source for Doppler tracking gravity wave experiments. A model devised to provide a quantitative description of the wet tropospheric fluctuation effect on the path delay of radio signals is used to assess the magnitude of both wet and dry fluctuations on various time scales (Treuhaft and Lanyi 1987). Normalized to daily Deep Space Network (DSN) water vapor radiometer (WVR) measurements, the model for wet fluctuations has agreed with WVR and very long baseline interferometry (VLBI) data on shorter time scales. The extension of the model to account for dry fluctuations is achieved by employing appropriate values for dry spatial variations and the scale height of the dry component. While this extension seems reasonable, it should be verified by experiment. It is the aim of this paper to estimate the magnitude of the problem and present potential solutions. The solutions presented do not span the set of all possibilities, but are discussed to establish the level to which the fluctuations might be removed.

II. THE LEVEL OF UNCALIBRATED TROPOSPHERIC FLUCTUATION

The essence of the model used to evaluate the level of tropospheric fluctuations as well as some of the calibration alternatives is found in Fig. 1. Wet or dry refractivity irregularities are envisioned as being frozen and blown across a site by the wind. Propagation delay statistics are obtained by integrating refractivity statistics over the geometry of the raypaths through the atmosphere. It is important to realize that temporal fluctuations, over a time interval T, are caused by spatial fluctuations of dimension V × T where V is the wind speed.

Typical Allan standard deviations from the model for DSN sites are shown in Fig. 2. The wet fluctuation was normalized by assuming an 8 m/sec wind speed and a 1 cm daily zenith delay fluctuation. With the caveats noted in Section I, the dry fluctuation was normalized by assuming an 8 m/sec wind speed and a 3 mm daily zenith fluctuation. This daily fluctuation level was derived from a very limited set of barometric pressure data and should be more extensively studied. As can be seen in the figure, which represents a calculation for 20 degree elevations, the single-path fluctuation level is 4×10^{-14} sec/sec and 9×10^{-15} sec/sec for the wet and dry components respectively at 1,000 seconds. At 40 degree elevations, the wet and dry 1,000 second Allan standard deviations are 2×10^{-14} sec/sec and 6×10^{-15} sec/sec respectively. This average DSN value is roughly 1.8 times that derived from Very Large Array (VLA) data, if the same wind speed is used (Armstrong and Sramek 1982). The difference is probably due to the higher altitude of the VLA site.

III. METHODS FOR REDUCING THE EFFECT OF TROPOSPHERIC FLUCTUATIONS

One possibility for reducing the effect of tropospheric fluctuations is to design an observation or analysis strategy which can separate the tropospheric signature from the gravity wave signature. In the Treuhaft and Lanyi (1987) reference, expressions for the statistical properties of tropospheric fluctuations are given. If the statistics of the gravity wave signature are significantly different, an observation sequence and/or parameter estimation filter can be designed to estimate the level of gravity wave and tropospheric signature. A simple example of this approach is the detection of gravity waves from binary stars or black holes (Wahlquist 1987, Wahlquist this volume). In that case, the periodic signature of the gravity wave can be extracted by observing for long periods of time and averaging the signal.

If the signature of the gravity wave is unknown or highly correlated with the tropospheric signature (*i.e.*, if the gravity wave and troposphere have similar power spectra), external calibration techniques should be considered. The most obvious external calibration technique is water vapor radiometry. While theoretical estimates of WVR performance indicate that the Allan standard deviation of fluctuations can be calibrated to 1×10^{-16} sec/sec for 1,000 second intervals, the data which demonstrate this capability are scarce. WVR data were successful in calibrating Very Large Array (VLA) phase fluctuations for some of the data sets examined (Resch *et al.* 1984). But in the Resch reference, there were times when the application of WVR data increased the phase residual. Recent comparisons of VLBI data (Herring 1988) to WVR zenith estimates show low frequency discrepancies on the order of 1 to 2 cm. Similar conclusions can be drawn from GPS data (Tralli *et al.* 1988). It may be necessary to understand the nature of these discrepancies and how they apply to fluctuation calibration. In short, although WVRs seem promising, a data base

showing consistent reduction of VLBI or Doppler residuals by applying WVR calibrations is missing.

Another possibility for calibration of both wet and dry fluctuations is using GPS satellite path delays along lines of sight close to that of the spacecraft. It will be assumed that GPS geometric, ionospheric, and instrumental effects are perfectly calibrated and that tropospheric fluctuations are the only source of residual delay error. The degree to which this assumption applies must be investigated. From the schematic picture of Fig. 1, one expects that, as two lines of sight get farther apart, the time scales on which they will have substantial correlation will get longer. That is, if, during their traversal of the troposphere, the average distance between a GPS raypath and that of a spacecraft is d, then there will be differential cancelling between the delays of each signal for time scales greater than d/v where v is the wind speed. Fig. 3 shows the model calculation for the difference between spacecraft and GPS delay rates induced by the dry troposphere. The delay rate for the tropospheric power spectrum is about 20% higher than the Allan standard deviation. The figure shows the total rate and the differenced rate for 20 degree and 40 degree elevations. It was assumed that the GPS satellite was 20 degrees in azimuth from the spacecraft line of sight, at the same elevation. It can be seen that for longer time scales, there is indeed differential cancelling between the GPS and spacecraft lines of sight. In particular, for 20 degree and 40 degree elevations, the dry fluctuation can be reduced to the level of 6×10^{-15} sec/sec and 2×10^{-15} sec/sec respectively. Data from GPS satellites and VLBI or Doppler experiments would be necessary to test this approach.

A third instrumental possibility is to use multiple receiving antennas separated by distances greater than the wind speed times the time scale of interest. For example, to reduce the fluctuation on time scales greater than 1,000 seconds, antennas separated by more than 8 km must be used. The fluctuation effect in the average of all the Doppler signals would be reduced relative to that in a single antenna by approximately $1/\sqrt{N}$ where N is the number of antennas used. If, for example, 2 to 3 antennas at Goldstone were used with 4 to 5 antennas at the VLA, a factor of 2 to 3 reduction in fluctuation error might be realized.

IV. SUMMARY

The levels of wet and dry tropospheric fluctuations have been estimated with the aid of a fluctuation model. The single-path wet fluctuation signatures at 20 degrees and 40 degrees elevation are 4×10^{-14} sec/sec and 2×10^{-14} sec/sec respectively, for 1,000 second intervals. The dry signatures are 9×10^{-15} sec/sec and 6×10^{-15} sec/sec. The wet signatures are of the order of the plasma contribution to the gravity wave detection error budget for Galileo experiments (*e.g.*, Armstrong this volume and references therein), but both wet and dry contributions will have to be addressed for potential K-band experiments.

Methods for reducing the contribution of atmospheric fluctuations in the Doppler data include observation and analysis techniques, water vapor radiometry, GPS tropospheric monitoring, and observations with multiple antenna systems. The level of remaining 1,000 second dry fluctuations using GPS calibration along a line of sight 20 degrees from the Doppler spacecraft was estimated to be 6×10^{-15} sec/sec and 2×10^{-15} sec/sec for 20 degree and 40 degree elevations. It was assumed that WVRs could calibrate the 1,000 second wet fluctuation to approximately 1×10^{-16} sec/sec.

This assertion must be validated with data. The GPS technique for tropospheric calibration must also be tested. What is suggested, in this paper, is that it may be possible to reduce the total fluctuation effect to the levels quoted. Experiments are required to justify choosing one calibration scenario and adopting it for gravity wave Doppler experiments. Other possibilities such as barometric arrays for calibrating the dry component should also be investigated.

ACKNOWLEDGEMENTS

This work was performed at the Jet Propulsion Laboratory, under contract with NASA.

REFERENCES

Armstrong, J. W., and Sramek, R. 1982, *Radio Science*, **17**, 1579.
Armstrong, J. W. "Advanced Doppler Tracking Experiment" (this volume).
Herring, T. A. 1988, private communication.
Resch, G. M., Hogg, D. E., and Napier, P. J. 1984, *Radio Science*, **19**, 411.
Tralli, D. M., Katsigiris, E. C., and Dixon, T. H. 1988, *EOS*, **69**, 332.
Treuhaft, R. N., and Lanyi, G. E. 1987, *Radio Science*, **22**, 251.
Wahlquist, H. 1987, *General Relativity and Gravitation*, **19**, 1101.
Wahlquist, H. "Detecting Gravity Waves from Binary Black Holes" (this volume).

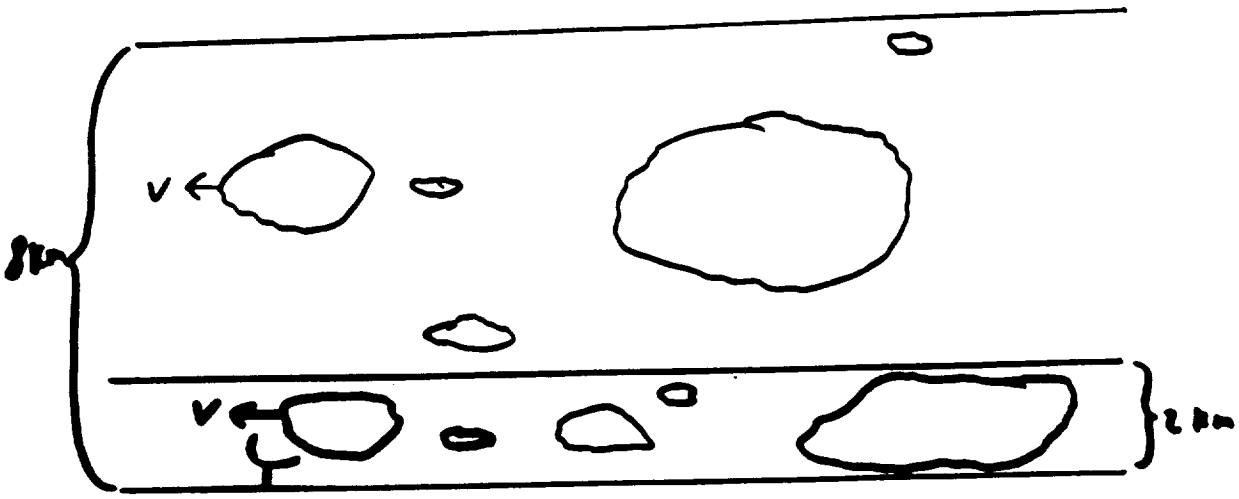

FIG. 1 — Schematic picture of the frozen flow model. The patches represent inhomogeneities in tropospheric refractivity, blown across a site with wind speed v. The 2 km and 8 km scale heights of the wet and dry tropospheres are indicated.

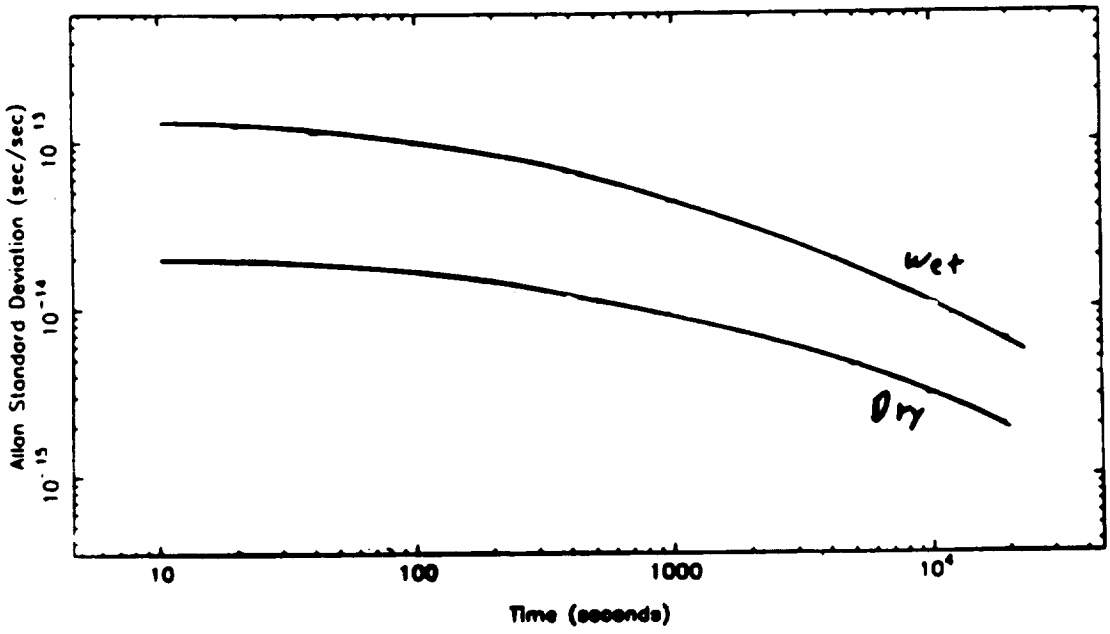

FIG. 2 — The model Allan standard deviation of the wet and dry tropospheres at 20 degrees elevation.

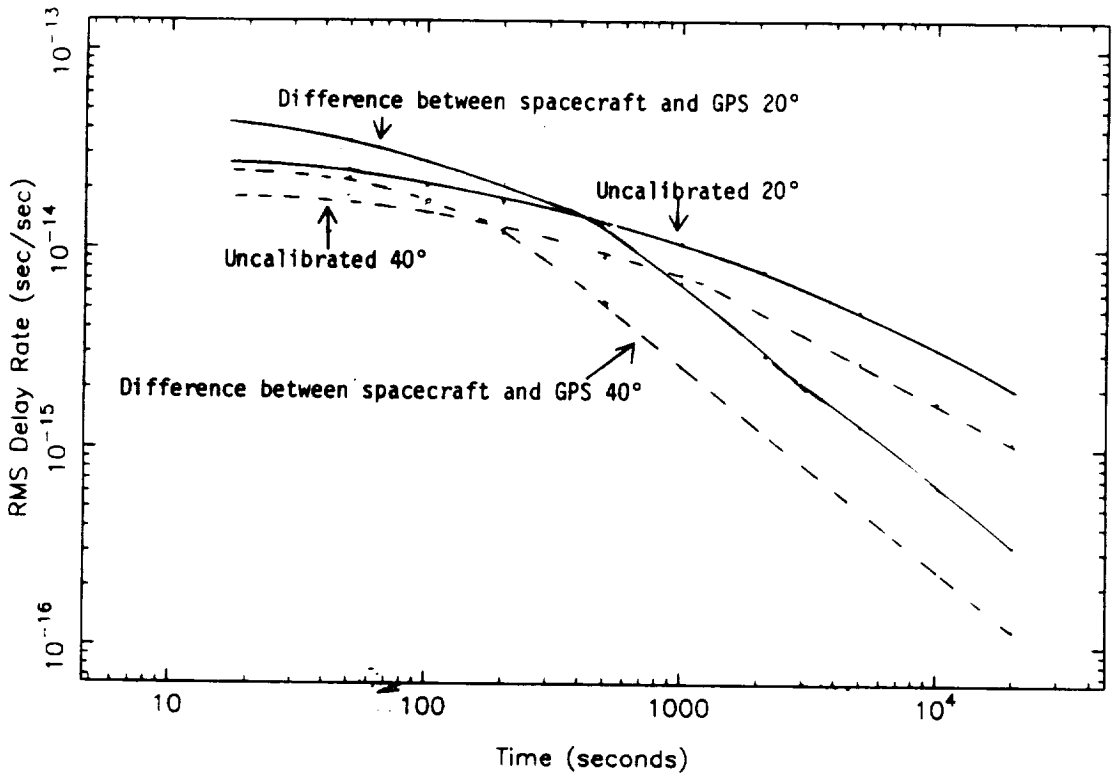

FIG. 3 — The model delay rate spectrum of the uncalibrated dry troposphere, and of the difference of the dry signature between the spacecraft and GPS lines of sight separated by 20 degrees in azimuth. The solid curves are for 20 degrees elevation and the dashed curves are for 40 degrees elevation.

DISCUSSION

BERTOTTI: You have mentioned the importance of correlating Doppler measurements at two different sites to reduce the tropospheric noise. I wish to report on a pilot experiment that will take place next month: the two Voyager spacecrafts will be tracked from Madrid (up and down) and from the VLBI station in Bologna, Italy (down) for eight passes. The correlation between the two Doppler signals will be measured.

SHAPIRO: Another method for troposphere calibration that would "work" (at a "useful" level) was conceived about two decades ago in the VLBI context: Horizontal arrays of long vertical tethers w/balloons at "well-spaced" vertical intervals on each tether, with each balloon instrument to measure relevant variables (temperature, relative humidity, pressure). This solution is, of course, horrendously expensive and would also pose a hazard to aircraft.

MALEKI: Do you mean that dispersion in the troposphere is identically zero at microwave wavelengths or is it too small to measure. If your answer is the latter, could you say how small it is?

TREUHAFT: I do not know the exact dispersion effect at X-band for water vapor. I believe it is a few orders of magnitude below 1 mm of delay. It should be checked. (Shapiro agreed with this qualitative assessment).

MATZNER: I'd like to point out that there is another method to probe the troposphere. This is atmospheric SONAR. This technique samples the lower few hundred meters of the atmosphere. It is being used, for instance, at Bell Laboratories to understand radio propagation through the atmosphere. Since the SONAR is responsive to density inhomogeneity, it presumably provides information in a linear combination of wet and dry contributions.

TREUHAFT: We would need density inhomogeneity information for altitudes greater than a few 100 meters, but SONAR is worth investigating. I should point out that gravity wave experiments at K-band will require extremely high precision tropospheric monitoring. So any technique which might work must be scrutinized for its ultimate accuracy, which would have to be at about 10^{-16} sec/sec at 1000 seconds to be useful.

A REVIEW OF ATOMIC CLOCK TECHNOLOGY, THE PERFORMANCE CAPABILITY OF PRESENT SPACEBORNE AND TERRESTRIAL ATOMIC CLOCKS, AND A LOOK TOWARD THE FUTURE

ROBERT F. C. VESSOT
Smithsonian Astrophysical Observatory
Cambridge, MA 02138

I. INTRODUCTION — A REVIEW OF ATOMIC CLOCK TECHNOLOGY

Clocks have played a strong role in the development of general relativity. The concept of the "proper clock" is presently best realized by atomic clocks, whose development as precision instruments has evolved very rapidly in the last decades. To put a historical prospective on this progress since the year AD 1000, Figure 1 shows the time stability of various clocks expressed in terms of seconds of time error over one day of operation. This stability of operation must not be confused with accuracy. Stability refers to the constancy of a clock operation as compared to that of some other clocks that serve as time references. Accuracy, on the other hand, is the ability to reproduce a previously defined frequency.

Table 1 outlines the issues that must be considered when we talk about accuracy and stability of clocks and oscillators. The late I. I. Rabi and J. R. Zacharias, in their work with atomic and molecular beams, were the first to realize that atoms were capable of being used as clocks, and N. F. Ramsey's invention of separated oscillatory fields made possible the first practical cesium clocks. In general, the most widely used resonances result from the hyperfine interaction of the nuclear magnetic dipole moment and that of the outermost electron, which is characteristic of hydrogen and the alkali atoms. During the past decade hyperfine resonances of ions have also been used, as will be seen later. Figure 2 shows, as an example, the hyperfine structure of ^{87}Rb with nuclear spin I = 3/2, $\nu_o = \Delta W/h = 6.834GHz$. Here $\Delta W = h\nu_o$ is the hyperfine separation energy and h is Planck's constant. The principal reason for both the accuracy and the stability of atomic clocks is the ability of obtaining very narrow hyperfine transition resonances by isolating the atom in some way so that only the applied stimulating microwave magnetic field is a significant source of perturbation. It is also important to make resonance transitions among hyperfine magnetic sublevels where separation is independent, at least to first order, of the magnetic field. In the case of ^{87}Rb, shown in Figure 2, this transition is between the F = 2, $m_F = 0$ and F = 1, and $m_F = 0$ hyperfine levels. In the case of ions stored in traps operating at high magnetic fields, one selects the trapping field to be consistent with a field-independent transition of the trapped atoms.

a) Detecting Atomic Transitions

Several techniques are used to detect the transitions in the hyperfine levels of atoms (or ions) so that information can be obtained to control the frequency of signal applied to the atoms or ions. The original technique is based on molecular beam apparatus where the linewidth of the atom was narrowed by extending the distance over which the microwave field is applied. The presence or absence of transitions is determined by the change in the effective dipole moment of atoms, which is observed by changes in the trajectory of atoms when they travel through highly inhomogeneous magnetic fields.

TABLE 1

CONCEPTS OF ACCURACY AND STABILITY

ACCURACY	STABILITY
• DEPENDS ON CONTROL AND UNDERSTANDING OF SYSTEMATICS	• A STATISTICAL CONCEPT allan variance <-----> SPECTRA
• VERY NARROW LINEWIDTHS	• A QUESTION OF NOISE/SIGNAL RATIO
• HIGH TRANSITION FREQUENCY	$\sigma(\tau) \propto \frac{1}{Q_{line}} \frac{\text{NOISE POWER}}{\text{SIGNAL POWER}}$
• WELL DETERMINED OFFSETS	$\sigma(\tau) \propto K \tau^{-1/2}$
• LOW LEVEL PERTURBATION FROM AMBIENT EFFECTS	• WE MUST NOT IGNORE NOISE OUTSIDE THE ATOMIC SYSTEM (e.g., receivers)

• ACCURACY CAPABILITY IS LIMITED BY THE STATISTICAL COMBINATIONS OF ALL UNCERTAINTIES

OBVIOUSLY - TO REALIZE *ACCURACY* CAPABILITY WE MUST ALLOW

ENOUGH AVERAGING TIME TO DEVELOP *STABILITY*, AND THIS TIME PERIOD

MUST BE COMPATIBLE WITH THE EXPECTED TIME VARIATION OF

SYSTEMATIC PERTURBATIONS.

In the case of masers and lasers we observe the microwave signal or the light that is coherently generated by an aggregate of stored atoms (or ions) undergoing self-stimulated transitions from regeneration or reflection of energy in a cavity (or between mirrors in the case of lasers). In the case of hydrogen masers, the signal is the familiar 21cm line of radio astronomy. This very low per signal (-100dBm) at 1,420,405,751.768Hz, is amplified and is used with synthesizers to control the phase of a 100MHz voltage-controlled, crystal oscillator.

In the past decade, with the advent of lasers that can be tuned to optical transitions involved in these "clock-like" ions and atoms, it has been possible to change the distribution of the population in the hyperfine levels by selectively emptying the unwanted hyperfine ground state levels of atoms (or ions) by "pumping" these atoms to higher energy states. This technique, which was pioneered by Kastler and Dehmelt in the 1950's, also allows several useful possibilities for very sensitive detection of hyperfine transitions made by the application of microwave signals.

In summary then, we presently use three methods to detect the transitions: 1) we can observe the energy of transition; 2) we can observe a change in atomic dipole moment; and 3) we can observe, by optical methods, whether or not atoms have made

transitions by exciting optical transitions from the selected ground state hyperfine levels to higher states and observing this process by monitoring either the absorption of the exciting light or the fluorescence of the atoms making spontaneous transitions from the upper state back down to a lower energy state.

b) The Quest for Narrow Resonances

Resonance linewidths of transitions depend on the length of time we can observe the atoms or ions in a relatively unperturbed manner. This essential feature of all atomic clocks has been a major focus of attention in the development of atomic clocks. Historically, the development began with atomic beams and cesium beam devices that have been in production commercially since the 1950's. The success of the cesium clocks led, in 1967, to the adoption of the hyperfine transition to Cesium 133 as the basis for the definition of the second. The second was defined as 9,192,641,770 periods of oscillation of the ground state hyperfine transition of ^{133}Cs. In 1983, the meter was defined in terms of the velocity of light as the distance light travels in 1/299,792,453 of a second. This makes possible a permanent value for ε_o, the permittivity of free space in the SI system, where the velocity of light is given as $c = (\mu_o\varepsilon_o)^{-1/2}$. (The SI value of μ_o has always been exactly $4\pi \times 10^{-7}$.)

Atomic beam devices depend on the time of flight atoms across the microwave interaction region. Even when low velocity atoms in the beam are selected, this type of apparatus in the primary standards laboratories is generally a few meters in length. Commercially available cesium beam devices are much shorter but still some 25cm in length. Figure 3 is a schematic sketch of a cesium beam tube resonator.

In the mid-1950's Dicke, Bender, and Carver found that alkali atoms could be immobilized in a glass cell filled with gas to buffer the atoms' thermal motion. Combinations of nitrogen and various inert gases can be chosen to reduce the temperature coefficient of the hyperfine resonance line of atoms when they are subject to collisions with buffer gases. This line-narrowing technique, in combination with optical pumping, led to the development in the late 1950's of commercially available rubidium gas cell devices and has since led to a very high level of production of rubidium gas cell standards with performance much superior to crystal controlled oscillators and very well suited to hostile vibration environments. These are small, lightweight, and frugal in their power requirements.

In 1960, Kleppner, Goldenberg, and Ramsey invented a storage technique that would work with atomic hydrogen, which led to their invention of the hydrogen maser. The heart of the maser is a quartz, Teflon-lined storage bottle, located in the uniform magnetic field region of a cavity resonator. Atoms enter, at thermal velocities of about 2×10^5 cm/sec, through a small hole, rattle about inside the bottle, and randomly emerge through the same hole. A storage time of about 5 seconds can be achieved with spherical bulbs having a volume of about 3 liters before oscillation is inhibited by wall collision effects that recombine the atoms or dephase the oscillating hyperfine interaction of the atoms. The dephasing effect is also accompanied by an average phase retardation per collision, which produces a wall collision frequency shift in the output signal. This frequency shift depends on the collision rate of atoms with the wall surface, and hence on the surface texture, which, though stable over time, varies from bulb to bulb depending on how it is coated. In our experience, the variability can be as large as 5 parts in 10^{13}. This lack of reproducibility limits the usefulness of the hydrogen maser as a primary standard.

The variability of the wall shift and the nature of hydrogen interactions with surfaces of various materials is the subject of ongoing study at SAO.

Another method of storage involves the use of ions in two forms of electromagnetic traps. The Penning trap uses a strong, static, magnetic field and an electrode configuration as shown in Figure 4. The residual motion of the ions have two basic frequencies. One is associated with the cyclotron motion of the ion in the magnetic field, the other with the electrostatic fields generated by the electrodes. The Paul traps, shown in Figure 5, works with a superposition of static and oscillating electric fields. This trap has been successfully used in a frequency standard of extraordinary long-term stability, which will be described later.

With the advent of tuneable lasers, it has become possible to use the momentum of absorbed optical photons as a means of slowing down a beam of atoms. The scheme is shown in Figure 6, where atoms (or ions) are shown entering from the left and a laser beam is shining on the atoms from the right. By tuning the light from the laser to be lower in frequency than the optical transition frequency of the atoms (or ions) by an amount equal to the Doppler shift owing to their motion, they will absorb the photons, and in so doing, undergo a change in the momentum of their motion. They reradiate the absorbed energy in random direction and later can reabsorb further energy from the directed beam of photons and, again radiate it; the process continuing many thousands of times for each atom. The result is to slow the atoms (or ions) down to the velocity of recoil of its randomly emitted photons. In the case shown in Figure 6 for magnesium 25, the atoms are slowed down, or cooled, to a kinetic temperature of 0.05K. It is possible to go even further with this process and to stop atoms or even to reverse their direction! Figure 7 describes a technique for slowing atoms, where the resonance frequency of the atoms is progressively Zeeman-shifted along the beam by the applications of a spatially varying magnetic field, which shifts the energy levels of the moving atoms to keep their resonance in tune with the laser beam and thus continue to absorb energy. Another method that has worked with *both* atoms and ions is to modulate the laser frequency so that groups of atoms, which have Doppler frequencies that follow the modulation, are retarded.

II. THE CURRENT STATUS OF ATOMIC CLOCKS - FREQUENCY STABILITY (1987-1988)

In the past 3 decades there has been an actively continuing program of atomic clock development, and it is, therefore, a bit risky to give an accurate portrayal of the situation at any point in time. Figure 8 is the writer's latest effort at putting together a picture of the frequency stability of a number of clocks (or oscillators) in terms of the Allan variance. The Allan variance, $\sigma(\tau)$, is a measure of the one-sigma value of the fractional frequency departure between pairs of adjacent frequency measurements, each of duration τ. The behavior of $\sigma(\tau)$ with τ depends on the spectral distribution of the frequency (or of the phase) fluctuations in the signal from the clock.

At the upper right of the figure is the Allan variance representation of a celestial clock — the millisecond pulsar. The variance data are made from the residuals of the frequency measurements after removing a linear drift rate of 9.07 parts in 10^{15}. As more and more data accumulate, and as more of these clock-like objects are discovered, I become increasingly sure that a very powerful timing

resource for testing general relativity and for studying cosmology will become available.

Below the pulsar line is a line representing the specification for spaceborne clocks used in the United States Global Positioning System (GPS), which is used for worldwide navigation and time transfer. to the left of the GPS specification are the specifications used to define the performance of small commercially available rubidium gas cell standards and commercially available cesium beam standards. Near to this line is performance observed from recently developed cesium beam clocks qualified for spaceborne use that have been developed and built by Kernco, Inc., Danvers, Massachusetts.

The performance of two newly developed clocks, that have been developed with the intention of eventual use in space, is shown below the GPS specification. Of these, upper trace is the Allan variance of the EG&G (Salem, Massachusetts) rubidium gas cell frequency standard with, and without, removal of its frequency drift. Slightly below the EG&G, rubidium gas cell data are data made from a small hydrogen maser developed by the Hughes Research Laboratory in Malibu, California. This maser operates with a very small storage volume located within a capacitively loaded resonator of small dimensions. In order for this system to oscillate, the quality factor, Q, of the resonator is enhanced by external amplification and feedback.

To the right of, and slightly below these new space clocks, is an estimate of the day-to-day to month-to-month variation of the international atomic time scale, TAI, at an Allan variance level slightly below 1 part in 10^{14}.

Below the TAI line is a very long plot that describes the behavior of the relative stability of two ^{199}Hg trapped-ion clocks, developed by Hewlett Packard by Cutler and his associates. These are located at the U.S. Naval Observatory in Washington, D.C. These clocks use the 40.5 GHz transition in the ground state of singly ionized mercury 199 atoms in a Paul trap. The residual motion of the cloud of trapped ions is cooled by collisions with helium gas admitted into the trap at pressure of about 15^{-5}Torr. This cools the atoms from a kinetic temperature of about 6000K to about 300K. The undisturbed lifetime of the atoms in the trap is about 40 minutes. The magnitude of the second-order Doppler frequency shifts, owing to the residual motion shown in Figure 4, is about 2 parts in 10^{12}; predictable to about 2 parts in 10^{13}. This is presently thought to be the major source of inaccuracy of these remarkably stable clocks.

The lowest trace shows the behavior of hydrogen masers (in this case the VLG series masers built by SAO), of the 23 which have built; 21 are in operation in observatories and tracking stations worldwide. A spaceborne version of this maser was developed and flown in the 1976 redshift test, and the design of this maser is presently being revised for long-terms (70 year operation in space. This maser's stability reaches a best value of about 4 parts in 10^{16} at about 10^3 seconds. For longer periods, the stability is degraded chiefly by systematic variations caused by thermal perturbations and by a very slow monotonic increase in the cavity resonance frequency.

Figure 9 shows a cross-section of the redeveloped SAO hydrogen maser for spaceborne use. This maser, since it has the same design parameters as the VLG masers, is expected to have comparable stability.

The dimensions, weights, and power requirements for these spaceborne clocks are summarized in Table 2.

TABLE 2

SIZE, WEIGHT AND POWER CONSUMPTION OF SPACEBORNE CLOCKS

	DIMENSIONS	WEIGHT	POWER
EG&G Rubidium Gas Cell Standard	11.3 x 21.2 x 17.5	4.5	13
Kernco Cesium Beam GPS Standard	20.3 x 3.3 x 38	12.2	27
Hughes Hydrogen Maser under Development	32.8 x 22.6 x 58.9	23	50
SAO Hydrogen Maser under Development	421cm. dia x 85.3	44	50

III. TRENDS OF DEVELOPMENT FOR FUTURE CLOCKS

The advent of tuneable lasers and the application of modern, low-temperature techniques have provided the stimulus for a number of fundamental changes in clock technology. It is now possible to change the states of atoms selectively and make more efficient use of atomic beam techniques. For example, in the cesium beam frequency standard shown schematically in Figure 3, only one of the 16 hyperfine magnetic sublevels is used to operate the clock. The others are scavenged away by cesium "Getters." Furthermore, the magnetic state selecting system will only deflect a narrow range of velocities. The resulting efficiency in the use of atoms is very small: only a few percent. The first magnet can be replaced by laser-induced transitions that pump nearly all the atoms into the desired $F = 4$, $m_F = 0$ transition. While the microwave interaction region can remain the same, the detection of the presence (or absence) of microwave transitions again can be done using the laser to pump atoms that have made "clock" transitions to the $F = 3$, $m_F = 0$ to an upper energy state. The presence (or absence) of such atoms is detected by observing the optical fluorescence of transitions back to the ground state. Besides improving the efficiency of flux usage and so improving the signal-to-noise ratio in cesium beam standards, and hence their stability, these laser techniques also make possible a substantial improvement in their accuracy. The second-order Doppler frequency correction is difficult to determine in the distribution of velocities of the beam in the present magnetically state selected primary frequency standards and this causes the principal source of uncertainty in the error budget that defines accuracy capability. Using laser techniques, there is very little disturbance in the easily predicted velocity distribution of the beam and the Doppler correction is far more accurately determined.

Better state selection techniques, using permanent magnets, are also available for atomic hydrogen masers. Normally the maser is operated with a single hexapole (or other multipole) magnet which focuses both the $F = 1$, $m_F = 0$ and $+1$ hyperfine sublevels of ground state atomic hydrogen into the storage bulb of the maser. The

inclusion of the unwanted F = 1, m_F = +1 state essentially doubles the population of atoms, the interatomic collision rate and, consequently, the rate of spin-exchange quenching of the oscillation. Not only is the storage lifetime adversely affected, systematic frequency shifts will result if collisions occur among atoms that are not symmetrically distributed among the F = 1, m_F = +1 and -1 states. Changes in the population of these states can result from changes in the magnetic field seen by the beam as it travels from the magnet to the storage bulb and, in practice, this sensitivity to ambient magnetic fields is far more serious than the residual second-order magnetic field shifts in the F = 1, $m_F = 0 \rightarrow F = 0$, m_F = 0 transition that are very well attenuated by magnetic shields surrounding the maser cavity-interaction space.

It is possible to eliminate the unwanted F = 1, m_F = +1 state by using adiabatic fast passage (AFP) technique to the population in the F = 1 manifold as shown in Figure 10. The beam is then refocussed into the maser bulb by a second magnet twice the length of the first. The inversion is performed by a combination of r.f. and d.c. fields applied to the beam as it passes through the "AFP region" shown in the figure. We are using this new state selection system in a new design of SAO maser.

Another program underway at SAO is research with an atomic hydrogen maser operating at temperatures below 1K using superfluid liquid helium to coat the surfaces of the hydrogen storage volume. So far, three groups of researchers have operated such masers: at MIT, at the University of British Columbia, and at Harvard/SAO. The maser technique allows extremely high precision measurements to be made of low-temperature, hydrogen-hydrogen, hydrogen-helium interactions both in the gas and in the storage vessel and on the surfaces of the storage vessel. From the viewpoint of clock technology, there appears to be an excellent possibility of producing signals with stability in the 10^{-18} region because of the combined benefits of the following low-temperature effects:

(1) The intrinsic storage time is hours in duration;

(2) Thermal noise, kT, per unit bandwidth is reduced;

(3) Both the collision cross-section and the velocity of the hydrogen atoms are smaller (the effective collision rate is reduced by a factor of about 500 so higher power can be obtained in the master output);

(4) Magnetic problems can be very effectively reduced using superconducting shields; and

(5) The stability of components is much better at low temperatures.

Figure 11 shows the stability expected from the SAO AFP maser and the cryogenically cooled maser.

In the fields of trapped ion standards using laser technology, the projected improvements expected by the Time and Frequency Research laboratory at the Jet Propulsion Laboratory is shown in Figure 12. The improvements shown are for Mercury 199. Work on a trapped ion system using Mercury 201 is in progress at the National Bureau of Standards and the expected stability of this device is shown by the dashed line.

The use of superconducting cavity resonators makes possible superb "fly wheel" oscillators to replace the presently used crystal-controlled oscillators. The combined stability of such an oscillator, locked to a mercury ion resonator with a lock loop time constant of about 1 hour, is shown in the heavy bottom line of Figure 12.

IV. CONCLUSION

One way to assess the potential usefulness of clocks in tests of relativity and gravitation is to express their performance in terms of the limits of their performance on measurements of velocity, distance, and angle. The stability of present (1988) hydrogen masers is shown as the plot labelled $\sigma_y(\tau)$ in Figure 13. Beneath it is another plot labelled $\sigma_{\Delta\tau}(\tau) = \tau\sigma_y(\tau)$, which is the one-sigma expectation of the time error in the next (figure) adjacent time interval, also of duration τ. The inner, right hand, vertical axis measures $\sigma_{\Delta\tau}(\tau)$.

In the case where we use electromagnetic signals to measure distance, the time error $\sigma_{\Delta\tau}(\tau)$ is readily converted to distance error by multiplying by the velocity of light. The right hand outer scale is such a measure of distance error. For example, if we continuously track a space vehicle, the clock-induced error in position expected between tracks made of 10^3 second duration, is about 3×10^2cm (or 0.3mm) with existing hydrogen masers. The one-sigma precision of range-rate measurements made during adjacent measurements of 10^4 second duration is about 1.8×10^{-5}cm/sec.

Angular resolution depends on the capability of time correlating the arrival of signals at both ends of a baseline of known length L (which can also be measured using time signals). The one-sigma resolution of angular measurements made τ seconds apart, is given by

$$\sigma_{\Delta\theta}(L,\tau\theta) = \frac{C\sigma_{\Delta\tau}(\tau)}{L_{\sin\theta}} \quad ,$$

where θ is the angle between the baseline and direction of the signal. For $\theta = \pi$, and a 3,000km baseline (intercontinental distances), $\sigma_{\delta\theta}(L, \tau,\theta) = 6 \times 10^{-14}$ radians. (This, of course, is not realized in terrestrial Very Long Baseline Interferometry owing to tropospheric and other systematic effects.) It is clear that, to realize this precision of measurement, the signal transmission paths both within the tracking station, and beyond its antenna must be free of phase perturbation. A measure of earth's tropospheric and 2 GHz ionospheric perturbation is shown in Figure 14 in terms of the Allan variance. The Ionospheric and tropospheric noise is shown by black dots labelled (a). These data were made during the 1976 SAO/NASA GP-A redshift experiment, using the 4-stage Scout Rocket system with a near-vertical trajectory going to 10,000 Km. altitude.

The ionospheric and tropospheric noise was removed by a 3-link Doppler cancelling system. The frequency residual after removing the predicted gravitational and relativistic effects for the entire 2-hour mission are shown in plot (b). The solid line in plot (b) is the Allan variance of the two ground-based masers used in the experiment. It is clear that the stability comparisons between the space and earth clocks and the two earth clocks are nearly the same and that the Doppler cancelling system is very effective at removing the combined propagation effects of the atmosphere, ionosphere, and rapidly ongoing path distance.

Future systems will best be operated from spaceborne terminals or space stations and will not be subject to earth's environment. Spaceborne clocks, with cryogenically operated masers or superconducting cavity oscillators, will make possible measurements one to two orders of magnitude more precisely than are shown in Figure 14. The present progress in spaceborne cryogenics is very encouraging. I believe that the most challenging future applications of ultra-high stability oscillators will be in cryogenically-cooled spaceborne systems involved in measuring relativistic and gravitational effects.

REFERENCES

Gerber, E.A., and Ballato, A. (eds.) 1985, *Precision Frequency Control*, Vol. 2, *Oscillators and Standards*, Academic Press, Inc.

Vanier, J., and Audoin, C., *Quantum Physics of Atomic Frequency Standards*, I.O.P. Publishing Limited, Adam Hilger, London, In press.

DISCUSSION

MALEKI: Let me comment on the mercury 199 clock. The HP clock has the dimensions Bob mentioned -- this is an effort to develop a mercury ion standard at JPL, and we expect our device would have dimensions of 50 cm x 50 cm x 50 cm when fully developed.

SHAPIRO: For the Hg 199 clock made by Hewlett-Packard, what are its physical dimensions and its present cost for an R&D model?

VESSOT: Two 6' racks. $600K +. I talked to Dr. G. M. R. Winkler of the USNO and his comment was: Present state does not allow uninterrupted operation for more than 6 months. No useful short term stability--only useful for 1-10 days of averaging. Used as prototype with an H maser as flywheel for day to day usefulness. "We must have a 10 day stable flywheel" for this system to be useful.

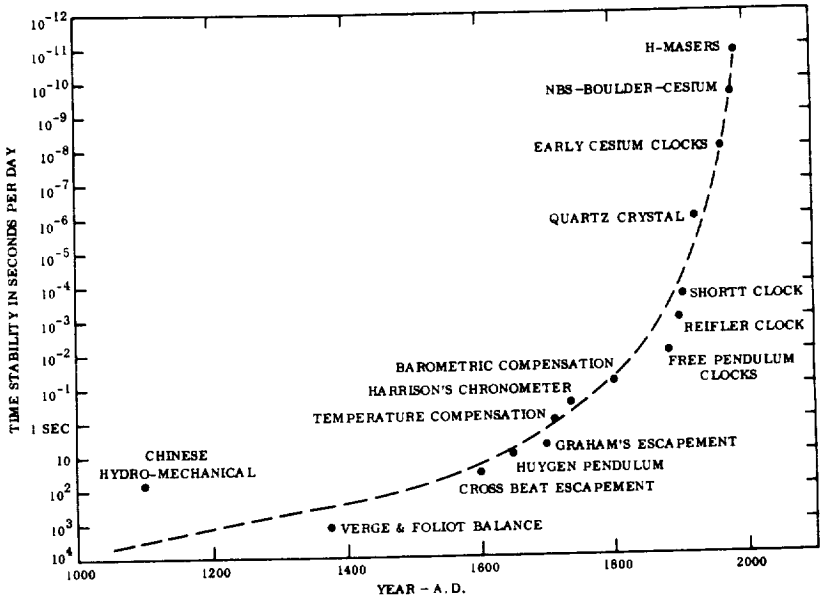

FIG. 1.—Performance of various clocks since 1000 AD

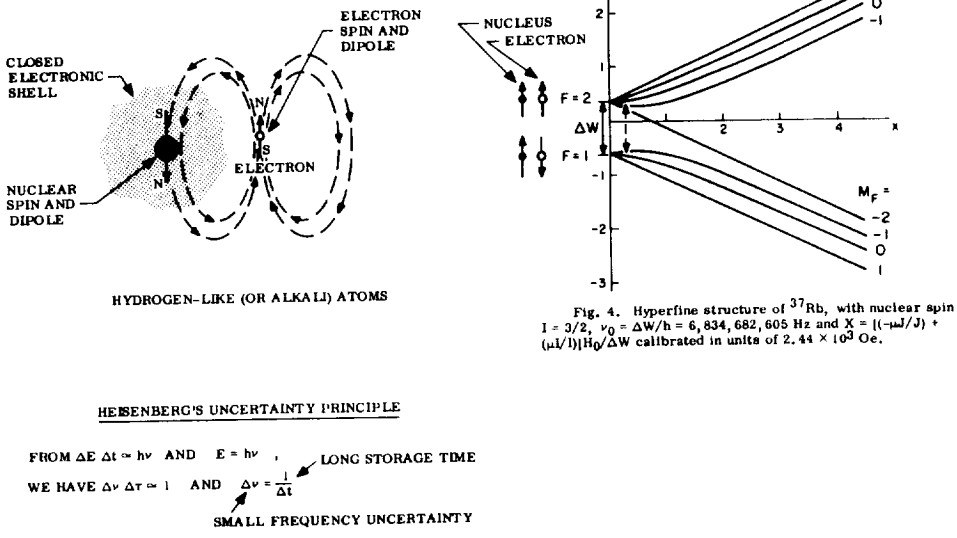

Fig. 4. Hyperfine structure of ^{37}Rb, with nuclear spin $I = 3/2$, $\nu_0 = \Delta W/h = 6,834,682,605$ Hz and $X = [(-\mu_J/J) + (\mu_I/I)]H_0/\Delta W$ calibrated in units of 2.44×10^3 Oe.

FIG. 2.—The hyperfine st ructure of a typical alkali atom

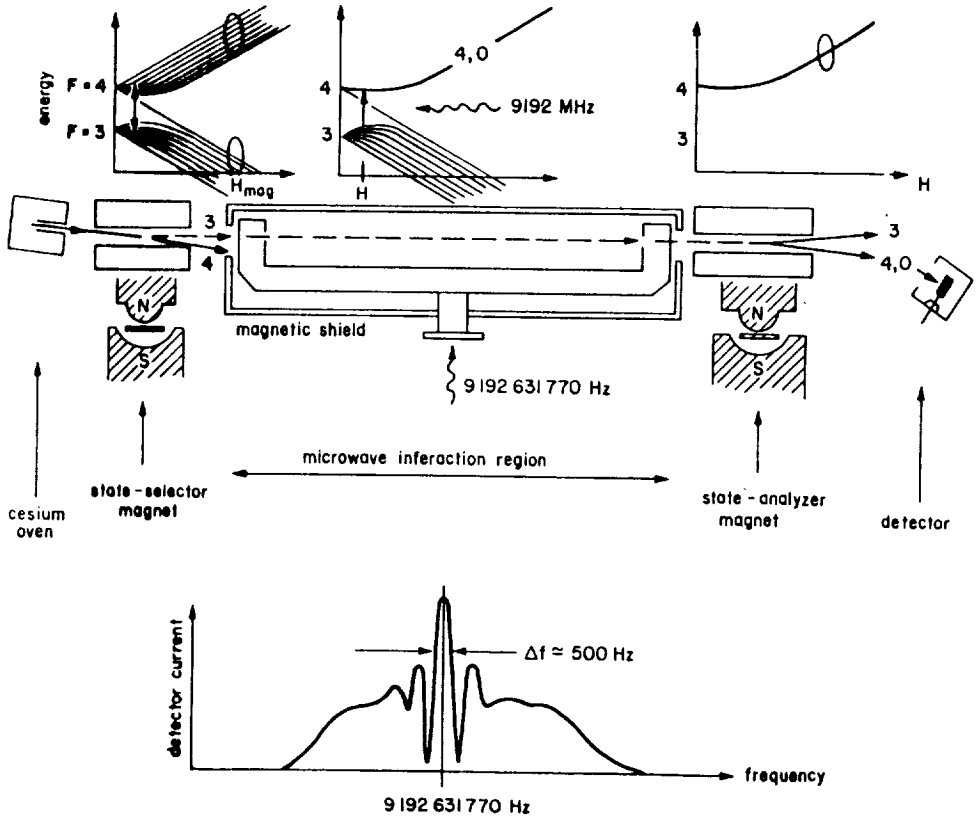

FIG. 3.—Schematic sketch of a cesium beam tube and the hyperfine structure of Cesium 133

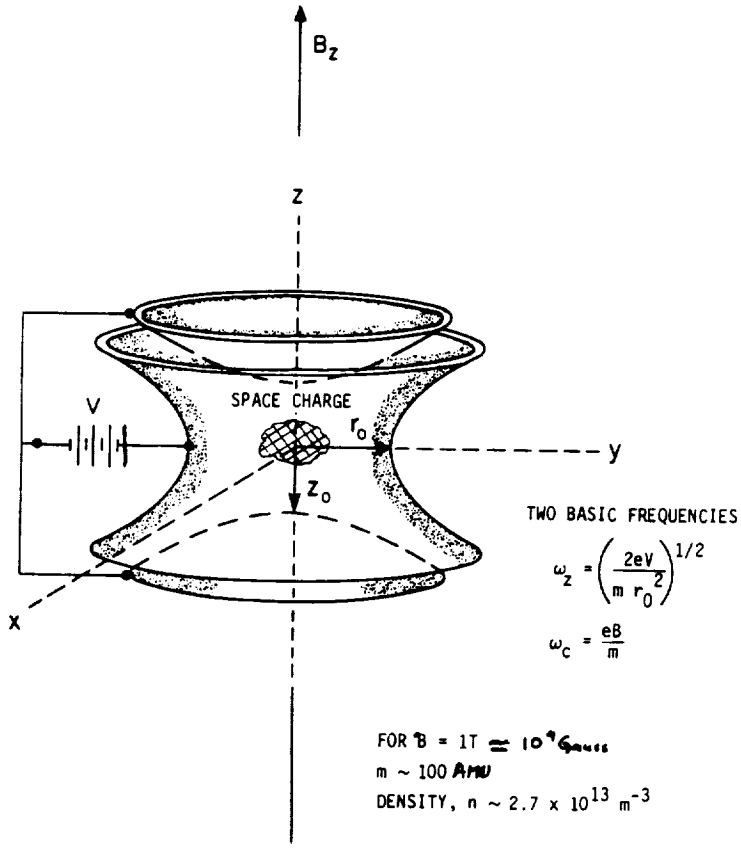

FIG. 4.—The Penning trap

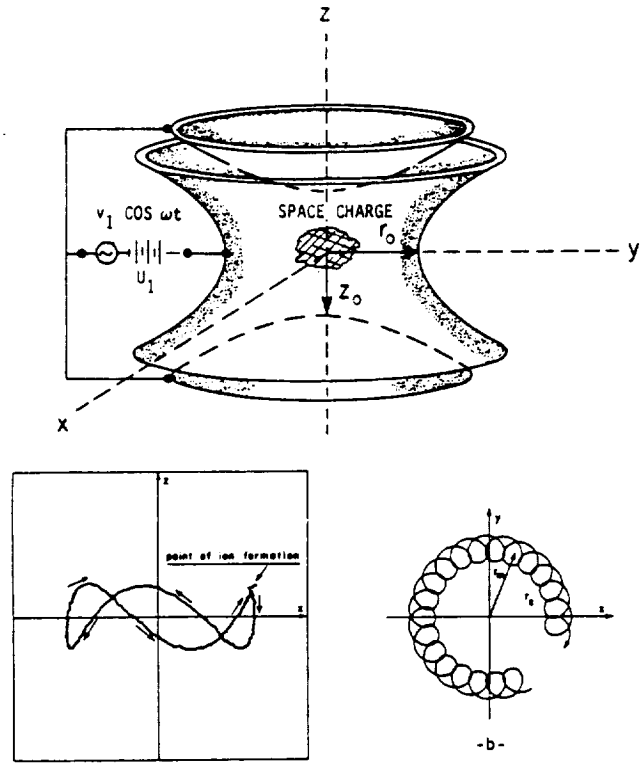

EXAMPLE FOR $^{199}Hg^+$ IONS: POTENTIAL WELL DEPTH ~ 10-30 eV
UNCOOLED SECOND-ORDER DOPPLER $\Delta f/f \sim 5.4 \times 10^{-13}$ (eV)$^{-1}$
TYPICALLY, KINETIC ENERGY IS 10% OF WELL DEPTH

FIG. 5.—The Paul trap

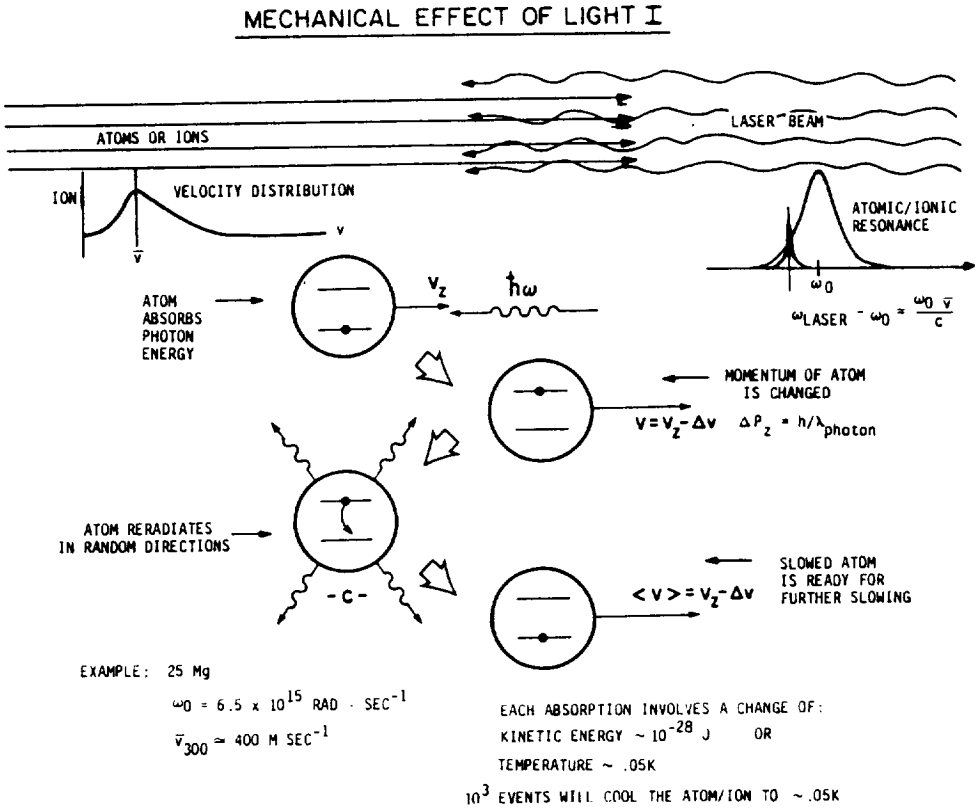

FIG. 6.—Slowing of atoms or ions by absorption of resonant radiation from a beam of light emitted by a laser.

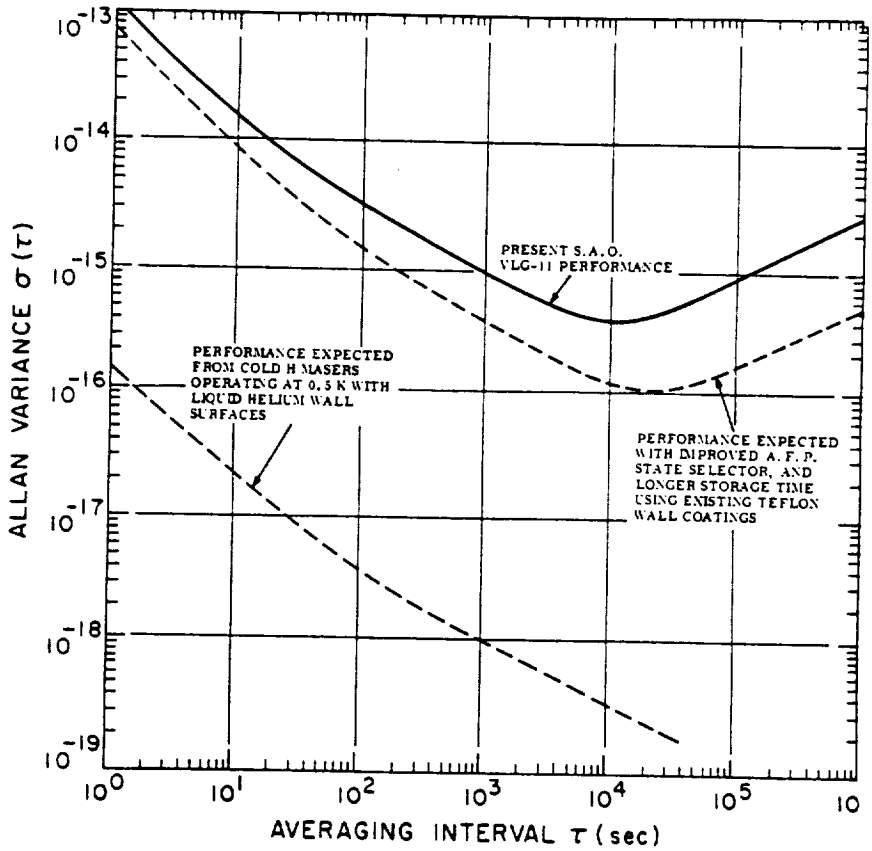

FIG. 11. – Stability expected from the SAO room temperature AFP maser with liquid helium storage container surfaces.

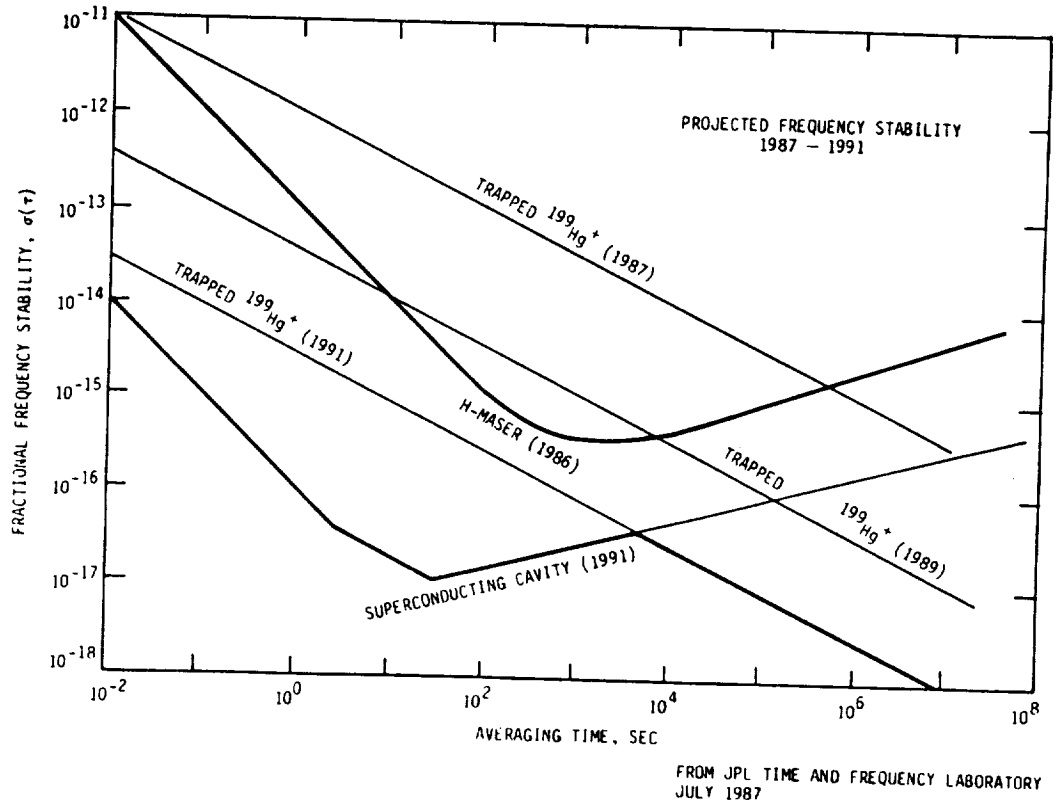

FIG. 12. – Frequency stability projections for trapped ion frequency standards and superconducting cavity stabilized oscillators.

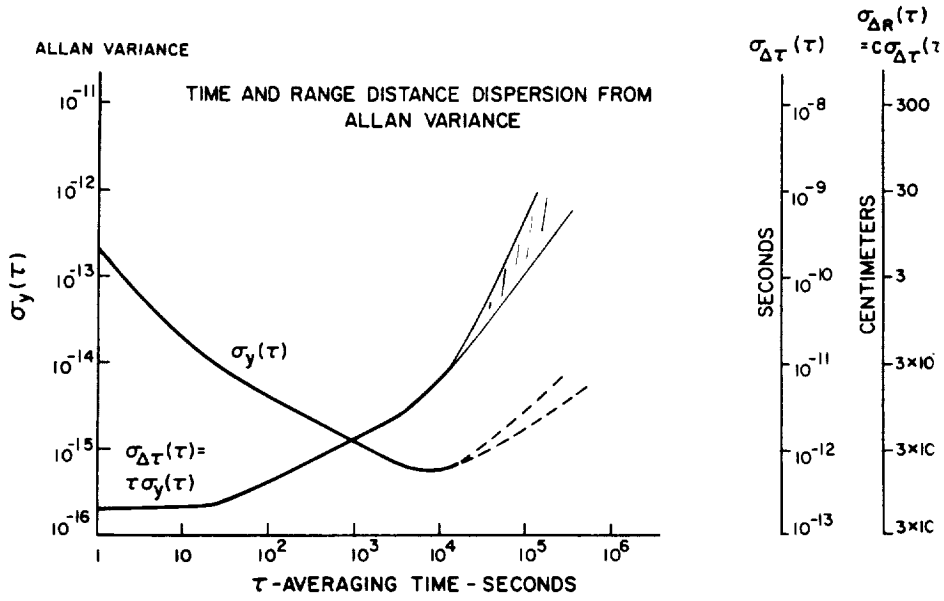

FIG. 13. – Atomic clock range and time error contributions to measurements made using electromagnetic signals.

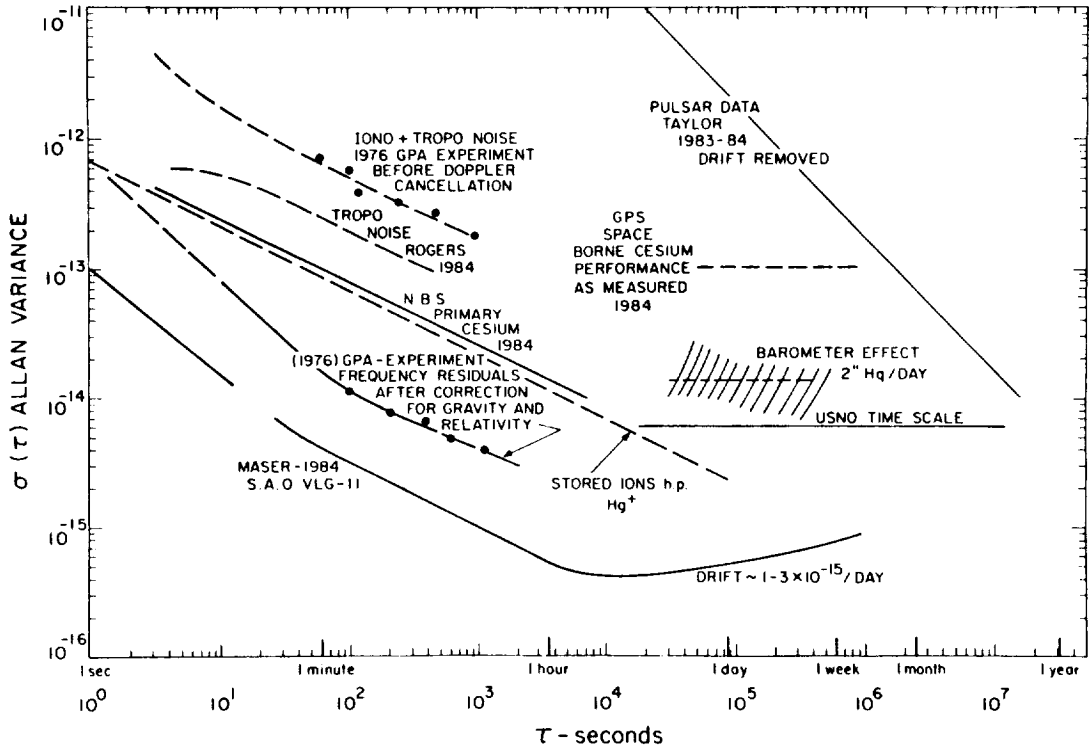

FIG. 14. – The effects of ionospheric and tropospheric fluctuations in earth-to-space signals at 2.2 GHz compared to hydrogen maser stability.

IMPROVED RANGING SYSTEMS

LARRY E. YOUNG
Jet Propulsion Laboratory

I. INTRODUCTION

Spacecraft range measurements have provided the most accurate tests, to date, of some relativistic gravitational parameters, even though the measurements were made with ranging systems having error budgets of about 10 meters (in *Relativistic Gravitation*). The thesis of this paper is that technology is now available to allow an improvement of two orders of magnitude in the accuracy of spacecraft ranging. The largest gains in accuracy result from the replacement of unstable analog components with high-speed digital circuits having precisely known delays and phase shifts.

II. ERROR SOURCES

Ranging instrumentation consists of a ground site transmitter, a spacecraft transponder (which receives the uplink ranging signal and coherently transmits a downlink), and a ground receiver which determines the time interval between uplink transmission and downlink reception. The time interval consists of the round trip, (vacuum) light travel time plus instrumental and media delays. The estimated magnitudes of some important error sources for the current ranging system, as well as for the proposed future system, are shown in the table below.

TABLE 1

ESTIMATED MAGNITUDES OF ERROR SOURCES

ERROR SOURCE	TODAY (TYPICAL)	FUTURE (+10 YEAR)
S/C Transponder Delay Change	500 cm	3 cm
Interplanetary Plasma	100 cm (X Up, S/X Down)	1 cm (Dual Up/Down)
Ionosphere	100 cm (4 cm IF GPS ION CAL)	1 cm (Dual Freq)
Tropospheric Delay	12 cm	0.5 cm
Antenna Multipath (SC and Ground)	50 cm	1 cm
Antenna Microwave Delay	30 cm	3 cm
GND Ranging Instrument (Random + Systematic)	100 cm	1 cm
Ground Frequency Standard	3 cm (5×10^{-15} Over 6 Hr)	<1 cm
Sta. Loc. & Earth Orient.	30 cm	3 cm
RSS of 2 Way Range Errors	533 cm	6 cm

III. REDUCTIONS OF ERROR IN FUTURE SYSTEMS

The above errors result from measuring and mapping media delays and from instrumental errors. The plasma mapping errors can be greatly reduced through the use of dual frequency transmissions for both uplink and downlink signals. Techniques have been suggested to reduce the tropospheric delay errors to the sub-cm level (Treuhaft 1988). Adequate improvements in the calibration accuracy for effects such as antenna delay and multipath, station coordinates, and earth orientation, are being developed to satisfy the requirements of VLBI and GPS measurements.

The dominant error sources in today's systems are instrumental. The largest contribution is the spacecraft transponder, which is difficult to calibrate after launch. Transponders have delay variations due to aging, temperature changes, radiation, signal amplitude changes, etc., that are a few per cent of the total analog delays. For the delay of 1 microsecond typical of a 1 MHz bandpass, delay variations of tens of nanoseconds result.

It would be possible to devise methods for in-flight calibration of the transponder delay, but the preferred solution is to directly reduce the error by developing a new digital transponder with a total analog delay of only a few nanoseconds. The key to this approach is high rate sampling of the broad band (~500 MHz) received signal, after minimal broad band analog processing (pre-amplification and bandpass filtering). All subsequent operations performed on the ranging and Doppler signals are digital, i.e., the outputs are uniquely determined by the inputs. The time delay of the digital operations depends only on the stability of the local frequency standard, and varies by less than 1 cm for typical spacecraft frequency standards.

Several advantages are obtained by using a digital design for transponders and for ground site transmitter/receivers. Some of these are listed below.

(1) The responses of digital circuit elements, such as filters, are exactly known, and not dependant on temperature, etc., (assumes the circuit remains purely "digital").

(2) Greater system design flexibility is allowed. For example, if two planetary landers are in the beam of the same earth antenna, their transponders could individually track the uplink range code (and carrier), and generate downlinks with orthogonal (between landers) "reconstructed" range codes coherent with the uplink signal received at each lander. The digital ground receiver would simultaneously track the two downlink signals to provide accurate differential Doppler and range measurements.

(3) Digital implementations allow improvements in power consumption, size, and reliability.

(4) Greater algorithmic flexibility is possible, as more operations and functions are available to the digital designer.

IV. CONCLUSION

It is now possible to design a spacecraft ranging system with anticipated measurement errors under 10 cm. The digital technology to track multiple ranging signals with cm-level accuracy has been demonstrated in the ROGUE GPS receiver. Development of custom GaAs chips to allow direct sampling of RF signals with 500 MHz bandwidth, followed by digital signal processing, is in process at JPL. The implementation of a 10 cm ranging system will probably not occur, however, until required for navigation. The utility of 10 cm range measurements for navigation is currently being studied at JPL. Potentially attractive navigation applications of accurate range include synergistic combinations of range and VLBI measurements. This combined data type could be applied, for example, to the relative navigation needed between a Mars rover and ascent vehicle, or to the determination of pre-encounter trajectory perturbations which would be used to pin down the target planet's ephemeris (grav-nav). Should the results of these studies indicate that 10 cm range data are valuable to navigation, components of improved range measurement systems could be installed on future spacecraft and at tracking sites, enabling more precise measurements of parameters used to test predictions of relativistic gravitational theories.

REFERENCES

September 1987, *Relativistic Gravitation: NASA's Present and Future Programs.*
Treuhaft, R. 1988, *"Tropospheric Monitoring Technology,"* these Proceedings.

DISCUSSION

SHAPIRO: Are there any firm plans (i.e., funds allocated and people assigned) for implementation of a 10 cm ranging system?

YOUNG: There is no current plan to implement 10 cm range measurements. A highly digital receiver will, however, be implemented by the mid 1990's. If studies on the navigation utility of 10 cm ranging have a positive result, that capability could be included in the revised receiver.

DRAG-FREE SATELLITE CONTROL

DANIEL B. DeBRA
Stanford University

A drag-free satellite cancels the effect of external disturbances. Although the forces may be small, a satellite is disturbed by residual air drag, radiation pressure, micrometeorite impact, and other small forces that act on its surface disturbing its orbit, which is principally determined by the gravity field. In some missions, these small perturbations that make the satellite deviate from its purely gravitational orbit are limiting. An internal unsupported proof mass is shielded by the satellite from the external disturbances. The position of the shield (or the main part of the satellite) is measured with respect to the internal proof mass, and this information is used to actuate a propulsion system which moves the satellite to follow the proof mass. Fig. 1 illustrates a drag-free control system. Since the proof mass is shielded it follows a purely gravitational orbit — as does the satellite following it — hence the name drag-free satellite. The idea was conceived by Lange (1964) and has been applied to many mission studies since.

In some cases, it is not necessary to cancel the disturbances, only to measure them so they may be taken into account. In such a case, an accelerometer may be a more suitable solution (for example, using the ONERA Cactus or the Bell Aerosystems MESA).

I. MISSIONS

In developing the concept of the drag-free satellite, Lange considered a number of applications. An obvious choice is when the gravitational path itself is an indicator of the gravity field, and thus disturbances decrease the accuracy with which geodesy can be studied from artificial satellites.

By observing the control effort applied to make the satellite drag-free, the disturbing forces can be measured. At low altitudes, these are predominantly atmospheric drag, so atmospheric density can be determined with unusually good spatial resolution.

A third application of the drag-free principle is to provide a uniquely weightless environment for instruments. If an instrument is used as the proof mass of the drag-free satellite, there are no support forces at all, and thus errors introduced by supports are completely removed. This feature is absolutely essential to the success of the Stanford gyro test of Relativity in which the gyros must be scrupulously free of any disturbances, so that changes in orientation they may undergo, due to their interaction with the gravity field, can be determined unambiguously.

Fourth, in a test of the principle of equivalence (proposed by Everitt and Worden 1974), the dynamic range of the measurements is greatly reduced if performed on-orbit and one of the two test masses is taken as the drag-free reference.

Fifth, when drag is cancelled, there is no uncertainty due to external disturbances, and an orbit can be predicted much farther into the future. This is useful for navigation satellites which must store and report their ephemerides (Space Department 1974).

useful for navigation satellites which must store and report their ephemerides (Space Department 1974).

II. SENSORS

The position of the satellite, with respect to the proof mass, must be detected without disturbing the proof mass. Capacitive sensors have proved successful, such as those developed at Stanford (Space Department 1974) and at the Office National d'Etudes et de Recherches Aerospatiales (ONERA) (Juillerat 1970). Optical sensors may produce even smaller disturbances, but are slightly less reliable by analytical comparison, though they offer the major advantage of providing a means of detecting a small proof mass inside a large cavity — a desirable feature for some missions. A shadowing technique, developed at the Johns Hopkins University Applied Physics Laboratory (APL) (Mobley *et al.* 1975), is similar to the small motion detector proposed by MATRA in a spinning satellite, in which the large detection was performed digitally by interrupting a series of pencil beams of light. A novel technique, developed by DeHoff (1975) at Stanford, excites fluorescence in a coating on the proof mass with ultraviolet light; the re-emission occurs in the infrared. Large motions can be detected using Schottky-barrier diodes without a serious internal reflection problem. The intensity of Beta emission has also been considered at APL, and a number of other novel schemes have been proposed.

III. ACTUATION

Any propulsion system is possible, from the use of the simplest compressed gas, such as nitrogen or Freon 14 (CF_4), to the exotic pulsed plasma Teflon engine, which has many advantages for extended missions. These systems are usually pulsed to provide the most efficient use of the propellant. Cryogens, which are needed to maintain a low-temperature environment, may also be used as a propellant for drag-free control as well as for attitude control. For example, liquid helium produces an effective propellant once the gas has warmed up to satellite body temperature. Since the flow must be continuous to provide cooling, differential proportional thrusting is employed, as the efficient use of propellant is not a consideration. On the Stanford gyro test of Relativity the He gas is at very low pressure (3 torr), but the specific impulse has been measured at 137 sec. The continuous thrust makes it possible to track the proof mass smoothly without significant error. This experiment is planned to carry a Global Positioning System (GPS) receiver. With negligible proof mass error signal, the GPS signal is a direct measure of the proof mass position, enabling the satellite to perform some very useful and important geodesy.

IV. CONTROL LAWS

If the satellite's angular velocity is slow compared with the bandwidth of the control system, the control can be considered for each axis separately. Simple lead compensation is a sufficient way of providing the rate information needed to damp the closed-loop behavior. As a result of mission requirements, or to obtain averaging of some of the disturbances between the satellite and the proof mass, the vehicle may spin at an angular velocity that is significant compared with the control bandwidth. Since the measurements are made in body axes, lead compensation will be applied incorrectly as viewed from inertial space. Lange (1964) provided a correction for this by including the necessary Coriolis terms due to the rotating coordinate frame in calculating the required velocity information. At ONERA, the position of the satellite, with respect to the proof mass, was measured each quarter of a revolution and the

sensors were interpreted according to their orientation in space, so that the information was actually gathered as an inertial measurement by indexing the information around to sequential sensors. Thus, even in a rotating satellite, the velocity information could be derived by a simple single-axis mechanization.

It is not always possible to place the proof mass at the mass center of the satellite. There is no interest in forcing the satellite housing to stay exactly centered on the proof mass, particularly if some of the relative motion is simply due to mutation of spin rather than a relative movement of the two mass centers that must be corrected. Sanz (1975) developed an estimator with which to subtract the part of the relative motion signal due to attitude motion in a spinning satellite. It was then possible to proceed with the control as if the proof mass was at the satellite mass center.

Most control laws, as originally conceived, are motivated by ideas of continual actuation. However, most propellants are not easily throttled, and for their effective use the thrusters are operated on-off. A dead zone is introduced into the control and this nonlinearity can cause some very interesting effects in a rotating satellite. Specifically, equilibria can exist beyond the edge of the dead zone when dead zones are established for each axis of the control. These equilibria are locations where the error signal produces a thrust equal to the centripetal acceleration of the mass center moving about the center of spin. Powell (1972) discovered these equilibria and developed circular dead bands and the techniques for mass center estimation to locate the pickoff null to coincide with the center of spin. With his techniques, spinning satellites, even with nonlinear control, can be made to operate as efficiently in their use of propellant as nonspinning satellites.

Some disturbances between the proof mass and the satellite have a gradient. Thus, if an external disturbance requires an error signal which will be correlated with the direction of the disturbance in space, averaging may not be obtained in a spinning satellite. Integral control is the solution to this problem; however, the calculations must be performed in a rotating coordinate frame. An inertially fixed external disturbance, which appears to rotate in the satellite coordinate frame, can be modelled as an oscillator and the benefits of integral control in inertial space are obtained (Tashker 1974).

V. ERROR SOURCES

For missions in which the path of the satellite must be as nearly gravitational as possible, it is important that disturbances between the satellite and the proof mass are made quite small. Solar radiation pressure acting on a typical satellite with an area-to-mass ratio of 0.01 m^2–kg^{-1} produces an acceleration of the order of 10^{-7} m–s^{-2}, thus the proof mass acceleration from internal disturbances must be kept several orders of magnitude smaller than that if improvements are to be realized. Disturbances from electric charge, gradients in magnetic fields, the radiometer effect due to temperature differences, radiation pressure due to temperature differences, and many other effects can be calculated and must be taken into account. With careful design these can all be kept below 10^{-11} m–s^{-2} using a proof mass of 20 mm diameter made of a heavy metal. The density must be high to reduce the area to mass ratio. An alloy of gold and platinum can also minimize magnetic susceptance (Space Department 1974).

the mass attraction between the satellite itself and the proof mass. The vehicle must be symmetrical, the location and the mass of the parts, especially those close to the proof mass, must be determined and compensating masses must be placed nearby to offset the mass attraction.

VI. FLIGHT EXPERIENCE

In 1972, the first drag-free satellite was launched. It provided a prediction capability for navigation satellites of 2 weeks, compared with the 12-hour limitation caused by the uncertainty in estimating atmospheric drag and radiation pressure. This three-axis control system demonstrated the principles and achieved a performance level of 5×10^{-11} m–s^{-2} (Space Department 1974) (see Fig. 1). Subsequent flights have been made with single-axis, drag-free satellites providing the drag-free performance in the in-track direction, which is most sensitive to error buildup, and using a passive eddy current repulsion suspension technique for the proof mass in the vertical direction and normal to the orbit plane. Pulse plasma thrusters provide lifetime potential of 7 years or more. With proper modelling of the attitude behavior, the equivalent prediction capability of 10^{-10} m–s^{-2} was achieved in 1982 with the NOVA navigation satellite (Eisner and Yionoulis 1982).

REFERENCES

DeHoff, R. L. 1975, "Minimum Thrustors Control of a Spinning Drag-free Satellite, Including the Design of a Large Cavity Optical Sensor," Ph.D. thesis, Stanford University.

Eisner, A., and Yionoulis, S. M. 1982, "NOVA-I — the 'Drag-free' Navigation Satellite," *ION — National Aerospace Meeting*.

Everitt, C. W. F., and Worden, P. W. 1974, "The Gyroscope Experiment: Test of the Equivalence of Gravitational and Inertial Mass Based on Cryogenic Techniques," *Proceedings of the International School of Physics "Enrico Fermi" Course LVI*.

Juillerat, R. 1970, "Physical Limitations in Sensors for a Drag-free Deep-space Probe," *Proceedings, Conference Experimental Tests of Gravitation Theories*, Office National d'Etudes et de Recherches Aerospatiales, Paris.

Lange, B. O. 1964, "The Drag-free Satellite," *AIAA J.*, **2**, 1590-1606.

Mobley, F. F., *et al.* 1975, "Electromagnetic Suspension for the TIP II Satellite," *13th Int. Conf. Magnetics*.

Powell, J. D. 1972, "Mass Center Estimation in Spinning Drag-free Satellites," *J. Spacecraft Rockets*, **9**, (6), 399-405.

Sanz, S. 1975, "Orientation and Three-dimensional Mass Center Estimation in a Rotating Drag-free Satellite," Ph.D. thesis, Stanford University.

Space Department of Johns Hopkins University 1974, Applied Physics Laboratory, and Guidance and Control Laboratory of Stanford University, "A Satellite Freed of all but Gravitational Forces: 'TRIAD I,'" *J. Spacecraft*, **11**, 637-44.

Tashker, M. G. 1974, "Integral Control of a Spinning Drag-free Satellite," Ph.D. thesis, Stanford University.

Tisson, J. 1972, *Influence des Rayonnements Spatiaux sur L'accelerometre* CACTUS, Note Technique ONERA No. 200, Office National d'Etudes et de Recherches Aerospatiales, Paris.

DISCUSSION

SHAPIRO: Have you considered the placement of optical corner reflectors on the GPB satellite to allow 'cross-checking', as part of the geodesy uses of the GPB flight?

DeBRA: Yes. It may not provide more or better information than the GPB continuous, but it is important to have a comparison of radio and optical data. It is our intention to add corner reflectors for whoever may wish to use them.

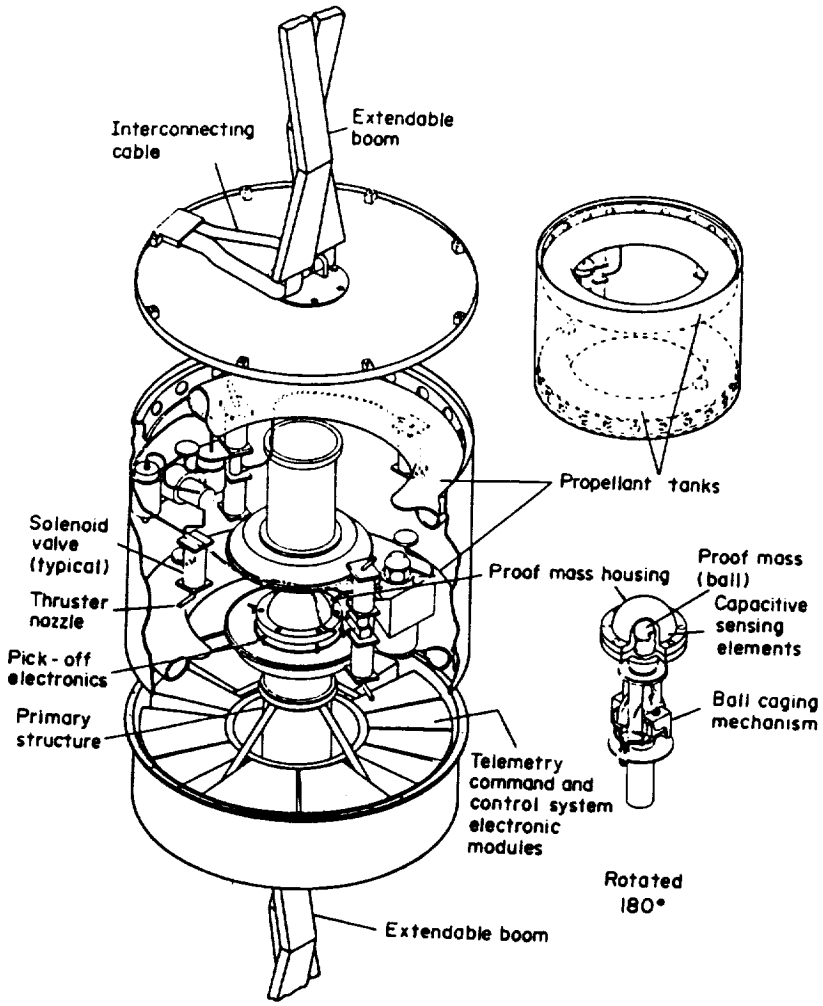

Figure 1
Cutaway drawing of the Stanford disturbance compensation system (DISCOS)

SUPERCONDUCTING GRAVITY GRADIOMETER AND A TEST OF INVERSE SQUARE LAW

M. V. MOODY AND H. J. PAIK
Department of Physics and Astronomy
University of Maryland, College Park, MD 20742

The equivalence principle prohibits the distinction of gravity from acceleration by a local measurement. However, by making a differential measurement of acceleration over a baseline, platform accelerations can be cancelled and gravity gradients detected. In an in-line superconducting gravity gradiometer, this differencing is accomplished with two spring-mass accelerometers in which the proof masses are confined to motion in a single degree of freedom and are coupled together by superconducting circuits. Platform motions appear as common mode accelerations and are cancelled by adjusting the ratio of two persistent currents in the sensing circuit. The sensing circuit is connected to a commercial SQUID amplifier to sense changes in the persistent currents generated by differential accelerations, *i.e.*, gravity gradients. A three-axis gravity gradiometer is formed by mounting six accelerometers on the faces of a precision cube, with the accelerometers on opposite faces of the cube forming one of three in-line gradiometers.

Such an instrument is being developed at the University of Maryland under support from NASA with the primary geophysical goal being a dedicated satellite mission for mapping the earth's gravity field. The goal for the sensitivity of this instrument was set by a 1983 workshop at 3×10^{-4} E $Hz^{-1/2}$. Additional scientific goals are a test of the inverse square law to a part in 10^{10} at 100 km, and a test of the Lense-Thirring effect by detecting the relativistic gravity magnetic terms in the gravity gradient tensor for the earth.

The expression representing the intrinsic spectral noise of the gradiometer consists of two terms: a Brownian motion noise term and an amplifier noise term. In addition to the scaling of the intrinsic spectral noise with one over the baseline squared, the determining parameters for the Brownian motion noise level are the mass, the temperature, and the quality factor; whereas, the determining parameters for the amplifier noise level are the resonance frequency and the energy resolution of the amplifier.

The intrinsic noise level for the three-axis gradiometer currently being tested is 2×10^{-3} E $Hz^{-1/2}$ and is limited by the amplifier noise term. In order to meet the 1983 workshop goal with a presently available commercial SQUID, the resonance frequency must be reduced. One way of accomplishing this reduction is by means of a superconducting negative spring. The negative spring consists of a superconducting disk with curved edges located in a short superconducting solenoid with a length less than the thickness of the disk. The negative spring has been demonstrated and is being incorporated into the latest model of the superconducting gravity gradiometer.

Though it appears that the goal for the intrinsic noise level can be met, the best sensitivity demonstrated in the laboratory to date is 0.05 E $Hz^{-1/2}$ at 1 Hz, degrading at lower frequencies. The source of this noise appears to be modulation of the earth's gravity by residual tilt noise. This modulation occurs as a result of sensitive axis misalignment and scale factor variations. In order to remove this and

other angular motion errors, a six-axis superconducting accelerometer is being developed at the University of Maryland under support from the Air Force Geophysics Lab. This device consists of a superconducting proof mass in the shape of an inverted cube. The motion of this proof mass is sensed in all six degrees of freedom (three angular and three linear) with superconducting bridge circuits. These bridge networks are modulated at six different frequencies and the signals are sensed with a single SQUID amplifier. This accelerometer has been designed to occupy the center of the precision cube of the gradiometer.

The gravity gradiometer project at the University of Maryland has progressed to the point where a study team has been formed to examine details and make recommendations to NASA with regard to a super-conducting Gravity Gradiometer Mission. The study team has drafted a report which will soon be published.

As previously mentioned, one of the scientific goals of such a mission(s) would be an inverse square law test to an accuracy of 1 part in 10^{10} at 100 km. This test would attempt to resolve a non-Newtonian potential by measuring the Laplacian of the earth's gravitational potential. In a circular polar orbit at 160 km altitude, which is preferred for the geophysical mission, the oblateness of the earth would be the source. With a mission duration of 180 days, the stated resolution could be achieved. However, this experiment is not a straightforward one. In order to minimize the effect of attitude rate variations, an inertial orientation must be chosen. One of the three sensitive axes could be oriented normal to the orbit plane to circumvent the limitation of 1 part in 10^5 that would be imposed by the axis misalignment. There still remains a challenge in matching the scale factors to 1 part in 10^{10} in the measurement bandwidth. This would require some sort of continuous cross-calibration of the gravity gradiometers.

DISCUSSION

NIETO: A two part question; (1) You don't need a shuttle mission, do you? (2) If you got the go-ahead yesterday, how long would it take you to prepare your package?

MOODY: No and mid 90's.

INERTIAL CORRECTIONS BY DYNAMIC ESTIMATION

DAVID SONNABEND

Jet Propulsion Laboratory,
California Institute of Technology

This paper presents the highlights of an Engineering Memorandum, "Dynamic Estimation for Floated Gradiometers," JPL EM 314-441, 6-5-88, by D. Sonnabend and W. M. McEneaney. The original impetus for the work was that gradiometers, in principle, measure components of the gravity gradient tensor, plus rotation effects, similar to centrifugal and Coriolis effects in accelerometers. The problem is that the rotation effects are often quite large, compared to the gradient, and that available inertial instruments can't measure them to adequate accuracy. The paper advances the idea that, if the instruments can be floated in a package subject to very low disturbances, a dynamic estimation, based on the Euler and translational equations of motion, plus models of all the instruments, can be used to greatly strengthen the estimates of the gradient and the rotation parameters. Moreover, symmetry constraints can be imposed directly in the filter, further strengthening the solution.

There are direct applications of these ideas to relativistic gravity experiments. First, the gradient tensor is really a subset of the Riemann tensor; so one can, in principle, make a direct measurement of curvature. Once the measurement model has been updated to a fully relativistic treatment of the rotation effects, the present estimation structure can be used to determine how well local curvature, and the PPN parameters, can be extracted, given the properties of the instrument ensemble. Gravitomagnetic effects may even be accessible, as suggested by Mashoon.

Another possibility, long advanced by Paik, would be the detection of "fifth force" terms in the geopotential. His idea is that, while the gradient tensor is traceless for any Newtonian potential, the addition of a consistent-type potential would lead to a non-zero trace, which should be readily measurable, in spite of large uncertainties in the earth's mass distribution. A problem here is that the centrifugal-like terms are not traceless; so again, dynamic estimation may help separate them from fifth force effects, if they exist.

The existing filter structure was devised to examine the measurement of the (Newtonian) geopotential, and does not stretch to cover either of these kinds of investigations. However, once a fully relativistic treatment of the gradient tensor, and of the rotation corrections, is available to us, it should not be hard to augment the filter state to include the uncertain parameters we are after; *i.e.*, some of the PPN parameters and the coefficients of one or more Yukawa potentials.

At present, the filter is built around a 14-element state vector, including the disturbance force on the instrument package, the instrument angular velocity and attitude, and 5 independent elements of the gradient tensor (assumed both symmetric and traceless). Possible measurements include linear and angular accelerometers, gyros, a star tracker, and a full tensor gradiometer. Any components of any of these measurements may be deleted. The effects of process noise are incorporated by means of Gauss-Markov processes for both air drag and gradient arising from variable geology. The latter is a very simple (but analytically tractable) scheme involving random mountains on a locally flat earth. While suitable for appraising the value of dynamic estimation in this scenario, several parts of the filter will need

to be upgraded to deal with a specific mission design. This is especially true if relativistic effects are to be included.

Finally, even for purely geophysical studies, it will be necessary to add a module that includes the errors in transforming from the instrument location and attitude to fixed earth (or other more or less inertial) coordinates. This will require the inclusion of satellite tracking in the measurement ensemble, a fairly extensive revision, particularly if a relativistic treatment is required. All of this could be done in a few months if support is available.

ULTRA-SENSITIVE INTERTIAL SENSORS VIA NEUTRAL-ATOM INTERFEROMETRY

JOHN F. CLAUSER

CQ825218

J. F. Clauser & Associates — Custom Sensor Development
975 Murrieta Blvd. #22, Livermore, California 94550

Upon looking at the various colossal interferometers, *etc.*, discussed at this conference to test gravitational theory, one cannot avoid feeling that easier approaches exist. It is the purpose of this paper to suggest such. We propose to use low-velocity, neutral-atom matter waves in place of electromagnetic waves in sensitive inertial interferometer configurations. For applications we consider spacecraft experiments to sense a drag-free condition, to measure the Lense-Thirring precession, to measure the gravito-magnetic effect and/or the earth's geopotential (depending on altitude), and to detect long period gravitational waves. Also, we consider a terrestrial precision test of the equivalence principle on spin-polarized atoms, capable of detecting effects of the 5th force. While the ideas described herein are preliminary, the orders of magnitude are sufficiently tantalizing to warrant further study. Although existing proposed designs may be adequate for some of these experiments, the use of matter-wave interferometry offers reduced complexity and cost, and an absence of cryogenics.

Contrast Sagnac interferometer experiments to measure the rotation rate of the earth with a passive single-circuit ring cavity. The Michelson Gale experiment employed light and a ring area several times that of a soccer field, achieving less than one fringe sensitivity. A recent neutron interferometry experiment by Werner Staudenmann and Colella achieved many fringe sensitivity with an interferometer that fits in one's hand! As a simple rule of thumb, a matter-wave interferometer employing particles with velocity, v, gains sensitivity over an electromagnetic one with the same area by a factor of c/v for rotations and $(c/v)^2$ for accelerations and gravity (Clauser 1987).

Although the spatial coherence of freely propagating atoms has been evident for some time, no one has yet built a separated beam interferometer. However, recently developed technology makes such a device feasible. For example, Sesko, Fan, and Wieman at JILA recently produced a beam of neutral cesium at 100 cm/sec with a single stage of laser cooling, and 15 cm/sec with a second stage. The temperature of the latter was 100 μK. The deBroglie wavelengths for these atoms are 30 and 200 Å, respectively.

An illustrative configuration for such a device (shown in Figure 1) employs a sequence of three equally spaced planar gratings. One choice for such gratings is to employ diffraction by the spatially periodic electric field of a nearly resonant standing-wave laser beam (the atomic analog of the Kapitza-Dirac effect). An advantage of this method is that it allows the grating to be blazed to high order through choice of laser power and detuning. A second choice is diffraction by a microfabricated, submicron-spaced grid. A third choice (requiring a slightly different geometry) is Davidson-Germer diffractive reflection by available large perfect silicon crystal faces, in which each face is a nearly perfect lattice plane.

In Figure 1, a laser-cooled and decelerated atomic beam is coherently divided at the first grating, propagates along two paths consisting of the sides of a rhombus, being redirected at the middle grating. The paths then superpose and recombine on the last grating, whereupon interference occurs. If the last grating is tilted slightly with respect to the others, a highly magnified transverse fringe pattern will be formed across this grating. The necessary conditions for coherence and nonvanishing fringe visibility can be satisfied for suitable choices of grating and atomic beam parameters. Detection of the fringes can be done by imaging the fluorescent light produced at the final grating, or by measuring the profile of the transmitted beam by standard atomic beam techniques (*e.g.*, ionization on hotwires).

If the interferometer described above is placed in a noninertial frame, it will exhibit a fringe shift. Let x be the distance between the outer two gradings, d (= $\lambda_{laser}/2$) be the grating split spacing, and n and 2n be the diffraction order at the end and middle gratings, respectively. Additionally, let $\hat{o}$ be a unit vector perpendicular to the plane of the paths, and $\hat{q}$ be a unit vector perpendicular to the line between the source and detector. Also, let Ω be the rotation rate vector, and a be the sum of the acceleration and gravity vectors. The phase shift δ (radians) that is due to rotation is given approximately by

$$\delta_{gyro} \approx \frac{2\pi x^2 n (\Omega \cdot \hat{o})}{d v}$$

while that due to gravity is given by

$$\delta_{grav.} \approx \frac{\pi x^2 n (a \cdot \hat{q})}{d v^2} \cdot \left(\frac{m_g}{m_i}\right)$$

The gyroscopic and gravitational sensitivities depend differently on particle velocity. Thus, a pair of matter-wave interferometers employing different velocity atoms (*e.g.*, *in-situ* along the same paths, but in different orders) can be used to determine both acceleration and rotation rate independently from a solution of the simultaneous equations. Six interferometers can sense all six components of the rotation rate and gravity plus acceleration vectors. With solid gratings (*e.g.*, crystal faces or a microfabricated grid), if soft X-rays or UV also propagate *in-situ* along the same paths, then the resulting electromagnetic fringes will form a reference to allow servo-stabilization of the grating positions against their low frequency thermal motion or other mechanical flexure.

Consider a spacecraft experiment to measure the Lense-Thirring precession, similar to the Stanford Gyroscope Experiment, but with the superconducting sphere and cryo-system replaced by the interferometer of Figure 1. For a count rate R, a fractional fringe $\pi/(R\tau)^{1/2}$ should be detectable, where τ (=1/f) is the integration time. For x ≈1–10 m, R = 10^6 is realistic. If the atomic beam is focused (*e.g.*, by additional lasers) this rate will be independent of x. Assume D = 0.5μ (or λ_{laser} = 9521Å) with Cs at 1 m/sec. The sensitivity to rotations is then Ω(rad sec^{-1} $H^{-1/2}$) = $7.8 \cdot 10^{-11} \times (m)^{-2}$. Thus an instrument with x = 100 m and $\tau \approx 1$ sec, or x = 10 m and $\tau \approx 10^4$ sec should sense Ω (Lense-

Thirring) $\approx 10^{-14}$. This sensitivity will improve inversely with v. The same instrument can be used for drag-free sensing with an accelerometer sensitivity of a (Gal $Hz^{-1/2}$) $\approx 1.6 \cdot 10^{-8} \times (m)^{-2}$. Although the interferometer can sense exact path equidistance (via the white fringe), spacecraft asymmetry may still cause a fixed imbalance. However, if the spacecraft rotates slowly about the star sensor axis ($\perp o$, $\perp q$), fringe variation synchronous with this rotation will constitute the usable signal and any fixed bias will cancel.

Gravitational gradients can be measured utilizing the same principles with a geometry in which the paths follow a two-loop structure (figure-eight with loops of equal area), shown in Figures 2a and 2b using Davidson-Germer diffraction by crystals). Because the circuits about the two loops are oppositely directed, the net area is zero. As a result, the interferometer will be insensitive to rotation, (except that it will also measure accelerational gradients such as those due to centrifugal acceleration). A gravitational field acting on one loop that is slightly different from that acting on the other, will yield a phase shift proportional to the difference. Thus, an interferometer with such geometry will measure gravitational gradients.

A spacecraft experiment with a gradiometer as per Figure 2a, with the same parameters as above, will have a sensitivity (for off-diagonal gradient components) of $da/dx \approx 1.3 \cdot 10^{-2}$ x' $(m)^{-3}$ E $Hz^{-1/2}$ Thus, a device with x' = 50m can detect a gravito-magnetic gradient of 10^{-8} E in $\tau \approx 50$ sec.

Consider next the sensitivity of a Figure 2b gradiometer to long-period gravitational waves. Such a wave will deflect the matter waves asymmetrically within the interferometer and act like a gravity gradient. For n = 1 the detectable strain, h, will be the fraction of a detectable fringe on the final grating divided by the extent x' of the device, *i.e.*, $h \approx \eta\ d\ x'^{-1}\ (R\tau)^{-1/2}$, independent of v. For a burst at 10^{-5} Hz, with $\tau = 10^5$, d = 1Å, x = 100 m and $R = 10^6$, the minium detectable strain is then $h \approx 10^{-17}$.

As a final application, consider a terrestrial experiment in the Fig. 1 configuration, with microfabricated gratings, with a B field gradient everywhere (within the domain of the paths) parallel to g. An oscillating magnetic field, applied to the apparatus, will cause spin flips detectable by a loss of fringe visibility at resonance. Suppose one adjusts (and/or shims) the magnetic gradient for minimum resonance width. This will occur when the Zeeman energy everywhere cancels the gravitational potential energy. The resonance frequency will be proportional to the ratio of the gravitational to inertial mass of the atom. If two species simultaneously propagate (*e.g.*, Rb^{85} and Rb^{87}), then the ratio of the species frequencies is the product of the magnetic moment ratio, the inertial mass ratio, and the gravitational mass ratio. The magnetic moment ratio can be precisely determined in an auxiliary resonance experiment as can the inertial mass ratio (*e.g.*, by measuring the corresponding ion cyclotron resonance frequency ratio, correcting for electron mass). Using field independent transitions, a high-precision Eötvös experiment results from this experiment sequence and a product of resonance frequency ratios. Performing the interferometer experiment at different altitudes then (in a fashion similar to the recent AFGL tower experiment) allows a measurement of the effects of a 5th force.

REFERENCES

Clauser, J. F. 1988, *Ultra-high Sensitivity Accelerometers and Gyroscopes Using Neutral Atom Matter-Have Interferometry*, Proc. of the International Workshop on Matter Wave Interferometry in Light of Schrödinger's Wave Mechanics 14 to16 September 1987, Technical Univ. of Vienna, and Atominstitut der österreichischen Universitäten (to appear in *Physica*

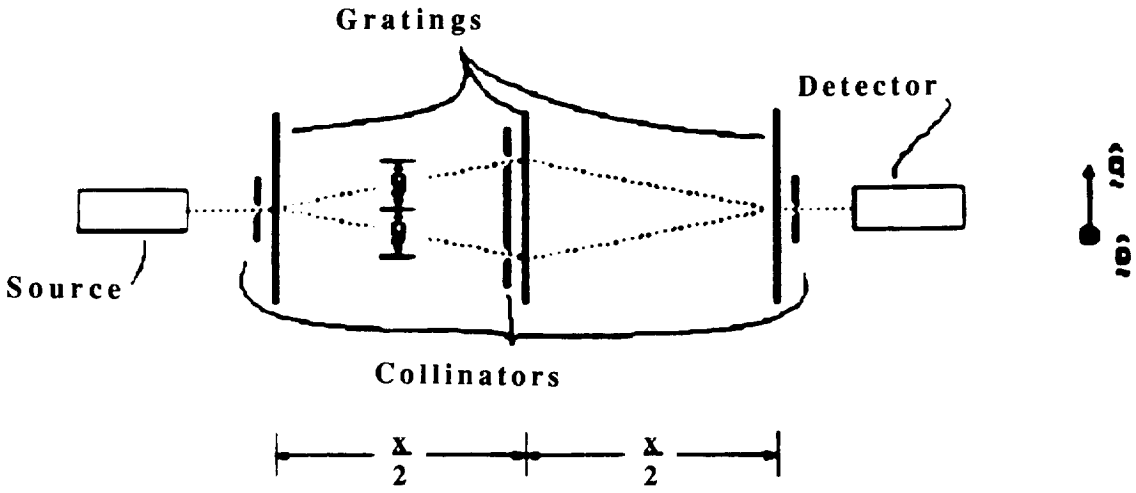

FIG. 1.— Separated Beam Interferometer

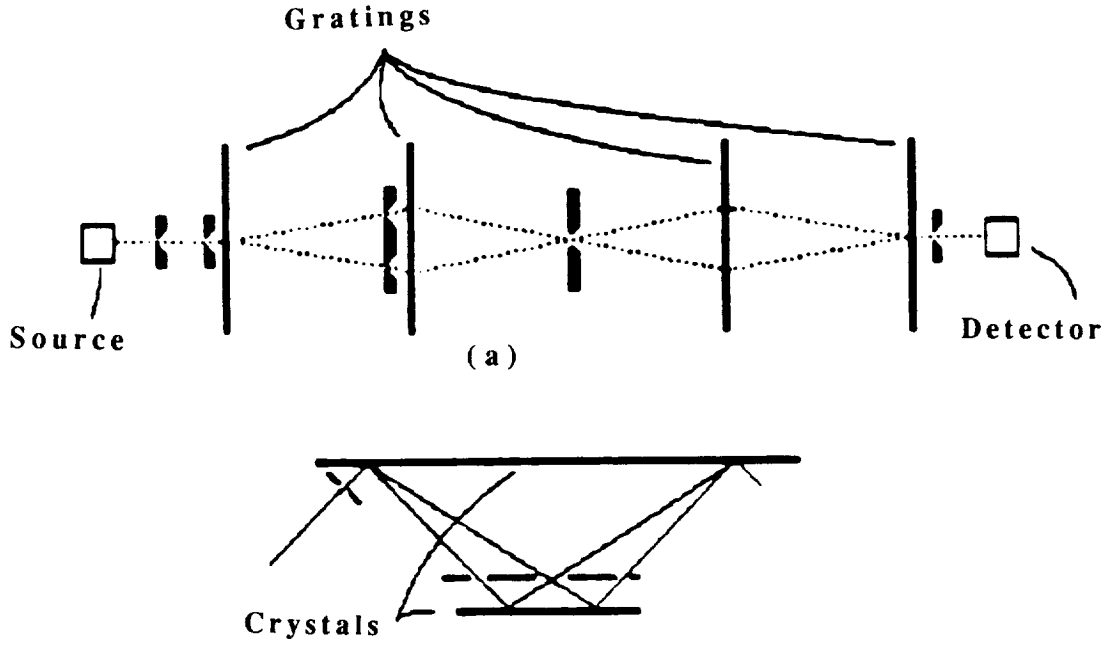

FIG. 2.—Gradiometer Configurations

DISCUSSION

FAIRBANK: Won't Newtonian forces overwhelm the signals you are trying to measure? Indeed, the Stanford experiment requires a nearly perfectly spherical ball, negligibly diamagnetic, etc. Minute deviations will cause anomalous precessions.

CLAUSER: If the spacecraft rotates slowly about the star tracer axis, then a fixed bias (e.g. due to spacecraft mass asymmetries) will yield no signal synchronous with the rotation. If an atom with J=0, I=0 (e.g. an alkaline earth or noble gas) is used, there wll be no magnetic influence on the atoms. For the configuration of Fig. 1, suppose the triangular areas of the input and output ends of the interferometer are imbalanced by a part in 10^{10}, due to a grating spacing error of 1mm out of 100m. Then a fringe shift comparable to that expected for the Lense-Thirring precession will be produced by a gravitational gradient of about 0.3 E, far greater than that expected in orbit. Warping of the spacecraft axis by thermal gradients and/or magnetostriction may cause a shift; however these can be removed by the aforementioned stabilization using the *in-situ* electromagnetic fringe reference.

WEISS: Won't thermal fluctuations wipe out your signal when you extrapolate the sensitivity to systems of large dimension, especially for your proposed gravitational wave detector?

CLAUSER: The proof masses are the atoms themselves, which are at 100 mK. The conditions for coherence (seeing fringes) are readily satisfied.

WEISS: No, I am referring to thermal fluctuations of the spacecraft and/or interferometer elements.

CLAUSER: Lets design a simple spacecraft and consider its primary bending mode. Suppose the instrument is 100 m long and is made from a carbon-fiber truss frame with 5:1 aspect ratio. This material has a density of 1.6 g cm^{-3} and an elastic modulus of 1.3×10^6 dyne cm^{-2}. A frame member cross section of 1 cm^2, yields an overall frame weight of 32 kg for two bars 100 m long. It will have a bending spring coefficient of x = 1.3 dyne per cm lateral end deflection. Putting kT/2 thermal energy at T=300K into this bending mode yields an end deflection of Dx_{rms} 1.8×10^{-3}m, which is about the same as the grating spacing time fringe fraction (1 part in 10^3) used for most of the experiments discussed above. OK, so you integrate a little longer. The exception is the proposed gravitational wave detector, which has a grating spacing 10^4 smaller, while a fringe is split to a part in 10^5. Thus, you are correct in fingering the gravitational wave detector as the most thermally sensitive. Its implementation thus requires a gain for the servo system that stabilizes the gratings relative to the electromagnetic fringe reference to be of order 10^6. I agree that such engineering is not trivial, but I think it is doable, and with due respect to the other contributors, less demanding than many of the proposals discussed at this conference. I propose this as an <u>easier</u> method to detect long period gravitational waves, not an <u>easy</u> method!

SONNABEND: What about the W^2 effects I mentioned in my talk on gradiometry. Won't these be important.

CLAUSER: I believe these effects represent centrifugal acceleration's lack of co-linearity. In a precision experiment, of course, the effect must be considered (as it was in Ref. 1). The effect was neglected here for simplicity of presentation. Since W is small in all of the experiments discussed here, W^2 effects will be correspondingly negligible.

SONNABEND: Your instrument does cancel out the w terms in your gradiometer, but not the w^2 and w term. In this respect, your instrument is the same as everyone else's. It measures the intrinsic tensor.

CLAUSER: You're right.

NASA
National Aeronautics and Space Administration

Report Documentation Page

1. Report No.	2. Government Accession No.	3. Recipient's Catalog No.
NASA CP-3046		

4. Title and Subtitle	5. Report Date
Relativistic Gravitational Experiments in Space	August 1989
	6. Performing Organization Code: EZ

7. Author(s)	8. Performing Organization Report No.
Ronald W. Hellings, Editor	
	10. Work Unit No.

9. Performing Organization Name and Address	11. Contract or Grant No.
NASA Headquarters Office of Space Science and Applications Astrophysics Division Washington, DC 20546-0001	
	13. Type of Report and Period Covered: Conference Publication
12. Sponsoring Agency Name and Address National Aeronautics and Space Administration Washington, DC 20546-0001	14. Sponsoring Agency Code

15. Supplementary Notes

16. Abstract

This report summarizes the results of a workshop on future gravitational physics space missions held in Annapolis, Maryland, June 28-30, 1988. The purpose of the workshop was to define generic technological requirements for such missions. NASA will use the results reported herein to direct its program of advanced technology development.

17. Key Words (Suggested by Author(s))	18. Distribution Statement
Gravity, Space, Interferometry	Unclassified - Unlimited Subject Category 90

19. Security Classif. (of this report)	20. Security Classif. (of this page)	21. No. of pages	22. Price
Unclassified	Unclassified	231	A11

NASA FORM 1626 OCT 86
For Sale by the National Technical Information Service, Springfield, VA 22161-2171

NASA-Langley, 1989

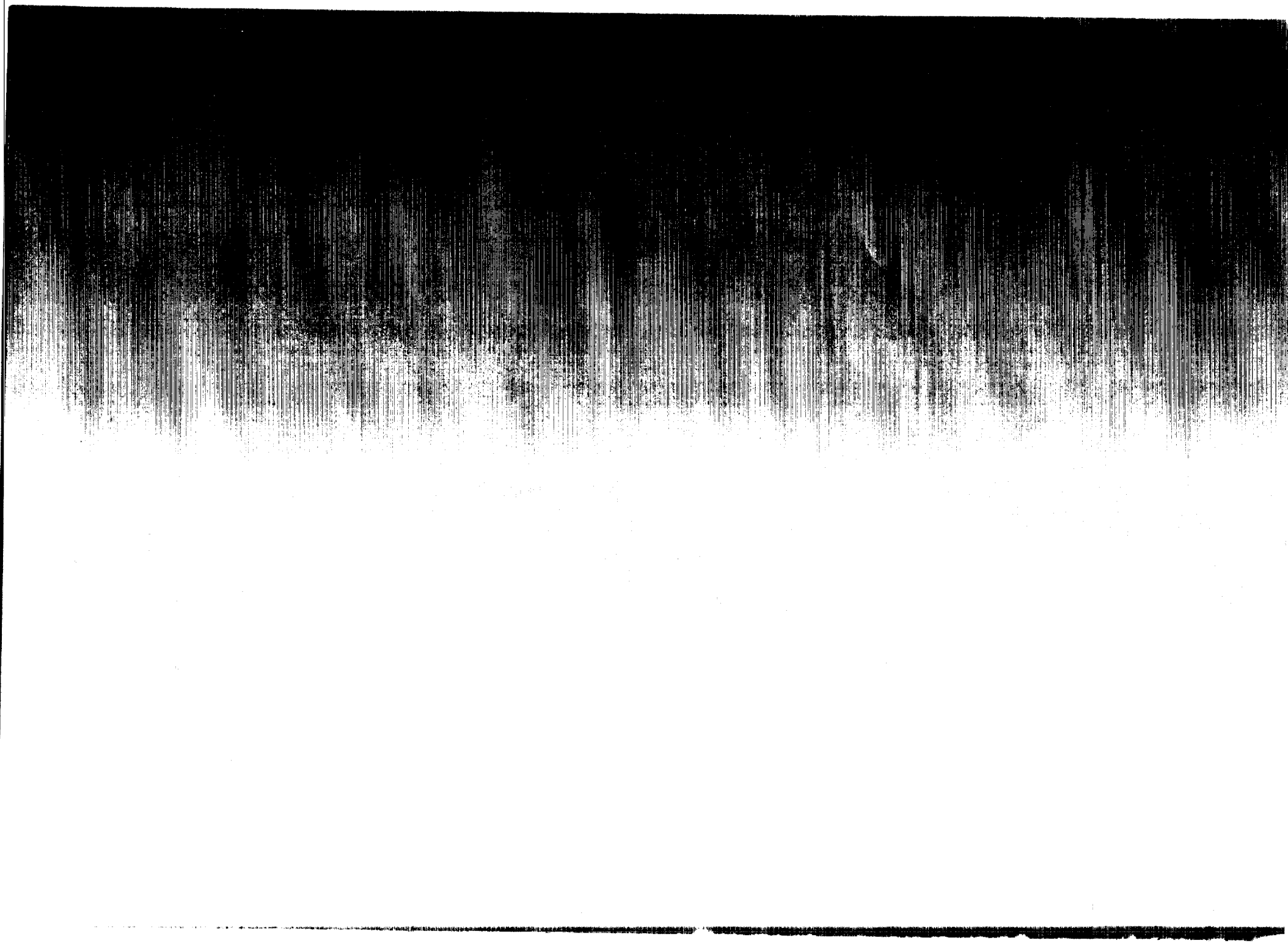

SPECIAL FOURTH-CLASS RATE
POSTAGE & FEES PAID
NASA
Permit No. G-27

POSTMASTER: If Undeliverable (Section 158 Postal Manual) Do Not Return